



Robust Design of Sensors and Functions in Vehicular Safety

Christoph Stöckle

Vollständiger Abdruck der von der Fakultät für Elektrotechnik und Informationstechnik der Technischen Universität München zur Erlangung des akademischen Grades eines

Doktors der Ingenieurwissenschaften (Dr.-Ing.)

genehmigten Dissertation.

Vorsitzender:

Prof. Dr.-Ing. habil. Erwin Biebl

Prüfende der Dissertation:

1. Prof. Dr.-Ing. Wolfgang Utschick
2. apl. Prof. Dr.-Ing. habil. Helmut Gräß

Die Dissertation wurde am 10.11.2021 bei der Technischen Universität München eingereicht und durch die Fakultät für Elektrotechnik und Informationstechnik am 05.07.2022 angenommen.

Für meine Familie

Danksagung

Diese Dissertation ist während meiner Tätigkeit als wissenschaftlicher Mitarbeiter an der Professur für Methoden der Signalverarbeitung (MSV) der Technischen Universität München (TUM) im Rahmen eines Kooperationsprojekts der Ingolstadt Institute der Technischen Universität München (INI.TUM), einer Kooperation von TUM, AUDI AG und Stadt Ingolstadt mit dem Ziel der Schaffung eines praxisnahen wissenschaftlichen Kompetenzzentrums, entstanden. Dies war nur möglich durch den Beitrag und die Unterstützung vieler Beteiligter, bei denen ich mich im Folgenden aufrichtig bedanken möchte.

Ganz besonders danken möchte ich meinem Doktorvater Univ.-Prof. Dr.-Ing. Wolfgang Utschick, der gleichzeitig auch der Leiter des MSV ist, für seine großartige Unterstützung während der ganzen Dauer des Projekts und darüber hinaus. Mit seiner ihm eigenen ganz besonderen Fähigkeit, methodische Zusammenhänge zwischen verschiedensten Anwendungsgebieten, die anderen verborgen bleiben, zu erkennen, hat er in ganz entscheidendem Maße zum Gelingen der Arbeit beigetragen und es ist nicht übertrieben, zu sagen, dass es ohne ihn die vorliegende Dissertation so nicht gegeben hätte. Eine nicht versiegende Quelle für inspirierende Ideen waren die vielen fachlichen Gespräche gerade auch auf dem gemeinsamen Arbeitsweg, die wie die vielen nicht-fachlichen Gespräche eine echte Bereicherung waren und mir auch in schwierigeren Phasen immer wieder neuen Mut gegeben haben. Dafür bin ich unendlich dankbar.

Ebenso dankbar bin ich meinen Betreuern Dr.-Ing. Stephan Herrmann und Dr.-Ing. Tobias Dirndorfer bei der AUDI AG, die diese Arbeit durch ihren Einsatz dort erst möglich gemacht haben. Durch ihre herausragende Expertise im von der Arbeit behandelten Anwendungsgebiet und ihr kontinuierliches Feedback haben sie viele ganz entscheidende Impulse aus Anwendungssicht gegeben und die Arbeit so in die richtige Richtung gelenkt.

Mein aufrichtiger Dank gilt auch meinem Mentor Apl. Prof. Dr.-Ing. habil. Helmut Gräß. Durch den glücklichen Umstand, dass er aufgrund seiner eigenen wissenschaftlichen Tätigkeit über eine ausgezeichnete Expertise bei auch für diese Dissertation relevanten Methoden verfügt, hat er mich nicht nur als Mentor in überfachlicher, sondern gerade auch in fachlicher Hinsicht unterstützt.

Bedanken möchte ich mich auch bei meinen Kollegen, die immer ein offenes Ohr für mich hatten und so die beste Grundlage für diese Arbeit geschaffen haben, die man sich wünschen kann. Ihre Hilfsbereitschaft und der Zusammenhalt, die ich erfahren durfte, sind einfach toll. An dieser Stelle möchte ich auch alle Studenten dankend erwähnen, mit denen ich arbeiten durfte und die im Rahmen ihrer eigenen Studienarbeiten zu dieser Dissertation beigetragen haben.

Mein Dank richtet sich auch an die Abteilungsleiter Dr.-Ing. Peter Bergmiller, Steffen Fey, Alexander Pesch und Dr.-Ing. Oliver Schlicht bei der AUDI AG. Sie sind dieser Arbeit immer aufgeschlossen gegenüberstanden und haben sie in den entscheidenden Phasen gefördert.

Und schließlich möchte ich mich ganz herzlich bei meiner Familie bedanken, vor allem bei meinen Eltern Michaela und Karl Heinz Stöckle. Sie haben mir durch ihre bedingungslose Liebe und ihr Verständnis immer den Rücken freigehalten, Rückhalt und neue Energie für diese Arbeit gegeben. Dafür bin ich unendlich dankbar.

München, November 2021

Abstract

Active safety functions that intervene in dangerous driving situations the driver is not able to control, e.g., by emergency braking or steering, have great potential to increase automotive safety by reducing the number as well as the severity of collisions. Such automated vehicular safety functions use the measurements of sensors sensing the environment of the vehicle in order to interpret the driving situation and trigger appropriate actions in dangerous driving situations such as emergency brake or steer interventions. As a consequence, they are typically very vulnerable to sensor imperfections and unavoidable measurement errors have a negative impact on both the safety and the satisfaction of the customer, which has to be taken into account when designing automated vehicular safety systems. Nevertheless, there is still no general design methodology with which both sensors and functions for a variety of automated vehicular safety systems can be systematically designed while taking both the unavoidable sensor measurement errors and the customer satisfaction into account.

Therefore, such a methodology for the robust design of automated vehicular safety systems considering unavoidable sensor measurement errors, which aims at designing them such that the customer requirements are fulfilled in a robust manner despite unavoidable sensor measurement errors, is developed in this thesis. To this end, ideas from integrated circuit design, a completely different application area, are transferred to the design of automated vehicular safety systems, which marks a paradigm shift, by exploiting the analogies to the integrated circuit design with a well-established worst-case design approach. In particular, three basic design problems are considered, which application engineers having to select sensors with appropriate properties and to adjust the functions in the development of automated vehicular safety systems are typically confronted with, namely, the function design for given sensors, the sensor design for a given function as well as the joint function and sensor design, which are formulated as optimization problems. Different possibilities for designing both functions and sensors of automated vehicular safety systems by solving the formulated optimization problems solely based on simulations of the automated vehicular safety system under design, which make the developed design methodology applicable to various automated vehicular safety systems, are suggested. Besides the Monte Carlo simulation, which

Abstract

is a straightforward possibility, the worst-case distance approach already applied in the integrated circuit design is considered as an alternative and adapted to the robust design of automated vehicular safety systems. They are compared with respect to the applicability to different automated vehicular safety systems, accuracy and computational complexity.

The developed methodology for the robust design of automated vehicular safety systems considering unavoidable sensor measurement errors is applied to two typical examples for automated vehicular safety systems, namely, an automatic emergency braking (AEB) and an automatic emergency steering (AES) system. The considered numerical examples demonstrate that the adaptation of the worst-case distance approach to the robust design of automated vehicular safety systems can significantly reduce the required number of simulations of the automated vehicular safety system under design by replacing an expensive Monte Carlo simulation requiring a huge number of simulations of the automated vehicular safety system for a comparable accuracy, and with this the computational complexity, the load for simulation servers as well as the time and expenses needed for the development of automated vehicular safety systems.

Contents

List of Figures	xiii
List of Tables	xxi
Acronyms	xxv
List of Symbols	xxvii
1 Introduction	1
1.1 Background and Motivation	1
1.2 Related Work and State of the Art	5
1.3 Contributions of the Thesis	6
1.4 Outline of the Thesis	8
2 System Model for Automated Vehicular Safety Systems	11
2.1 Mathematical Representation of the Driving Scenario	11
2.2 Stochastic Model of the Automated Vehicular Safety System	16
2.2.1 Stochastic Model of the Sensors	16
2.2.2 Mathematical Model of the Automated Vehicular Safety Function	18
3 Robust System Design	21
3.1 Problem Formulation for Robust System Design	21
3.2 Simulation-Based Robust System Design	26
3.2.1 Monte-Carlo-Based Robust System Design	26
3.2.2 Worst-Case-Distance-Based Robust System Design	33
4 Robust Design of Automated Vehicular Safety Systems	47
4.1 Problem Formulation for Robust Design of Automated Vehicular Safety Systems	47
4.1.1 Function Design	47

Contents

4.1.2	Sensor Design	50
4.1.3	Joint Function and Sensor Design	52
4.2	Quality Measure for Robust Design of Automated Vehicular Safety Systems	57
5	Simulation-Based Robust Design of Automated Vehicular Safety Systems	71
5.1	Monte-Carlo-Based Robust Design of Automated Vehicular Safety Systems	72
5.2	Worst-Case-Distance-Based Robust Design of Automated Vehicular Safety Systems	77
5.2.1	Direct Application of Worst-Case Distance Approach to Robust Design of Automated Vehicular Safety Systems	80
5.2.2	Adaptation of Worst-Case Distance Approach to Robust Design of Automated Vehicular Safety Systems	88
6	Robust Design of an Automatic Emergency Braking System	109
6.1	System Model for the Automatic Emergency Braking System	109
6.1.1	Mathematical Representation of the Driving Scenario for the Robust Design of the Automatic Emergency Braking System	110
6.1.2	Stochastic Model of the Automatic Emergency Braking System	117
6.2	Robust Function and Sensor Design for the Automatic Emergency Braking System	121
6.2.1	Probability of Fulfilling the Specification for the Customer Satisfaction in Case of the TTC-Based Decision Rule	123
6.2.2	Probability of Fulfilling the Specification for the Customer Satisfaction in Case of Error-Free Relative Velocity Measurements	128
6.3	Numerical Examples for the Robust Design of the Automatic Emergency Braking System	132
6.3.1	One Driving Scenario, TTC-Based Decision Rule and Error-Free Relative Velocity Measurements	132
6.3.2	Several Driving Scenarios, Set of Decision Rules and Error-Free Relative Velocity Measurements	144
6.3.3	Erroneous Distance and Relative Velocity Measurements	156
7	Robust Design of an Automatic Emergency Steering System	173
7.1	System Model for the Automatic Emergency Steering System	173

7.1.1	Mathematical Representation of the Driving Scenario for the Robust Design of the Automatic Emergency Steering System	174
7.1.2	Stochastic Model of the Automatic Emergency Steering System	179
7.2	Robust Function and Sensor Design for the Automatic Emergency Steering System	181
7.3	Numerical Examples for the Robust Design of the Automatic Emergency Steering System	183
8	Conclusion	191
8.1	Summary	191
8.2	Future Work	195
A	Probability that the Statistical Parameters s Lie in $\hat{\mathcal{A}}_{s,b,i}$	199
B	Properties Implied by Statistical Independence of Sensor Measurement Errors	205
C	Closed-Form Solutions of Differential Equations Describing Vehicle Motion	209
C.1	Vehicle Motion with Constant Longitudinal Acceleration	209
C.2	Vehicle Motion with Constant Lateral Acceleration	211
	Bibliography	215

List of Figures

1.1	The five phases involved in an accident according to the ACEA as well as the relevance of active, passive and tertiary safety in those phases (taken from [4]).	4
1.2	General setting in which an automated vehicular safety function is embedded.	4
2.1	A typical driving scenario.	12
2.2	State of a vehicle at time t	13
2.3	Trajectories of exemplary driving maneuvers of a vehicle with $[x(t_{\text{start}}), y(t_{\text{start}}), v(t_{\text{start}}), \psi(t_{\text{start}})]^T = [0, 0, 20 \frac{\text{m}}{\text{s}}, 0]^T$, $r_{\text{min}} = 5 \text{ m}$ and different inputs a_{lon} and a_{lat} depicted at time instants $t = 0, 0.5 \text{ s}, 1 \text{ s}, 1.5 \text{ s}, 2 \text{ s}$ from $t_{\text{start}} = 0$ (left) to $t_{\text{end}} = 2 \text{ s}$ (right).	15
2.4	General mathematical model of automated vehicular safety systems including sensor measurement errors.	16
3.1	Approximate number $M_{\text{req.}}$ of samples or observations and system simulations in the Monte Carlo simulation required for estimating the probability $Y = 0.99$ of fulfilling the performance specifications with the desired confidence level κ for the corresponding confidence interval $[\hat{Y}_M - \Delta Y, \hat{Y}_M + \Delta Y]$	34
3.2	Exemplary individual parameter acceptance region partition $\mathcal{A}_{s,L,i}$ with a finite lower bound $f_{L,i}$ (green area including orange boundary) and the corresponding approximate individual parameter acceptance region partition $\hat{\mathcal{A}}_{s,L,i}$ defined by the worst-case distance $\beta_{L,i}$ (horizontally striped area including violet linear boundary) for two statistical parameters $\mathbf{s} = [s_1, s_2]^T$	36

LIST OF FIGURES

3.3 Exemplary individual parameter acceptance region partition $\mathcal{A}_{s,U,i}$ with a finite upper bound $f_{U,i}$ (green area including orange boundary) and the corresponding approximate individual parameter acceptance region partition $\hat{\mathcal{A}}_{s,U,i}$ defined by the worst-case distance $\beta_{U,i}$ (vertically striped area including magenta linear boundary) for two statistical parameters $\mathbf{s} = [s_1, s_2]^T$ 37

3.4 Intersection of two exemplary individual parameter acceptance region partitions $\mathcal{A}_{s,L,i}$ with a finite lower bound $f_{L,i}$ and $\mathcal{A}_{s,U,i}$ with a finite upper bound $f_{U,i}$ (green area including orange boundaries) as well as the corresponding approximate individual parameter acceptance region partitions $\hat{\mathcal{A}}_{s,L,i}$ and $\hat{\mathcal{A}}_{s,U,i}$ defined by the worst-case distances $\beta_{L,i}$ and $\beta_{U,i}$ (horizontally and vertically striped areas including violet and magenta linear boundaries, respectively) for two statistical parameters $\mathbf{s} = [s_1, s_2]^T$ 38

4.1 Basic design problems in the development of automated vehicular safety systems. 48

4.2 Function design for the set $\mathcal{F} = \{f_1, f_2, f_3\}$ of decision rules with one adjustable function parameter $\varphi = \varphi \in \mathbb{R}$ 49

4.3 Sensor design for one sensor parameter $\sigma = \sigma \in \mathcal{S} = \mathbb{R}^+$ 51

4.4 Joint function and sensor design for one sensor parameter $\sigma = \sigma \in \mathcal{S} = \mathbb{R}^+$ and the set $\mathcal{F} = \{f_1, f_2, f_3\}$ of decision rules f with one adjustable function parameter $\varphi = \varphi \in \mathbb{R}$, where $f = f_1$, $Q_1 < Q_2 < Q_3 = Q_{\min} < Q_4$ and $C_1 < C_2 < C_3 = C_{\min}(f_1) < C_4 < C_5$ 55

4.5 Joint function and sensor design for one sensor parameter $\sigma = \sigma \in \mathcal{S} = \mathbb{R}^+$ and the set $\mathcal{F} = \{f_1, f_2, f_3\}$ of decision rules f with one adjustable function parameter $\varphi = \varphi \in \mathbb{R}$, where $f = f_2 = f_{\text{opt}}$, $Q_1 < Q_2 < Q_3 = Q_{\min} < Q_4$ and $C_1 < C_2 = C_{\min}(f_2) = C_{\min}^* < C_3 < C_4 < C_5$ 55

4.6 Joint function and sensor design for one sensor parameter $\sigma = \sigma \in \mathcal{S} = \mathbb{R}^+$ and the set $\mathcal{F} = \{f_1, f_2, f_3\}$ of decision rules f with one adjustable function parameter $\varphi = \varphi \in \mathbb{R}$, where $f = f_3$, $Q_1 < Q_2 < Q_3 = Q_{\min} < Q_4$ and $C_1 < C_2 < C_3 < C_4 = C_{\min}(f_3) < C_5$ 56

- 4.7 Design space \mathcal{D} in joint function and sensor design for one sensor parameter $\sigma = \sigma \in \mathcal{S} = \mathbb{R}^+$, the set $\mathcal{F} = \{f_1, f_2, f_3\}$ of decision rules f with one adjustable function parameter $\varphi = \varphi \in \mathbb{R}$ and the scenario set $\mathcal{X} = \{\xi_1, \xi_2, \xi_3, \xi_4\}$, where $f = f_1$ 68
- 4.8 Design space \mathcal{D} in joint function and sensor design for one sensor parameter $\sigma = \sigma \in \mathcal{S} = \mathbb{R}^+$, the set $\mathcal{F} = \{f_1, f_2, f_3\}$ of decision rules f with one adjustable function parameter $\varphi = \varphi \in \mathbb{R}$ and the scenario set $\mathcal{X} = \{\xi_1, \xi_2, \xi_3, \xi_4\}$, where $f = f_2$ 68
- 4.9 Design space \mathcal{D} in joint function and sensor design for one sensor parameter $\sigma = \sigma \in \mathcal{S} = \mathbb{R}^+$, the set $\mathcal{F} = \{f_1, f_2, f_3\}$ of decision rules f with one adjustable function parameter $\varphi = \varphi \in \mathbb{R}$ and the scenario set $\mathcal{X} = \{\xi_1, \xi_2, \xi_3, \xi_4\}$, where $f = f_3$ 69
- 5.1 Exemplary individual error acceptance region partition $\mathcal{A}_{\varepsilon,b,i}$, $b \in \{\text{L}, \text{U}\}$, (green area possibly including dashed orange boundary) with either a finite lower bound $q_{\text{L},i}$ if $b = \text{L}$ or a finite upper bound $q_{\text{U},i}$ if $b = \text{U}$ for $E = 1$ sensor measurement error $\varepsilon[n]$ at a time instant t_n under the assumption that the function must not decide for an intervention based on the sensor measurements $\mathbf{y}[n_1]$ at the time instant t_{n_1} and based on the sensor measurements $\mathbf{y}[n_2]$ at the time instant t_{n_2} using the decision rule $f(\cdot; \varphi)$ such that $q_i \geq q_{\text{L},i}$ if $b = \text{L}$ or $q_i \leq q_{\text{U},i}$ if $b = \text{U}$, and its relationship to the error regions $\bar{\mathcal{I}}_{\varepsilon,n}$ without intervention, where $f(\mathbf{y}[n]; \varphi) = 0$, approximated by the error regions $\hat{\bar{\mathcal{I}}}_{\varepsilon,n}$ corresponding to the worst-case distances β_n (horizontally and vertically striped areas including dashed violet and magenta linear boundaries, respectively) in the plane where $\varepsilon[n] = \mu_n$ for $n \neq n_1, n_2$. 90

LIST OF FIGURES

- 5.2 Exemplary individual error acceptance region partition $\mathcal{A}_{\varepsilon,b,i}$, $b \in \{L, U\}$, (green area possibly including dashed orange boundary) with either a finite lower bound $q_{L,i}$ if $b = L$ or a finite upper bound $q_{U,i}$ if $b = U$ for $E = 1$ sensor measurement error $\varepsilon[n]$ at a time instant t_n under the assumption that the function must decide for an intervention based on the sensor measurements $\mathbf{y}[n_3]$ and $\mathbf{y}[n_4]$ at the time instants t_{n_3} and t_{n_4} at least once using the decision rule $f(\cdot; \varphi)$ such that $q_i \geq q_{L,i}$ if $b = L$ or $q_i \leq q_{U,i}$ if $b = U$, and its relationship to the error regions $\bar{\mathcal{T}}_{\varepsilon,n}$ without intervention, where $f(\mathbf{y}[n]; \varphi) = 0$ and $\boldsymbol{\mu}$ is not included, approximated by the error regions $\hat{\bar{\mathcal{T}}}_{\varepsilon,n}$ corresponding to the worst-case distances β_n (horizontally and vertically striped areas including dashed violet and magenta linear boundaries, respectively) in the plane where $\varepsilon[n] = \mu_n$ for $n \neq n_3, n_4$ 98
- 5.3 Exemplary individual error acceptance region partition $\mathcal{A}_{\varepsilon,b,i}$, $b \in \{L, U\}$, (green area possibly including dashed orange boundary) with either a finite lower bound $q_{L,i}$ if $b = L$ or a finite upper bound $q_{U,i}$ if $b = U$ for $E = 1$ sensor measurement error $\varepsilon[n]$ at a time instant t_n under the assumption that the function must decide for an intervention based on the sensor measurements $\mathbf{y}[n_3]$ and $\mathbf{y}[n_4]$ at the time instants t_{n_3} and t_{n_4} at least once using the decision rule $f(\cdot; \varphi)$ such that $q_i \geq q_{L,i}$ if $b = L$ or $q_i \leq q_{U,i}$ if $b = U$, and its relationship to the error regions $\bar{\mathcal{T}}_{\varepsilon,n}$ without intervention, where $f(\mathbf{y}[n]; \varphi) = 0$ and $\boldsymbol{\mu}$ is partially included, approximated by the error regions $\hat{\bar{\mathcal{T}}}_{\varepsilon,n}$ corresponding to the worst-case distances β_n (horizontally and vertically striped areas including dashed violet and magenta linear boundaries, respectively) in the plane where $\varepsilon[n] = \mu_n$ for $n \neq n_3, n_4$ 99
- 6.1 Driving scenario considered for the robust design of an AEB system at time t 110

- 6.2 Probability that the sensor measurement errors ε lie in the error region $\mathcal{I}_{\varepsilon,n}$ with intervention at the time instant t_n and fulfill the condition for triggering an emergency brake intervention at the time instant t_n for $\sigma_v = 0$, $x_0 = 10$ m, $v_0 = -10 \frac{\text{m}}{\text{s}}$, $f_s = 1$ kHz and the TTC-based decision rule $f_{\text{TTC}}(\cdot; \varphi)$ as well as the lower bound $t_{n_{\min}} = 0.45$ s and the upper bound $t_{n_{\max}} = 0.5$ s of the time interval in which the emergency brake intervention with the constant deceleration $a = 10 \frac{\text{m}}{\text{s}^2}$ has to be triggered to fulfill the specification $0 = x_{\min} \leq x_{\text{end}} \leq x_{\max} = 0.5$ m for the customer satisfaction. 134
- 6.3 Probability that the discrete time index n_b of the time instant $t_b = n_b/f_s$ at which the emergency brake intervention is triggered is the discrete time index n'_b of the time instant $t_{n'_b} = n'_b/f_s$ for $\sigma_v = 0$, $x_0 = 10$ m, $v_0 = -10 \frac{\text{m}}{\text{s}}$, $f_s = 1$ kHz and the TTC-based decision rule $f_{\text{TTC}}(\cdot; \varphi)$ as well as the lower bound $t_{n_{\min}} = 0.45$ s and the upper bound $t_{n_{\max}} = 0.5$ s of the time interval in which the emergency brake intervention with the constant deceleration $a = 10 \frac{\text{m}}{\text{s}^2}$ has to be triggered to fulfill the specification $0 = x_{\min} \leq x_{\text{end}} \leq x_{\max} = 0.5$ m for the customer satisfaction. . . . 135
- 6.4 Probability that the considered AEB system fulfills the specification $x_{\min} \leq x_{\text{end}} \leq x_{\max}$ for the customer satisfaction vs. the function parameter φ (a) and the standard deviation σ_x of the sensor measurement errors in the measured distance (b) for $\sigma_v = 0$, $x_0 = 10$ m, $v_0 = -10 \frac{\text{m}}{\text{s}}$, $f_s = 1$ kHz, $a = 10 \frac{\text{m}}{\text{s}^2}$, $x_{\min} = 0$, $x_{\max} = 0.5$ m and the TTC-based decision rule $f_{\text{TTC}}(\cdot; \varphi)$ with the optimal function parameter value φ_{opt} determined by the function design for $\sigma_x = 0.3$ m and the maximal tolerable standard deviation $\sigma_{x,\text{max}}$ of the sensor measurement errors in the measured distance determined by the sensor design for $\varphi = 0.51$ s and $P_{\min} = 0.99$, respectively. 137

LIST OF FIGURES

6.5 Contour lines of the probability that the considered AEB system fulfills the specification $x_{\min} \leq x_{\text{end}} \leq x_{\max}$ for the customer satisfaction for $\sigma_v = 0$, $x_0 = 10$ m, $v_0 = -10 \frac{\text{m}}{\text{s}}$, $f_s = 1$ kHz, $a = 10 \frac{\text{m}}{\text{s}^2}$, $x_{\min} = 0$, $x_{\max} = 0.5$ m and the TTC-based decision rule $f_{\text{TTC}}(\cdot; \varphi)$ with the optimal function parameter value φ_{opt} and the maximal tolerable standard deviation $\sigma_{x, \max}$ of the sensor measurement errors in the measured distance determined by the joint function and sensor design for $P_{\min} = 0.99$ 138

6.6 Probability that the considered AEB system fulfills the specification $x_{\min} \leq x_{\text{end}} \leq x_{\max}$ for the customer satisfaction for $v_0 = -10 \frac{\text{m}}{\text{s}}$ and $v_0 = -20 \frac{\text{m}}{\text{s}}$ as well as the minimum thereof, i.e., the quality measure Q , vs. the function parameter φ for $\sigma_x = 0.1$ m, $\sigma_v = 0$, $x_0 = 50$ m, $f_s = 1$ kHz, $a = 10 \frac{\text{m}}{\text{s}^2}$, $x_{\min} = 0$, $x_{\max} = 0.5$ m and the TTC-based decision rule $f_{\text{TTC}}(\cdot; \varphi)$ 145

6.7 Probability that the considered AEB system fulfills the specification $x_{\min} \leq x_{\text{end}} \leq x_{\max}$ for the customer satisfaction for $v_0 = -10 \frac{\text{m}}{\text{s}}$ and $v_0 = -20 \frac{\text{m}}{\text{s}}$ as well as the minimum thereof, i.e., the quality measure Q , vs. the function parameter φ for $\sigma_x = 0.1$ m, $\sigma_v = 0$, $x_0 = 50$ m, $f_s = 1$ kHz, $a = 10 \frac{\text{m}}{\text{s}^2}$, $x_{\min} = 0$, $x_{\max} = 0.5$ m and the advanced TTC-based decision rule $f_{\text{adv. TTC}}(\cdot; \varphi)$ with the optimal function parameter value φ_{opt} determined by the function design. 146

6.8 Probability that the considered AEB system fulfills the specification $x_{\min} \leq x_{\text{end}} \leq x_{\max}$ for the customer satisfaction for $v_0 = -10 \frac{\text{m}}{\text{s}}$ and $v_0 = -20 \frac{\text{m}}{\text{s}}$ as well as the minimum thereof, i.e., the quality measure Q , vs. the function parameter φ for $\sigma_x = 0.1$ m, $\sigma_v = 0$, $x_0 = 50$ m, $f_s = 1$ kHz, $a = 10 \frac{\text{m}}{\text{s}^2}$, $x_{\min} = 0$, $x_{\max} = 0.5$ m and the BTN-based decision rule $f_{\text{BTN}}(\cdot; \varphi)$ 147

6.9 Contour lines of the probability that the considered AEB system fulfills the specification $x_{\min} \leq x_{\text{end}} \leq x_{\max}$ for the customer satisfaction for $v_0 = -10 \frac{\text{m}}{\text{s}}$ and $v_0 = -20 \frac{\text{m}}{\text{s}}$ at height 0.99, which are the boundaries of the respective individual design space partitions $\mathcal{D}(\xi_1)$ and $\mathcal{D}(\xi_2)$ in the joint function and sensor design in case of $P_{\min} = 0.99$, for $\sigma_v = 0$, $x_0 = 50$ m, $f_s = 1$ kHz, $a = 10 \frac{\text{m}}{\text{s}^2}$, $x_{\min} = 0$, $x_{\max} = 0.5$ m and the TTC-based decision rule $f_{\text{TTC}}(\cdot; \varphi)$ 150

6.10 Contour lines of the probability that the considered AEB system fulfills the specification $x_{\min} \leq x_{\text{end}} \leq x_{\max}$ for the customer satisfaction for $v_0 = -10 \frac{\text{m}}{\text{s}}$ and $v_0 = -20 \frac{\text{m}}{\text{s}}$ as well as of the minimum thereof, i.e., the quality measure Q , at height 0.99, which are the boundaries of the respective individual design space partitions $\mathcal{D}(\xi_1)$ and $\mathcal{D}(\xi_2)$ and design space \mathcal{D} in the joint function and sensor design in case of $P_{\min} = 0.99$, for $\sigma_v = 0$, $x_0 = 50 \text{ m}$, $f_s = 1 \text{ kHz}$, $a = 10 \frac{\text{m}}{\text{s}^2}$, $x_{\min} = 0$, $x_{\max} = 0.5 \text{ m}$ and the advanced TTC-based decision rule $f_{\text{adv. TTC}}(\cdot; \varphi)$ 151

6.11 Contour lines of the probability that the considered AEB system fulfills the specification $x_{\min} \leq x_{\text{end}} \leq x_{\max}$ for the customer satisfaction for $v_0 = -10 \frac{\text{m}}{\text{s}}$ and $v_0 = -20 \frac{\text{m}}{\text{s}}$ as well as of the minimum thereof, i.e., the quality measure Q , at height 0.99, which are the boundaries of the respective individual design space partitions $\mathcal{D}(\xi_1)$ and $\mathcal{D}(\xi_2)$ and design space \mathcal{D} in the joint function and sensor design in case of $P_{\min} = 0.99$, for $\sigma_v = 0$, $x_0 = 50 \text{ m}$, $f_s = 1 \text{ kHz}$, $a = 10 \frac{\text{m}}{\text{s}^2}$, $x_{\min} = 0$, $x_{\max} = 0.5 \text{ m}$ and the BTN-based decision rule $f_{\text{BTN}}(\cdot; \varphi)$ with the optimal function parameter value φ_{opt} and the maximal tolerable standard deviation $\sigma_{x, \max}$ of the sensor measurement errors in the measured distance determined by the joint function and sensor design in case of $P_{\min} = 0.99$ 152

List of Tables

1.1	Levels of driving automation defined by SAE International standard J3016 (taken from [3]).	2
6.1	Optimal function parameter value φ_{opt} for the considered AEB system determined by the function design for $\sigma_v = 0$, $x_0 = 10$ m, $v_0 = -10 \frac{\text{m}}{\text{s}}$, $f_s = 1$ kHz, $a = 10 \frac{\text{m}}{\text{s}^2}$, $x_{\text{min}} = 0$, $x_{\text{max}} = 0.5$ m, the TTC-based decision rule $f_{\text{TTC}}(\cdot; \varphi)$ and various values of the standard deviation σ_x of the sensor measurement errors in the measured distance as well as the resulting probability $P(x_{\text{min}} \leq x_{\text{end}} \leq x_{\text{max}})$ of fulfilling the specification for the customer satisfaction.	139
6.2	Maximal tolerable standard deviation $\sigma_{x,\text{max}}$ of the sensor measurement errors in the measured distance for the considered AEB system determined by the sensor design for $\sigma_v = 0$, $x_0 = 10$ m, $v_0 = -10 \frac{\text{m}}{\text{s}}$, $f_s = 1$ kHz, $a = 10 \frac{\text{m}}{\text{s}^2}$, $x_{\text{min}} = 0$, $x_{\text{max}} = 0.5$ m, the TTC-based decision rule $f_{\text{TTC}}(\cdot; \varphi)$, $P_{\text{min}} = 0.99$ and various values of the function parameter φ	141
6.3	Probability $P(x_{\text{min}} \leq x_{\text{end}} \leq x_{\text{max}})$ that the considered AEB system fulfills the specification $x_{\text{min}} \leq x_{\text{end}} \leq x_{\text{max}}$ for the customer satisfaction for $x_0 = 10$ m, $v_0 = -10 \frac{\text{m}}{\text{s}}$, $f_s = 1$ kHz, $a = 10 \frac{\text{m}}{\text{s}^2}$, $x_{\text{min}} = 0$, $x_{\text{max}} = 0.5$ m and the TTC-based decision rule $f_{\text{TTC}}(\cdot; \varphi)$	157

6.4 Absolute error $\left| \hat{P}_{10^5}(x_{\min} \leq x_{\text{end}} \leq x_{\max}) - P(x_{\min} \leq x_{\text{end}} \leq x_{\max}) \right|$ between the Monte-Carlo-based estimate $\hat{P}_{10^5}(x_{\min} \leq x_{\text{end}} \leq x_{\max})$ from $M = 10^5$ simulations of the considered AEB system and the actual probability $P(x_{\min} \leq x_{\text{end}} \leq x_{\max})$ of fulfilling the specification $x_{\min} \leq x_{\text{end}} \leq x_{\max}$ for the customer satisfaction for $x_0 = 10$ m, $v_0 = -10 \frac{\text{m}}{\text{s}}$, $f_s = 1$ kHz, $a = 10 \frac{\text{m}}{\text{s}^2}$, $x_{\min} = 0$, $x_{\max} = 0.5$ m and the TTC-based decision rule $f_{\text{TTC}}(\cdot; \varphi)$ 160

6.5 Absolute error $\left| \hat{P}(x_{\min} \leq x_{\text{end}} \leq x_{\max}) - P(x_{\min} \leq x_{\text{end}} \leq x_{\max}) \right|$ between the worst-case-distance-based approximation $\hat{P}(x_{\min} \leq x_{\text{end}} \leq x_{\max})$ and the actual probability $P(x_{\min} \leq x_{\text{end}} \leq x_{\max})$ of fulfilling the specification $x_{\min} \leq x_{\text{end}} \leq x_{\max}$ for the customer satisfaction by the considered AEB system for $x_0 = 10$ m, $v_0 = -10 \frac{\text{m}}{\text{s}}$, $f_s = 1$ kHz, $a = 10 \frac{\text{m}}{\text{s}^2}$, $x_{\min} = 0$, $x_{\max} = 0.5$ m and the TTC-based decision rule $f_{\text{TTC}}(\cdot; \varphi)$ 163

6.6 Absolute error $\left| \hat{P}(x_{\min} \leq x_{\text{end}} \leq x_{\max}) - P(x_{\min} \leq x_{\text{end}} \leq x_{\max}) \right|$ between the worst-case-distance-based approximation $\hat{P}(x_{\min} \leq x_{\text{end}} \leq x_{\max})$ and the actual probability $P(x_{\min} \leq x_{\text{end}} \leq x_{\max})$ of fulfilling the specification $x_{\min} \leq x_{\text{end}} \leq x_{\max}$ for the customer satisfaction by the considered AEB system, i.e., the accurate Monte-Carlo-based estimate $\hat{P}_{10^8}(x_{\min} \leq x_{\text{end}} \leq x_{\max})$ from $M = 10^8$ simulations of the AEB system used as ground truth, for $x_0 = 10$ m, $v_0 = -10 \frac{\text{m}}{\text{s}}$, $f_s = 1$ kHz, $a = 10 \frac{\text{m}}{\text{s}^2}$, $x_{\min} = 0$, $x_{\max} = 0.5$ m and the BTN-based decision rule $f_{\text{BTN}}(\cdot; \varphi)$ 165

6.7 Probability $P(x_{\min} \leq x_{\text{end}} \leq x_{\max})$ that the considered AEB system fulfills the specification $x_{\min} \leq x_{\text{end}} \leq x_{\max}$ for the customer satisfaction, i.e., the accurate Monte-Carlo-based estimate $\hat{P}_{10^8}(x_{\min} \leq x_{\text{end}} \leq x_{\max})$ from $M = 10^8$ simulations of the AEB system used as ground truth, for $x_0 = 10$ m, $v_0 = -10 \frac{\text{m}}{\text{s}}$, $f_s = 1$ kHz, $a = 10 \frac{\text{m}}{\text{s}^2}$, $x_{\min} = 0$, $x_{\max} = 0.5$ m and the BTN-based decision rule $f_{\text{BTN}}(\cdot; \varphi)$ 167

6.8 Absolute error

$\left| \hat{P}_{10^5}(x_{\min} \leq x_{\text{end}} \leq x_{\max}) - P(x_{\min} \leq x_{\text{end}} \leq x_{\max}) \right|$ between
 the Monte-Carlo-based estimate $\hat{P}_{10^5}(x_{\min} \leq x_{\text{end}} \leq x_{\max})$ from
 $M = 10^5$ simulations of the considered AEB system and the actual
 probability $P(x_{\min} \leq x_{\text{end}} \leq x_{\max})$ of fulfilling the specification
 $x_{\min} \leq x_{\text{end}} \leq x_{\max}$ for the customer satisfaction, i.e., the accurate
 Monte-Carlo-based estimate $\hat{P}_{10^8}(x_{\min} \leq x_{\text{end}} \leq x_{\max})$ from
 $M = 10^8$ simulations of the AEB system used as ground truth,
 for $x_0 = 10$ m, $v_0 = -10 \frac{\text{m}}{\text{s}}$, $f_s = 1$ kHz, $a = 10 \frac{\text{m}}{\text{s}^2}$, $x_{\min} = 0$,
 $x_{\max} = 0.5$ m and the BTN-based decision rule $f_{\text{BTN}}(\cdot; \varphi)$ 168

Acronyms

ACC	Adaptive Cruise Control
ACEA	European Automobile Manufacturers Association called Association des Constructeurs Européens d'Automobiles
ADAS	advanced driver assistance system
AEB	automatic emergency braking
AES	automatic emergency steering
BTN	brake-threat-number
cdf	cumulative distribution function
HMI	human-machine interface
i.i.d.	independent and identically distributed
MC	Monte Carlo
MSE	mean squared error
pdf	probability density function
pmf	probability mass function
SAE	Society of Automotive Engineers
TTC	time-to-collision
UT	Unscented Transformation
V2X	vehicle-to-everything

Acronyms

WCD worst-case distance

List of Symbols

\mathbf{A}	some matrix
\mathbf{a}	some vector
$ \mathbf{A} $	elementwise absolute value of a matrix \mathbf{A}
$\partial\mathcal{A}$	boundary of a set \mathcal{A}
$\text{cl}(\mathcal{A})$	closure of a set \mathcal{A}
$\det(\mathbf{A})$	determinant of a matrix \mathbf{A}
$\text{diag}(\mathbf{a})$	diagonal matrix whose diagonal elements are the elements of the vector \mathbf{a}
$\mathbf{A} \odot \mathbf{B}$	Hadamard/elementwise product of matrices \mathbf{A} and \mathbf{B}
\mathbb{N}	set of positive integers
\mathbb{N}_0	set of non-negative integers
n	discrete time index
\mathbb{R}	set of real numbers
\mathbb{R}^+	set of positive real numbers
\mathbb{R}_0^+	set of non-negative real numbers
t	continuous time
$\mathbf{x}[n]$	discrete-time signal
$\mathbf{x}(t)$	continuous-time signal
$\dot{\mathbf{x}}(t)$	derivative $\frac{d}{dt}\mathbf{x}(t)$ of $\mathbf{x}(t)$ with respect to time t

Introduction 1

The first chapter explains the background behind and the motivation for the robust design of sensors and functions¹ considering sensor measurement errors in vehicular safety before it gives an overview of related work representing the state of the art, states the contributions of the thesis and ends with an outline of it.

1.1 Background and Motivation

Currently, the automotive sector faces and is exposed to four disruptive technology-driven trends, namely, electrification, connectivity, diverse mobility and autonomous driving, which have been identified by the study whose results have been published in [1]. While electrification, connectivity and diverse mobility refer to electric vehicles, i.e., vehicles with electric motors, the communication of vehicles with each other, the infrastructure, the cloud or any other entity that may affect them called vehicle-to-everything (V2X) communication and the shift from car ownership to car sharing, respectively, autonomous driving is about self-driving vehicles, which do not need human input for performing the dynamic driving task, and has become a term that is more and more used synonymously with automated driving.

The SAE International standard J3016 of the Society of Automotive Engineers (SAE) published in [2] and summarized in [3] categorizes the driving automation into six levels, which are shown in Table 1.1. The degree of driving automation increases from level 0 to level 5. While the human driver alone performs the driving task in level 0, a driver assistance system executes either steering or acceleration/deceleration in level 1 and one or more driver assistance systems execute both steering and acceleration/deceleration in level 2 for specific driving modes, i.e., types of driving scenarios with characteristic dynamic driving task requirements, e.g., merging on a highway, with the expectation that the human driver performs all remaining aspects of the dynamic driving task. In levels 3 and 4, an automated driving system performs all aspects of the dynamic driving task for specific driving modes with and without the

¹In automotive engineering, the word “function” refers to an application implemented in a vehicle in order to fulfill a particular purpose and is not to be confused with a mathematical function.

SAE Level	Name	Narrative Definition
Human driver monitors the driving environment		
0	No Automation	the full-time performance by the human driver of all aspects of the dynamic driving task, even when enhanced by warning or intervention systems
1	Driver Assistance	the driving mode-specific execution by a driver assistance system of either steering or acceleration/deceleration using information about the driving environment and with the expectation that the human driver performs all remaining aspects of the dynamic driving task
2	Partial Automation	the driving mode-specific execution by one or more driver assistance systems of both steering and acceleration/deceleration using information about the driving environment and with the expectation that the human driver performs all remaining aspects of the dynamic driving task
Automated driving system (“system”) monitors the driving environment		
3	Conditional Automation	the driving mode-specific performance by an automated driving system of all aspects of the dynamic driving task with the expectation that the human driver will respond appropriately to a request to intervene
4	High Automation	the driving mode-specific performance by an automated driving system of all aspects of the dynamic driving task, even if a human driver does not respond appropriately to a request to intervene
5	Full Automation	the full-time performance by an automated driving system of all aspects of the dynamic driving task under all roadway and environmental conditions that can be managed by a human driver

Table 1.1: Levels of driving automation defined by SAE International standard J3016 (taken from [3]).

expectation that the human driver will respond appropriately to a request to intervene, respectively. Finally, level 5 is characterized by the full-time performance of all aspects of the dynamic driving task by an automated driving system under all roadway and environmental conditions that can be managed by a human driver.

Although a lot of research is still required in order to make the vision of full automation come true, several advanced driver assistance systems (ADASs) that perform at least temporarily single aspects of the dynamic driving task are already available. In general, the operation mode of driver assistance systems can be classified by the type of vehicle guidance into three categories [4]. Category A consists of informing functions, which only indirectly affect the vehicle guidance by providing the human driver with information from the environment perception via the human-machine interface (HMI). Typical examples are the traffic sign recognition, which informs the driver about detected traffic signs, e.g., by displaying the current speed limit, and the lane departure warning, which informs the driver about an unintended departure of the current driving lane, e.g., by a vibration of the steering wheel. In contrast to the functions of category A, the continuously automating functions forming category B have direct influence on the vehicle guidance, which comes with a division of the execution of the dynamic driving task among the human driver and the functions while the human driver can always override the functions. Typically, those functions are comfort functions like the Adaptive Cruise Control (ACC), which automatically adapts the velocity of the vehicle to that of the vehicle driving in front of it, and the lane keep assist, which automatically steers to keep the vehicle in the current driving lane. As the functions of category B, the intervening emergency functions forming category C directly influence the vehicle guidance. However, in contrast to the functions of category B, they do this only in near-accident situations that cannot be controlled by the human driver and, as they are superior in these situations, the human driver cannot override them. Typically, those functions are vehicular safety functions like automatic emergency braking (AEB) and automatic emergency steering (AES) functions, whose goal is to automatically brake in front of and evade obstacles, respectively.

Such vehicular safety functions form a part of vehicular safety, where three domains, namely, active, passive and tertiary safety, can be distinguished with respect to the five phases involved in an accident according to the European Automobile Manufacturers Association called Association des Constructeurs Européens d'Automobiles (ACEA) [4]. While active safety is relevant in the first three phases and passive safety in the phases 3 and 4, tertiary safety is relevant in the last phase as illustrated in Figure 1.1. The first phase is normal driving, which ends with the occurrence of a critical situation, which starts the phase of danger. The point of no accident avoidance marks the

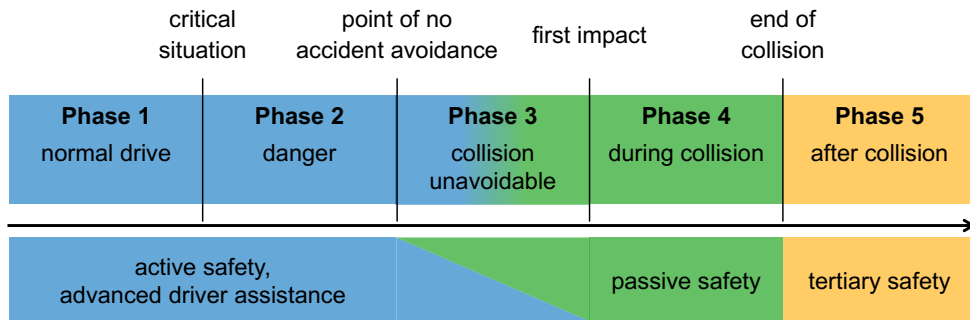


Figure 1.1: The five phases involved in an accident according to the ACEA as well as the relevance of active, passive and tertiary safety in those phases (taken from [4]).

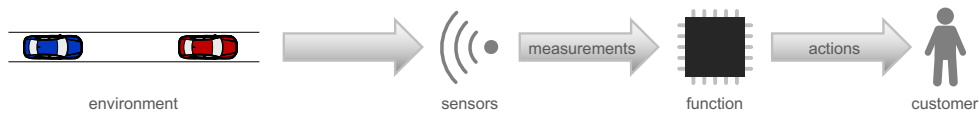


Figure 1.2: General setting in which an automated vehicular safety function is embedded.

transition from this phase to the subsequent phase, in which a collision is unavoidable. This phase is followed by the phase during the collision from the first impact to the end of the collision, which is the beginning of the last phase, namely, the phase after the collision. The goal of active safety is to prevent the occurrence of a critical situation in the first phase, defuse an occurred critical situation in the second phase or reduce the force of the unavoidable impact in the third phase while passive safety aims at protecting the occupants during an unavoidable collision in the phases 3 and 4, e.g., by an airbag. In the last phase after the collision, rescue actions have to be taken, e.g., an emergency call, which is the task of tertiary safety.

Active safety functions that intervene in dangerous driving situations the driver is not able to control like AEB and AES functions have great potential to increase automotive safety by reducing the number as well as the severity of collisions. As depicted in Figure 1.2, such automated vehicular safety functions use the measurements of sensors sensing the environment of the vehicle in order to interpret the driving situation and trigger appropriate actions in dangerous driving situations, e.g., an emergency brake or steer intervention. Consequently, they are typically very vulnerable to sensor imperfections and unavoidable measurement errors have a negative impact on both the safety and the satisfaction of the customer. For example, sensor measurement

errors in AEB and AES systems cause the problem that an emergency brake or steer intervention might not be triggered although it is necessary or, on the contrary, a false alarm might occur. Therefore, these unavoidable sensor measurement errors have to be taken into account.

1.2 Related Work and State of the Art

The following works deal with the uncertainty vehicular safety systems are exposed to as caused by sensor measurement errors and errors in the prediction of the unknown future evolution of a situation, and represent the state of the art. For calculating the collision probability under measurement and prediction uncertainty, [5–10] present Monte-Carlo-based methods whereas [11] replaces the expensive Monte Carlo sampling by the Unscented Transformation (UT) and [12, 13] provide analytical solutions. Collision detection algorithms using the collision probability computed by Monte-Carlo-, UT- and machine-learning-based methods are compared in [14]. [15] presents a criticality measure, which can be used for trajectory planning including collision avoidance in the presence of measurement and prediction errors, and [16] a method for motion planning in automated driving under measurement and prediction uncertainty while [17–19] discuss collision avoidance systems whose decision for an intervention explicitly takes the measurement and prediction uncertainty into account. Methods for identifying the optimal emergency maneuver considering the pedestrian’s injury risk, positioning errors and uncertain future movements are described in [20, 21].

The fusion of data from different sensors in autonomous vehicles requires accurate estimates of the location uncertainty resulting from the sensor measurement errors to achieve a high fusion accuracy. Therefore, [22] tackles the problem of predicting the location uncertainty in form of covariance matrices based on a neural network.

Based on Monte Carlo simulations, [23] investigates the effect of sensor measurement errors on the uncertainty of collision warning criteria used in collision warning systems, [24] examines their impact on the performance of a situation assessment algorithm for a collision prevention assistant and [25] analyzes their influence on the accuracy of predicted collision parameters like the time-to-collision (TTC) used in predictive passive safety systems. The authors of [11] use the UT also for computing the probability distribution of the TTC under measurement uncertainty in [26]. Closed-form expressions for the probability distributions of criticality measures used in ADASs like the TTC, which are subject to the uncertainty in the prediction of the future evolution of a situation and sensor measurement errors, are derived in [27]. The framework presented there is applied in [28] in order to analyze the impact of predic-

tion uncertainty and sensor measurement errors on the performance of AEB systems. While closed-form expressions for the worst-case performance of a collision avoidance system in the presence of prediction and measurement errors are derived in [29], [30] presents a statistical analysis of the vehicle motion estimation from features in the environment under the influence of sensor measurement errors using closed-form expressions and [31] obtains analytical results for the relationship between sensor measurement errors and the resulting errors in the pose of the vehicle determined by odometry.

A methodology for setting the parameters of rear-end collision warning and avoidance algorithms based on statistical performance metrics that allow to take the uncertainty caused by erroneous sensor measurements of the current state in the driving scenario and predictions of the unknown future development of the state into account is proposed by the authors of [32]. In [33], a measure for the robustness of decision functions used in active safety systems for deciding on interventions to sensor measurement errors is introduced, which can also help to derive requirements for the errors and tune the decision functions, i.e., adjust the values of their parameters. [34] uses analytic statistical modeling for the analysis of object detection with stereo vision for collision warning, which makes it possible to predict the uncertainty in object location and obtain optimal thresholds in the presence of measurement errors. In [35, 36], sensor parameters are derived from requirements for the vehicle localization accuracy based on a probabilistic model taking sensor measurement errors into account. However, there is still no general design methodology with which both sensors and functions for a variety of automated vehicular safety systems can be systematically designed while taking both the unavoidable sensor measurement errors and the customer satisfaction into account in contrast to other areas of engineering science, e.g., civil and mechanical engineering as well as integrated circuit design, where general design procedures were introduced early on to deal with unavoidable parameter tolerances and deficiencies as well as their influence on the system performance [37–43].

1.3 Contributions of the Thesis

In this thesis, a new methodology for the robust design of automated vehicular safety systems considering unavoidable sensor measurement errors, which aims at designing them such that the customer requirements are fulfilled in a robust manner despite unavoidable sensor measurement errors, is developed. To this end, ideas from integrated circuit design, a completely different application area, are transferred to the design of automated vehicular safety systems, which marks a paradigm shift, by exploiting the

analogies to the integrated circuit design with the well-established worst-case design approach presented in [39–43]. The result is the first general design methodology with which both sensors and functions for a variety of automated vehicular safety systems can be systematically designed while taking both the unavoidable sensor measurement errors and the customer satisfaction into account.

In particular, three basic design problems are considered, which application engineers having to select sensors with appropriate properties and to adjust the functions in the development of automated vehicular safety systems are typically confronted with, namely, the function design for given sensors, the sensor design for a given function as well as the joint function and sensor design. Each of these three basic design problems is formulated as an optimization problem, whose solution yields the optimal sensor parameter values, the best decision rule for triggering the respective action by the function and the optimal function parameter values of the automated vehicular safety system under design with respect to a quality measure that is defined to measure to what extent the function meets the customer requirements in a robust manner despite the unavoidable sensor measurement errors. Moreover, application engineers are provided with design spaces that represent the requirements the sensors have to fulfill such that the customer requirements are met in a robust manner despite the unavoidable sensor measurement errors to the desired extent, which is of particular importance for the overall design task in an industrial environment. The solution of the optimization problems formulated for the sensor as well as joint function and sensor design minimizes the costs inside the design spaces such that the customer requirements are met in a robust manner despite the unavoidable sensor measurement errors to the desired extent at minimal costs.

Different possibilities for a simulation-based evaluation of the quality measure are suggested, which allows to design both functions and sensors of automated vehicular safety systems by solving the formulated optimization problems solely based on simulations of the automated vehicular safety system under design and makes the developed design methodology applicable to various automated vehicular safety systems. Besides the Monte Carlo simulation, which is a straightforward possibility, the worst-case distance approach already applied in the integrated circuit design is considered as an alternative and adapted to the robust design of automated vehicular safety systems. They are compared with respect to the applicability to different automated vehicular safety systems, accuracy and computational complexity.

The developed methodology for the robust design of automated vehicular safety systems considering unavoidable sensor measurement errors is applied to two typical examples for automated vehicular safety systems, namely, an AEB and an AES system,

which, in part, has already been published in [44–46] for the AEB system and in [47] for the AES system. These application examples provide a complete picture of the system model, the formulation of the design problems at hand as optimization problems using the proposed design methodology and their solution based on closed-form expressions for the quality measure or solely based on simulations of the AEB or AES system under design without the need for deriving closed-form expressions for the quality measure. Deriving such closed-form expressions would also not be viable for the complex automated vehicular safety systems in practice and therefore the developers of such systems have to resort to a simulation-based design. In particular, the model of the AEB system has been kept as simple as possible in order to illustrate the basic principle of the design methodology and allow for the derivation of results in closed form at several points for an accurate evaluation of the design methodology. The considered numerical examples demonstrate that the adaptation of the worst-case distance approach to the robust design of automated vehicular safety systems can significantly reduce the required number of simulations of the automated vehicular safety system under design by replacing an expensive Monte Carlo simulation requiring a huge number of simulations of the automated vehicular safety system for a comparable accuracy, and with this the computational complexity, the load for simulation servers as well as the time and expenses needed for the development of automated vehicular safety systems.

A tutorial-style explanation of how the ideas from the integrated circuit design can be transferred to the design of automated vehicular safety systems and the resulting methodology allows to systematically design both functions and sensors such that the customer requirements are fulfilled in a robust manner despite unavoidable sensor measurement errors can be found in [48].

1.4 Outline of the Thesis

After introducing the system model in Chapter 2, Chapter 3 gives a general overview of a robust system design as performed in integrated circuit design. Based on this, the proposed methodology for the robust design of automated vehicular safety systems considering unavoidable sensor measurement errors is developed by formulating the design tasks at hand as optimization problems and defining the used quality measure in Chapter 4 while Chapter 5 deals with the simulation-based evaluation of this quality measure for the design of automated vehicular safety systems solely based on simulations of the automated vehicular safety system under design. The developed design methodology is applied to the robust design of an AEB system and an AES system in Chapter 6 and Chapter 7, respectively. Finally, Chapter 8 concludes the thesis with a

1.4 Outline of the Thesis

summary and an outline of possible future work.

System Model for Automated Vehicular Safety Systems 2

Formulating the robust function and sensor design considering sensor measurement errors for automated vehicular safety systems as optimization problems, which allow for a systematic solution of the design problems, requires a mathematical model of the overall system. This system model can be split into a mathematical representation of the considered driving scenario in which the automated vehicular safety system is applied and a stochastic model of the automated vehicular safety system itself including sensor measurement errors.

2.1 Mathematical Representation of the Driving Scenario

As illustrated in Figure 2.1, a driving scenario consists of the ego vehicle, which is equipped with the automated vehicular safety system under consideration, and one or more standing or moving objects, which might be other road users like other vehicles, motorcycles, bicycles and pedestrians or obstacles on the road, e.g., building material deposited at construction sites. The objects considered in this thesis are vehicles, and the motion of each vehicle in general and the ego vehicle in particular during a driving maneuver is described by the following system of differential equations for curvilinear motion from [49]:

$$\dot{x}(t) = v(t) \cos(\psi(t)), \quad (2.1)$$

$$\dot{y}(t) = v(t) \sin(\psi(t)), \quad (2.2)$$

$$\dot{v}(t) = a_{\text{lon}}, \quad (2.3)$$

$$\dot{\psi}(t) = \min\left(\frac{a_{\text{lat}}}{v(t)}, \frac{v(t)}{r_{\text{min}}}\right). \quad (2.4)$$

In this motion model, which is an extension of the standard curvilinear motion model stated in [50] by the turn radius r_{min} of the vehicle, the state of the vehicle at time t is represented by the state vector $[x(t), y(t), v(t), \psi(t)]^T$ consisting of four state

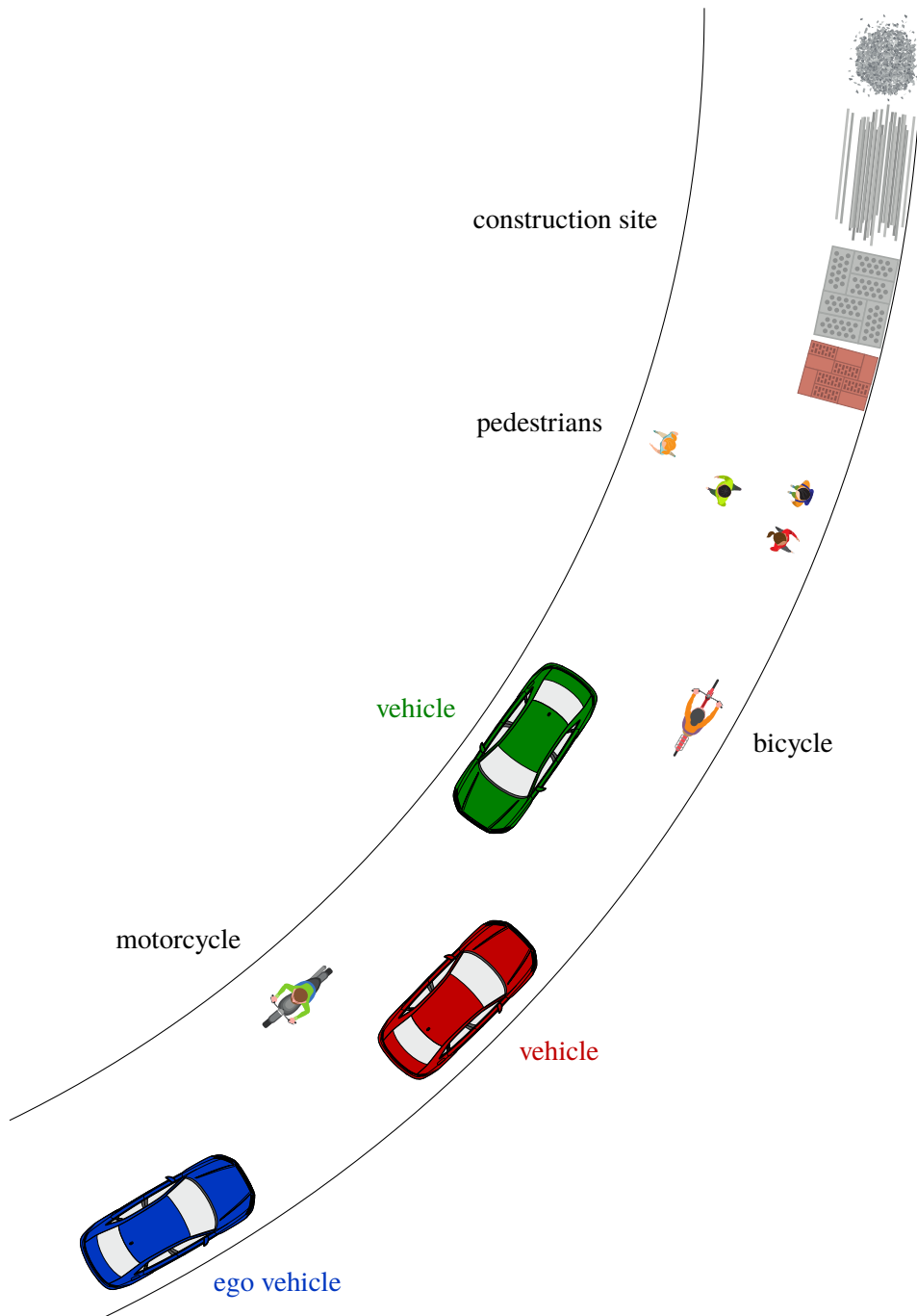


Figure 2.1: A typical driving scenario.

2.1 Mathematical Representation of the Driving Scenario

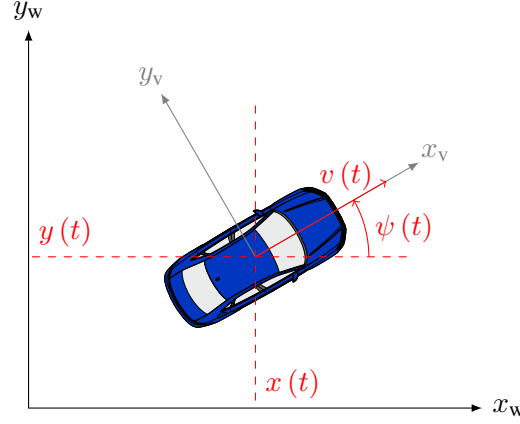


Figure 2.2: State of a vehicle at time t .

variables, which are the coordinates $x(t)$ and $y(t)$ of its center of gravity with respect to the x_w - and y_w -axis of a world coordinate system determining its position, its longitudinal velocity $v(t)$ and its yaw angle $\psi(t)$ with respect to the world coordinate system at time t as visualized in Figure 2.2. Furthermore, a_{lon} and a_{lat} are the longitudinal and the lateral acceleration, respectively.

Solving the system of differential equations for a given initial state $[x(t_{start}), y(t_{start}), v(t_{start}), \psi(t_{start})]^T$ of the vehicle at the beginning of the driving maneuver starting at time t_{start} and ending at time t_{end} yields the trajectory during the driving maneuver given by the function

$$[t_{start}, t_{end}] \rightarrow \mathbb{R}^4, t \mapsto \begin{bmatrix} x(t) \\ y(t) \\ v(t) \\ \psi(t) \end{bmatrix}, \quad (2.5)$$

i.e., the sequence of states $[x(t), y(t), v(t), \psi(t)]^T$ for the time t in the time interval $[t_{start}, t_{end}]$. Apart from special cases where a closed-form solution exists, the system of differential equations has to be solved numerically as that of more complex motion models like the single- and twin-track motion models (see, e.g., [51]), which can easily be used instead of the curvilinear motion model considered in this thesis for increased model accuracy.

Once the trajectory for the time interval $[t_{start}, t_{end}]$ is known, the state $[x(t), y(t), v(t), \psi(t)]^T$ of the vehicle at time $t \in [t_{start}, t_{end}]$ completely determines the position of all points of its contour at time t . The contour is represented by a sequence of

points and each point is defined by its time-independent coordinates in the vehicle coordinate system whose x_v - and y_v -axis are aligned with the longitudinal and lateral axis of the vehicle, respectively, and whose origin is fixed at its center of gravity as visualized in Figure 2.2. If a point of the contour has the coordinates (x_v, y_v) in the vehicle coordinate system of the vehicle with the state $[x(t), y(t), v(t), \psi(t)]^T$ at time t , its coordinates $(x_w(t), y_w(t))$ in the world coordinate system are given by the coordinate transformation

$$\begin{bmatrix} x_w(t) \\ y_w(t) \end{bmatrix} = \begin{bmatrix} \cos(\psi(t)) & -\sin(\psi(t)) \\ \sin(\psi(t)) & \cos(\psi(t)) \end{bmatrix} \begin{bmatrix} x_v \\ y_v \end{bmatrix} + \begin{bmatrix} x(t) \\ y(t) \end{bmatrix} \quad (2.6)$$

from coordinates in the vehicle coordinate system to coordinates in the world coordinate system.

Hence, each driving maneuver of a vehicle starting at time $t_{\text{start}} \geq t_0$ and ending at time $t_{\text{end}} \geq t_{\text{start}}$ in the considered driving scenario starting at time t_0 is completely characterized by the initial state $[x(t_{\text{start}}), y(t_{\text{start}}), v(t_{\text{start}}), \psi(t_{\text{start}})]^T$ of the vehicle at the beginning of the driving maneuver, the longitudinal and the lateral acceleration a_{lon} and a_{lat} , respectively, as well as the turn radius r_{min} of the vehicle. The trajectories of exemplary driving maneuvers with $[x(t_{\text{start}}), y(t_{\text{start}}), v(t_{\text{start}}), \psi(t_{\text{start}})]^T = [0, 0, 20 \frac{\text{m}}{\text{s}}, 0]^T$, $r_{\text{min}} = 5 \text{ m}$ and the three different inputs $a_{\text{lon}} = -5 \frac{\text{m}}{\text{s}^2}$ and $a_{\text{lat}} = 0$, $a_{\text{lon}} = 0$ and $a_{\text{lat}} = 5 \frac{\text{m}}{\text{s}^2}$ as well as $a_{\text{lon}} = -5 \frac{\text{m}}{\text{s}^2}$ and $a_{\text{lat}} = 5 \frac{\text{m}}{\text{s}^2}$ are depicted in Figure 2.3 at time instants $t = 0, 0.5 \text{ s}, 1 \text{ s}, 1.5 \text{ s}, 2 \text{ s}$ from $t_{\text{start}} = 0$ to $t_{\text{end}} = 2 \text{ s}$. Assuming that the final state of each involved vehicle in the considered driving scenario at the end of a driving maneuver is its initial state at the beginning of the subsequent driving maneuver, the state of the whole dynamic system at time t can be described by N state variables collected in the state vector $\mathbf{x}(t) \in \mathbb{R}^N$, which are the state variables of the involved vehicles at this time instant or combinations thereof that are relevant for the considered automated vehicular safety system, and the whole considered driving scenario, to which the considered automated vehicular safety system is exposed, can be represented by N_ξ scenario parameters collected in the vector $\boldsymbol{\xi} \in \mathbb{R}^{N_\xi}$, which are the elements of the initial state vector $\mathbf{x}_0 = \mathbf{x}(t_0)$ of the dynamic system at the beginning of the driving scenario, the time instants at which driving maneuvers of the involved vehicles not initiated by the automated vehicular safety system start, their longitudinal and lateral accelerations during these driving maneuvers, their turn radii as well as the coordinates of the points sufficiently describing their contours in the vehicle coordinate systems.

2.1 Mathematical Representation of the Driving Scenario

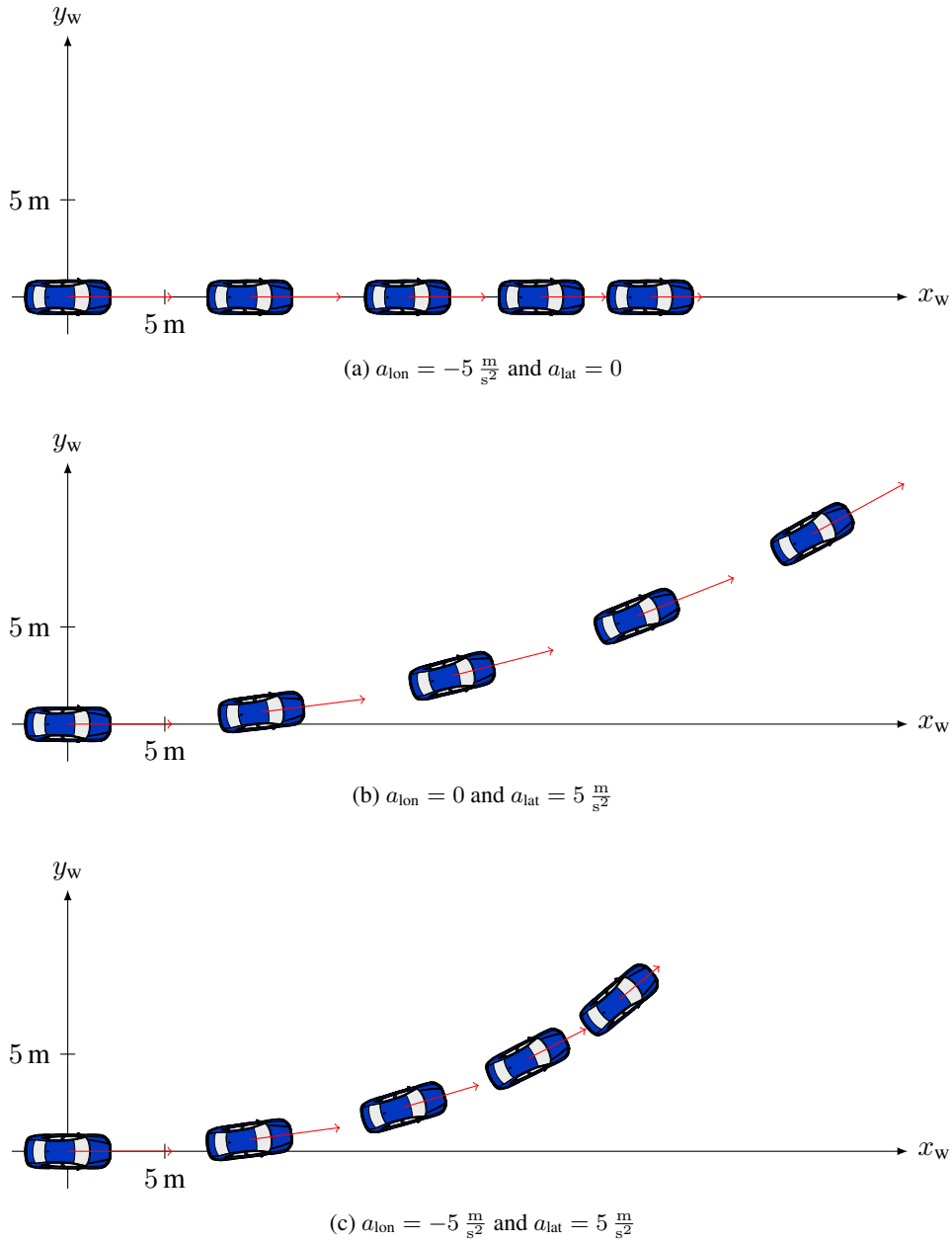


Figure 2.3: Trajectories of exemplary driving maneuvers of a vehicle with $[x(t_{\text{start}}), y(t_{\text{start}}), v(t_{\text{start}}), \psi(t_{\text{start}})]^T = [0, 0, 20 \frac{\text{m}}{\text{s}}, 0]^T$, $r_{\text{min}} = 5 \text{ m}$ and different inputs a_{lon} and a_{lat} depicted at time instants $t = 0, 0.5 \text{ s}, 1 \text{ s}, 1.5 \text{ s}, 2 \text{ s}$ from $t_{\text{start}} = 0$ (left) to $t_{\text{end}} = 2 \text{ s}$ (right).

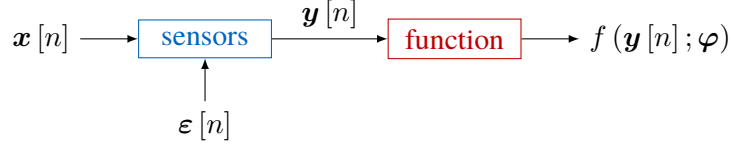


Figure 2.4: General mathematical model of automated vehicular safety systems including sensor measurement errors.

2.2 Stochastic Model of the Automated Vehicular Safety System

A general mathematical model of automated vehicular safety systems including sensor measurement errors is depicted in Figure 2.4. It consists of a stochastic model of the sensors including their measurement errors and a mathematical model of the automated vehicular safety function.

2.2.1 Stochastic Model of the Sensors

The sensors take measurements with a sampling rate f_s at time instants

$$t_n = \frac{n}{f_s} \quad (2.7)$$

with the discrete time index $n = 0, 1, \dots$ and deliver the measurement vector $\mathbf{y}[n] \in \mathbb{R}^M$ consisting of the measurements of M quantities observed by the sensors at the time instant t_n based on the state $\mathbf{x}[n] = \mathbf{x}(t_n)$ of the dynamic system at the time instant t_n under the influence of E measurement errors made by the sensors at the time instant t_n , which are collected in the error vector $\boldsymbol{\varepsilon}[n] \in \mathbb{R}^E$. Consequently, the measurements $\mathbf{y}[n]$ are a function of the state $\mathbf{x}[n]$ and the measurement errors $\boldsymbol{\varepsilon}[n]$:

$$\mathbf{y} : \mathbb{R}^N \times \mathbb{R}^E \rightarrow \mathbb{R}^M, (\mathbf{x}[n], \boldsymbol{\varepsilon}[n]) \mapsto \mathbf{y}[n] = \mathbf{y}(\mathbf{x}[n], \boldsymbol{\varepsilon}[n]). \quad (2.8)$$

In the special case of directly measuring the $N = M$ state variables $\mathbf{x}[n]$ with $E = M$ additive measurement errors $\boldsymbol{\varepsilon}[n]$ at the time instant t_n , for example, this function is the sum of the state $\mathbf{x}[n]$ and the measurement errors $\boldsymbol{\varepsilon}[n]$, i.e.,

$$\mathbf{y}[n] = \mathbf{y}(\mathbf{x}[n], \boldsymbol{\varepsilon}[n]) = \mathbf{x}[n] + \boldsymbol{\varepsilon}[n]. \quad (2.9)$$

The unavoidable sensor measurement errors $\boldsymbol{\varepsilon}[n]$ are modeled as random variables forming a discrete-time stochastic process $\{\boldsymbol{\varepsilon}[n] : n \in \mathbb{N}_0\}$ where the measurement errors $\boldsymbol{\varepsilon}[n_1]$ and $\boldsymbol{\varepsilon}[n_2]$ at different time instants t_{n_1} and t_{n_2} , $n_1, n_2 \in \mathbb{N}_0, n_1 \neq n_2$,

are assumed to be statistically independent. Furthermore, the measurement errors $\varepsilon [n]$ at the time instant t_n are assumed to be Gaussian and follow the normal distribution with mean $\boldsymbol{\mu}_n \in \mathbb{R}^E$ and covariance matrix $\mathbf{C}_n \in \mathbb{R}^{E \times E}$, i.e., $\varepsilon [n] \sim \mathcal{N}(\boldsymbol{\mu}_n, \mathbf{C}_n)$ has the probability density function (pdf)

$$f_{\varepsilon[n]}(\varepsilon [n]) = \frac{1}{\sqrt{(2\pi)^E \det(\mathbf{C}_n)}} \exp\left(-\frac{1}{2}(\varepsilon [n] - \boldsymbol{\mu}_n)^T \mathbf{C}_n^{-1} (\varepsilon [n] - \boldsymbol{\mu}_n)\right), \quad (2.10)$$

where the mean $\boldsymbol{\mu}_n$ and the covariance matrix \mathbf{C}_n might depend on the state $\mathbf{x} [n]$ and thus on the time instant t_n . The dependence of the mean $\boldsymbol{\mu}_n$ and the covariance matrix \mathbf{C}_n on the state $\mathbf{x} [n]$ is represented by the functions

$$\boldsymbol{\mu}(\cdot; \boldsymbol{\sigma}_\mu) : \mathbb{R}^N \rightarrow \mathbb{R}^E, \mathbf{x} [n] \mapsto \boldsymbol{\mu}_n = \boldsymbol{\mu}(\mathbf{x} [n]; \boldsymbol{\sigma}_\mu) \quad (2.11)$$

parameterized by the parameter vector $\boldsymbol{\sigma}_\mu \in \mathbb{R}^{N_\mu}$ consisting of N_μ parameters depending on the choice of the sensors and

$$\mathbf{C}(\cdot; \boldsymbol{\sigma}_C) : \mathbb{R}^N \rightarrow \mathbb{R}^{E \times E}, \mathbf{x} [n] \mapsto \mathbf{C}_n = \mathbf{C}(\mathbf{x} [n]; \boldsymbol{\sigma}_C) \quad (2.12)$$

parameterized by the parameter vector $\boldsymbol{\sigma}_C \in \mathbb{R}^{N_C}$ consisting of N_C parameters depending on the choice of the sensors too, respectively. Systematic sensor measurement errors, which might result from a wrong calibration of the sensors for example, can be incorporated in form of a non-zero mean $\boldsymbol{\mu}_n$ of the sensor measurement errors $\varepsilon [n]$ whereas $\boldsymbol{\mu}_n = \mathbf{0}$ holds in the absence of any systematic sensor measurement errors. An example for a state-dependent and thus time-dependent covariance matrix of the sensor measurement errors is

$$\mathbf{C}_n = \mathbf{C}(\mathbf{x} [n]; \boldsymbol{\sigma}_C) = \text{diag}(|\mathbf{x} [n]| \odot \boldsymbol{\sigma}_C) \quad (2.13)$$

in the special case of $E = M$ additive measurement errors $\varepsilon [n]$ when directly measuring the $N = M$ state variables $\mathbf{x} [n]$ at the time instant t_n according to (2.9). As it is a diagonal matrix, the sensor measurement errors $\varepsilon [n]$ at the time instant t_n are uncorrelated and statistically independent. Its i -th diagonal element, the variance of the i -th of the sensor measurement errors $\varepsilon [n]$ at the time instant t_n , is the product between the absolute value of the i -th of the state variables $\mathbf{x} [n]$ at the time instant t_n and the i -th of the parameters $\boldsymbol{\sigma}_C \in (\mathbb{R}^+)^E$, and increases with increasing absolute value of the respective state variable that is measured. With increasing parameters $\boldsymbol{\sigma}_C$, the variances also increase. Hence, the parameters $\boldsymbol{\sigma}_C$ can be interpreted as a relative measure for the measurement accuracy of the sensors with respect to the absolute values of the state variables $\mathbf{x} [n]$.

In certain scenarios, the assumption of Gaussian sensor measurement errors $\varepsilon [n]$ might be justified [23] and their Gaussian covariance matrix C_n could also result from signal processing with a filter like the Extended Kalman Filter [5]. Even if this Gaussian assumption is not justified, one can still proceed with the Gaussian random variables $\varepsilon [n]$, which can be considered as a kind of virtual sensor measurement errors, as they can be transformed by an appropriate function

$$\mathbf{T} : \mathbb{R}^E \rightarrow \mathbb{R}^{E'}, \varepsilon [n] \mapsto \varepsilon' [n] = \mathbf{T} (\varepsilon [n]) \quad (2.14)$$

to random variables $\varepsilon' [n]$ with a different probability distribution modeling the actual sensor measurement errors and this transformation can be considered to be part of the sensors. If the function

$$\mathbf{y}' : \mathbb{R}^N \times \mathbb{R}^{E'} \rightarrow \mathbb{R}^M, (\mathbf{x} [n], \varepsilon' [n]) \mapsto \mathbf{y} [n] = \mathbf{y}' (\mathbf{x} [n], \varepsilon' [n]) \quad (2.15)$$

maps the actual sensor measurement errors $\varepsilon' [n]$ together with the state $\mathbf{x} [n]$ to the measurements $\mathbf{y} [n]$ at the time instant t_n as the function \mathbf{y} in (2.8) maps the virtual sensor measurement errors $\varepsilon [n]$ together with the state $\mathbf{x} [n]$ to the measurements $\mathbf{y} [n]$ at the time instant t_n , the latter can be expressed as

$$\mathbf{y} (\mathbf{x} [n], \varepsilon [n]) = \mathbf{y}' (\mathbf{x} [n], \varepsilon' [n]) = \mathbf{y}' (\mathbf{x} [n], \mathbf{T} (\varepsilon [n])), \quad (2.16)$$

where the transformation \mathbf{T} from virtual to actual sensor measurement errors is embedded.

In this stochastic model of the sensors, the sensors are determined by the $N_\sigma = N_\mu + N_C + 1$ sensor parameters collected in the vector

$$\boldsymbol{\sigma} = \begin{bmatrix} \boldsymbol{\sigma}_\mu \\ \boldsymbol{\sigma}_C \\ f_s \end{bmatrix} \in \mathbb{R}^{N_\sigma}, \quad (2.17)$$

namely, the N_μ parameters $\boldsymbol{\sigma}_\mu$ and the N_C parameters $\boldsymbol{\sigma}_C$ of the mean and the covariance of their measurement errors, respectively, as well as their sampling rate f_s , which describe their properties.

2.2.2 Mathematical Model of the Automated Vehicular Safety Function

The automated vehicular safety function derives safety-relevant information from the sensor measurements $\mathbf{y} [n]$ at the time instant t_n in order to interpret the current driving situation and uses a decision rule in order to decide on whether to intervene by

triggering an appropriate action for mitigating a dangerous driving situation, e.g., an emergency brake or steer intervention. Such a decision rule can be represented by a decision function

$$f(\cdot; \boldsymbol{\varphi}) : \mathbb{R}^M \rightarrow \{0, 1\}, \mathbf{y}[n] \mapsto f(\mathbf{y}[n]; \boldsymbol{\varphi}) \quad (2.18)$$

parameterized by the parameter vector $\boldsymbol{\varphi} = [\varphi_1, \varphi_2, \dots, \varphi_{N_\varphi}]^T \in \mathbb{R}^{N_\varphi}$ consisting of N_φ adjustable parameters $\varphi_i, i = 1, 2, \dots, N_\varphi$. It maps the measurements $\mathbf{y}[n]$ to the function value $f(\mathbf{y}[n]; \boldsymbol{\varphi})$, which can only be 0 or 1. As long as the decision rule is not fulfilled, i.e., $f(\mathbf{y}[n]; \boldsymbol{\varphi}) = 0$, the function does not trigger the respective action, and, as soon as the decision rule is fulfilled for the measurements $\mathbf{y}[n]$ at a time instant t_n , i.e., $f(\mathbf{y}[n]; \boldsymbol{\varphi}) = 1$, the function triggers the respective action. The smallest n for which $f(\mathbf{y}[n]; \boldsymbol{\varphi}) = 1$ is the discrete time index

$$n_d = \min_{n \in \mathbb{N}_0} n \quad \text{s.t.} \quad f(\mathbf{y}[n]; \boldsymbol{\varphi}) = 1 \quad (2.19)$$

that corresponds to the time instant

$$t_d = t_{n_d} = \frac{n_d}{f_s} \quad (2.20)$$

at which the measurements $\mathbf{y}[n_d]$ leading to triggering the action are made. The time that elapses between this time instant t_d and the time instant

$$t_a = t_d + \delta = \frac{n_d}{f_s} + \delta \quad (2.21)$$

at which the triggered action starts due to latencies, e.g., caused by evaluating the decision rule, is captured by a fixed delay $\delta \in \mathbb{R}_0^+$.

Once an action is triggered by the function, this intervention is performed automatically such that the driver does not have any control over it as it is assumed that the driver cannot handle the detected dangerous driving situation alone. In this mathematical model of the automated vehicular safety function, the function is determined by the N_φ adjustable parameters $\boldsymbol{\varphi}$ of its decision rule.

Robust System Design 3

In other areas of engineering science, e.g., civil and mechanical engineering as well as integrated circuit design, general design procedures were introduced early on to deal with unavoidable parameter tolerances and deficiencies as well as their influence on the system performance [37–43]. Due to several analogies, the well-established worst-case design approach applied to integrated circuits in [39–43] is of particular interest for the robust design of automated vehicular safety systems considering sensor measurement errors and helps to formulate it as optimization problems based on the mathematical model for automated vehicular safety systems introduced in the previous chapter. Before formulating these optimization problems in the next chapter, this chapter gives a general overview of such a robust system design in order to understand how it can be transferred to the robust design of automated vehicular safety systems.

3.1 Problem Formulation for Robust System Design

The system performance is measured in terms of N_f performance properties f_i , $i = 1, 2, \dots, N_f$, collected in the performance vector $\mathbf{f} = [f_1, f_2, \dots, f_{N_f}]^T \in \mathbb{R}^{N_f}$. These performance properties \mathbf{f} are quantities of interest that have to lie in certain acceptance intervals such that the system is considered to operate in a proper or acceptable way, e.g., the minimum output voltage of an integrated circuit. The acceptance interval for the i^{th} performance property f_i is denoted as $[f_{L,i}, f_{U,i}]$ with the lower and upper bound $f_{L,i}$ and $f_{U,i}$, respectively. If a lower bound $f_{L,i}$ does not exist, $f_{L,i} \rightarrow -\infty$, and if an upper bound $f_{U,i}$ does not exist, $f_{U,i} \rightarrow \infty$. Hence, the performance acceptance region can be expressed as

$$\mathcal{A}_{\mathbf{f}} = \{ \mathbf{f} \in \mathbb{R}^{N_f} : f_{L,i} \leq f_i \leq f_{U,i}, i = 1, 2, \dots, N_f \}. \quad (3.1)$$

It is the set of all values of the performance properties \mathbf{f} that lie in the acceptance intervals and can thus be represented by the intersection of the individual performance acceptance region partitions

$$\mathcal{A}_{\mathbf{f},L,i} = \{ \mathbf{f} \in \mathbb{R}^{N_f} : f_i \geq f_{L,i} \} \text{ and } \mathcal{A}_{\mathbf{f},U,i} = \{ \mathbf{f} \in \mathbb{R}^{N_f} : f_i \leq f_{U,i} \}, \quad (3.2)$$

in the i^{th} of which only the i^{th} performance property f_i is restricted to not lie below the lower bound $f_{L,i}$ and above the upper bound $f_{U,i}$ of the corresponding acceptance interval $[f_{L,i}, f_{U,i}]$, respectively:

$$\mathcal{A}_f = \bigcap_{i=1}^{N_f} \mathcal{A}_{f,L,i} \cap \mathcal{A}_{f,U,i}. \quad (3.3)$$

In the special cases $f_{L,i} \rightarrow -\infty$ and $f_{U,i} \rightarrow \infty$, the corresponding individual performance acceptance region partitions simplify to $\mathcal{A}_{f,L,i} = \mathbb{R}^{N_f}$ and $\mathcal{A}_{f,U,i} = \mathbb{R}^{N_f}$, respectively.

The performance properties \mathbf{f} are dependent on N_p parameters p_j , $j = 1, 2, \dots, N_p$, of the system collected in the parameter vector $\mathbf{p} = [p_1, p_2, \dots, p_{N_p}]^T \in \mathbb{R}^{N_p}$, e.g., the oxide thickness, the length and the width of transistors in an integrated circuit, and thus a function of them:

$$\mathbf{f} : \mathbb{R}^{N_p} \rightarrow \mathbb{R}^{N_f}, \mathbf{p} \mapsto \mathbf{f}(\mathbf{p}). \quad (3.4)$$

For this function, there is usually no closed-form expression of $\mathbf{f}(\mathbf{p})$ due to the high complexity of systems in practice like an integrated circuit such that the evaluation of \mathbf{f} at given parameter values \mathbf{p} requires a numerical simulation of the system. It maps the given parameter values \mathbf{p} , which are the input of the simulation, to the respective values of the performance properties \mathbf{f} , which are the output of the simulation. The N_p parameters \mathbf{p} of a system can be split into N_d deterministic design parameters d_j , $j = 1, 2, \dots, N_d$, N_s statistical parameters s_j , $j = 1, 2, \dots, N_s$, and N_θ operating parameters θ_j , $j = 1, 2, \dots, N_\theta$, collected in the vectors $\mathbf{d} = [d_1, d_2, \dots, d_{N_d}]^T \in \mathbb{R}^{N_d}$, $\mathbf{s} = [s_1, s_2, \dots, s_{N_s}]^T \in \mathbb{R}^{N_s}$ and $\boldsymbol{\theta} = [\theta_1, \theta_2, \dots, \theta_{N_\theta}]^T \in \mathbb{R}^{N_\theta}$, respectively:

$$\mathbf{p} = \begin{bmatrix} \mathbf{d} \\ \mathbf{s} \\ \boldsymbol{\theta} \end{bmatrix}. \quad (3.5)$$

In contrast to the deterministic design parameters \mathbf{d} like the length and width of transistors in an integrated circuit, the values of the statistical parameters \mathbf{s} fluctuate as, e.g., the oxide thickness and the perturbations of length and width of transistors in manufactured integrated circuits due to unavoidable manufacturing tolerances. These parameters are modeled by Gaussian random variables, i.e., $\mathbf{s} \sim \mathcal{N}(\mathbf{s}_0, \mathbf{C})$ has the pdf

$$f_s(\mathbf{s}) = \frac{1}{\sqrt{(2\pi)^{N_s} \det(\mathbf{C})}} \exp\left(-\frac{1}{2}(\mathbf{s} - \mathbf{s}_0)^T \mathbf{C}^{-1}(\mathbf{s} - \mathbf{s}_0)\right), \quad (3.6)$$

3.1 Problem Formulation for Robust System Design

with the mean s_0 and the covariance matrix C . As a consequence, the performance properties $\mathbf{f} = \mathbf{f}(\mathbf{p}) = \mathbf{f}(\mathbf{d}, \mathbf{s}, \boldsymbol{\theta})$, which are a function of these statistical parameters \mathbf{s} , are random variables as well and their values fluctuate too as, e.g., in manufactured integrated circuits. Because of these fluctuations, the performance properties \mathbf{f} might or might not lie in the acceptance intervals $[f_{L,i}, f_{U,i}]$, $i = 1, 2, \dots, N_f$, such that the system might fulfill or violate the performance specifications $f_{L,i} \leq f_i \leq f_{U,i}$, $i = 1, 2, \dots, N_f$, defined by the acceptance intervals. The fluctuations of the statistical parameter values can be taken into account by using the probability Y that the system fulfills all given performance specifications, which is the definition of the yield in [42] for manufactured integrated circuits, as quality measure:

$$Y = P \left(\bigwedge_{i=1}^{N_f} f_{L,i} \leq f_i \leq f_{U,i} \right) = P(\mathbf{f} \in \mathcal{A}_f). \quad (3.7)$$

The yield measures the percentage of manufactured integrated circuits with an acceptable performance whereas $1 - Y$ is a measure for the percentage of manufactured integrated circuits with an unacceptable performance, which have to be rejected. The design goal is to determine the values for the deterministic design parameters \mathbf{d} of the system under design such that the probability Y that the system fulfills all given performance specifications becomes maximum. Focusing on this goal, the robust system design can be formulated as the following optimization problem:

$$\mathbf{d}_{\text{opt}} = \underset{\mathbf{d} \in N_d}{\text{argmax}} Y. \quad (3.8)$$

The maximization of the probability Y of fulfilling the performance specifications, the quality measure, with respect to the deterministic design parameters \mathbf{d} for system optimization results in the optimal values \mathbf{d}_{opt} for the deterministic design parameters \mathbf{d} of the system under design.

Besides the classes of deterministic design parameters \mathbf{d} and statistical parameters \mathbf{s} , the operating parameters $\boldsymbol{\theta}$, e.g., the temperature an integrated circuit is exposed to, form a third class of the parameters \mathbf{p} . In contrast to the statistical parameters \mathbf{s} , they are ranging parameters for which no statistical knowledge in form of a probability distribution is available but only a range of possible values. The range of the j^{th} operating parameter θ_j can be defined by the tolerance interval $[\theta_{L,j}, \theta_{U,j}]$ in which it may lie with the lower bound $\theta_{L,j}$ and the upper bound $\theta_{U,j}$. Combining the tolerance intervals $[\theta_{L,j}, \theta_{U,j}]$ of all N_θ operating parameters $\theta_j, j = 1, 2, \dots, N_\theta$, via the

Cartesian product yields the tolerance region

$$\begin{aligned} T_{\boldsymbol{\theta}} &= \{ \boldsymbol{\theta} \in \mathbb{R}^{N_{\boldsymbol{\theta}}} : \theta_{L,j} \leq \theta_j \leq \theta_{U,j}, j = 1, 2, \dots, N_{\boldsymbol{\theta}} \} \\ &= [\theta_{L,1}, \theta_{U,1}] \times [\theta_{L,2}, \theta_{U,2}] \times \dots \times [\theta_{L,N_{\boldsymbol{\theta}}}, \theta_{U,N_{\boldsymbol{\theta}}}] . \end{aligned} \quad (3.9)$$

As the performance properties $\mathbf{f} = \mathbf{f}(\mathbf{p}) = \mathbf{f}(\mathbf{d}, \mathbf{s}, \boldsymbol{\theta})$ are a function of the deterministic design parameters \mathbf{d} , statistical parameters \mathbf{s} and operating parameters $\boldsymbol{\theta}$, the probability $Y = Y(\mathbf{d}, \boldsymbol{\theta})$ of fulfilling the performance specifications is a function of both the deterministic design parameters \mathbf{d} and the operating parameters $\boldsymbol{\theta}$:

$$Y : \mathbb{R}^{N_d} \times \mathbb{R}^{N_{\boldsymbol{\theta}}} \rightarrow [0, 1], (\mathbf{d}, \boldsymbol{\theta}) \mapsto Y(\mathbf{d}, \boldsymbol{\theta}). \quad (3.10)$$

Consequently, the optimal values \mathbf{d}_{opt} for the deterministic design parameters \mathbf{d} of the system under design obtained by the maximization of the probability Y of fulfilling the performance specifications in (3.8) are dependent on the operating parameters $\boldsymbol{\theta}$. So far, it has been assumed that the operating parameters $\boldsymbol{\theta}$ are fixed, i.e., have specific values that do not change over time, such that the optimal values \mathbf{d}_{opt} for the deterministic design parameters \mathbf{d} have to be obtained only once for these values of the operating parameters $\boldsymbol{\theta}$ by the maximization (3.8) in the design phase. However, the operating parameters $\boldsymbol{\theta}$ are ranging parameters whose nature is that their values can vary within the tolerance region $T_{\boldsymbol{\theta}}$. Due to the dependency of the optimal values \mathbf{d}_{opt} for the deterministic design parameters \mathbf{d} on the operating parameters $\boldsymbol{\theta}$, these optimal values \mathbf{d}_{opt} , which have been obtained by the maximization (3.8) for one instance of the operating parameters $\boldsymbol{\theta}$ in the design phase, are not optimal anymore when the values of the operating parameters $\boldsymbol{\theta}$ deviate from this one instance. Therefore, the deterministic design parameters \mathbf{d} would have to be adapted to the values of the operating parameters $\boldsymbol{\theta}$ by the maximization (3.8) whenever they change, which is impossible in case of already manufactured integrated circuits whose deterministic design parameters \mathbf{d} like the transistor length and width cannot be changed anymore. In order to overcome this problem, the optimal values \mathbf{d}_{opt} for the deterministic design parameters \mathbf{d} have to be made independent of the operating parameters $\boldsymbol{\theta}$. This independence can be achieved by taking the whole tolerance region $T_{\boldsymbol{\theta}}$ of the operating parameters $\boldsymbol{\theta}$ already in the design phase before manufacturing the integrated circuits into account, i.e., by determining the optimal values \mathbf{d}_{opt} for the deterministic design parameters \mathbf{d} such that they are optimal not only for one instance of the operating parameters $\boldsymbol{\theta}$ but for the whole tolerance region $T_{\boldsymbol{\theta}}$ of them. One possibility for this is using the worst-case probability of fulfilling the performance specifications, i.e., the minimum probability

$$Y_{\text{WC}} = \min_{\boldsymbol{\theta} \in T_{\boldsymbol{\theta}}} Y \quad (3.11)$$

3.1 Problem Formulation for Robust System Design

of fulfilling the performance specifications in the whole tolerance region T_θ of the operating parameters θ , as new quality measure. By maximizing this new quality measure, the optimal values \mathbf{d}_{opt} for the deterministic design parameters \mathbf{d} of the system under design can be obtained again as in [42] for integrated circuits:

$$\mathbf{d}_{\text{opt}} = \operatorname{argmax}_{\mathbf{d} \in N_d} Y_{\text{WC}} = \operatorname{argmax}_{\mathbf{d} \in N_d} \min_{\theta \in T_\theta} Y. \quad (3.12)$$

The minimization of the probability $Y = Y(\mathbf{d}, \theta)$ of fulfilling the performance specifications, which is a function of both the deterministic design parameters \mathbf{d} and the operating parameters θ , with respect to the operating parameters θ eliminates the dependency on the operating parameters θ such that the resulting worst-case probability $Y_{\text{WC}} = Y_{\text{WC}}(\mathbf{d})$ of fulfilling the performance specifications is a function of the deterministic design parameters \mathbf{d} only:

$$Y_{\text{WC}} : \mathbb{R}^{N_d} \rightarrow [0, 1], \mathbf{d} \mapsto Y_{\text{WC}}(\mathbf{d}). \quad (3.13)$$

This makes the optimal values \mathbf{d}_{opt} for the deterministic design parameters \mathbf{d} obtained by maximizing the worst-case probability Y_{WC} of fulfilling the performance specifications independent of the operating parameters θ as desired.

Another possibility for making the optimal values \mathbf{d}_{opt} for the deterministic design parameters \mathbf{d} independent of the operating parameters θ , which, however is not considered in the following and just stated for completeness, is using the alternative probability

$$Y = P \left(\forall \theta \in T_\theta : \bigwedge_{i=1}^{N_f} f_{L,i} \leq f_i \leq f_{U,i} \right) = P(\forall \theta \in T_\theta : \mathbf{f} \in \mathcal{A}_f) \quad (3.14)$$

for the maximization (3.8) as in [43], which incorporates the whole tolerance region T_θ of the operating parameters θ . It is the probability that the system fulfills all given performance specifications not only for one instance of the operating parameters θ but for the whole tolerance region T_θ of them. Due to the incorporation of the whole range T_θ of the operating parameters θ , the so defined probability Y is already independent of them and a function of the deterministic design parameters \mathbf{d} only as the worst-case probability Y_{WC} of fulfilling the performance specifications, for which this property has been enforced artificially:

$$Y : \mathbb{R}^{N_d} \rightarrow [0, 1], \mathbf{d} \mapsto Y(\mathbf{d}). \quad (3.15)$$

Again, this makes the optimal values \mathbf{d}_{opt} for the deterministic design parameters \mathbf{d} obtained by maximizing the probability Y independent of the operating parameters θ as desired.

3.2 Simulation-Based Robust System Design

The maximization of the quality measure, i.e., the worst-case probability Y_{WC} of fulfilling the performance specifications in (3.12), requires several evaluations of the probability Y of fulfilling the performance specifications. As there is usually no closed-form expression for the performance properties \mathbf{f} as a function of the parameters \mathbf{p} defined in (3.4) and it can only be evaluated by numerical simulations of the system, this is also the case for the probability Y of fulfilling the performance specifications as a function of the deterministic design parameters \mathbf{d} and operating parameters $\boldsymbol{\theta}$ defined in (3.10).

3.2.1 Monte-Carlo-Based Robust System Design

A straightforward possibility for obtaining a value of the probability Y of fulfilling the performance specifications for given deterministic design parameters \mathbf{d} and operating parameters $\boldsymbol{\theta}$ at least approximately is estimating it by a Monte Carlo simulation. In the Monte Carlo simulation, M realizations $\mathbf{s}_1, \mathbf{s}_2, \dots, \mathbf{s}_M$ of all involved random variables, i.e., the statistical parameters \mathbf{s} , are generated at random according to their probability distribution, which might be the Gaussian distribution $\mathcal{N}(\mathbf{s}_0, \mathbf{C})$ with the pdf in (3.6) or any other probability distribution. Each realization \mathbf{s}_m , $m = 1, 2, \dots, M$, together with given deterministic design parameters \mathbf{d} and operating parameters $\boldsymbol{\theta}$, which form the parameters

$$\mathbf{p}_m = \begin{bmatrix} \mathbf{d} \\ \mathbf{s}_m \\ \boldsymbol{\theta} \end{bmatrix}, \quad (3.16)$$

is mapped to the respective values $\mathbf{f}_m = \mathbf{f}(\mathbf{p}_m) = \mathbf{f}(\mathbf{d}, \mathbf{s}_m, \boldsymbol{\theta})$ of the performance properties \mathbf{f} according to (3.4) by a system simulation. In these M random experiments, it is counted how often the values of the samples \mathbf{f}_m of the performance properties \mathbf{f} lie in the acceptance intervals $[f_{L,i}, f_{U,i}]$, $i = 1, 2, \dots, N_{\mathbf{f}}$, to obtain the frequency

$$\hat{Y}_M = \frac{M_{1,M}}{M} \quad (3.17)$$

of fulfilling all performance specifications $f_{L,i} \leq f_i \leq f_{U,i}$, $i = 1, 2, \dots, N_{\mathbf{f}}$, associated with these acceptance intervals, i.e., $\mathbf{f}_m \in \mathcal{A}_{\mathbf{f}}$, which is an estimate for the probability Y of fulfilling these performance specifications, i.e., $\mathbf{f} \in \mathcal{A}_{\mathbf{f}}$, which is defined in (3.7).

Defining the performance acceptance function as the indicator function

$$\delta_{\mathcal{A}_f} : \mathbb{R}^{N_f} \rightarrow \{0, 1\}, \mathbf{f} \mapsto \delta_{\mathcal{A}_f}(\mathbf{f}) = \begin{cases} 1, & \mathbf{f} \in \mathcal{A}_f \\ 0, & \mathbf{f} \notin \mathcal{A}_f \end{cases}, \quad (3.18)$$

which indicates whether $\mathbf{f} \in \mathcal{A}_f$, i.e., the performance properties \mathbf{f} fulfill all performance specifications, with the function value 1, allows to express the number of the samples \mathbf{f}_m of the performance properties \mathbf{f} that fulfill all performance specifications and the frequency of fulfilling all performance specifications in the Monte Carlo simulation as

$$M_{1,M} = \sum_{m=1}^M \delta_{\mathcal{A}_f}(\mathbf{f}_m) \quad (3.19)$$

and

$$\hat{Y}_M = \frac{1}{M} \sum_{m=1}^M \delta_{\mathcal{A}_f}(\mathbf{f}_m), \quad (3.20)$$

respectively. Hence, the Monte Carlo simulation can be interpreted as an estimator, which estimates the probability Y of fulfilling the performance specifications from the random observations $\mathbf{f}_m = \mathbf{f}(\mathbf{d}, \mathbf{s}_m, \boldsymbol{\theta})$, $m = 1, 2, \dots, M$:

$$\hat{Y}_M : (\mathbb{R}^{N_f})^M \rightarrow [0, 1], (\mathbf{f}_1, \mathbf{f}_2, \dots, \mathbf{f}_M) \mapsto \hat{Y}_M(\mathbf{f}_1, \mathbf{f}_2, \dots, \mathbf{f}_M). \quad (3.21)$$

As the samples $\mathbf{s}_1, \mathbf{s}_2, \dots, \mathbf{s}_M$ of the statistical parameters \mathbf{s} are independent and identically distributed (i.i.d.) according to the probability distribution of \mathbf{s} , the corresponding outputs $\delta_{\mathcal{A}_f}(\mathbf{f}_m) = \delta_{\mathcal{A}_f}(\mathbf{f}(\mathbf{d}, \mathbf{s}_m, \boldsymbol{\theta}))$, $m = 1, 2, \dots, M$, of the performance acceptance function $\delta_{\mathcal{A}_f}$, each of which is 1 with the probability

$$\begin{aligned} P(\delta_{\mathcal{A}_f}(\mathbf{f}_m) = 1) &= P(\delta_{\mathcal{A}_f}(\mathbf{f}(\mathbf{d}, \mathbf{s}_m, \boldsymbol{\theta})) = 1) \\ &= P(\delta_{\mathcal{A}_f}(\mathbf{f}(\mathbf{d}, \mathbf{s}, \boldsymbol{\theta})) = 1) = P(\delta_{\mathcal{A}_f}(\mathbf{f}) = 1) \\ &= P(\mathbf{f} \in \mathcal{A}_f) = Y \end{aligned} \quad (3.22)$$

and 0 with the probability

$$P(\delta_{\mathcal{A}_f}(\mathbf{f}_m) = 0) = 1 - P(\delta_{\mathcal{A}_f}(\mathbf{f}_m) = 1) = 1 - Y, \quad (3.23)$$

are the results of Bernoulli trials whose success probability is the probability Y of fulfilling the performance specifications and thus i.i.d. Bernoulli random variables forming a Bernoulli process. As a consequence, the number $M_{1,M}$ of the samples \mathbf{f}_m of the performance properties \mathbf{f} in the M Bernoulli trials with the success probability

Y that fulfill all performance specifications, which represents a success in those trials, is a binomially distributed random variable with the probability mass function (pmf)

$$f_{M_{1,M}}(k) = P(M_{1,M} = k) = \binom{M}{k} Y^k (1 - Y)^{M-k} \quad (3.24)$$

and the possible values $k = 0, 1, \dots, M$, which is denoted as $M_{1,M} \sim \mathcal{B}(M, Y)$. As the mean and variance of the i.i.d. Bernoulli distributed random variables $\delta_{\mathcal{A}_f}(\mathbf{f}_m)$ are

$$\begin{aligned} E[\delta_{\mathcal{A}_f}(\mathbf{f}_m)] &= 1 \cdot P(\delta_{\mathcal{A}_f}(\mathbf{f}_m) = 1) + 0 \cdot P(\delta_{\mathcal{A}_f}(\mathbf{f}_m) = 0) \\ &= P(\delta_{\mathcal{A}_f}(\mathbf{f}_m) = 1) = Y \end{aligned} \quad (3.25)$$

and

$$\begin{aligned} \text{Var}[\delta_{\mathcal{A}_f}(\mathbf{f}_m)] &= E[\delta_{\mathcal{A}_f}^2(\mathbf{f}_m)] - E^2[\delta_{\mathcal{A}_f}(\mathbf{f}_m)] \\ &= 1 \cdot P(\delta_{\mathcal{A}_f}(\mathbf{f}_m) = 1) + 0 \cdot P(\delta_{\mathcal{A}_f}(\mathbf{f}_m) = 0) - Y^2 \\ &= Y - Y^2 = Y(1 - Y), \end{aligned} \quad (3.26)$$

respectively, the corresponding binomially distributed random variable $M_{1,M}$, which is expressed as the sum of these random variables $\delta_{\mathcal{A}_f}(\mathbf{f}_m)$ in (3.19), has the mean

$$E[M_{1,M}] = \sum_{m=1}^M E[\delta_{\mathcal{A}_f}(\mathbf{f}_m)] = \sum_{m=1}^M Y = MY \quad (3.27)$$

and the variance

$$\text{Var}[M_{1,M}] = \sum_{m=1}^M \text{Var}[\delta_{\mathcal{A}_f}(\mathbf{f}_m)] = \sum_{m=1}^M Y(1 - Y) = MY(1 - Y). \quad (3.28)$$

Furthermore, the estimate \hat{Y}_M for the probability Y of fulfilling the performance specifications is a scaled version of the binomially distributed random variable $M_{1,M}$ in the interval $[0, 1]$ as expressed in (3.17) with the pmf

$$\begin{aligned} f_{\hat{Y}_M}(y) &= P(\hat{Y}_M = y) = P\left(\frac{M_{1,M}}{M} = y\right) = P(M_{1,M} = My) \\ &= f_{M_{1,M}}(My) = \binom{M}{My} Y^{My} (1 - Y)^{M(1-y)}, \end{aligned} \quad (3.29)$$

the possible values $y = 0, \frac{1}{M}, \dots, 1$, the mean

$$E[\hat{Y}_M] = \frac{E[M_{1,M}]}{M} = \frac{MY}{M} = Y \quad (3.30)$$

and the variance

$$\text{Var} \left[\hat{Y}_M \right] = \frac{\text{Var} [M_{1,M}]}{M^2} = \frac{MY(1-Y)}{M^2} = \frac{Y(1-Y)}{M}. \quad (3.31)$$

Since the expected value $E \left[\hat{Y}_M \right]$ of the estimate is the true probability Y of fulfilling the performance specifications, the estimator $\hat{Y}_M = \hat{Y}_M(\mathbf{f}_1, \mathbf{f}_2, \dots, \mathbf{f}_M)$ for the probability Y of fulfilling the performance specifications stated in (3.21) is unbiased. In case of an unbiased estimator, the mean squared error (MSE) between the estimate and the parameter to be estimated is given by the variance of the estimate. Hence, the MSE between the estimate \hat{Y}_M and the true probability Y of fulfilling the performance specifications is

$$E \left[\left(\hat{Y}_M - Y \right)^2 \right] = \text{Var} \left[\hat{Y}_M \right] = \frac{Y(1-Y)}{M} \xrightarrow{M \rightarrow \infty} 0, \quad (3.32)$$

which converges to 0 as the number of samples or observations \mathbf{f}_m and system simulations M in the Monte Carlo simulation tends to infinity.

Chebyshev's inequality applied to the estimate, i.e., the random variable \hat{Y}_M , reads

$$P \left(\left| \hat{Y}_M - E \left[\hat{Y}_M \right] \right| \geq \varepsilon \right) \leq \frac{\text{Var} \left[\hat{Y}_M \right]}{\varepsilon^2} \quad (3.33)$$

for all $\varepsilon > 0$. With the mean of the estimate \hat{Y}_M in (3.30) and its variance in (3.31), this inequality becomes

$$P \left(\left| \hat{Y}_M - Y \right| \geq \varepsilon \right) \leq \frac{Y(1-Y)}{M\varepsilon^2}. \quad (3.34)$$

Hence,

$$P \left(\left| \hat{Y}_M - Y \right| > \varepsilon \right) \leq P \left(\left| \hat{Y}_M - Y \right| \geq \varepsilon \right) \leq \frac{Y(1-Y)}{M\varepsilon^2} \xrightarrow{M \rightarrow \infty} 0, \quad (3.35)$$

which implies that

$$P \left(\left| \hat{Y}_M - Y \right| > \varepsilon \right) \xrightarrow{M \rightarrow \infty} 0. \quad (3.36)$$

This means that the estimate \hat{Y}_M converges in probability to the true probability Y of fulfilling the performance specifications to be estimated as the number of samples or observations \mathbf{f}_m and system simulations M in the Monte Carlo simulation tends to infinity, which is also known as the weak law of large numbers:

$$\hat{Y}_M \xrightarrow{p} Y \quad \text{for } M \rightarrow \infty. \quad (3.37)$$

Therefore, the estimator $\hat{Y}_M = \hat{Y}_M(\mathbf{f}_1, \mathbf{f}_2, \dots, \mathbf{f}_M)$ for the probability Y of fulfilling the performance specifications stated in (3.21) is consistent.

The statistical knowledge about the estimate \hat{Y}_M is completely captured by its pmf $f_{\hat{Y}_M}(y)$ stated in (3.29). Theoretically, the required number of samples or observations \mathbf{f}_m and system simulations M in the Monte Carlo simulation for a desired estimation accuracy, e.g., specified in form of a confidence interval $[\hat{Y}_M - \Delta Y, \hat{Y}_M + \Delta Y]$ of length $2 \Delta Y$ around the random estimate \hat{Y}_M which shall contain the true probability Y of fulfilling the performance specifications with a desired probability κ , the desired confidence level, could be derived from it. Unfortunately, it cannot be derived in closed form due to the special structure of the pmf $f_{\hat{Y}_M}(y)$ of the estimate \hat{Y}_M , which is a scaled binomially distributed random variable. However, an approximation of the underlying binomial distribution by a Gaussian distribution makes the derivation of such a closed-form expression for the required number of samples or observations \mathbf{f}_m and system simulations M in the Monte Carlo simulation possible.

The Central Limit Theorem applied to the number of the samples \mathbf{f}_m of the performance properties \mathbf{f} that fulfill all performance specifications, i.e., the binomially distributed random variable $M_{1,M}$ expressed as the sum of the i.i.d. Bernoulli distributed random variables $\delta_{A_f}(\mathbf{f}_m)$ in (3.19) with the mean (3.27) and the variance (3.28), states that the corresponding standardized random variable

$$\tilde{M}_{1,M} = \frac{M_{1,M} - \mathbb{E}[M_{1,M}]}{\sqrt{\text{Var}[M_{1,M}]}} = \frac{M_{1,M} - MY}{\sqrt{MY(1-Y)}} \quad (3.38)$$

converges in distribution to a standard normal random variable as the number of samples \mathbf{f}_m and system simulations M in the Monte Carlo simulation tends to infinity:

$$\tilde{M}_{1,M} \xrightarrow{d} \mathcal{N}(0, 1) \quad \text{for } M \rightarrow \infty. \quad (3.39)$$

This means that the cumulative distribution function (cdf) of this standardized random variable $\tilde{M}_{1,M}$ converges to the cdf

$$\Phi(x) = \frac{1}{\sqrt{2\pi}} \int_{-\infty}^x e^{-\xi^2/2} d\xi \quad (3.40)$$

of the standard normal distribution for all $x \in \mathbb{R}$:

$$P(\tilde{M}_{1,M} \leq x) \xrightarrow{M \rightarrow \infty} \Phi(x). \quad (3.41)$$

Thus, the standardized random variable $\tilde{M}_{1,M}$ can be considered to be approximately Gaussian with mean $\mathbb{E}[\tilde{M}_{1,M}] = 0$ and variance $\text{Var}[\tilde{M}_{1,M}] = 1$ if the number

of samples \mathbf{f}_m and system simulations M in the Monte Carlo simulation is large, which has to be the case for a high estimation accuracy anyway. From this, it can be concluded that for a large number of samples \mathbf{f}_m and system simulations M in the Monte Carlo simulation, the binomially distributed random variable

$$M_{1,M} = \sqrt{MY(1-Y)}\tilde{M}_{1,M} + MY \quad (3.42)$$

corresponding to the standardized random variable $\tilde{M}_{1,M}$ in (3.38) is approximately Gaussian with the mean

$$\mathbb{E}[M_{1,M}] = \sqrt{MY(1-Y)}\mathbb{E}[\tilde{M}_{1,M}] + MY = MY \quad (3.43)$$

and the variance

$$\begin{aligned} \text{Var}[M_{1,M}] &= \text{Var}\left[\sqrt{MY(1-Y)}\tilde{M}_{1,M}\right] = MY(1-Y)\text{Var}[\tilde{M}_{1,M}] \\ &= MY(1-Y) \end{aligned} \quad (3.44)$$

as also stated in (3.27) and (3.28), respectively. This explains why the Gaussian distribution $\mathcal{N}(MY, MY(1-Y))$ can be used as an approximation for the binomial distribution $\mathcal{B}(M, Y)$ if M is large. As a consequence, the estimate \hat{Y}_M , which is just a scaled version of the number $M_{1,M}$ of the samples \mathbf{f}_m that fulfill all performance specifications in the Monte Carlo simulation as can be seen in (3.17), is approximately Gaussian as well with the mean and the variance given by (3.30) and (3.31), respectively. Since the corresponding standardized random variable

$$\tilde{Y}_M = \frac{\hat{Y}_M - \mathbb{E}[\hat{Y}_M]}{\sqrt{\text{Var}[\hat{Y}_M]}} = \frac{\hat{Y}_M - Y}{\sqrt{Y(1-Y)/M}} \quad (3.45)$$

is thus approximately Gaussian with zero mean and unit variance, the cdf of the estimate \hat{Y}_M can be expressed as

$$\begin{aligned} F_{\hat{Y}_M}(y) &= P(\hat{Y}_M \leq y) = P\left(\frac{\hat{Y}_M - Y}{\sqrt{Y(1-Y)/M}} \leq \frac{y - Y}{\sqrt{Y(1-Y)/M}}\right) \\ &= P\left(\tilde{Y}_M \leq \frac{y - Y}{\sqrt{Y(1-Y)/M}}\right) \approx \Phi\left(\frac{y - Y}{\sqrt{Y(1-Y)/M}}\right). \end{aligned} \quad (3.46)$$

With this expression and the fact that

$$\hat{Y}_M - \Delta Y \leq Y \leq \hat{Y}_M + \Delta Y \Leftrightarrow Y - \Delta Y \leq \hat{Y}_M \leq Y + \Delta Y, \quad (3.47)$$

the probability that the confidence interval $[\hat{Y}_M - \Delta Y, \hat{Y}_M + \Delta Y]$ of length $2 \Delta Y$ around the estimate \hat{Y}_M contains the true probability Y of fulfilling the performance specifications can be written as

$$\begin{aligned}
 & P\left(\hat{Y}_M - \Delta Y \leq Y \leq \hat{Y}_M + \Delta Y\right) \\
 &= P\left(Y - \Delta Y \leq \hat{Y}_M \leq Y + \Delta Y\right) \\
 &= P\left(\hat{Y}_M \leq Y + \Delta Y\right) - P\left(\hat{Y}_M \leq Y - \Delta Y\right) \\
 &= F_{\hat{Y}_M}(Y + \Delta Y) - F_{\hat{Y}_M}(Y - \Delta Y) \\
 &\approx \Phi\left(\frac{\Delta Y}{\sqrt{Y(1-Y)/M}}\right) - \Phi\left(-\frac{\Delta Y}{\sqrt{Y(1-Y)/M}}\right) \\
 &= \Phi\left(\frac{\Delta Y}{\sqrt{Y(1-Y)/M}}\right) - \left(1 - \Phi\left(\frac{\Delta Y}{\sqrt{Y(1-Y)/M}}\right)\right) \\
 &= 2\Phi\left(\frac{\Delta Y}{\sqrt{Y(1-Y)/M}}\right) - 1.
 \end{aligned} \tag{3.48}$$

From this, it can be concluded that the following condition has to be fulfilled such that the confidence interval $[\hat{Y}_M - \Delta Y, \hat{Y}_M + \Delta Y]$ around the estimate \hat{Y}_M contains the true probability Y of fulfilling the performance specifications with the probability κ , the desired confidence level, i.e., $P\left(\hat{Y}_M - \Delta Y \leq Y \leq \hat{Y}_M + \Delta Y\right) = \kappa$:

$$2\Phi\left(\frac{\Delta Y}{\sqrt{Y(1-Y)/M}}\right) - 1 \approx \kappa. \tag{3.49}$$

This condition can be rewritten as

$$\frac{\Delta Y}{\sqrt{Y(1-Y)/M}} \approx \Phi^{-1}\left(\frac{\kappa + 1}{2}\right) \tag{3.50}$$

and finally as a condition for the number of samples or observations f_m and system simulations M in the Monte Carlo simulation:

$$M \approx \frac{Y(1-Y)}{\Delta Y^2} \left(\Phi^{-1}\left(\frac{\kappa + 1}{2}\right)\right)^2 = M_{\text{req.}}. \tag{3.51}$$

$M_{\text{req.}}$ is the approximate number of samples or observations f_m and system simulations in the Monte Carlo simulation required for estimating the probability Y of fulfilling the performance specifications by the estimator $\hat{Y}_M = \hat{Y}_M(\mathbf{f}_1, \mathbf{f}_2, \dots, \mathbf{f}_M)$

from (3.21) with the desired confidence level κ for the corresponding confidence interval $[\hat{Y}_M - \Delta Y, \hat{Y}_M + \Delta Y]$. Assuming that the true probability of fulfilling the performance specifications is $Y = 0.99$, this number $M_{\text{req.}}$ is plotted over the half confidence interval length ΔY for the desired confidence levels $\kappa = 0.9, 0.95, 0.99$ and over the desired confidence level κ for the half confidence interval lengths $\Delta Y = 0.01, 0.001, 0.0001$ in Figure 3.1. The approximate required number $M_{\text{req.}}$ of samples or observations f_m and system simulations in the Monte Carlo simulation increases if the half confidence interval length ΔY decreases or the desired confidence level κ increases. Especially if the half confidence interval length ΔY is already small, a further reduction of it leads to a significant increase in the approximate required number $M_{\text{req.}}$ of samples or observations f_m and system simulations in the Monte Carlo simulation.

So, it can be concluded that estimating the probability Y of fulfilling the performance specifications by a Monte Carlo simulation has a beneficial advantage but also an important drawback. On the one hand, it can be implemented easily and it is easy to apply it to different systems due to its generality. On the other hand, however, a large number M of system simulations has to be performed in order to obtain an accurate estimate, i.e., an estimate \hat{Y}_M with a high confidence level κ for a small confidence interval $[\hat{Y}_M - \Delta Y, \hat{Y}_M + \Delta Y]$ around it with a small half length ΔY , which might lead to a prohibitively large computational complexity in practice.

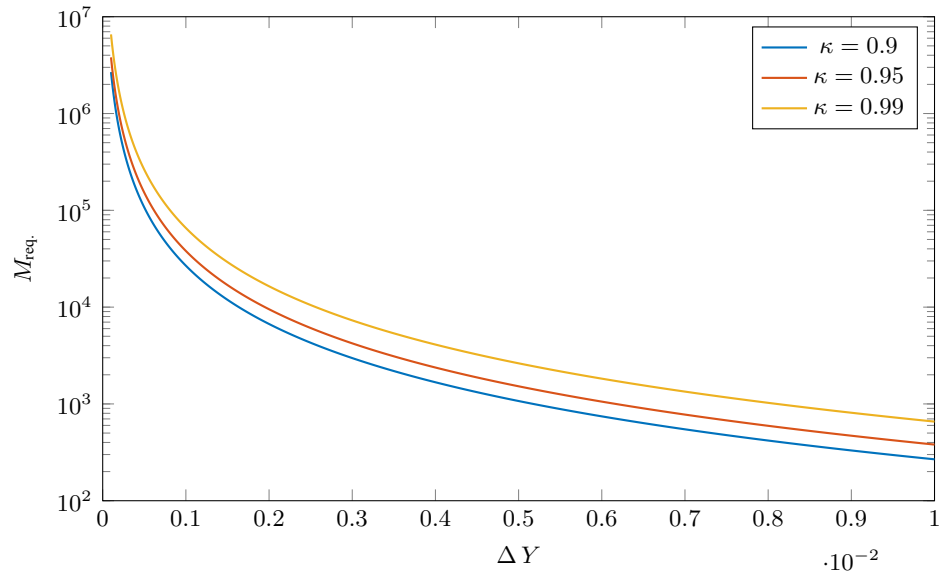
3.2.2 Worst-Case-Distance-Based Robust System Design

The problem of the large number M of system simulations to be performed in order to obtain an accurate Monte-Carlo-based estimate \hat{Y}_M for the probability Y of fulfilling the performance specifications can be overcome by exploiting the fact that the probability Y of fulfilling the performance specifications, which has been defined in (3.7) as the probability that all performance properties f lie in the acceptance intervals and thus in the performance acceptance region \mathcal{A}_f defined in (3.1), is equivalent to the probability that the statistical parameters s lie in a corresponding parameter acceptance region \mathcal{A}_s :

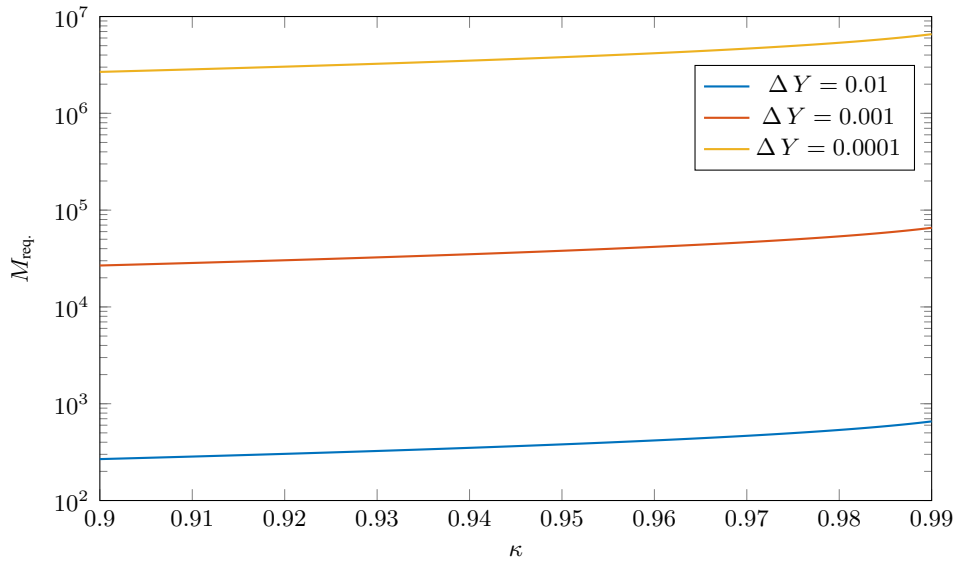
$$Y = P(f \in \mathcal{A}_f) = P(s \in \mathcal{A}_s). \quad (3.52)$$

This parameter acceptance region is defined as

$$\begin{aligned} \mathcal{A}_s &= \{s \in \mathbb{R}^{N_s} : f \in \mathcal{A}_f\} \\ &= \{s \in \mathbb{R}^{N_s} : f_{L,i} \leq f_i \leq f_{U,i}, i = 1, 2, \dots, N_f\}, \end{aligned} \quad (3.53)$$



(a) M_{req} . vs. ΔY .



(b) M_{req} . vs. κ .

Figure 3.1: Approximate number M_{req} . of samples or observations and system simulations in the Monte Carlo simulation required for estimating the probability $Y = 0.99$ of fulfilling the performance specifications with the desired confidence level κ for the corresponding confidence interval $[\hat{Y}_M - \Delta Y, \hat{Y}_M + \Delta Y]$.

i.e., the set of all values of the statistical parameters \mathbf{s} that are mapped to performance properties \mathbf{f} lying in the acceptance intervals and thus correspond to a system fulfilling the performance specifications. Analogously to the performance acceptance region, the parameter acceptance region can also be represented by the intersection of the individual parameter acceptance region partitions

$$\mathcal{A}_{\mathbf{s},L,i} = \{\mathbf{s} \in \mathbb{R}^{N_s} : f_i \geq f_{L,i}\} = \{\mathbf{s} \in \mathbb{R}^{N_s} : \mathbf{f} \in \mathcal{A}_{\mathbf{f},L,i}\} \quad (3.54)$$

and

$$\mathcal{A}_{\mathbf{s},U,i} = \{\mathbf{s} \in \mathbb{R}^{N_s} : f_i \leq f_{U,i}\} = \{\mathbf{s} \in \mathbb{R}^{N_s} : \mathbf{f} \in \mathcal{A}_{\mathbf{f},U,i}\}, \quad (3.55)$$

the i^{th} of which are the sets of all values of the statistical parameters \mathbf{s} that are mapped to values of the i^{th} performance property f_i that do not lie below the lower bound $f_{L,i}$ and above the upper bound $f_{U,i}$ of the corresponding acceptance interval $[f_{L,i}, f_{U,i}]$, respectively:

$$\mathcal{A}_{\mathbf{s}} = \bigcap_{i=1}^{N_f} \mathcal{A}_{\mathbf{s},L,i} \cap \mathcal{A}_{\mathbf{s},U,i}. \quad (3.56)$$

In the special cases $f_{L,i} \rightarrow -\infty$ and $f_{U,i} \rightarrow \infty$, the corresponding individual parameter acceptance region partitions simplify to $\mathcal{A}_{\mathbf{s},L,i} = \mathbb{R}^{N_s}$ and $\mathcal{A}_{\mathbf{s},U,i} = \mathbb{R}^{N_s}$, respectively. Exemplary individual parameter acceptance region partitions $\mathcal{A}_{\mathbf{s},L,i}$ with a finite lower bound $f_{L,i}$ and $\mathcal{A}_{\mathbf{s},U,i}$ with a finite upper bound $f_{U,i}$ for a performance property f_i that is a function of only two statistical parameters $\mathbf{s} = [s_1, s_2]^T$ are the green areas in Figure 3.2 and Figure 3.3, where $f_i > f_{L,i}$ and $f_i < f_{U,i}$, respectively, including the orange boundaries, where $f_i = f_{L,i}$ and $f_i = f_{U,i}$, respectively. Although the boundaries of the individual parameter acceptance region partitions are typically considered to be smooth, this does not have to be the case. The intersection of two individual parameter acceptance region partitions $\mathcal{A}_{\mathbf{s},L,i}$ and $\mathcal{A}_{\mathbf{s},U,i}$, i.e.,

$$\begin{aligned} \mathcal{A}_{\mathbf{s},L,i} \cap \mathcal{A}_{\mathbf{s},U,i} &= \{\mathbf{s} \in \mathbb{R}^{N_s} : f_i \geq f_{L,i}\} \cap \{\mathbf{s} \in \mathbb{R}^{N_s} : f_i \leq f_{U,i}\} \\ &= \{\mathbf{s} \in \mathbb{R}^{N_s} : f_{L,i} \leq f_i \leq f_{U,i}\}, \end{aligned} \quad (3.57)$$

where the i^{th} performance property f_i lies in its acceptance interval $[f_{L,i}, f_{U,i}]$ such that the i^{th} performance specification $f_{L,i} \leq f_i \leq f_{U,i}$ defined by this acceptance interval is fulfilled, is illustrated in Figure 3.4 for the two exemplary individual parameter acceptance region partitions $\mathcal{A}_{\mathbf{s},L,i}$ and $\mathcal{A}_{\mathbf{s},U,i}$ from Figure 3.2 and Figure 3.3, respectively.

The probability that the statistical parameters \mathbf{s} lie in the parameter acceptance region $\mathcal{A}_{\mathbf{s}}$ and thus the probability Y of fulfilling the performance specifications could

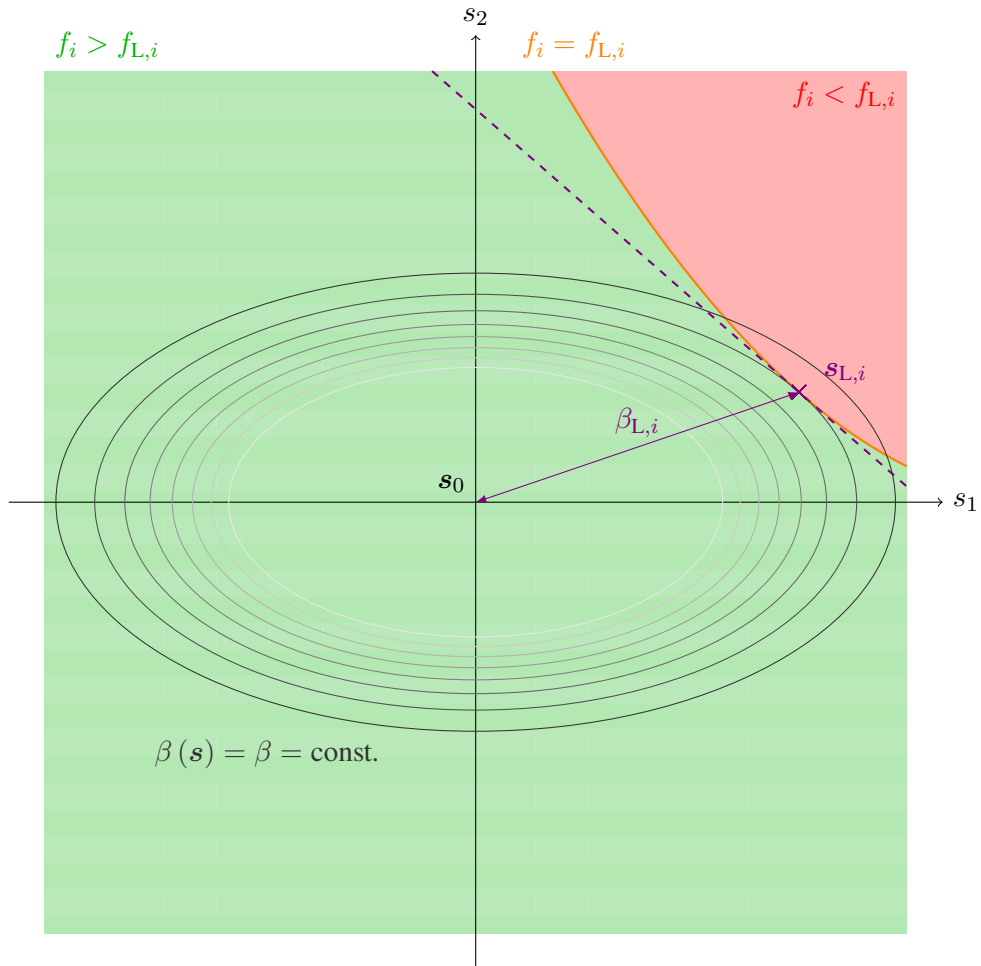


Figure 3.2: Exemplary individual parameter acceptance region partition $\mathcal{A}_{s,L,i}$ with a finite lower bound $f_{L,i}$ (green area including orange boundary) and the corresponding approximate individual parameter acceptance region partition $\hat{\mathcal{A}}_{s,L,i}$ defined by the worst-case distance $\beta_{L,i}$ (horizontally striped area including violet linear boundary) for two statistical parameters $\mathbf{s} = [s_1, s_2]^T$.

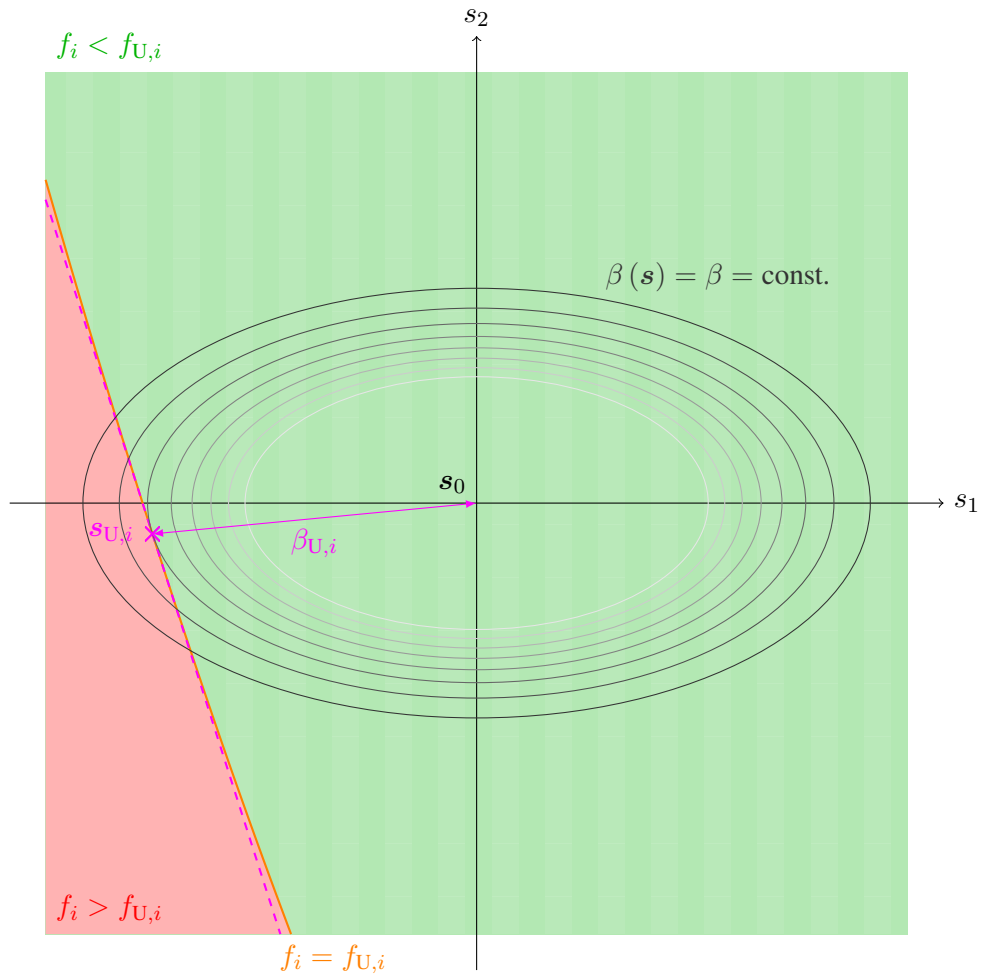


Figure 3.3: Exemplary individual parameter acceptance region partition $\mathcal{A}_{s,U,i}$ with a finite upper bound $f_{U,i}$ (green area including orange boundary) and the corresponding approximate individual parameter acceptance region partition $\hat{\mathcal{A}}_{s,U,i}$ defined by the worst-case distance $\beta_{U,i}$ (vertically striped area including magenta linear boundary) for two statistical parameters $\mathbf{s} = [s_1, s_2]^T$.

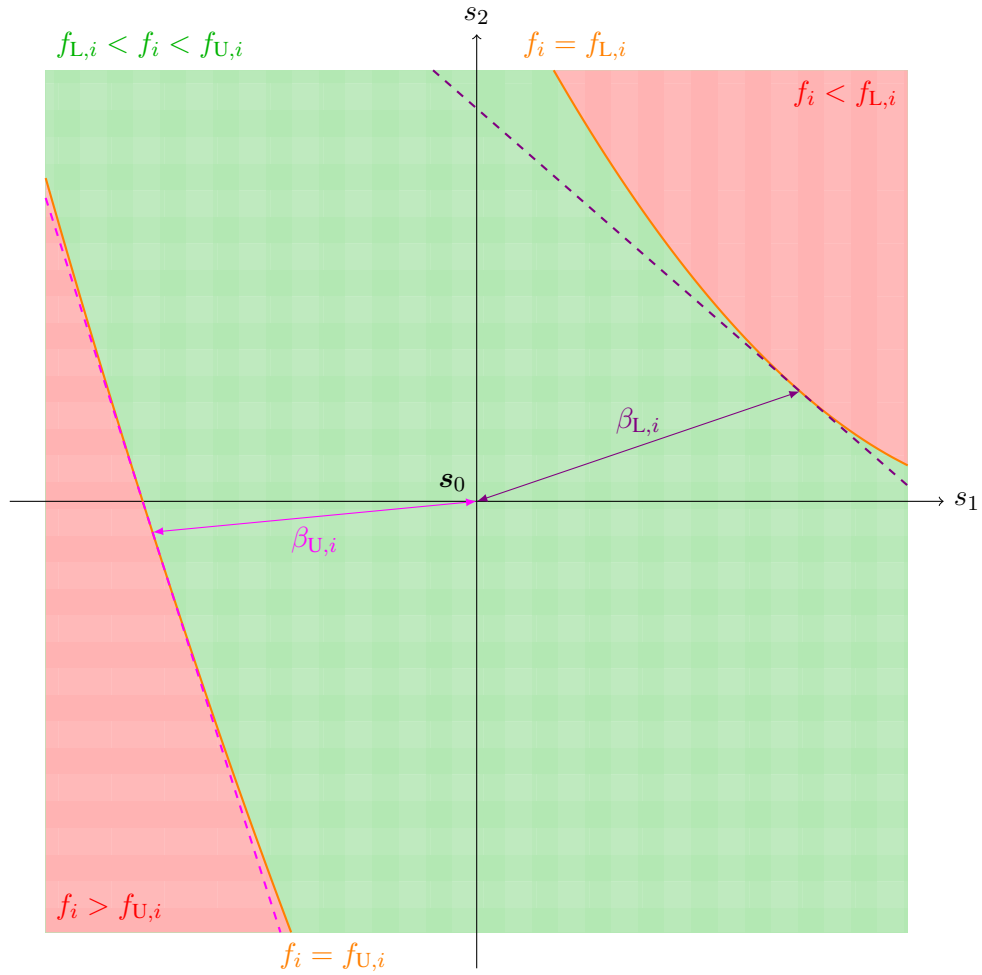


Figure 3.4: Intersection of two exemplary individual parameter acceptance region partitions $\mathcal{A}_{s,L,i}$ with a finite lower bound $f_{L,i}$ and $\mathcal{A}_{s,U,i}$ with a finite upper bound $f_{U,i}$ (green area including orange boundaries) as well as the corresponding approximate individual parameter acceptance region partitions $\hat{\mathcal{A}}_{s,L,i}$ and $\hat{\mathcal{A}}_{s,U,i}$ defined by the worst-case distances $\beta_{L,i}$ and $\beta_{U,i}$ (horizontally and vertically striped areas including violet and magenta linear boundaries, respectively) for two statistical parameters $\mathbf{s} = [s_1, s_2]^T$.

theoretically be obtained by integrating the multivariate Gaussian pdf $f_s(\mathbf{s})$ of the statistical parameters \mathbf{s} given by (3.6) in the parameter acceptance region \mathcal{A}_s :

$$\begin{aligned} Y &= P(\mathbf{s} \in \mathcal{A}_s) = \int_{\mathcal{A}_s} f_s(\mathbf{s}) \, d\mathbf{s} \\ &= \frac{1}{\sqrt{(2\pi)^{N_s} \det(\mathbf{C})}} \int_{\{\mathbf{s} \in \mathbb{R}^{N_s} : \mathbf{f} \in \mathcal{A}_f\}} \exp\left(-\frac{1}{2}(\mathbf{s} - \mathbf{s}_0)^T \mathbf{C}^{-1}(\mathbf{s} - \mathbf{s}_0)\right) \, d\mathbf{s}. \end{aligned} \quad (3.58)$$

Unfortunately, there are two problems that render this integration intractable in practice. First, the boundary of the parameter acceptance region \mathcal{A}_s as illustrated by the orange curves in Figure 3.4 for two statistical parameters $\mathbf{s} = [s_1, s_2]^T$ can only be determined by many system simulations and, second, the integration of the multivariate Gaussian pdf $f_s(\mathbf{s})$ of the statistical parameters \mathbf{s} in the parameter acceptance region \mathcal{A}_s with a possibly highly nonlinear boundary can only be performed numerically, which comes with a high computational complexity. In order to overcome both problems at the same time, one can resort to approximating the boundary of the parameter acceptance region \mathcal{A}_s by just a few system simulations such that the integration in the resulting simplified parameter acceptance region becomes easy. This can be achieved by so-called worst-case distances.

The worst-case distances for a finite lower bound $f_{L,i}$ and for a finite upper bound $f_{U,i}$ of the acceptance interval for the i^{th} performance property f_i are defined as

$$\beta_{L,i} = \min_{\mathbf{s} \in \mathbb{R}^{N_s}} \beta(\mathbf{s}) \quad \text{s.t.} \quad f_i \leq f_{L,i}, \quad (3.59)$$

and

$$\beta_{U,i} = \min_{\mathbf{s} \in \mathbb{R}^{N_s}} \beta(\mathbf{s}) \quad \text{s.t.} \quad f_i \geq f_{U,i}, \quad (3.60)$$

respectively, where $\beta(\mathbf{s})$ measures the distance between the statistical parameters \mathbf{s} and their mean \mathbf{s}_0 . The worst-case distance $\beta_{b,i}$, $b \in \{L, U\}$, is the smallest distance between the mean \mathbf{s}_0 of the statistical parameters \mathbf{s} , at which their multivariate Gaussian pdf $f_s(\mathbf{s})$ has its peak and which is assumed to lie in the corresponding individual parameter acceptance region partition $\mathcal{A}_{s,b,i}$, and the boundary of the corresponding individual parameter acceptance region partition $\mathcal{A}_{s,b,i}$, where the i^{th} performance specification $f_{L,i} \leq f_i \leq f_{U,i}$ is barely fulfilled, i.e., $f_i = f_{b,i}$. As distance measure $\beta(\mathbf{s})$ for the distance between the statistical parameters \mathbf{s} and their mean \mathbf{s}_0 , the Mahalanobis distance is chosen, i.e.,

$$\beta^2(\mathbf{s}) = (\mathbf{s} - \mathbf{s}_0)^T \mathbf{C}^{-1}(\mathbf{s} - \mathbf{s}_0), \quad (3.61)$$

in order to take the covariance matrix \mathbf{C} of the statistical parameters \mathbf{s} into account and thereby link the distance measure $\beta(\mathbf{s})$ to their pdf $f_{\mathbf{s}}(\mathbf{s})$:

$$f_{\mathbf{s}}(\mathbf{s}) = \frac{1}{\sqrt{(2\pi)^{N_s} \det(\mathbf{C})}} \exp\left(-\frac{1}{2}\beta^2(\mathbf{s})\right). \quad (3.62)$$

As a consequence, the set of all statistical parameter values \mathbf{s} that have the same distance $\beta(\mathbf{s}) = \beta = \text{const.}$ from their mean \mathbf{s}_0 , i.e., all equidistant points \mathbf{s} , is the set of all statistical parameter values \mathbf{s} for which their pdf $f_{\mathbf{s}}(\mathbf{s})$ has the same value, i.e., a contour line of the pdf $f_{\mathbf{s}}(\mathbf{s})$:

$$\begin{aligned} \{\mathbf{s} \in \mathbb{R}^{N_s} : \beta(\mathbf{s}) = \beta\} &= \left\{ \mathbf{s} \in \mathbb{R}^{N_s} : f_{\mathbf{s}}(\mathbf{s}) = \frac{\exp\left(-\frac{1}{2}\beta^2\right)}{\sqrt{(2\pi)^{N_s} \det(\mathbf{C})}} \right\} \\ &= \left\{ \mathbf{s} \in \mathbb{R}^{N_s} : (\mathbf{s} - \mathbf{s}_0)^T \mathbf{C}^{-1} (\mathbf{s} - \mathbf{s}_0) = \beta^2 \right\}. \end{aligned} \quad (3.63)$$

In general, these sets for different constant distances β are hyperellipsoids whose center is the mean \mathbf{s}_0 of the statistical parameters \mathbf{s} and, in case of the two statistical parameters $\mathbf{s} = [s_1, s_2]^T$ in Figure 3.2 and Figure 3.3, they are the gray ellipses centered at their mean \mathbf{s}_0 . Along each ellipse, their bivariate Gaussian pdf $f_{\mathbf{s}}(\mathbf{s})$ as well as their distance $\beta(\mathbf{s}) = \beta$ from their mean \mathbf{s}_0 is constant, which increases if the ellipse becomes larger. Hence, in each of the two figures, the statistical parameter values $\mathbf{s} = [s_1, s_2]^T$ on the largest of the shown ellipses, which intersects the orange boundary of the individual parameter acceptance region partition $\mathcal{A}_{\mathbf{s},b,i}$, $b \in \{\text{L}, \text{U}\}$, in two points, have the largest distance $\beta(\mathbf{s}) = \beta$ from their mean \mathbf{s}_0 . If the ellipse is decreased such that the resulting smaller ellipse still intersects the boundary of the individual parameter acceptance region partition $\mathcal{A}_{\mathbf{s},b,i}$ in two points, these two points represent statistical parameter values $\mathbf{s} = [s_1, s_2]^T$ that have a smaller distance $\beta(\mathbf{s}) = \beta$ from their mean \mathbf{s}_0 than the ones on the larger ellipse. If this procedure is continued, the two points where the decreasing ellipse and the boundary of the individual parameter acceptance region partition $\mathcal{A}_{\mathbf{s},b,i}$ intersect converge to a single point $\mathbf{s}_{b,i}$, $b \in \{\text{L}, \text{U}\}$, where the ellipse touches the boundary of the individual parameter acceptance region partition $\mathcal{A}_{\mathbf{s},b,i}$ and which is represented by a cross. As an even smaller ellipse like the smallest of the shown ellipses would not have any point with the boundary of the individual parameter acceptance region partition $\mathcal{A}_{\mathbf{s},b,i}$ in common, this single point $\mathbf{s}_{b,i}$ represents the statistical parameter values $\mathbf{s} = [s_1, s_2]^T$ on the boundary of the individual parameter acceptance region partition $\mathcal{A}_{\mathbf{s},b,i}$ that have the smallest distance $\beta(\mathbf{s})$ from their mean \mathbf{s}_0 , which thus is the worst-case distance

$\beta_{b,i}$ for the bound $f_{b,i}$, $b \in \{L, U\}$, of the acceptance interval for the i^{th} performance property f_i . In general, the smallest hyperellipsoid on which all statistical parameters \mathbf{s} have the same distance β from their mean \mathbf{s}_0 and that has a point with the boundary of the individual parameter acceptance region partition $\mathcal{A}_{\mathbf{s},b,i}$ in common touches this boundary at the point $\mathbf{s}_{b,i}$ where the statistical parameters \mathbf{s} on this boundary have the smallest distance $\beta(\mathbf{s})$ from their mean \mathbf{s}_0 , namely, the worst-case distance $\beta_{b,i}$:

$$\beta_{b,i} = \beta(\mathbf{s}_{b,i}). \quad (3.64)$$

The boundary of the individual parameter acceptance region partition $\mathcal{A}_{\mathbf{s},b,i}$, $b \in \{L, U\}$, can be approximated by linearizing it with a tangential hyperplane that touches it at the point $\mathbf{s}_{b,i}$ where the statistical parameters \mathbf{s} on this boundary have the smallest distance from their mean \mathbf{s}_0 , i.e., the worst-case distance $\beta_{b,i}$, to obtain an approximate individual parameter acceptance region partition $\hat{\mathcal{A}}_{\mathbf{s},b,i}$ bounded by this tangential hyperplane. For the two statistical parameters $\mathbf{s} = [s_1, s_2]^T$ in Figure 3.2 and Figure 3.3, the tangential hyperplane approximating the orange boundary of the individual parameter acceptance region partition $\mathcal{A}_{\mathbf{s},L,i}$, where $f_i = f_{L,i}$, is the violet tangential line and the tangential hyperplane approximating the orange boundary of the individual parameter acceptance region partition $\mathcal{A}_{\mathbf{s},U,i}$, where $f_i = f_{U,i}$, is the magenta tangential line, and the resulting approximate individual parameter acceptance region partitions $\hat{\mathcal{A}}_{\mathbf{s},L,i}$ and $\hat{\mathcal{A}}_{\mathbf{s},U,i}$ are the horizontally and vertically striped areas bounded by these violet and magenta tangential lines, respectively.

As derived in Appendix A, the probability that the statistical parameters \mathbf{s} lie in the approximate individual parameter acceptance region partition $\hat{\mathcal{A}}_{\mathbf{s},b,i}$ can be computed as follows to approximate the probability that the statistical parameters \mathbf{s} lie in the individual parameter acceptance region partition $\mathcal{A}_{\mathbf{s},b,i}$, $b \in \{L, U\}$:

$$P(\mathbf{s} \in \mathcal{A}_{\mathbf{s},b,i}) \approx P(\mathbf{s} \in \hat{\mathcal{A}}_{\mathbf{s},b,i}) = \Phi(\beta_{b,i}). \quad (3.65)$$

So, the integration of the multivariate Gaussian pdf of the statistical parameters \mathbf{s} in the approximate individual parameter acceptance region partition $\hat{\mathcal{A}}_{\mathbf{s},b,i}$ to obtain the probability $P(\mathbf{s} \in \hat{\mathcal{A}}_{\mathbf{s},b,i})$ that the statistical parameters \mathbf{s} lie in the approximate individual parameter acceptance region partition $\hat{\mathcal{A}}_{\mathbf{s},b,i}$ and thus approximately the probability $P(\mathbf{s} \in \mathcal{A}_{\mathbf{s},b,i})$ that they lie in the actual individual parameter acceptance region partition $\mathcal{A}_{\mathbf{s},b,i}$ simplifies to one evaluation of the standard normal cdf $\Phi(x)$ at the worst-case distance $\beta_{b,i}$. The peak of the multivariate Gaussian pdf of the statistical parameters \mathbf{s} at their mean \mathbf{s}_0 has to lie in the individual parameter acceptance region partition $\mathcal{A}_{\mathbf{s},b,i}$, $b \in \{L, U\}$, and it has to be rather concentrated around its

peak in order to be able to achieve a large probability $P(\mathbf{s} \in \mathcal{A}_{\mathbf{s},b,i})$ that the statistical parameters \mathbf{s} lie in the individual parameter acceptance region partition $\mathcal{A}_{\mathbf{s},b,i}$ and thus the corresponding performance specification $f_i \geq f_{L,i}$ if $b = L$ or $f_i \leq f_{U,i}$ if $b = U$ is fulfilled, which is a requirement for achieving a high probability Y of fulfilling all performance specifications $f_{L,i} \leq f_i \leq f_{U,i}$, $i = 1, 2, \dots, N_f$. In addition, the maximum of the multivariate Gaussian pdf of the statistical parameters \mathbf{s} along the boundary of the individual parameter acceptance region partition $\mathcal{A}_{\mathbf{s},b,i}$ occurs exactly where the tangential hyperplane, the boundary of the corresponding approximate individual parameter acceptance region partition $\hat{\mathcal{A}}_{\mathbf{s},b,i}$, touches it and thus the approximation error between them is zero. Hence, the approximation has the advantageous property that the multivariate Gaussian pdf of the statistical parameters \mathbf{s} is small where the approximation error between the boundaries of the individual parameter acceptance region partition $\mathcal{A}_{\mathbf{s},b,i}$ and the corresponding approximate individual parameter acceptance region partition $\hat{\mathcal{A}}_{\mathbf{s},b,i}$ is large such that the approximation of the probability $P(\mathbf{s} \in \mathcal{A}_{\mathbf{s},b,i})$ that the statistical parameters \mathbf{s} lie in the individual parameter acceptance region partition $\mathcal{A}_{\mathbf{s},b,i}$ by the probability $P(\mathbf{s} \in \hat{\mathcal{A}}_{\mathbf{s},b,i})$ that they lie in the corresponding approximate individual parameter acceptance region partition $\hat{\mathcal{A}}_{\mathbf{s},b,i}$ is accurate. Moreover, the boundaries of the actual and approximate individual parameter acceptance region partitions $\mathcal{A}_{\mathbf{s},b,i}$ and $\hat{\mathcal{A}}_{\mathbf{s},b,i}$, respectively, might touch or intersect at more than one point, where the approximation error is zero as well.

The approximation of the probability $P(\mathbf{s} \in \mathcal{A}_{\mathbf{s},b,i})$ that the statistical parameters \mathbf{s} lie in the individual parameter acceptance region partition $\mathcal{A}_{\mathbf{s},b,i}$, $b \in \{L, U\}$, by the probability $P(\mathbf{s} \in \hat{\mathcal{A}}_{\mathbf{s},b,i})$ that they lie in the approximate individual parameter acceptance region partition $\hat{\mathcal{A}}_{\mathbf{s},b,i}$ using the worst-case distance $\beta_{b,i}$ in (3.65) allows to approximate the probability $P(\mathbf{s} \in \mathcal{A}_{\mathbf{s},L,i} \cap \mathcal{A}_{\mathbf{s},U,i})$ that they lie in the intersection $\mathcal{A}_{\mathbf{s},L,i} \cap \mathcal{A}_{\mathbf{s},U,i}$ of the two individual parameter acceptance region partitions $\mathcal{A}_{\mathbf{s},L,i}$ and $\mathcal{A}_{\mathbf{s},U,i}$. Such an intersection $\mathcal{A}_{\mathbf{s},L,i} \cap \mathcal{A}_{\mathbf{s},U,i}$, which is illustrated in Figure 3.4 for the two exemplary individual parameter acceptance region partitions $\mathcal{A}_{\mathbf{s},L,i}$ and $\mathcal{A}_{\mathbf{s},U,i}$ from Figure 3.2 and Figure 3.3, respectively, with two statistical parameters $\mathbf{s} = [s_1, s_2]^T$, is given by (3.57). It is the set of all statistical parameters \mathbf{s} for which the i^{th} performance property f_i lies in its acceptance interval $[f_{L,i}, f_{U,i}]$ such that the i^{th} performance specification $f_{L,i} \leq f_i \leq f_{U,i}$ defined by this acceptance interval is fulfilled. Therefore, the probability that the statistical parameters \mathbf{s} lie in the intersection $\mathcal{A}_{\mathbf{s},L,i} \cap \mathcal{A}_{\mathbf{s},U,i}$ is the probability that the i^{th} performance property f_i lies in its acceptance interval

$[f_{L,i}, f_{U,i}]$ and can be expressed as

$$\begin{aligned}
 P(\mathbf{s} \in \mathcal{A}_{\mathbf{s},L,i} \cap \mathcal{A}_{\mathbf{s},U,i}) &= P(f_{L,i} \leq f_i \leq f_{U,i}) \\
 &= P(f_i \leq f_{U,i}) - P(f_i < f_{L,i}) \\
 &= P(f_i \leq f_{U,i}) - (1 - P(f_i \geq f_{L,i})) \\
 &= P(\mathbf{s} \in \mathcal{A}_{\mathbf{s},U,i}) - (1 - P(\mathbf{s} \in \mathcal{A}_{\mathbf{s},L,i})) \\
 &= P(\mathbf{s} \in \mathcal{A}_{\mathbf{s},L,i}) + P(\mathbf{s} \in \mathcal{A}_{\mathbf{s},U,i}) - 1.
 \end{aligned} \tag{3.66}$$

Using (3.65), this probability can be approximated by

$$P(\mathbf{s} \in \mathcal{A}_{\mathbf{s},L,i} \cap \mathcal{A}_{\mathbf{s},U,i}) \approx \Phi(\beta_{L,i}) + \Phi(\beta_{U,i}) - 1 \tag{3.67}$$

if both the lower bound $f_{L,i}$ and the upper bound $f_{U,i}$ of the acceptance interval for the i^{th} performance property f_i corresponding to the individual parameter acceptance region partitions $\mathcal{A}_{\mathbf{s},L,i}$ and $\mathcal{A}_{\mathbf{s},U,i}$ with the worst-case distances $\beta_{L,i}$ and $\beta_{U,i}$, respectively, are finite. If only one of the two bounds $f_{L,i}$ and $f_{U,i}$ of the acceptance interval for the i^{th} performance property f_i , namely, $f_{b,i}$, $b \in \{L, U\}$, is finite while the other bound $f_{\bar{b},i}$ is not finite, the individual parameter acceptance region partition that corresponds to the bound $f_{\bar{b},i}$ of the acceptance interval for the i^{th} performance property f_i that is not finite is $\mathcal{A}_{\mathbf{s},\bar{b},i} = \mathbb{R}^{N_s}$ such that the intersection $\mathcal{A}_{\mathbf{s},L,i} \cap \mathcal{A}_{\mathbf{s},U,i} = \mathcal{A}_{\mathbf{s},b,i} \cap \mathcal{A}_{\mathbf{s},\bar{b},i}$ of the two individual parameter acceptance region partitions $\mathcal{A}_{\mathbf{s},L,i}$ and $\mathcal{A}_{\mathbf{s},U,i}$ simplifies to the individual parameter acceptance region partition $\mathcal{A}_{\mathbf{s},b,i}$ that corresponds to the finite bound $f_{b,i}$ of the acceptance interval for the i^{th} performance property f_i , i.e., $\mathcal{A}_{\mathbf{s},L,i} \cap \mathcal{A}_{\mathbf{s},U,i} = \mathcal{A}_{\mathbf{s},b,i}$. In this case, the probability $P(\mathbf{s} \in \mathcal{A}_{\mathbf{s},L,i} \cap \mathcal{A}_{\mathbf{s},U,i})$ that the statistical parameters \mathbf{s} lie in the intersection $\mathcal{A}_{\mathbf{s},L,i} \cap \mathcal{A}_{\mathbf{s},U,i}$ of the two individual parameter acceptance region partitions $\mathcal{A}_{\mathbf{s},L,i}$ and $\mathcal{A}_{\mathbf{s},U,i}$ consequently simplifies to the probability $P(\mathbf{s} \in \mathcal{A}_{\mathbf{s},b,i})$ that they lie in the individual parameter acceptance region partition $\mathcal{A}_{\mathbf{s},b,i}$ that corresponds to the finite bound $f_{b,i}$ of the acceptance interval for the i^{th} performance property f_i and can be approximated by the corresponding worst-case distance $\beta_{b,i}$ as stated in (3.65), i.e., $P(\mathbf{s} \in \mathcal{A}_{\mathbf{s},L,i} \cap \mathcal{A}_{\mathbf{s},U,i}) = P(\mathbf{s} \in \mathcal{A}_{\mathbf{s},b,i}) \approx \Phi(\beta_{b,i})$. To sum up,

$$P(\mathbf{s} \in \mathcal{A}_{\mathbf{s},L,i} \cap \mathcal{A}_{\mathbf{s},U,i}) \approx \begin{cases} \Phi(\beta_{U,i}), & f_{L,i} \rightarrow -\infty \\ \Phi(\beta_{L,i}), & f_{U,i} \rightarrow \infty \\ \Phi(\beta_{L,i}) + \Phi(\beta_{U,i}) - 1, & \text{otherwise} \end{cases} . \tag{3.68}$$

Since the parameter acceptance region $\mathcal{A}_{\mathbf{s}}$ is the intersection of all intersections of two individual parameter acceptance region partitions $\mathcal{A}_{\mathbf{s},L,i}$ and $\mathcal{A}_{\mathbf{s},U,i}$,

$i = 1, 2, \dots, N_f$, according to (3.56), the probability that the statistical parameters \mathbf{s} do not lie in the parameter acceptance region \mathcal{A}_s can be expressed as

$$\begin{aligned} P(\mathbf{s} \notin \mathcal{A}_s) &= P\left(\mathbf{s} \notin \bigcap_{i=1}^{N_f} \mathcal{A}_{s,L,i} \cap \mathcal{A}_{s,U,i}\right) = P\left(\bigvee_{i=1}^{N_f} \mathbf{s} \notin \mathcal{A}_{s,L,i} \cap \mathcal{A}_{s,U,i}\right) \\ &\approx \sum_{i=1}^{N_f} P(\mathbf{s} \notin \mathcal{A}_{s,L,i} \cap \mathcal{A}_{s,U,i}) = \sum_{i=1}^{N_f} 1 - P(\mathbf{s} \in \mathcal{A}_{s,L,i} \cap \mathcal{A}_{s,U,i}). \end{aligned} \quad (3.69)$$

With (3.68), the probability Y of fulfilling all performance specifications $f_{L,i} \leq f_i \leq f_{U,i}$ defined by the acceptance intervals $[f_{L,i}, f_{U,i}]$ for the performance properties f_i , $i = 1, 2, \dots, N_f$, can be approximated by

$$\begin{aligned} Y &= P(\mathbf{f} \in \mathcal{A}_f) = P(\mathbf{s} \in \mathcal{A}_s) = 1 - P(\mathbf{s} \notin \mathcal{A}_s) \\ &\approx 1 - \sum_{i=1}^{N_f} 1 - P(\mathbf{s} \in \mathcal{A}_{s,L,i} \cap \mathcal{A}_{s,U,i}) \\ &\approx 1 - \sum_{i=1}^{N_f} 1 - \begin{cases} \Phi(\beta_{U,i}), & f_{L,i} \rightarrow -\infty \\ \Phi(\beta_{L,i}), & f_{U,i} \rightarrow \infty \\ \Phi(\beta_{L,i}) + \Phi(\beta_{U,i}) - 1, & \text{otherwise} \end{cases} \end{aligned} \quad (3.70)$$

So, the integration of the multivariate Gaussian pdf of the statistical parameters \mathbf{s} in the parameter acceptance region \mathcal{A}_s from (3.58) to obtain the probability Y of fulfilling the performance specifications is simplified to approximating this probability Y by evaluating the standard normal cdf $\Phi(x)$ at the worst-case distances $\beta_{b,i}$, $i = 1, 2, \dots, N_f$, $b = L, U$. Each required worst-case distance $\beta_{b,i}$ can be determined by solving the optimization problem (3.59) if $b = L$ and (3.60) if $b = U$, i.e., an optimization minimizing the distance between the statistical parameters \mathbf{s} on the boundary of the corresponding individual parameter acceptance region partition $\mathcal{A}_{s,b,i}$ and their mean \mathbf{s}_0 without determining the whole boundary of the parameter acceptance region \mathcal{A}_s . These optimizations just require a few system simulations, which are automatically chosen by an appropriate optimization method for solving these optimizations in a smart way serving the achievement of the optimization goal, and thus replace a computationally expensive Monte Carlo simulation, which just chooses an extensive amount of system simulations according to the underlying probability distribution in a brute-force way for estimating the probability of interest, i.e., the probability Y of fulfilling the performance specifications, by a few relevant simulations that deliver the

3.2 *Simulation-Based Robust System Design*

required information for approximating this probability. This is the reason why approximating the probability Y of fulfilling the performance specifications by worst-case distances can lead to a significant reduction of computational complexity in the robust system design as compared to estimating it by a Monte Carlo simulation when a high estimation accuracy is required.

Robust Design of Automated Vehicular Safety Systems

4

After giving a general overview of a robust system design as performed in integrated circuit design by the previous chapter as a preparation, this chapter demonstrates the analogies between such a robust system design and the robust design of automated vehicular safety systems considering sensor measurement errors, and explains how it can be transferred to the design of automated vehicular safety systems. Based on this and the mathematical model for automated vehicular safety systems introduced in Chapter 2, the robust design of automated vehicular safety systems considering sensor measurement errors is formulated as optimization problems. This finally results in a methodology for the robust function and sensor design that allows to systematically design both functions and sensors of automated vehicular safety systems by solving the formulated optimization problems such that the customer requirements are fulfilled in a robust manner despite unavoidable sensor measurement errors.

4.1 Problem Formulation for Robust Design of Automated Vehicular Safety Systems

Application engineers having to select sensors with appropriate properties and to adjust the functions in the development of automated vehicular safety systems are typically confronted with the three basic design problems illustrated in Figure 4.1, namely, the function design for given sensors, the sensor design for a given function as well as the joint function and sensor design.

4.1.1 Function Design

In the function design, where the sensors to be used in the automated vehicular safety system under design and, in particular, the properties of their measurement errors in form of a probability distribution are given already, the design goal is to adapt the function to the given sensors such that it meets the requirements of the customers in a robust manner despite the unavoidable sensor measurement errors. Similarly to

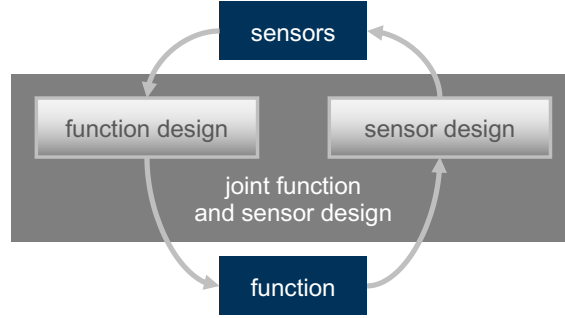


Figure 4.1: Basic design problems in the development of automated vehicular safety systems.

the robust system design where the quality measure is maximized with respect to the deterministic design parameters d of the system under design in order to determine the optimal values d_{opt} for them as formulated in (3.8) with the probability Y of fulfilling the performance specifications as the quality measure, a quality measure Q , which measures to what extent the function meets the customer requirements in a robust manner despite the unavoidable sensor measurement errors, can be maximized with respect to the decision rule f from a set \mathcal{F} of predefined decision rules for triggering the respective action by the function and its adjustable parameters φ in order to determine the best decision rule f_{opt} and the optimal function parameter values φ_{opt} with respect to this quality measure Q . Formally, this systematic approach for the function design can be formulated as the following optimization problem:

$$(f_{\text{opt}}, \varphi_{\text{opt}}) = \underset{f \in \mathcal{F}, \varphi \in \mathbb{R}^{N_\varphi}}{\text{argmax}} Q. \quad (4.1)$$

The quality measure $Q = Q(f, \varphi)$ depends on both the decision rule f and the function parameters φ , and is thus a function of them:

$$Q : \mathcal{F} \times \mathbb{R}^{N_\varphi} \rightarrow \mathbb{R}, (f, \varphi) \mapsto Q(f, \varphi). \quad (4.2)$$

Solving the optimization problem (4.1) determines the best decision rule f_{opt} by ranking all predefined decision rules f in \mathcal{F} with respect to the maximal quality level

$$Q_{\text{max}}(f) = \max_{\varphi \in \mathbb{R}^{N_\varphi}} Q(f, \varphi) \quad (4.3)$$

that they can achieve when adjusting the function parameters φ in order to choose the best decision rule f_{opt} of them based on this ranking, which is the decision rule f

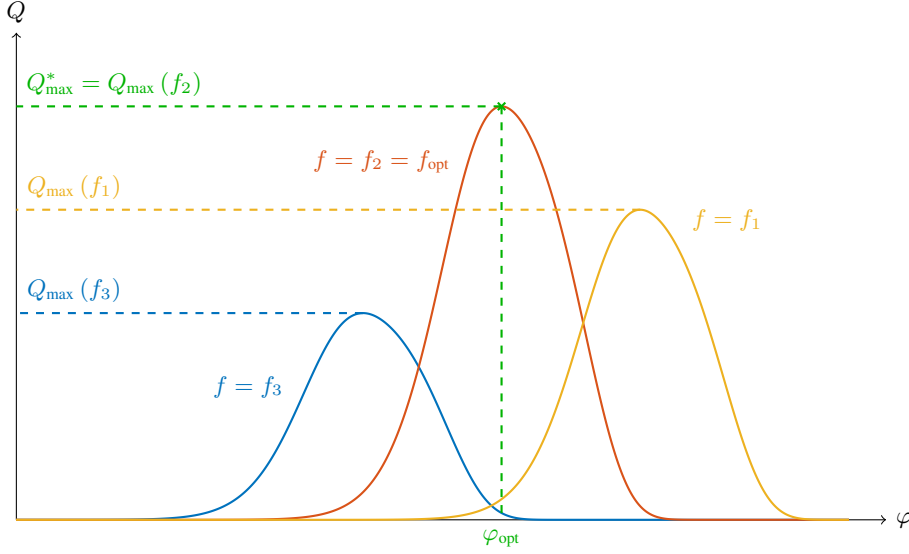


Figure 4.2: Function design for the set $\mathcal{F} = \{f_1, f_2, f_3\}$ of decision rules with one adjustable function parameter $\varphi = \varphi \in \mathbb{R}$.

whose maximal achievable quality level $Q_{\max}(f)$ is the highest maximal achievable quality level

$$Q_{\max}^* = \max_{f \in \mathcal{F}} Q_{\max}(f) = \max_{f \in \mathcal{F}} \max_{\varphi \in \mathbb{R}^{N_\varphi}} Q(f, \varphi) = \max_{f \in \mathcal{F}, \varphi \in \mathbb{R}^{N_\varphi}} Q(f, \varphi) \quad (4.4)$$

of all f in \mathcal{F} . The function parameter values φ corresponding to this highest maximal achievable quality level Q_{\max}^* , i.e., for which $Q(f_{\text{opt}}, \varphi) = Q_{\max}^*$, are the optimal function parameter values φ_{opt} . Using the so obtained best decision rule $f_{\text{opt}}(\cdot; \varphi_{\text{opt}})$ with the optimal function parameters φ_{opt} for triggering the respective action by the function ensures that the highest quality level Q_{\max}^* that can be achieved with the given sensors is reached and thus the requirements of the customers are met in a robust manner despite the unavoidable sensor measurement errors to the greatest possible extent.

The quality measure Q is illustrated in Figure 4.2 as a function of one function parameter $\varphi = \varphi \in \mathbb{R}$ for three different decision rules f_1 , f_2 and f_3 , each of which can be used for triggering the respective action by the function and whose only adjustable function parameter φ is φ . If the set \mathcal{F} of predefined decision rules for triggering the respective action by the function consists of f_1 , f_2 and f_3 , the function is designed for given sensors, i.e., given sensor parameters σ , by maximizing the

quality measure Q with respect to the decision rule f from $\mathcal{F} = \{f_1, f_2, f_3\}$ and the single function parameter φ according to the optimization problem (4.1). This maximization of the quality measure Q results in the best decision rule $f_{\text{opt}} = f_2$ and the corresponding optimal function parameter $\varphi_{\text{opt}} = \varphi_{\text{opt}}$, for which the highest maximal achievable quality level Q_{max}^* of all f in \mathcal{F} is reached, i.e., $Q = Q_{\text{max}}^*$. This is highlighted in Figure 4.2. The highest maximal achievable quality level Q_{max}^* of all f in \mathcal{F} according to (4.4) is the maximal achievable quality level $Q_{\text{max}}(f_2)$ of the second decision rule f_2 according to (4.3) while the maximal achievable quality level $Q_{\text{max}}(f_1)$ of the first decision rule f_1 is smaller and the maximal achievable quality level $Q_{\text{max}}(f_3)$ of the third decision rule f_3 is even smaller. Based on the ranking of the decision rules f in \mathcal{F} with respect to the maximal achievable quality level $Q_{\text{max}}(f)$, i.e., $Q_{\text{max}}(f_3) < Q_{\text{max}}(f_1) < Q_{\text{max}}(f_2) = Q_{\text{max}}^*$, the first decision rule f_1 is better than the third decision rule f_3 and the second decision rule $f_2 = f_{\text{opt}}$ is better than the first decision rule f_1 and thus the best one.

4.1.2 Sensor Design

In the sensor design, where the function to be used in the automated vehicular safety system under design is given already, the design goal is to determine which requirements the sensors have to fulfill such that the given function meets the requirements of the customers in a robust manner despite the unavoidable sensor measurement errors, and appropriate sensors fulfilling these requirements. The desired extent to which the function meets the requirements of the customers in a robust manner despite the unavoidable sensor measurement errors can be expressed in form of a required minimum quality level Q_{min} .

The quality measure $Q = Q(\sigma)$ depends on the sensor parameters σ , and is thus a function of them:

$$Q : \mathcal{S} \rightarrow \mathbb{R}, \sigma \mapsto Q(\sigma). \quad (4.5)$$

The set of all sensor parameter values σ in the possible domain $\mathcal{S} \subseteq \mathbb{R}^{N_\sigma}$ for which the quality measure $Q = Q(\sigma)$ does not lie below this required minimum quality level Q_{min} is the design space

$$\mathcal{D} = \{\sigma \in \mathcal{S} : Q \geq Q_{\text{min}}\} \quad (4.6)$$

from which the application engineer has to choose the sensor parameter values σ such that the customer requirements are met in a robust manner despite the unavoidable sensor measurement errors to the desired extent. Hence, the application engineer is provided with an entire design space \mathcal{D} that represents the requirements the sensors have

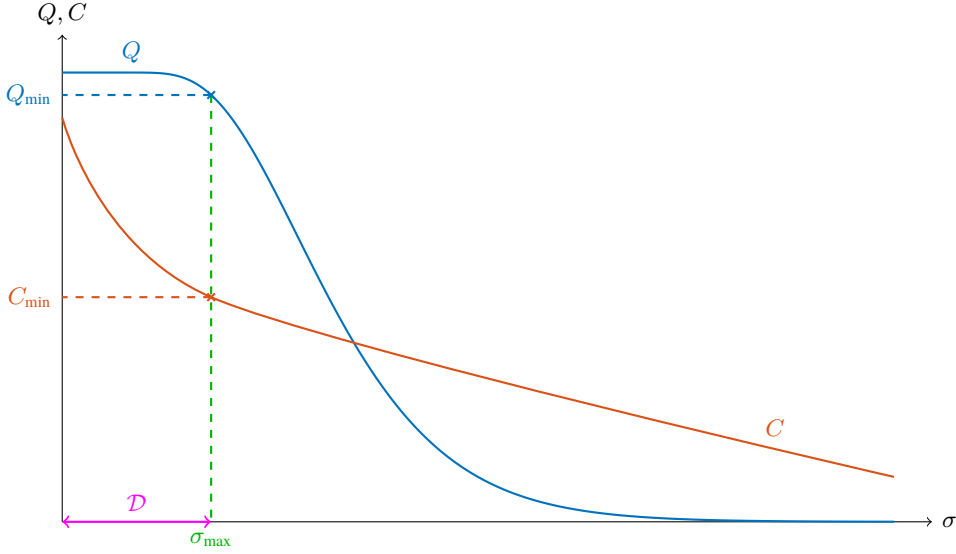


Figure 4.3: Sensor design for one sensor parameter $\sigma = \sigma \in \mathcal{S} = \mathbb{R}^+$.

to fulfill, which is of particular importance for the overall design task in an industrial environment. An example for such a design space \mathcal{D} can be seen in Figure 4.3, where the quality measure Q is illustrated as a function of one sensor parameter $\sigma = \sigma$, which is considered to be the only sensor parameter σ whose value can be chosen in the sensor design and to be positive, i.e., $\mathcal{S} = \mathbb{R}^+$. This design space \mathcal{D} is the interval $(0, \sigma_{\max}]$ of the sensor parameter σ , where the quality measure Q does not lie below the required minimum quality level Q_{\min} and whose upper limit is σ_{\max} .

Inside such a design space \mathcal{D} , costs $C = C(\sigma)$ which depend on the sensor parameters σ , i.e., a cost function

$$C : \mathbb{R}^{N_\sigma} \rightarrow \mathbb{R}, \sigma \mapsto C(\sigma), \quad (4.7)$$

can be minimized with respect to the sensor parameters σ in order to optimize a relevant objective, e.g., minimize the costs of the sensors, and determine the optimal sensor parameter values σ_{opt} with respect to the costs C and the quality measure Q . Formally formulating this systematic approach for the sensor design leads to the following optimization problem, where the design space \mathcal{D} is incorporated by the constraint:

$$\sigma_{\text{opt}} = \underset{\sigma \in \mathcal{S}}{\operatorname{argmin}} C \quad \text{s.t.} \quad \sigma \in \mathcal{D}. \quad (4.8)$$

This optimization problem is equivalent to the optimization problem

$$\sigma_{\text{opt}} = \underset{\sigma \in \mathcal{S}}{\operatorname{argmin}} C \quad \text{s.t.} \quad Q \geq Q_{\min}. \quad (4.9)$$

The choice of sensors whose sensor parameters σ have the optimal sensor parameter values σ_{opt} obtained by solving this optimization problem guarantees that the quality measure Q does not lie below the required minimum quality level Q_{\min} and thus the customer requirements are met in a robust manner despite the unavoidable sensor measurement errors to the desired extent at minimal costs

$$C_{\min} = \min_{\sigma \in \mathcal{S}} C \quad \text{s.t.} \quad Q \geq Q_{\min}. \quad (4.10)$$

Besides the quality measure Q as a function of the only sensor parameter $\sigma = \sigma \in \mathbb{R}^+$ whose value can be chosen in the sensor design, also possible costs C are illustrated as a function of this sensor parameter σ in Figure 4.3. As these costs C monotonically decrease when the sensor parameter σ increases, the cost function C is minimal if and only if σ is maximal. This converts the minimization of the cost function C in the stated optimization problem (4.9) of the sensor design into the maximization of the sensor parameter σ . As a consequence, the sensors are designed for a given function, i.e., a given decision rule f and given function parameters φ , by determining the largest value of the sensor parameter σ inside the design space \mathcal{D} , which is the upper limit σ_{\max} of the design space \mathcal{D} highlighted in Figure 4.3.

4.1.3 Joint Function and Sensor Design

The joint function and sensor design is a combination of the two aforementioned design problems, where neither the sensors nor the function of the automated vehicular safety system under design are given. The design goal is to determine both the sensors and the function such that the function meets the requirements of the customers in a robust manner despite the unavoidable sensor measurement errors. Formally, the joint function and sensor design can also be formulated as an optimization problem:

$$(\sigma_{\text{opt}}, f_{\text{opt}}, \varphi_{\text{opt}}) = \underset{\sigma \in \mathcal{S}, f \in \mathcal{F}, \varphi \in \mathbb{R}^{N_\varphi}}{\operatorname{argmin}} C \quad \text{s.t.} \quad Q \geq Q_{\min}. \quad (4.11)$$

This optimization problem is an extension of the optimization problem (4.9) for the sensor design by additional optimization variables such that the costs C are not only minimized with respect to the sensor parameters σ in the possible domain $\mathcal{S} \subseteq \mathbb{R}^{N_\sigma}$ but also with respect to the decision rule f from a set \mathcal{F} of predefined decision rules and its adjustable parameters φ while ensuring that the quality measure Q does not lie

below the required minimum quality level Q_{\min} and thus the customer requirements are met in a robust manner despite the unavoidable sensor measurement errors to the desired extent. While the cost function describing the costs $C = C(\sigma)$ as a function of the sensor parameters σ is still the same as that for the sensor design in (4.7), the quality measure $Q = Q(\sigma, f, \varphi)$ is now considered to be a function of all optimization variables, i.e., the sensor parameters σ and the additional optimization variables, namely, the decision rule f and the function parameters φ :

$$Q : \mathcal{S} \times \mathcal{F} \times \mathbb{R}^{N_\varphi} \rightarrow \mathbb{R}, (\sigma, f, \varphi) \mapsto Q(\sigma, f, \varphi). \quad (4.12)$$

Due to the larger number of optimization variables providing more degrees of freedom for solving the optimization problem, the minimal costs

$$C_{\min}^* = \min_{\sigma \in \mathcal{S}, f \in \mathcal{F}, \varphi \in \mathbb{R}^{N_\varphi}} C \quad \text{s.t.} \quad Q \geq Q_{\min} \quad (4.13)$$

resulting from the solution of the optimization problem (4.11) for the joint function and sensor design are as small as or even smaller than the minimal costs C_{\min} resulting from the solution of the optimization problem (4.9) for the sensor design in (4.10). This demonstrates the power of the joint function and sensor design as compared to the sensor design, where reaching smaller minimal costs C_{\min} is restricted by the given function, i.e., the given decision rule f and the given function parameters φ , which would possibly allow to reach smaller minimal costs C_{\min} if they could be chosen appropriately. Solving the optimization problem (4.11) for the joint function and sensor design determines the best decision rule f_{opt} by ranking all predefined decision rules f with respect to the minimal costs

$$C_{\min}(f) = \min_{\sigma \in \mathcal{S}, \varphi \in \mathbb{R}^{N_\varphi}} C(\sigma) \quad \text{s.t.} \quad Q(\sigma, f, \varphi) \geq Q_{\min} \quad (4.14)$$

that they allow to reach for a given required minimum quality level Q_{\min} by choosing the sensor parameters σ and adjusting the function parameters φ in order to choose the best decision rule f_{opt} of them based on this ranking, which is the decision rule f for which the minimal reachable costs $C_{\min}(f)$ are the smallest minimal reachable costs

$$\begin{aligned} C_{\min}^* &= \min_{f \in \mathcal{F}} C_{\min}(f) = \min_{f \in \mathcal{F}} \min_{\sigma \in \mathcal{S}, \varphi \in \mathbb{R}^{N_\varphi}} C(\sigma) \quad \text{s.t.} \quad Q(\sigma, f, \varphi) \geq Q_{\min} \\ &= \min_{\sigma \in \mathcal{S}, f \in \mathcal{F}, \varphi \in \mathbb{R}^{N_\varphi}} C(\sigma) \quad \text{s.t.} \quad Q(\sigma, f, \varphi) \geq Q_{\min} \end{aligned} \quad (4.15)$$

of all f in \mathcal{F} . The sensor parameter values σ and function parameter values φ corresponding to these smallest minimal reachable costs C_{\min}^* , i.e., for which $C(\sigma, f_{\text{opt}}, \varphi) =$

C_{\min}^* , are the optimal sensor parameters values σ_{opt} and the optimal function parameter values φ_{opt} , respectively. Using the so obtained best decision rule $f_{\text{opt}}(\cdot; \varphi_{\text{opt}})$ with the optimal function parameters φ_{opt} for triggering the respective action by the function in combination with sensors whose sensor parameters σ have the obtained optimal sensor parameter values σ_{opt} guarantees that the quality measure Q does not lie below the required minimum quality level Q_{\min} and thus the customer requirements are met in a robust manner despite the unavoidable sensor measurement errors to the desired extent at minimal costs C_{\min}^* .

The constraint of the optimization problem (4.11) again defines the design space, which, in case of the joint function and sensor design, is the set

$$\mathcal{D} = \{(\sigma, f, \varphi) \in \mathcal{S} \times \mathcal{F} \times \mathbb{R}^{N_\varphi} : Q \geq Q_{\min}\}, \quad (4.16)$$

from which the application engineer has to choose the sensor parameter values σ , the decision rule f and the function parameter values φ such that the constraint is fulfilled, i.e., the quality measure Q is not smaller than the required minimum quality level Q_{\min} and thus the customer requirements are met in a robust manner despite the unavoidable sensor measurement errors to the desired extent. Consequently, the optimization problem (4.11) to be solved for the joint function and sensor design can also be expressed in terms of this design space \mathcal{D} the application engineer is provided with:

$$(\sigma_{\text{opt}}, f_{\text{opt}}, \varphi_{\text{opt}}) = \underset{\sigma \in \mathcal{S}, f \in \mathcal{F}, \varphi \in \mathbb{R}^{N_\varphi}}{\text{argmin}} C \quad \text{s.t.} \quad (\sigma, f, \varphi) \in \mathcal{D}. \quad (4.17)$$

So, the optimal sensor parameter values σ_{opt} , the best decision rule f_{opt} and the optimal function parameter values φ_{opt} are the sensor parameter values σ , the decision rule f and the function parameter values φ inside the design space \mathcal{D} for which the costs C are minimum.

This is illustrated in Figure 4.4, Figure 4.5 and Figure 4.6, which show the contour lines of the quality measure Q considered as a function of one sensor parameter $\sigma = \sigma \in \mathcal{S} = \mathbb{R}^+$ and one function parameter $\varphi = \varphi \in \mathbb{R}$ for three different decision rules f_1, f_2 and f_3 , respectively. Along each contour line, the quality measure Q has one of the constant values Q_1, Q_2, Q_3 and Q_4 sorted in ascending order such that $Q_1 < Q_2 < Q_3 < Q_4$. As for the function design before, φ is assumed to be the only adjustable function parameter φ of each predefined decision rule f in the set $\mathcal{F} = \{f_1, f_2, f_3\}$, from which the decision rule for triggering the respective action by the function is to be chosen, also for the joint function and sensor design while σ is considered to be the only sensor parameter σ whose value is to be chosen from the

4.1 Problem Formulation for Robust Design of Automated Vehicular Safety Systems

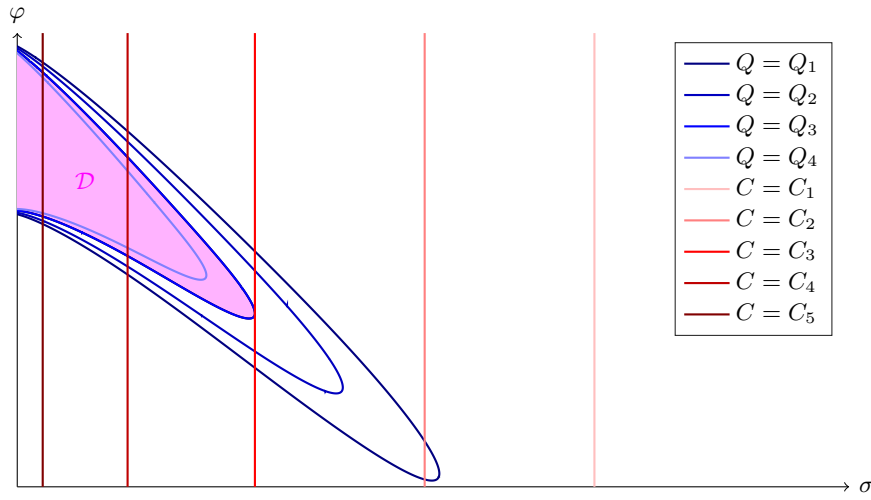


Figure 4.4: Joint function and sensor design for one sensor parameter $\sigma = \sigma \in \mathcal{S} = \mathbb{R}^+$ and the set $\mathcal{F} = \{f_1, f_2, f_3\}$ of decision rules f with one adjustable function parameter $\varphi = \varphi \in \mathbb{R}$, where $f = f_1$, $Q_1 < Q_2 < Q_3 = Q_{\min} < Q_4$ and $C_1 < C_2 < C_3 = C_{\min}(f_1) < C_4 < C_5$.

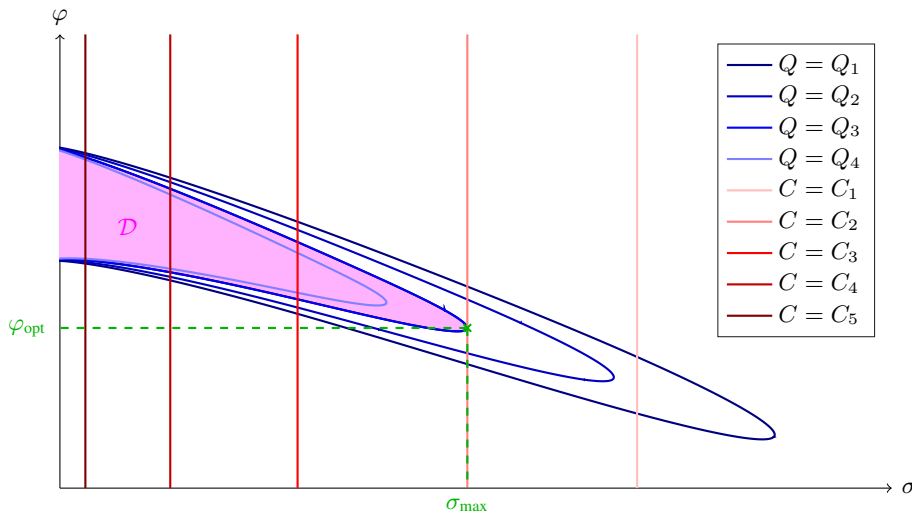


Figure 4.5: Joint function and sensor design for one sensor parameter $\sigma = \sigma \in \mathcal{S} = \mathbb{R}^+$ and the set $\mathcal{F} = \{f_1, f_2, f_3\}$ of decision rules f with one adjustable function parameter $\varphi = \varphi \in \mathbb{R}$, where $f = f_2 = f_{\text{opt}}$, $Q_1 < Q_2 < Q_3 = Q_{\min} < Q_4$ and $C_1 < C_2 = C_{\min}(f_2) = C_{\min}^* < C_3 < C_4 < C_5$.

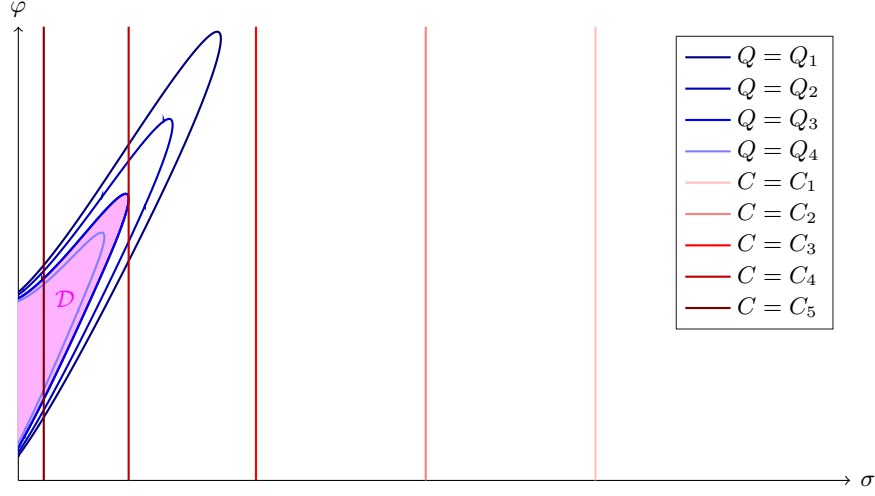


Figure 4.6: Joint function and sensor design for one sensor parameter $\sigma = \sigma \in \mathcal{S} = \mathbb{R}^+$ and the set $\mathcal{F} = \{f_1, f_2, f_3\}$ of decision rules f with one adjustable function parameter $\varphi = \varphi \in \mathbb{R}$, where $f = f_3$, $Q_1 < Q_2 < Q_3 = Q_{\min} < Q_4$ and $C_1 < C_2 < C_3 < C_4 = C_{\min}(f_3) < C_5$.

possible domain $\mathcal{S} = \mathbb{R}^+$ as in the sensor design before. Besides the contour lines of the quality measure Q , the design space \mathcal{D} corresponding to the required minimum quality level $Q_{\min} = Q_3$ is shown. It is the magenta region where the sensor parameter σ , the decision rule f and the function parameter φ correspond to a quality measure Q that does not lie below the required minimum quality level $Q_{\min} = Q_3$, which is bounded by the contour lines of the quality measure Q along which the quality measure Q is exactly Q_3 such that the required minimum quality level Q_{\min} is just reached. In addition, also the contour lines of the costs C which have already been considered in the sensor design before and monotonically decrease with increasing sensor parameter value σ are shown. Along each contour line, the costs C have one of the constant values C_1, C_2, C_3, C_4 and C_5 sorted in ascending order such that $C_1 < C_2 < C_3 < C_4 < C_5$. In Figure 4.4, Figure 4.5 and Figure 4.6, it can be observed that the minimal reachable costs $C_{\min}(f)$ corresponding to the maximal sensor parameter σ inside the design space \mathcal{D} , where $Q \geq Q_{\min} = Q_3$, according to (4.14) are $C_{\min}(f_1) = C_3$ for the first decision rule f_1 , $C_{\min}(f_2) = C_2$ for the second decision rule f_2 and $C_{\min}(f_3) = C_4$ for the third decision rule f_3 , respectively. Based on the ranking of the decision rules f in \mathcal{F} with respect to the minimal reachable costs $C_{\min}(f)$, i.e., $C_{\min}(f_2) = C_2 < C_{\min}(f_1) = C_3 < C_{\min}(f_3) = C_4$, the first decision

rule f_1 is better than the third decision rule f_3 and the second decision rule f_2 is better than the first decision rule f_1 . Hence, the second decision rule f_2 is the best decision rule f_{opt} of all decision rules in \mathcal{F} and the corresponding minimal reachable costs $C_{\min}(f_2) = C_2$ are the smallest minimal reachable costs C_{\min}^* according to (4.15), i.e., $f_{\text{opt}} = f_2$ and $C_{\min}^* = C_{\min}(f_2) = C_2$. The function parameter value φ and the sensor parameter value σ corresponding to these smallest minimal reachable costs C_{\min}^* are the optimal function parameter value φ_{opt} and the optimal sensor parameter value σ_{max} , respectively. This solution of the stated optimization problem (4.11) for the joint function and sensor design is highlighted by the green cross in Figure 4.5. As the costs C monotonically decrease when the sensor parameter σ increases, which converts the minimization of the cost function C in the stated optimization problem (4.11) for the joint function and sensor design into the maximization of the sensor parameter σ , the optimal sensor parameter value σ_{max} leading to the smallest minimal reachable costs C_{\min}^* is the maximal value of the sensor parameter σ inside the design space \mathcal{D} .

4.2 Quality Measure for Robust Design of Automated Vehicular Safety Systems

In the robust system design, the probability Y of fulfilling the performance specifications defined in (3.7) can be used as quality measure, which measures to what extent systems meet the performance specifications, in order to design the systems by the maximization (3.8) of this quality measure. This can be translated to the robust design of automated vehicular safety systems considering sensor measurement errors in order to come up with an appropriate quality measure Q , which measures to what extent the function meets the customer requirements in a robust manner despite the unavoidable sensor measurement errors, and can be used in the formulated optimization problems (4.1), (4.9) and (4.11) of the function design, the sensor design as well as the joint function and sensor design, respectively.

When an automated vehicular safety system intervenes by triggering an action, relevant quantities, e.g., the final distance from an obstacle after an emergency brake intervention, have to lie in certain acceptance intervals such that the intervention is acceptable and the customer is satisfied with the system. So, the customer satisfaction can be measured in terms of these quantities, i.e., N_q customer satisfaction properties q_i , $i = 1, 2, \dots, N_q$, collected in the customer satisfaction vector $\mathbf{q} = [q_1, q_2, \dots, q_{N_q}]^T \in \mathbb{R}^{N_q}$. The acceptance intervals in which these customer satisfaction properties \mathbf{q} have to lie such that the customer is satisfied and which might be user-dependent can be chosen in a user-specific way and the acceptance interval for the

i^{th} customer satisfaction property q_i is denoted as $[q_{L,i}, q_{U,i}]$ with the lower and upper bound $q_{L,i}$ and $q_{U,i}$, respectively. If a lower bound $q_{L,i}$ does not exist, $q_{L,i} \rightarrow -\infty$, and if an upper bound $q_{U,i}$ does not exist, $q_{U,i} \rightarrow \infty$. Those acceptance intervals are specifications for the customer satisfaction and represent the customer requirements that have to be met.

The customer satisfaction properties $\mathbf{q} = [q_1, q_2, \dots, q_{N_q}]^T$ and the corresponding acceptance intervals $[q_{L,i}, q_{U,i}]$, $i = 1, 2, \dots, N_q$, play the role of the performance properties $\mathbf{f} = [f_1, f_2, \dots, f_{N_f}]^T$ and the corresponding acceptance intervals $[f_{L,i}, f_{U,i}]$, $i = 1, 2, \dots, N_f$. Analogously to the performance acceptance region \mathcal{A}_f given by (3.1), a customer satisfaction acceptance region

$$\mathcal{A}_q = \{\mathbf{q} \in \mathbb{R}^{N_q} : q_{L,i} \leq q_i \leq q_{U,i}, i = 1, 2, \dots, N_q\} \quad (4.18)$$

can be defined. It is the set of all values of the customer satisfaction properties \mathbf{q} that lie in the acceptance intervals and can thus be represented by the intersection of the individual customer satisfaction acceptance region partitions

$$\mathcal{A}_{q,L,i} = \{\mathbf{q} \in \mathbb{R}^{N_q} : q_i \geq q_{L,i}\} \text{ and } \mathcal{A}_{q,U,i} = \{\mathbf{q} \in \mathbb{R}^{N_q} : q_i \leq q_{U,i}\} \quad (4.19)$$

as the performance acceptance region \mathcal{A}_f by the intersection of the individual performance acceptance region partitions $\mathcal{A}_{f,L,i}$ and $\mathcal{A}_{f,U,i}$ given by (3.2) in (3.3):

$$\mathcal{A}_q = \bigcap_{i=1}^{N_q} \mathcal{A}_{q,L,i} \cap \mathcal{A}_{q,U,i}. \quad (4.20)$$

In the i^{th} of these individual customer satisfaction acceptance region partitions $\mathcal{A}_{q,L,i}$ and $\mathcal{A}_{q,U,i}$ into which the customer satisfaction acceptance region \mathcal{A}_q is decomposed, only the i^{th} customer satisfaction property q_i is restricted to not lie below the lower bound $q_{L,i}$ and above the upper bound $q_{U,i}$ of the corresponding acceptance interval $[q_{L,i}, q_{U,i}]$, respectively. In the special cases $q_{L,i} \rightarrow -\infty$ and $q_{U,i} \rightarrow \infty$, the corresponding individual customer satisfaction acceptance region partitions simplify to $\mathcal{A}_{q,L,i} = \mathbb{R}^{N_q}$ and $\mathcal{A}_{q,U,i} = \mathbb{R}^{N_q}$, respectively.

Triggering an action by the function of an automated vehicular safety system based on the sensor measurements and thus the customer satisfaction properties \mathbf{q} are dependent on the sensor parameters $\boldsymbol{\sigma}$ determining the used sensors, the sensor measurement errors $\varepsilon[n]$ at the $n_{\text{end}} + 1$ time instants t_n , $n = 0, 1, \dots, n_{\text{end}}$, in the

considered time interval collected in the vector

$$\boldsymbol{\varepsilon} = \begin{bmatrix} \varepsilon_1 \\ \varepsilon_2 \\ \vdots \\ \varepsilon_{E(n_{\text{end}}+1)} \end{bmatrix} = \begin{bmatrix} \boldsymbol{\varepsilon}[0] \\ \boldsymbol{\varepsilon}[1] \\ \vdots \\ \boldsymbol{\varepsilon}[n_{\text{end}}] \end{bmatrix} \in \mathbb{R}^{E(n_{\text{end}}+1)}, \quad (4.21)$$

the decision rule f used by the function for triggering the action, the function parameters $\boldsymbol{\varphi}$ determining the function and the scenario parameters $\boldsymbol{\xi}$ representing the considered driving scenario, to which the automated vehicular safety system is exposed. Hence, the customer satisfaction properties \boldsymbol{q} are a function of the sensor parameters $\boldsymbol{\sigma}$, the sensor measurement errors $\boldsymbol{\varepsilon}$ in the considered time interval, the decision rule f , the function parameters $\boldsymbol{\varphi}$ and the scenario parameters $\boldsymbol{\xi}$:

$$\boldsymbol{q} : \mathcal{S} \times \mathbb{R}^{E(n_{\text{end}}+1)} \times \mathcal{F} \times \mathbb{R}^{N_{\boldsymbol{\varphi}}} \times \mathcal{X} \rightarrow \mathbb{R}^{N_{\boldsymbol{q}}}, (\boldsymbol{\sigma}, \boldsymbol{\varepsilon}, f, \boldsymbol{\varphi}, \boldsymbol{\xi}) \mapsto \boldsymbol{q}(\boldsymbol{\sigma}, \boldsymbol{\varepsilon}, f, \boldsymbol{\varphi}, \boldsymbol{\xi}). \quad (4.22)$$

Here, \mathcal{X} denotes the set of the driving scenarios for which the automated vehicular safety system is to be designed such that the customer requirements are fulfilled and the customer is satisfied with the system in these scenarios, i.e., the set of the scenario parameters $\boldsymbol{\xi} = [\xi_1, \xi_2, \dots, \xi_{N_{\boldsymbol{\xi}}}]^T \in \mathbb{R}^{N_{\boldsymbol{\xi}}}$ of the driving scenarios each of which the automated vehicular safety system under design is supposed to handle in an acceptable way by fulfilling the specifications for the customer satisfaction.

In the introduced system model for automated vehicular safety systems, the sensor measurement errors $\boldsymbol{\varepsilon}[n]$ at the time instant t_n are assumed to be Gaussian and follow the normal distribution $\mathcal{N}(\boldsymbol{\mu}_n, \boldsymbol{C}_n)$ with the pdf $f_{\boldsymbol{\varepsilon}[n]}(\boldsymbol{\varepsilon}[n])$ given by (2.10), where $\boldsymbol{\mu}_n \in \mathbb{R}^E$ and $\boldsymbol{C}_n \in \mathbb{R}^{E \times E}$ are the mean and covariance matrix, respectively. As the sensor measurement errors $\boldsymbol{\varepsilon}[n_1]$ and $\boldsymbol{\varepsilon}[n_2]$ at different time instants t_{n_1} and t_{n_2} , $n_1, n_2 \in \{0, 1, \dots, n_{\text{end}}\}$, $n_1 \neq n_2$, are assumed to be statistically independent in addition, the pdf of the vector $\boldsymbol{\varepsilon}$ stated in (4.21), which consists of the sensor measurement errors $\boldsymbol{\varepsilon}[n]$ at all time instants t_n , $n = 0, 1, \dots, n_{\text{end}}$, in the considered

time interval, reads

$$\begin{aligned}
 f_{\varepsilon}(\varepsilon) &= \prod_{n=0}^{n_{\text{end}}} f_{\varepsilon[n]}(\varepsilon[n]) \\
 &= \prod_{n=0}^{n_{\text{end}}} \frac{1}{\sqrt{(2\pi)^E \det(\mathbf{C}_n)}} \exp\left(-\frac{1}{2}(\varepsilon[n] - \boldsymbol{\mu}_n)^T \mathbf{C}_n^{-1}(\varepsilon[n] - \boldsymbol{\mu}_n)\right) \\
 &= \frac{1}{\sqrt{(2\pi)^{E(n_{\text{end}}+1)} \prod_{n=0}^{n_{\text{end}}} \det(\mathbf{C}_n)}} \\
 &\quad \cdot \exp\left(-\frac{1}{2} \sum_{n=0}^{n_{\text{end}}} (\varepsilon[n] - \boldsymbol{\mu}_n)^T \mathbf{C}_n^{-1}(\varepsilon[n] - \boldsymbol{\mu}_n)\right).
 \end{aligned} \tag{4.23}$$

With

$$\boldsymbol{\mu} = \begin{bmatrix} \boldsymbol{\mu}_0 \\ \boldsymbol{\mu}_1 \\ \vdots \\ \boldsymbol{\mu}_{n_{\text{end}}} \end{bmatrix} \in \mathbb{R}^{E(n_{\text{end}}+1)} \tag{4.24}$$

and

$$\mathbf{C} = \begin{bmatrix} \mathbf{C}_0 & \mathbf{0} & \cdots & \mathbf{0} \\ \mathbf{0} & \mathbf{C}_1 & \cdots & \mathbf{0} \\ \vdots & \vdots & \ddots & \vdots \\ \mathbf{0} & \mathbf{0} & \cdots & \mathbf{C}_{n_{\text{end}}} \end{bmatrix} \in \mathbb{R}^{E(n_{\text{end}}+1) \times E(n_{\text{end}}+1)}, \tag{4.25}$$

it can be rewritten as

$$f_{\varepsilon}(\varepsilon) = \frac{1}{\sqrt{(2\pi)^{E(n_{\text{end}}+1)} \det(\mathbf{C})}} \exp\left(-\frac{1}{2}(\varepsilon - \boldsymbol{\mu})^T \mathbf{C}^{-1}(\varepsilon - \boldsymbol{\mu})\right) \tag{4.26}$$

because

$$\det(\mathbf{C}) = \prod_{n=0}^{n_{\text{end}}} \det(\mathbf{C}_n) \tag{4.27}$$

and

$$\begin{aligned}
 (\boldsymbol{\varepsilon} - \boldsymbol{\mu})^T \mathbf{C}^{-1} (\boldsymbol{\varepsilon} - \boldsymbol{\mu}) &= \begin{bmatrix} (\boldsymbol{\varepsilon}[0] - \boldsymbol{\mu}_0)^T & (\boldsymbol{\varepsilon}[1] - \boldsymbol{\mu}_1)^T & \cdots & (\boldsymbol{\varepsilon}[n_{\text{end}}] - \boldsymbol{\mu}_{n_{\text{end}}})^T \end{bmatrix} \\
 &\quad \cdot \begin{bmatrix} \mathbf{C}_0^{-1} & \mathbf{0} & \cdots & \mathbf{0} \\ \mathbf{0} & \mathbf{C}_1^{-1} & \cdots & \mathbf{0} \\ \vdots & \vdots & \ddots & \vdots \\ \mathbf{0} & \mathbf{0} & \cdots & \mathbf{C}_{n_{\text{end}}}^{-1} \end{bmatrix} \begin{bmatrix} \boldsymbol{\varepsilon}[0] - \boldsymbol{\mu}_0 \\ \boldsymbol{\varepsilon}[1] - \boldsymbol{\mu}_1 \\ \vdots \\ \boldsymbol{\varepsilon}[n_{\text{end}}] - \boldsymbol{\mu}_{n_{\text{end}}} \end{bmatrix} \\
 &= \sum_{n=0}^{n_{\text{end}}} (\boldsymbol{\varepsilon}[n] - \boldsymbol{\mu}_n)^T \mathbf{C}_n^{-1} (\boldsymbol{\varepsilon}[n] - \boldsymbol{\mu}_n).
 \end{aligned} \tag{4.28}$$

So, the sensor measurement errors $\boldsymbol{\varepsilon}$ are Gaussian with mean $E[\boldsymbol{\varepsilon}] = \boldsymbol{\mu}$ and covariance matrix $E[(\boldsymbol{\varepsilon} - \boldsymbol{\mu})(\boldsymbol{\varepsilon} - \boldsymbol{\mu})^T] = \mathbf{C}$, i.e., $\boldsymbol{\varepsilon} \sim \mathcal{N}(\boldsymbol{\mu}, \mathbf{C})$. As a consequence, the customer satisfaction properties $\mathbf{q} = \mathbf{q}(\boldsymbol{\sigma}, \boldsymbol{\varepsilon}, f, \boldsymbol{\varphi}, \boldsymbol{\xi})$, which are a function of these random sensor measurement errors $\boldsymbol{\varepsilon}$, are random variables as well and might lie inside or outside the acceptance intervals $[q_{L,i}, q_{U,i}]$, $i = 1, 2, \dots, N_q$, such that the specifications $q_{L,i} \leq q_i \leq q_{U,i}$, $i = 1, 2, \dots, N_q$, for the customer satisfaction defined by the acceptance intervals are fulfilled or violated. Hence, the Gaussian random variables $\boldsymbol{\varepsilon} \sim \mathcal{N}(\boldsymbol{\mu}, \mathbf{C})$ modeling the unavoidable sensor measurement errors play the role of the statistical parameters $\mathbf{s} \sim \mathcal{N}(\mathbf{s}_0, \mathbf{C})$ because the performance properties $\mathbf{f} = \mathbf{f}(\mathbf{p}) = \mathbf{f}(\mathbf{d}, \mathbf{s}, \boldsymbol{\theta})$ corresponding to the customer satisfaction properties $\mathbf{q} = \mathbf{q}(\boldsymbol{\sigma}, \boldsymbol{\varepsilon}, f, \boldsymbol{\varphi}, \boldsymbol{\xi})$ are a function of these random statistical parameters \mathbf{s} and the specifications $f_{L,i} \leq f_i \leq f_{U,i}$, $i = 1, 2, \dots, N_f$, for them in form of acceptance intervals $[f_{L,i}, f_{U,i}]$, $i = 1, 2, \dots, N_f$, are conceptually the same. As the probability Y of fulfilling all given performance specifications defined in (3.7) is used as quality measure for the robust system design, the probability of fulfilling all given specifications for the customer satisfaction can be used as quality measure Q for the robust design of automated vehicular safety systems in order to take the unavoidable sensor measurement errors into account:

$$Q = P \left(\bigwedge_{i=1}^{N_q} q_{L,i} \leq q_i \leq q_{U,i} \right) = P(\mathbf{q} \in \mathcal{A}_q). \tag{4.29}$$

While the probability Y of fulfilling the performance specifications measures to what extent systems fulfill the performance specifications, this quality measure Q measures to what extent the function fulfills the specifications for the customer satisfaction and thus the customer requirements in a robust manner despite the unavoidable sensor

measurement errors. As the optimal deterministic design parameter values \mathbf{d}_{opt} for a system under design are determined by the solution of the optimization problem (3.8), where the probability Y of fulfilling the performance specifications is maximized, the optimal sensor parameter values $\boldsymbol{\sigma}_{\text{opt}}$, the best decision rule f_{opt} and the optimal function parameter values $\boldsymbol{\varphi}_{\text{opt}}$ for an automated vehicular safety system under design can be determined by solving the formulated optimization problems (4.1), (4.9) and (4.11) of the function design, the sensor design as well as the joint function and sensor design, respectively, where the probability $P(\mathbf{q} \in \mathcal{A}_q)$ of fulfilling the specifications for the customer satisfaction is used as quality measure Q . This emphasizes that the sensor parameters $\boldsymbol{\sigma}$, the decision rule f and the function parameters $\boldsymbol{\varphi}$ play the role of the deterministic design parameters \mathbf{d} .

The automated vehicular safety system under design is supposed to handle all driving scenarios $\boldsymbol{\xi}$ from the scenario set \mathcal{X} , which might be a whole range of such scenario parameters $\boldsymbol{\xi}$. Conceptually, these scenario parameters $\boldsymbol{\xi}$ from the scenario set \mathcal{X} can be treated like the operating parameters $\boldsymbol{\theta}$ from the tolerance region T_θ in the robust system design as ranging parameters for which no statistical knowledge in form of a probability distribution is available but only a range of possible values. Analogously to the tolerance region T_θ of the operating parameters $\boldsymbol{\theta}$ in (3.9), the scenario set can be expressed as

$$\begin{aligned} \mathcal{X} &= \{ \boldsymbol{\xi} \in \mathbb{R}^{N_\xi} : \xi_{L,j} \leq \xi_j \leq \xi_{U,j}, j = 1, 2, \dots, N_\xi \} \\ &= [\xi_{L,1}, \xi_{U,1}] \times [\xi_{L,2}, \xi_{U,2}] \times \dots \times [\xi_{L,N_\xi}, \xi_{U,N_\xi}] \end{aligned} \quad (4.30)$$

if the j^{th} scenario parameter ξ_j ranges from the lower bound $\xi_{L,j}$ to the upper bound $\xi_{U,j}$ and thus may lie in the tolerance interval $[\xi_{L,j}, \xi_{U,j}]$.

The dependence of the customer satisfaction properties $\mathbf{q} = \mathbf{q}(\boldsymbol{\sigma}, \boldsymbol{\varepsilon}, f, \boldsymbol{\varphi}, \boldsymbol{\xi})$ on the sensor parameters $\boldsymbol{\sigma}$, the sensor measurement errors $\boldsymbol{\varepsilon}$, the decision rule f , the function parameters $\boldsymbol{\varphi}$ and the scenario parameters $\boldsymbol{\xi}$ makes the probability $P(\mathbf{q} \in \mathcal{A}_q)$ of fulfilling the specifications for the customer satisfaction and thus the quality measure $Q = Q(\boldsymbol{\sigma}, f, \boldsymbol{\varphi}, \boldsymbol{\xi})$ set to this probability in (4.29) a function of the sensor parameters $\boldsymbol{\sigma}$, the decision rule f , the function parameters $\boldsymbol{\varphi}$ and the scenario parameters $\boldsymbol{\xi}$:

$$Q : \mathcal{S} \times \mathcal{F} \times \mathbb{R}^{N_\varphi} \times \mathcal{X} \rightarrow [0, 1], (\boldsymbol{\sigma}, f, \boldsymbol{\varphi}, \boldsymbol{\xi}) \mapsto Q(\boldsymbol{\sigma}, f, \boldsymbol{\varphi}, \boldsymbol{\xi}) = P(\mathbf{q} \in \mathcal{A}_q). \quad (4.31)$$

Consequently, the optimal sensor parameter values $\boldsymbol{\sigma}_{\text{opt}}$, the best decision rule f_{opt} and the optimal function parameter values $\boldsymbol{\varphi}_{\text{opt}}$ of the automated vehicular safety system under design obtained by solving the optimization problems (4.1), (4.9) and (4.11) of the function design, the sensor design as well as the joint function and sensor

design, respectively, are dependent on the scenario parameters ξ and thus on the driving scenario characterized by them. So far, it has been assumed that the scenario parameters ξ are fixed, i.e., have specific values that correspond to the only driving scenario the automated vehicular safety system under design is supposed to handle, such that the optimal sensor parameter values σ_{opt} , the best decision rule f_{opt} and the optimal function parameter values φ_{opt} have to be obtained only once for these values of the scenario parameters ξ by solving the optimization problems (4.1), (4.9) and (4.11) in the design phase. However, the automated vehicular safety system under design shall not handle only one driving scenario with the fixed scenario parameters ξ but all driving scenarios with the various scenario parameter values ξ from the scenario set \mathcal{X} . Due to the dependency of the optimal sensor parameter values σ_{opt} , the best decision rule f_{opt} and the optimal function parameter values φ_{opt} on the scenario parameters ξ , these optimal values σ_{opt} and φ_{opt} as well as this best decision rule f_{opt} , which have been obtained by solving the optimization problems (4.1), (4.9) and (4.11) for one instance of the scenario parameters ξ in the design phase, are not optimal anymore when the values of the scenario parameters ξ of the driving scenario to which the automated vehicular safety system is exposed deviate from this one instance. Therefore, the sensor parameters σ , the decision rule f and the function parameters φ would have to be adapted to the values of the scenario parameters ξ by solving the optimization problems (4.1), (4.9) and (4.11) whenever they change. Although this might be possible for the decision rule f and the function parameters φ , it is impossible for the sensor parameters σ in case of already installed sensors whose parameters σ like the variances of their measurement errors cannot be changed anymore. In order to overcome this problem, the optimal sensor parameter values σ_{opt} , the best decision rule f_{opt} and the optimal function parameter values φ_{opt} have to be made independent of the scenario parameters ξ . This independence can be achieved by taking all scenarios ξ from the scenario set \mathcal{X} already in the design phase into account, i.e., by determining the optimal sensor parameter values σ_{opt} , the best decision rule f_{opt} and the optimal function parameter values φ_{opt} such that they are optimal not only for one instance of the scenario parameters ξ but for the various values of them from the scenario set \mathcal{X} . In the robust system design, the worst-case probability Y_{WC} of fulfilling the performance specifications defined by (3.11) as the minimum of the probability Y of fulfilling the performance specifications in the whole tolerance region T_{θ} of the operating parameters θ corresponding to the scenario parameters ξ is used instead of the probability Y of fulfilling the performance specifications as quality measure in order to eliminate the dependency of the optimal deterministic design parameter values d_{opt} corresponding to the optimal sensor parameter values σ_{opt} , the best decision rule

f_{opt} and the optimal function parameter values φ_{opt} on the operating parameters θ . Analogously, the worst-case probability $P_{\text{WC}}(\mathbf{q} \in \mathcal{A}_{\mathbf{q}})$ of fulfilling the specifications for the customer satisfaction defined by

$$P_{\text{WC}}(\mathbf{q} \in \mathcal{A}_{\mathbf{q}}) = \min_{\xi \in \mathcal{X}} P(\mathbf{q} \in \mathcal{A}_{\mathbf{q}}) \quad (4.32)$$

as the minimum of the probability $P(\mathbf{q} \in \mathcal{A}_{\mathbf{q}})$ that the specifications for the customer satisfaction are fulfilled in all driving scenarios with the various scenario parameter values ξ from the scenario set \mathcal{X} can be used instead of the probability $P(\mathbf{q} \in \mathcal{A}_{\mathbf{q}})$ that the specifications for the customer satisfaction are fulfilled as quality measure Q in order to eliminate the dependency of the optimal sensor parameter values σ_{opt} , the best decision rule f_{opt} and the optimal function parameter values φ_{opt} on the scenario parameters ξ . By solving the optimization problems (4.1), (4.9) and (4.11) of the function design, the sensor design as well as the joint function and sensor design, respectively, with this quality measure

$$Q = P_{\text{WC}}(\mathbf{q} \in \mathcal{A}_{\mathbf{q}}) = \min_{\xi \in \mathcal{X}} P(\mathbf{q} \in \mathcal{A}_{\mathbf{q}}) = \min_{\xi \in \mathcal{X}} P\left(\bigwedge_{i=1}^{N_{\mathbf{q}}} q_{\text{L},i} \leq q_i \leq q_{\text{U},i}\right), \quad (4.33)$$

the optimal sensor parameter values σ_{opt} , the best decision rule f_{opt} and the optimal function parameter values φ_{opt} of the automated vehicular safety system under design can be obtained again. The minimization of the probability $P(\mathbf{q} \in \mathcal{A}_{\mathbf{q}})$ that the specifications for the customer satisfaction are fulfilled, which is a function of the sensor parameters σ , the decision rule f , the function parameters φ and the scenario parameters ξ as stated in (4.31), with respect to the scenario parameters ξ makes the resulting worst-case probability $P_{\text{WC}}(\mathbf{q} \in \mathcal{A}_{\mathbf{q}})$ of fulfilling the specifications for the customer satisfaction and thus the quality measure $Q = Q(\sigma, f, \varphi)$ independent of the scenario parameters ξ as desired and a function of the sensor parameters σ , the decision rule f and the function parameters φ only:

$$Q : \mathcal{S} \times \mathcal{F} \times \mathbb{R}^{N_{\varphi}} \rightarrow [0, 1], (\sigma, f, \varphi) \mapsto Q(\sigma, f, \varphi) = P_{\text{WC}}(\mathbf{q} \in \mathcal{A}_{\mathbf{q}}). \quad (4.34)$$

If this quality measure Q defined by (4.33) has the value $Q_0 \in [0, 1]$, the minimum of the probability $P(\mathbf{q} \in \mathcal{A}_{\mathbf{q}})$ that the specifications for the customer satisfaction are fulfilled in all driving scenarios ξ from the scenario set \mathcal{X} is

$$\min_{\xi \in \mathcal{X}} P(\mathbf{q} \in \mathcal{A}_{\mathbf{q}}) = P_{\text{WC}}(\mathbf{q} \in \mathcal{A}_{\mathbf{q}}) = Q = Q_0. \quad (4.35)$$

This guarantees that the probability $P(\mathbf{q} \in \mathcal{A}_{\mathbf{q}})$ of fulfilling the specifications for the customer satisfaction is at least Q_0 in each driving scenario ξ from the scenario set \mathcal{X}

4.2 Quality Measure for Robust Design of Automated Vehicular Safety Systems

because $\min_{\xi \in \mathcal{X}} P(\mathbf{q} \in \mathcal{A}_q)$ would not be Q_0 contradicting (4.35) if $P(\mathbf{q} \in \mathcal{A}_q) < Q_0$ in at least one driving scenario $\xi \in \mathcal{X}$:

$$Q = \min_{\xi \in \mathcal{X}} P(\mathbf{q} \in \mathcal{A}_q) = Q_0 \Rightarrow P(\mathbf{q} \in \mathcal{A}_q) \geq Q_0 \quad \forall \xi \in \mathcal{X}. \quad (4.36)$$

In general, the probability $P(\mathbf{q} \in \mathcal{A}_q)|_{\xi=\xi'}$ of fulfilling the specifications for the customer satisfaction in a specific driving scenario ξ' from the scenario set \mathcal{X} cannot be smaller than the worst-case probability $P_{\text{WC}}(\mathbf{q} \in \mathcal{A}_q)$ of fulfilling these specifications, i.e.,

$$P(\mathbf{q} \in \mathcal{A}_q)|_{\xi=\xi'} \geq \min_{\xi \in \mathcal{X}} P(\mathbf{q} \in \mathcal{A}_q) = P_{\text{WC}}(\mathbf{q} \in \mathcal{A}_q) \quad \forall \xi' \in \mathcal{X}, \quad (4.37)$$

and the scenarios ξ' from the scenario set \mathcal{X} for which the corresponding probability $P(\mathbf{q} \in \mathcal{A}_q)|_{\xi=\xi'}$ of fulfilling the specifications for the customer satisfaction is equal to the worst-case probability $P_{\text{WC}}(\mathbf{q} \in \mathcal{A}_q)$ of fulfilling these specifications and thus minimum are the worst cases forming the set

$$\mathcal{X}_{\text{WC}} = \left\{ \xi' \in \mathcal{X} : P(\mathbf{q} \in \mathcal{A}_q)|_{\xi=\xi'} = \min_{\xi \in \mathcal{X}} P(\mathbf{q} \in \mathcal{A}_q) \right\} \quad (4.38)$$

of worst-case driving scenarios.

If the worst-case probability $P_{\text{WC}}(\mathbf{q} \in \mathcal{A}_q)$ of fulfilling the specifications for the customer satisfaction is used as quality measure Q in the optimization problems (4.9) and (4.11) of the sensor design as well as the joint function and sensor design, respectively, the required minimum quality level Q_{min} in the constraint of these optimization problems is the required minimum worst-case probability P_{min} of fulfilling these specifications:

$$Q_{\text{min}} = P_{\text{min}}. \quad (4.39)$$

The constraint of both optimization problems thus reads

$$P_{\text{WC}}(\mathbf{q} \in \mathcal{A}_q) = \min_{\xi \in \mathcal{X}} P(\mathbf{q} \in \mathcal{A}_q) \geq P_{\text{min}}. \quad (4.40)$$

If the probability $P(\mathbf{q} \in \mathcal{A}_q)$ of fulfilling the specifications for the customer satisfaction is at least P_{min} in each driving scenario ξ from the scenario set \mathcal{X} , the minimum of this probability in all driving scenarios $\xi \in \mathcal{X}$ is at least P_{min} . On the other hand, the probability $P(\mathbf{q} \in \mathcal{A}_q)$ of fulfilling the specifications for the customer satisfaction is at least P_{min} in each driving scenario ξ from the scenario set \mathcal{X} if the minimum of this probability in all driving scenarios $\xi \in \mathcal{X}$ is at least P_{min} as otherwise this minimum would be smaller than P_{min} contradicting the assumption that it is at least

P_{\min} . Therefore, the constraint (4.40) of the optimization problems (4.9) and (4.11) of the sensor design as well as the joint function and sensor design, respectively, is equivalent to

$$P(\mathbf{q} \in \mathcal{A}_q) \geq P_{\min} \quad \forall \xi \in \mathcal{X}. \quad (4.41)$$

Consequently, the design space \mathcal{D} defined in (4.6) from which the sensor parameter values σ have to be chosen in the sensor design such that the constraint (4.40) of the optimization problem (4.9) is fulfilled and thus the customer requirements are met in a robust manner despite the unavoidable sensor measurement errors to the desired extent can be expressed as

$$\begin{aligned} \mathcal{D} &= \{\sigma \in \mathcal{S} : P_{\text{WC}}(\mathbf{q} \in \mathcal{A}_q) \geq P_{\min}\} \\ &= \left\{ \sigma \in \mathcal{S} : \min_{\xi \in \mathcal{X}} P(\mathbf{q} \in \mathcal{A}_q) \geq P_{\min} \right\} \\ &= \{\sigma \in \mathcal{S} : P(\mathbf{q} \in \mathcal{A}_q) \geq P_{\min} \quad \forall \xi \in \mathcal{X}\} \\ &= \bigcap_{\xi' \in \mathcal{X}} \left\{ \sigma \in \mathcal{S} : P(\mathbf{q} \in \mathcal{A}_q) |_{\xi=\xi'} \geq P_{\min} \right\} = \bigcap_{\xi' \in \mathcal{X}} \mathcal{D}(\xi'). \end{aligned} \quad (4.42)$$

So, the design space \mathcal{D} is the intersection of the individual design space partitions

$$\mathcal{D}(\xi') = \left\{ \sigma \in \mathcal{S} : P(\mathbf{q} \in \mathcal{A}_q) |_{\xi=\xi'} \geq P_{\min} \right\} \quad (4.43)$$

for all driving scenarios ξ' from the scenario set \mathcal{X} and decomposed into them. The individual design space partition $\mathcal{D}(\xi')$ for the driving scenario $\xi' \in \mathcal{X}$ is the set of all sensor parameter values σ in the possible domain \mathcal{S} leading to a probability $P(\mathbf{q} \in \mathcal{A}_q)$ of fulfilling the specifications for the customer satisfaction that is at least $P_{\min} = Q_{\min}$ in the driving scenario ξ' while the design space \mathcal{D} is the set of all sensor parameter values $\sigma \in \mathcal{S}$ for which this probability $P(\mathbf{q} \in \mathcal{A}_q)$ is at least $P_{\min} = Q_{\min}$ in all driving scenarios ξ from the scenario set \mathcal{X} and thus the quality measure Q is at least Q_{\min} as required.

Analogously to the design space \mathcal{D} of the sensor design in (4.42), the design space \mathcal{D} defined in (4.16) from which the sensor parameter values σ , the decision rule f and the function parameter values φ have to be chosen in the joint function and sensor design such that the constraint (4.40) of the optimization problem (4.11) is fulfilled and thus the customer requirements are met in a robust manner despite the unavoidable sensor measurement errors to the desired extent can also be decomposed into individual design space partitions

$$\mathcal{D}(\xi') = \left\{ (\sigma, f, \varphi) \in \mathcal{S} \times \mathcal{F} \times \mathbb{R}^{N_\varphi} : P(\mathbf{q} \in \mathcal{A}_q) |_{\xi=\xi'} \geq P_{\min} \right\} \quad (4.44)$$

for all driving scenarios ξ' from the scenario set \mathcal{X} and expressed as the intersection of them:

$$\begin{aligned}
 \mathcal{D} &= \{(\sigma, f, \varphi) \in \mathcal{S} \times \mathcal{F} \times \mathbb{R}^{N_\varphi} : P_{\text{WC}}(\mathbf{q} \in \mathcal{A}_q) \geq P_{\min}\} \\
 &= \{(\sigma, f, \varphi) \in \mathcal{S} \times \mathcal{F} \times \mathbb{R}^{N_\varphi} : P(\mathbf{q} \in \mathcal{A}_q) \geq P_{\min} \forall \xi \in \mathcal{X}\} \\
 &= \bigcap_{\xi' \in \mathcal{X}} \{(\sigma, f, \varphi) \in \mathcal{S} \times \mathcal{F} \times \mathbb{R}^{N_\varphi} : P(\mathbf{q} \in \mathcal{A}_q)|_{\xi=\xi'} \geq P_{\min}\} \quad (4.45) \\
 &= \bigcap_{\xi' \in \mathcal{X}} \mathcal{D}(\xi').
 \end{aligned}$$

Here, the individual design space partition $\mathcal{D}(\xi')$ for the driving scenario $\xi' \in \mathcal{X}$ is the set of all sensor parameter values σ in the possible domain \mathcal{S} , decision rules f from the set \mathcal{F} of predefined decision rules and function parameter values φ leading to a probability $P(\mathbf{q} \in \mathcal{A}_q)$ of fulfilling the specifications for the customer satisfaction that is at least $P_{\min} = Q_{\min}$ in the driving scenario ξ' while the design space \mathcal{D} is the set of all sensor parameter values $\sigma \in \mathcal{S}$, decision rules $f \in \mathcal{F}$ and function parameter values φ for which this probability $P(\mathbf{q} \in \mathcal{A}_q)$ is at least $P_{\min} = Q_{\min}$ in all driving scenarios ξ' from the scenario set \mathcal{X} and thus the quality measure Q is at least Q_{\min} as required. This is illustrated in Figure 4.7, Figure 4.8 and Figure 4.9 for one sensor parameter $\sigma = \sigma \in \mathcal{S} = \mathbb{R}^+$, the set $\mathcal{F} = \{f_1, f_2, f_3\}$ of three decision rules f with one adjustable function parameter $\varphi = \varphi \in \mathbb{R}$ and the scenario set $\mathcal{X} = \{\xi_1, \xi_2, \xi_3, \xi_4\}$ consisting of four driving scenarios ξ . The blue, red, yellow and green curves are the contour lines along which the probability $P(\mathbf{q} \in \mathcal{A}_q)$ of fulfilling the specifications for the customer satisfaction is equal to the required minimum worst-case probability P_{\min} in the driving scenarios ξ_1, ξ_2, ξ_3 and ξ_4 , respectively, and the boundaries of the individual design space partitions $\mathcal{D}(\xi_1), \mathcal{D}(\xi_2), \mathcal{D}(\xi_3)$ and $\mathcal{D}(\xi_4)$ highlighted by the blue, red, yellow and green areas in which the probability $P(\mathbf{q} \in \mathcal{A}_q)$ of fulfilling the specifications for the customer satisfaction does not lie below the required minimum worst-case probability P_{\min} in the driving scenarios ξ_1, ξ_2, ξ_3 and ξ_4 , respectively. The intersection of the individual design space partitions $\mathcal{D}(\xi_1), \mathcal{D}(\xi_2), \mathcal{D}(\xi_3)$ and $\mathcal{D}(\xi_4)$ yields the design space \mathcal{D} highlighted by the magenta areas, in which the quality measure Q , i.e., the minimum of the probability $P(\mathbf{q} \in \mathcal{A}_q)$ of fulfilling the specifications for the customer satisfaction in the four driving scenarios ξ_1, ξ_2, ξ_3 and ξ_4 , does not lie below the required minimum quality level $Q_{\min} = P_{\min}$.

The constraint (4.40) of the optimization problems (4.9) and (4.11) in the robust sensor as well as joint function and sensor design guarantees that the designed automated vehicular safety system fulfills the specifications for the customer satisfaction at least with the required minimum worst-case probability $P_{\min} = Q_{\min}$ in all considered

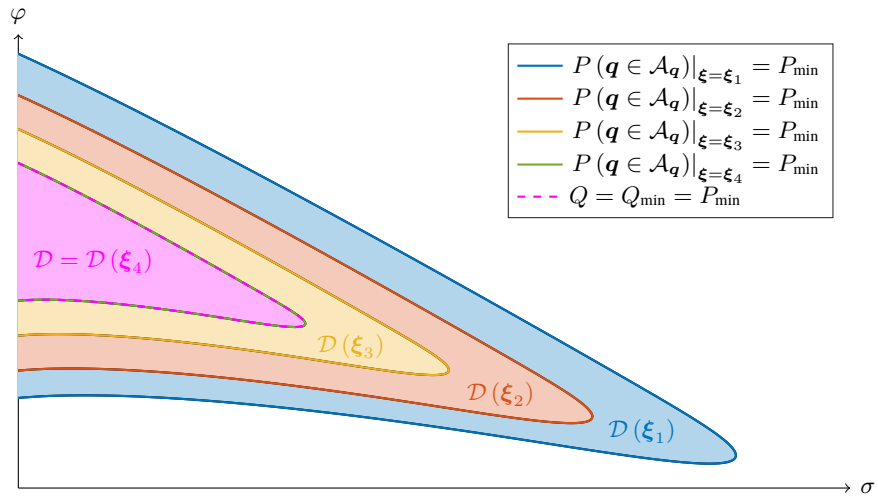


Figure 4.7: Design space \mathcal{D} in joint function and sensor design for one sensor parameter $\sigma = \sigma \in \mathcal{S} = \mathbb{R}^+$, the set $\mathcal{F} = \{f_1, f_2, f_3\}$ of decision rules f with one adjustable function parameter $\varphi = \varphi \in \mathbb{R}$ and the scenario set $\mathcal{X} = \{\xi_1, \xi_2, \xi_3, \xi_4\}$, where $f = f_1$.

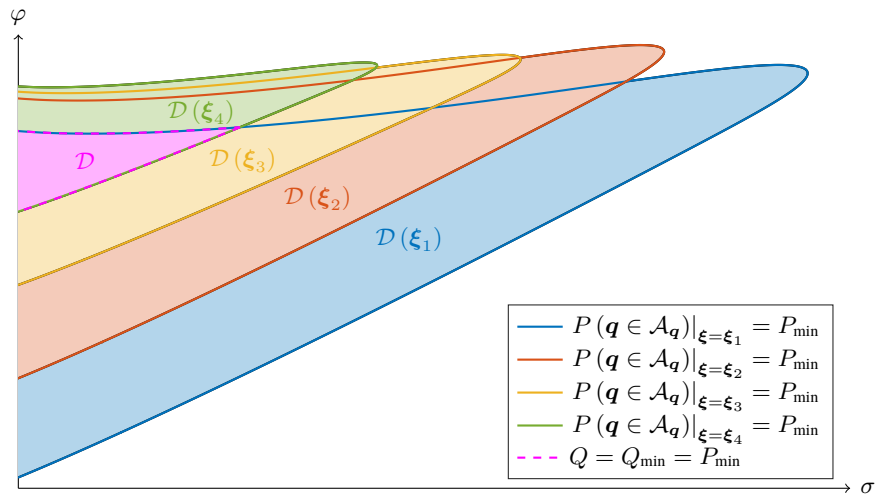


Figure 4.8: Design space \mathcal{D} in joint function and sensor design for one sensor parameter $\sigma = \sigma \in \mathcal{S} = \mathbb{R}^+$, the set $\mathcal{F} = \{f_1, f_2, f_3\}$ of decision rules f with one adjustable function parameter $\varphi = \varphi \in \mathbb{R}$ and the scenario set $\mathcal{X} = \{\xi_1, \xi_2, \xi_3, \xi_4\}$, where $f = f_2$.

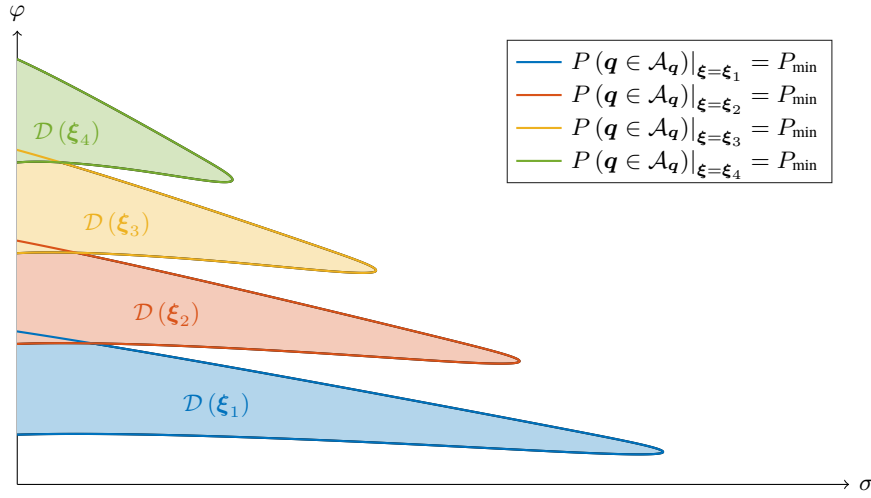


Figure 4.9: Design space \mathcal{D} in joint function and sensor design for one sensor parameter $\sigma = \sigma \in \mathcal{S} = \mathbb{R}^+$, the set $\mathcal{F} = \{f_1, f_2, f_3\}$ of decision rules f with one adjustable function parameter $\varphi = \varphi \in \mathbb{R}$ and the scenario set $\mathcal{X} = \{\xi_1, \xi_2, \xi_3, \xi_4\}$, where $f = f_3$.

driving scenarios from the scenario set \mathcal{X} , which determines the customer satisfaction as well as the reliability and safety of the system. Increasing the required minimum quality level Q_{\min} , i.e., the required minimum worst-case probability P_{\min} , increases the customer satisfaction as well as the reliability and safety of the system but might also increase the minimal costs C_{\min} resulting from solving the optimization problems (4.9) and (4.11) of the robust sensor as well as joint function and sensor design. Therefore, a trade-off has to be found by choosing the required minimum quality level Q_{\min} appropriately. This is a decision that has to be made by the management, which can be based on user studies or on the desired probability of fulfilling the specifications in system assessment tests like those of the New Car Assessment Programme (NCAP).

Simulation-Based Robust Design of Automated Vehicular Safety Systems 5

In the previous chapter, the robust design of automated vehicular safety systems considering sensor measurement errors has been formulated as optimization problems using a probabilistic quality measure Q based on analogies to a robust system design as performed in integrated circuit design. Solving these optimization problems (4.1), (4.9) and (4.11) of the robust function design, sensor design as well as joint function and sensor design, respectively, requires several evaluations of the quality measure Q . As there is usually no closed-form expression for the quality measure Q , it has to be evaluated based on simulations of the automated vehicular safety system under design. This chapter suggests different possibilities for such a simulation-based evaluation of the quality measure Q based on analogies to a robust system design as performed in integrated circuit design again. This eventually leads to a methodology for the robust function and sensor design that allows to systematically design both functions and sensors of automated vehicular safety systems by solving the formulated optimization problems solely based on simulations of the automated vehicular safety system under design such that the customer requirements are fulfilled in a robust manner despite unavoidable sensor measurement errors.

Apart from simple automated vehicular safety systems in idealized scenarios, there is usually no closed-form expression for the customer satisfaction properties q as a function of the sensor parameters σ , the sensor measurement errors ε , the decision rule f , the function parameters φ and the scenario parameters ξ defined in (4.22) due to the high complexity of automated vehicular safety systems in practice. Hence, the evaluation of q at given sensor parameters σ , sensor measurement errors ε , a given decision rule f , given function parameters φ and scenario parameters ξ requires a numerical simulation of the automated vehicular safety system. It maps the given sensor parameters σ , sensor measurement errors ε , the given decision rule f , the given function parameters φ and scenario parameters ξ , which are the input of the simulation, to the respective values of the customer satisfaction properties q , which

are the output of the simulation. As there is usually no closed-form expression for the customer satisfaction properties \mathbf{q} as a function of the sensor parameters $\boldsymbol{\sigma}$, the sensor measurement errors $\boldsymbol{\varepsilon}$, the decision rule f , the function parameters $\boldsymbol{\varphi}$ and the scenario parameters $\boldsymbol{\xi}$, and it can only be evaluated by numerical simulations of the automated vehicular safety system apart from simple automated vehicular safety systems in idealized scenarios, this is also the case for the probability $P(\mathbf{q} \in \mathcal{A}_q)$ that the customer satisfaction properties \mathbf{q} lie in the acceptance intervals and thus fulfill the specifications for the customer satisfaction as a function of the sensor parameters $\boldsymbol{\sigma}$, the decision rule f , the function parameters $\boldsymbol{\varphi}$ and the scenario parameters $\boldsymbol{\xi}$ given in (4.31) and the worst-case probability $P_{\text{WC}}(\mathbf{q} \in \mathcal{A}_q)$ of fulfilling the specifications for the customer satisfaction, i.e., the quality measure Q , as a function of the sensor parameters $\boldsymbol{\sigma}$, the decision rule f and the function parameters $\boldsymbol{\varphi}$ given in (4.34). There are different possibilities for obtaining values of the probability $P(\mathbf{q} \in \mathcal{A}_q)$ that the specifications for the customer satisfaction are fulfilled, from which a value of the quality measure Q can be obtained by minimizing the probability $P(\mathbf{q} \in \mathcal{A}_q)$ with respect to the scenario parameters $\boldsymbol{\xi}$ according to the definition of the quality measure Q as the worst-case probability $P_{\text{WC}}(\mathbf{q} \in \mathcal{A}_q)$ of fulfilling the specifications for the customer satisfaction in (4.33).

5.1 Monte-Carlo-Based Robust Design of Automated Vehicular Safety Systems

As the Monte Carlo simulation can be used in the robust system design as an estimator in order to approximately obtain a value of the probability $P(\mathbf{f} \in \mathcal{A}_f)$ that the performance specifications are fulfilled for given deterministic design parameters \mathbf{d} and operating parameters $\boldsymbol{\theta}$, the Monte Carlo simulation can also be used as an estimator in order to obtain a value of the probability $P(\mathbf{q} \in \mathcal{A}_q)$ that the specifications for the customer satisfaction are fulfilled for given sensor parameters $\boldsymbol{\sigma}$, a given decision rule f , given function parameters $\boldsymbol{\varphi}$ and scenario parameters $\boldsymbol{\xi}$ at least approximately. In the Monte Carlo simulation, M realizations $\boldsymbol{\varepsilon}_1, \boldsymbol{\varepsilon}_2, \dots, \boldsymbol{\varepsilon}_M$ of all involved random variables, i.e., the sensor measurement errors $\boldsymbol{\varepsilon}$, are generated at random according to their probability distribution, which is the Gaussian distribution $\mathcal{N}(\boldsymbol{\mu}, \mathbf{C})$ with the pdf in (4.26). Each realization $\boldsymbol{\varepsilon}_m, m = 1, 2, \dots, M$, of the sensor measurement errors $\boldsymbol{\varepsilon}$ together with given sensor parameters $\boldsymbol{\sigma}$, a given decision rule f , given function parameters $\boldsymbol{\varphi}$ and scenario parameters $\boldsymbol{\xi}$ is mapped to the respective values $\mathbf{q}_m = \mathbf{q}(\boldsymbol{\sigma}, \boldsymbol{\varepsilon}_m, f, \boldsymbol{\varphi}, \boldsymbol{\xi})$ of the customer satisfaction properties \mathbf{q} according to (4.22) by a simulation of the automated vehicular safety system. In these M random experiments, it is counted how often the values of the samples \mathbf{q}_m of the customer

satisfaction properties \mathbf{q} lie in the acceptance intervals $[q_{L,i}, q_{U,i}]$, $i = 1, 2, \dots, N_{\mathbf{q}}$, to obtain their number $M_{1,M}$ and the frequency

$$\hat{P}_M(\mathbf{q} \in \mathcal{A}_{\mathbf{q}}) = \frac{M_{1,M}}{M} \quad (5.1)$$

of fulfilling all specifications $q_{L,i} \leq q_i \leq q_{U,i}$, $i = 1, 2, \dots, N_{\mathbf{q}}$, for the customer satisfaction associated with these acceptance intervals, i.e., $\mathbf{q}_m \in \mathcal{A}_{\mathbf{q}}$, which is an estimate for the probability $P(\mathbf{q} \in \mathcal{A}_{\mathbf{q}})$ of fulfilling these specifications for the customer satisfaction.

Defining the acceptance function for the customer satisfaction as the indicator function

$$\delta_{\mathcal{A}_{\mathbf{q}}} : \mathbb{R}^{N_{\mathbf{q}}} \rightarrow \{0, 1\}, \mathbf{q} \mapsto \delta_{\mathcal{A}_{\mathbf{q}}}(\mathbf{q}) = \begin{cases} 1, & \mathbf{q} \in \mathcal{A}_{\mathbf{q}}, \\ 0, & \mathbf{q} \notin \mathcal{A}_{\mathbf{q}}, \end{cases} \quad (5.2)$$

which indicates whether $\mathbf{q} \in \mathcal{A}_{\mathbf{q}}$, i.e., the customer satisfaction properties \mathbf{q} fulfill all specifications for the customer satisfaction, with the function value 1, allows to express the number of the samples \mathbf{q}_m of the customer satisfaction properties \mathbf{q} that fulfill all specifications for the customer satisfaction and the frequency of fulfilling all specifications for the customer satisfaction in the Monte Carlo simulation as

$$M_{1,M} = \sum_{m=1}^M \delta_{\mathcal{A}_{\mathbf{q}}}(\mathbf{q}_m) \quad (5.3)$$

and

$$\hat{P}_M(\mathbf{q} \in \mathcal{A}_{\mathbf{q}}) = \frac{1}{M} \sum_{m=1}^M \delta_{\mathcal{A}_{\mathbf{q}}}(\mathbf{q}_m), \quad (5.4)$$

respectively. Hence, the Monte Carlo simulation can be interpreted as an estimator, which estimates the probability $P(\mathbf{q} \in \mathcal{A}_{\mathbf{q}})$ of fulfilling the specifications for the customer satisfaction from the random observations $\mathbf{q}_m = \mathbf{q}(\boldsymbol{\sigma}, \boldsymbol{\varepsilon}_m, \mathbf{f}, \boldsymbol{\varphi}, \boldsymbol{\xi})$, $m = 1, 2, \dots, M$:

$$\hat{P}_M(\mathbf{q} \in \mathcal{A}_{\mathbf{q}}) : (\mathbb{R}^{N_{\mathbf{q}}})^M \rightarrow [0, 1], (\mathbf{q}_1, \mathbf{q}_2, \dots, \mathbf{q}_M) \mapsto \hat{P}_M(\mathbf{q} \in \mathcal{A}_{\mathbf{q}}). \quad (5.5)$$

The samples $\mathbf{q}_1, \mathbf{q}_2, \dots, \mathbf{q}_M$ of the customer satisfaction properties \mathbf{q} correspond to the samples $\mathbf{f}_1, \mathbf{f}_2, \dots, \mathbf{f}_M$ of the performance properties \mathbf{f} while the probability $P(\mathbf{q} \in \mathcal{A}_{\mathbf{q}})$ of fulfilling the specifications for the customer satisfaction corresponds to the probability $P(\mathbf{f} \in \mathcal{A}_{\mathbf{f}})$ of fulfilling the performance specifications. As the estimate \hat{Y}_M for the probability Y of fulfilling the performance specifications is a scaled version of a binomially distributed random variable in the interval $[0, 1]$ with the

pmf $f_{\hat{Y}_M}(y)$ in (3.29), the possible values $y = 0, \frac{1}{M}, \dots, 1$, the mean $E[\hat{Y}_M] = Y$ and the variance $\text{Var}[\hat{Y}_M] = \frac{Y(1-Y)}{M}$, the estimate $\hat{P}_M(\mathbf{q} \in \mathcal{A}_q)$ for the probability $P(\mathbf{q} \in \mathcal{A}_q)$ of fulfilling the specifications for the customer satisfaction is also a scaled version of a binomially distributed random variable in the interval $[0, 1]$ with the pmf

$$f_{\hat{P}_M(\mathbf{q} \in \mathcal{A}_q)}(p) = \binom{M}{Mp} (P(\mathbf{q} \in \mathcal{A}_q))^{Mp} (1 - P(\mathbf{q} \in \mathcal{A}_q))^{M(1-p)}, \quad (5.6)$$

the possible values $p = 0, \frac{1}{M}, \dots, 1$, the mean

$$E[\hat{P}_M(\mathbf{q} \in \mathcal{A}_q)] = P(\mathbf{q} \in \mathcal{A}_q) \quad (5.7)$$

and the variance

$$\text{Var}[\hat{P}_M(\mathbf{q} \in \mathcal{A}_q)] = \frac{P(\mathbf{q} \in \mathcal{A}_q)(1 - P(\mathbf{q} \in \mathcal{A}_q))}{M}. \quad (5.8)$$

As the estimator \hat{Y}_M for the probability Y of fulfilling the performance specifications, the estimator $\hat{P}_M(\mathbf{q} \in \mathcal{A}_q)$ for the probability $P(\mathbf{q} \in \mathcal{A}_q)$ of fulfilling the specifications for the customer satisfaction is unbiased with the MSE

$$\begin{aligned} E\left[\left(\hat{P}_M(\mathbf{q} \in \mathcal{A}_q) - P(\mathbf{q} \in \mathcal{A}_q)\right)^2\right] &= \text{Var}[\hat{P}_M(\mathbf{q} \in \mathcal{A}_q)] \\ &= \frac{P(\mathbf{q} \in \mathcal{A}_q)(1 - P(\mathbf{q} \in \mathcal{A}_q))}{M} \quad (5.9) \\ &\xrightarrow{M \rightarrow \infty} 0 \end{aligned}$$

converging to 0 as the number of samples or observations \mathbf{q}_m and simulations of the automated vehicular safety system M in the Monte Carlo simulation tends to infinity and consistent, which means that the estimate $\hat{P}_M(\mathbf{q} \in \mathcal{A}_q)$ converges in probability to the true probability $P(\mathbf{q} \in \mathcal{A}_q)$ as the number of simulations M tends to infinity:

$$\hat{P}_M(\mathbf{q} \in \mathcal{A}_q) \xrightarrow{p} P(\mathbf{q} \in \mathcal{A}_q) \quad \text{for } M \rightarrow \infty. \quad (5.10)$$

The statistical knowledge about the estimate $\hat{P}_M(\mathbf{q} \in \mathcal{A}_q)$ for the probability $P(\mathbf{q} \in \mathcal{A}_q)$ of fulfilling the specifications for the customer satisfaction is completely captured by its pmf $f_{\hat{P}_M(\mathbf{q} \in \mathcal{A}_q)}(p)$ stated in (5.6). Theoretically, the required number of samples or observations \mathbf{q}_m and simulations of the automated vehicular safety system M in the Monte Carlo simulation for a desired estimation accuracy, e.g., specified in form of a confidence interval $[\hat{P}_M(\mathbf{q} \in \mathcal{A}_q) - \Delta P, \hat{P}_M(\mathbf{q} \in \mathcal{A}_q) + \Delta P]$ of length

$2 \Delta P$ around the random estimate $\hat{P}_M(\mathbf{q} \in \mathcal{A}_q)$ for the probability $P(\mathbf{q} \in \mathcal{A}_q)$ of fulfilling the specifications for the customer satisfaction which shall contain the true probability $P(\mathbf{q} \in \mathcal{A}_q)$ with a desired probability κ , the desired confidence level, could be derived from it. Unfortunately, it cannot be derived in closed form due to the special structure of the pmf $f_{\hat{P}_M(\mathbf{q} \in \mathcal{A}_q)}(p)$ of the estimate $\hat{P}_M(\mathbf{q} \in \mathcal{A}_q)$ for the probability of fulfilling the specifications for the customer satisfaction, which is a scaled binomially distributed random variable.

If the number of samples \mathbf{q}_m and simulations of the automated vehicular safety system M in the Monte Carlo simulation is large, which has to be the case for a high estimation accuracy anyway, however, the estimate $\hat{P}_M(\mathbf{q} \in \mathcal{A}_q)$ for the probability $P(\mathbf{q} \in \mathcal{A}_q)$ of fulfilling the specifications for the customer satisfaction is approximately Gaussian with the mean and the variance given by (5.7) and (5.8), respectively, as well as the cdf

$$\begin{aligned} F_{\hat{P}_M(\mathbf{q} \in \mathcal{A}_q)}(p) &= P\left(\hat{P}_M(\mathbf{q} \in \mathcal{A}_q) \leq p\right) \\ &\approx \Phi\left(\frac{p - P(\mathbf{q} \in \mathcal{A}_q)}{\sqrt{P(\mathbf{q} \in \mathcal{A}_q)(1 - P(\mathbf{q} \in \mathcal{A}_q))/M}}\right) \end{aligned} \quad (5.11)$$

due to the Central Limit Theorem. This is in accordance with the fact that the estimate \hat{Y}_M for the probability $Y = P(\mathbf{f} \in \mathcal{A}_f)$ of fulfilling the performance specifications corresponding to the probability $P(\mathbf{q} \in \mathcal{A}_q)$ of fulfilling the specifications for the customer satisfaction is approximately Gaussian with the mean $E[\hat{Y}_M] = Y$ and the variance $\text{Var}[\hat{Y}_M] = \frac{Y(1-Y)}{M}$ as well as the cdf $F_{\hat{Y}_M}(y)$ given by (3.46) due to the Central Limit Theorem if the number of samples \mathbf{f}_m and system simulations M in the Monte Carlo simulation is large. As the probability $P(\hat{Y}_M - \Delta Y \leq Y \leq \hat{Y}_M + \Delta Y)$ that the confidence interval $[\hat{Y}_M - \Delta Y, \hat{Y}_M + \Delta Y]$ of length $2 \Delta Y$ around the estimate \hat{Y}_M contains the true probability $Y = P(\mathbf{f} \in \mathcal{A}_f)$ of fulfilling the performance specifications is written as in (3.48), the probability that the confidence interval $[\hat{P}_M(\mathbf{q} \in \mathcal{A}_q) - \Delta P, \hat{P}_M(\mathbf{q} \in \mathcal{A}_q) + \Delta P]$ of length $2 \Delta P$ around the estimate $\hat{P}_M(\mathbf{q} \in \mathcal{A}_q)$ contains the true probability $P(\mathbf{q} \in \mathcal{A}_q)$ of fulfilling the specifications for the customer satisfaction can be written as

$$\begin{aligned} &P\left(\hat{P}_M(\mathbf{q} \in \mathcal{A}_q) - \Delta P \leq P(\mathbf{q} \in \mathcal{A}_q) \leq \hat{P}_M(\mathbf{q} \in \mathcal{A}_q) + \Delta P\right) \\ &= P\left(P(\mathbf{q} \in \mathcal{A}_q) - \Delta P \leq \hat{P}_M(\mathbf{q} \in \mathcal{A}_q) \leq P(\mathbf{q} \in \mathcal{A}_q) + \Delta P\right) \\ &\approx 2 \Phi\left(\frac{\Delta P}{\sqrt{P(\mathbf{q} \in \mathcal{A}_q)(1 - P(\mathbf{q} \in \mathcal{A}_q))/M}}\right) - 1. \end{aligned} \quad (5.12)$$

From (3.48), it has been concluded that the number of samples or observations f_m and system simulations M in the Monte Carlo simulation has to fulfill the condition (3.51) such that the confidence interval $\left[\hat{Y}_M - \Delta Y, \hat{Y}_M + \Delta Y \right]$ of length $2 \Delta Y$ around the estimate \hat{Y}_M contains the true probability Y of fulfilling the performance specifications with the probability κ , the desired confidence level, i.e., $P\left(\hat{Y}_M - \Delta Y \leq Y \leq \hat{Y}_M + \Delta Y\right) = \kappa$. Analogously, it can be concluded from (5.12) that the number of samples or observations q_m and simulations of the automated vehicular safety system M in the Monte Carlo simulation has to fulfill the following condition such that the confidence interval $\left[\hat{P}_M(\mathbf{q} \in \mathcal{A}_q) - \Delta P, \hat{P}_M(\mathbf{q} \in \mathcal{A}_q) + \Delta P \right]$ of length $2 \Delta P$ around the estimate $\hat{P}_M(\mathbf{q} \in \mathcal{A}_q)$ contains the true probability $P(\mathbf{q} \in \mathcal{A}_q)$ of fulfilling the specifications for the customer satisfaction with the probability κ , the desired confidence level, i.e.,

$$P\left(\hat{P}_M(\mathbf{q} \in \mathcal{A}_q) - \Delta P \leq P(\mathbf{q} \in \mathcal{A}_q) \leq \hat{P}_M(\mathbf{q} \in \mathcal{A}_q) + \Delta P\right) = \kappa : \quad (5.13)$$

$$M \approx \frac{P(\mathbf{q} \in \mathcal{A}_q)(1 - P(\mathbf{q} \in \mathcal{A}_q))}{\Delta P^2} \left(\Phi^{-1} \left(\frac{\kappa + 1}{2} \right) \right)^2 = M_{\text{req.}}. \quad (5.14)$$

$M_{\text{req.}}$ is the approximate number of samples or observations q_m and simulations of the automated vehicular safety system in the Monte Carlo simulation required for estimating the probability $P(\mathbf{q} \in \mathcal{A}_q)$ of fulfilling the specifications for the customer satisfaction by the estimator $\hat{P}_M(\mathbf{q} \in \mathcal{A}_q)$ from (5.5) with the desired confidence level κ for the corresponding confidence interval $\left[\hat{P}_M(\mathbf{q} \in \mathcal{A}_q) - \Delta P, \hat{P}_M(\mathbf{q} \in \mathcal{A}_q) + \Delta P \right]$. Assuming that the true probability of fulfilling the specifications for the customer satisfaction is $P(\mathbf{q} \in \mathcal{A}_q) = 0.99$, plotting this number $M_{\text{req.}}$ over the half confidence interval length ΔP for the desired confidence levels $\kappa = 0.9, 0.95, 0.99$ and over the desired confidence level κ for the half confidence interval lengths $\Delta P = 0.01, 0.001, 0.0001$ yields the same plots as plotting the approximate number $M_{\text{req.}}$ of samples or observations f_m and system simulations in the Monte Carlo simulation required for estimating the probability Y of fulfilling the performance specifications with the desired confidence level κ for the corresponding confidence interval $\left[\hat{Y}_M - \Delta Y, \hat{Y}_M + \Delta Y \right]$ over the half confidence interval length ΔY for the desired confidence levels $\kappa = 0.9, 0.95, 0.99$ and over the desired confidence level κ for the half confidence interval lengths $\Delta Y = 0.01, 0.001, 0.0001$ assuming that the true probability Y of fulfilling the performance specifications is $Y = P(\mathbf{q} \in \mathcal{A}_q) = 0.99$ in Figure 3.1 with ΔY replaced by ΔP . The approximate required number $M_{\text{req.}}$ of samples or observations q_m and simulations of the automated vehicular safety system in the Monte Carlo simulation increases if the half confidence interval length ΔP

decreases or the desired confidence level κ increases. Especially if the half confidence interval length ΔP is already small, a further reduction of it leads to a significant increase in the approximate required number $M_{\text{req.}}$ of samples or observations \mathbf{q}_m and simulations of the automated vehicular safety system in the Monte Carlo simulation.

So, it can be concluded that estimating the probability $P(\mathbf{q} \in \mathcal{A}_q)$ of fulfilling the specifications for the customer satisfaction by a Monte Carlo simulation has a beneficial advantage but also an important drawback. On the one hand, it can be implemented easily and it is easy to apply it to different automated vehicular safety systems due to its generality. On the other hand, however, a large number M of simulations of the automated vehicular safety system has to be performed in order to obtain an accurate estimate $\hat{P}_M(\mathbf{q} \in \mathcal{A}_q)$ for the probability $P(\mathbf{q} \in \mathcal{A}_q)$ of fulfilling the specifications for the customer satisfaction with a high confidence level κ for a small confidence interval $[\hat{P}_M(\mathbf{q} \in \mathcal{A}_q) - \Delta P, \hat{P}_M(\mathbf{q} \in \mathcal{A}_q) + \Delta P]$ around it with a small half length ΔP , which might lead to a prohibitively large computational complexity in practice.

5.2 Worst-Case-Distance-Based Robust Design of Automated Vehicular Safety Systems

The problem of the large number M of simulations of the automated vehicular safety system to be performed in order to obtain an accurate Monte-Carlo-based estimate $\hat{P}_M(\mathbf{q} \in \mathcal{A}_q)$ for the probability $P(\mathbf{q} \in \mathcal{A}_q)$ of fulfilling the specifications for the customer satisfaction can be overcome as follows. The customer satisfaction properties \mathbf{q} , the corresponding acceptance intervals $[q_{L,i}, q_{U,i}]$, $i = 1, 2, \dots, N_q$, the sensor measurement errors ε and the customer satisfaction acceptance region \mathcal{A}_q defined by (4.18) play the role of the performance properties \mathbf{f} , the corresponding acceptance intervals $[f_{L,i}, f_{U,i}]$, $i = 1, 2, \dots, N_f$, the statistical parameters s and the performance acceptance region \mathcal{A}_f defined by (3.1), respectively. Analogously to the parameter acceptance region \mathcal{A}_s defined by (3.53), an error acceptance region

$$\begin{aligned} \mathcal{A}_\varepsilon &= \left\{ \varepsilon \in \mathbb{R}^{E(n_{\text{end}}+1)} : \mathbf{q} \in \mathcal{A}_q \right\} \\ &= \left\{ \varepsilon \in \mathbb{R}^{E(n_{\text{end}}+1)} : q_{L,i} \leq q_i \leq q_{U,i}, i = 1, 2, \dots, N_q \right\} \end{aligned} \quad (5.15)$$

can be defined. It is the set of all values of the sensor measurement errors ε that are mapped to customer satisfaction properties \mathbf{q} lying in the acceptance intervals and thus correspond to an automated vehicular safety system fulfilling the specifications for the customer satisfaction. The probability $P(\varepsilon \in \mathcal{A}_\varepsilon)$ that the sensor measurement errors

ε lie in the error acceptance region \mathcal{A}_ε is equivalent to the probability $P(\mathbf{q} \in \mathcal{A}_q)$ that the automated vehicular safety system fulfills all given specifications for the customer satisfaction such that all customer satisfaction properties \mathbf{q} lie in the acceptance intervals and thus in the customer satisfaction acceptance region \mathcal{A}_q :

$$P(\mathbf{q} \in \mathcal{A}_q) = P(\varepsilon \in \mathcal{A}_\varepsilon). \quad (5.16)$$

Analogously to the performance acceptance region \mathcal{A}_f , the parameter acceptance region \mathcal{A}_s and the customer satisfaction acceptance region \mathcal{A}_q , the error acceptance region \mathcal{A}_ε can also be represented by the intersection of individual error acceptance region partitions

$$\mathcal{A}_{\varepsilon,L,i} = \left\{ \varepsilon \in \mathbb{R}^{E(n_{\text{end}}+1)} : q_i \geq q_{L,i} \right\} = \left\{ \varepsilon \in \mathbb{R}^{E(n_{\text{end}}+1)} : \mathbf{q} \in \mathcal{A}_{q,L,i} \right\} \quad (5.17)$$

and

$$\mathcal{A}_{\varepsilon,U,i} = \left\{ \varepsilon \in \mathbb{R}^{E(n_{\text{end}}+1)} : q_i \leq q_{U,i} \right\} = \left\{ \varepsilon \in \mathbb{R}^{E(n_{\text{end}}+1)} : \mathbf{q} \in \mathcal{A}_{q,U,i} \right\}, \quad (5.18)$$

the i^{th} of which are the sets of all values of the sensor measurement errors ε that are mapped to values of the i^{th} customer satisfaction property q_i that do not lie below the lower bound $q_{L,i}$ and above the upper bound $q_{U,i}$ of the corresponding acceptance interval $[q_{L,i}, q_{U,i}]$, respectively:

$$\mathcal{A}_\varepsilon = \bigcap_{i=1}^{N_q} \mathcal{A}_{\varepsilon,L,i} \cap \mathcal{A}_{\varepsilon,U,i}. \quad (5.19)$$

In the special cases $q_{L,i} \rightarrow -\infty$ and $q_{U,i} \rightarrow \infty$, the corresponding individual error acceptance region partitions simplify to $\mathcal{A}_{\varepsilon,L,i} = \mathbb{R}^{E(n_{\text{end}}+1)}$ and $\mathcal{A}_{\varepsilon,U,i} = \mathbb{R}^{E(n_{\text{end}}+1)}$, respectively. The green areas, where $f_i > f_{L,i}$ and $f_i < f_{U,i}$, including the orange boundaries, where $f_i = f_{L,i}$ and $f_i = f_{U,i}$, in Figure 3.2 and Figure 3.3 representing exemplary individual parameter acceptance region partitions $\mathcal{A}_{s,L,i}$ with a finite lower bound $f_{L,i}$ and $\mathcal{A}_{s,U,i}$ with a finite upper bound $f_{U,i}$, respectively, for a performance property f_i that is a function of only two statistical parameters $\mathbf{s} = [s_1, s_2]^T$ also represent exemplary individual error acceptance region partitions $\mathcal{A}_{\varepsilon,L,i}$ with a finite lower bound $q_{L,i}$ and $\mathcal{A}_{\varepsilon,U,i}$ with a finite upper bound $q_{U,i}$, respectively, for a customer satisfaction property q_i that is a function of only two sensor measurement errors $\varepsilon = [\varepsilon_1, \varepsilon_2]^T$ when replacing f_i by q_i , $f_{L,i}$ by $q_{L,i}$, $f_{U,i}$ by $q_{U,i}$, s_1 by ε_1 , s_2 by ε_2 and the mean \mathbf{s}_0 of the statistical parameters \mathbf{s} by the mean $\boldsymbol{\mu}$ of the sensor measurement errors ε . While $q_i = q_{L,i}$ and $q_i = q_{U,i}$ along the orange boundary, $q_i > q_{L,i}$ and

$q_i < q_{U,i}$ in the green areas of Figure 3.2 and Figure 3.3, respectively. After the replacement of $f_i, f_{L,i}, f_{U,i}, s_1, s_2$ and \mathbf{s}_0 by $q_i, q_{L,i}, q_{U,i}, \varepsilon_1, \varepsilon_2$ and $\boldsymbol{\mu}$, respectively, the illustration of the intersection $\mathcal{A}_{\mathbf{s},L,i} \cap \mathcal{A}_{\mathbf{s},U,i}$ of the two exemplary individual parameter acceptance region partitions $\mathcal{A}_{\mathbf{s},L,i}$ and $\mathcal{A}_{\mathbf{s},U,i}$ from Figure 3.2 and Figure 3.3 in Figure 3.4 can also be seen as an illustration of the intersection

$$\begin{aligned} \mathcal{A}_{\varepsilon,L,i} \cap \mathcal{A}_{\varepsilon,U,i} &= \left\{ \boldsymbol{\varepsilon} \in \mathbb{R}^{E(n_{\text{end}}+1)} : q_i \geq q_{L,i} \right\} \cap \left\{ \boldsymbol{\varepsilon} \in \mathbb{R}^{E(n_{\text{end}}+1)} : q_i \leq q_{U,i} \right\} \\ &= \left\{ \boldsymbol{\varepsilon} \in \mathbb{R}^{E(n_{\text{end}}+1)} : q_{L,i} \leq q_i \leq q_{U,i} \right\} \end{aligned} \quad (5.20)$$

of two individual error acceptance region partitions $\mathcal{A}_{\varepsilon,L,i}$ and $\mathcal{A}_{\varepsilon,U,i}$ for the two exemplary individual error acceptance region partitions $\mathcal{A}_{\varepsilon,L,i}$ and $\mathcal{A}_{\varepsilon,U,i}$ represented by Figure 3.2 and Figure 3.3. In such an intersection of two individual error acceptance region partitions $\mathcal{A}_{\varepsilon,L,i}$ and $\mathcal{A}_{\varepsilon,U,i}$, the i^{th} customer satisfaction property q_i lies in its acceptance interval $[q_{L,i}, q_{U,i}]$ such that the i^{th} specification $q_{L,i} \leq q_i \leq q_{U,i}$ for the customer satisfaction defined by this acceptance interval is fulfilled.

The probability that the sensor measurement errors $\boldsymbol{\varepsilon}$ lie in the error acceptance region $\mathcal{A}_{\boldsymbol{\varepsilon}}$ and thus the probability $P(\mathbf{q} \in \mathcal{A}_{\mathbf{q}})$ of fulfilling the specifications for the customer satisfaction could theoretically be obtained by integrating the multivariate Gaussian pdf $f_{\boldsymbol{\varepsilon}}(\boldsymbol{\varepsilon})$ of the sensor measurement errors $\boldsymbol{\varepsilon}$ given by (4.26) in the error acceptance region $\mathcal{A}_{\boldsymbol{\varepsilon}}$:

$$\begin{aligned} P(\mathbf{q} \in \mathcal{A}_{\mathbf{q}}) &= P(\boldsymbol{\varepsilon} \in \mathcal{A}_{\boldsymbol{\varepsilon}}) = \int_{\mathcal{A}_{\boldsymbol{\varepsilon}}} f_{\boldsymbol{\varepsilon}}(\boldsymbol{\varepsilon}) \, d\boldsymbol{\varepsilon} \\ &= \frac{1}{\sqrt{(2\pi)^{E(n_{\text{end}}+1)} \det(\mathbf{C})}} \\ &\quad \cdot \int_{\{\boldsymbol{\varepsilon} \in \mathbb{R}^{E(n_{\text{end}}+1)} : \mathbf{q} \in \mathcal{A}_{\mathbf{q}}\}} \exp\left(-\frac{1}{2}(\boldsymbol{\varepsilon} - \boldsymbol{\mu})^T \mathbf{C}^{-1}(\boldsymbol{\varepsilon} - \boldsymbol{\mu})\right) \, d\boldsymbol{\varepsilon}. \end{aligned} \quad (5.21)$$

Unfortunately, there are two problems that render this integration intractable in practice. First, the boundary of the error acceptance region $\mathcal{A}_{\boldsymbol{\varepsilon}}$ as illustrated by the orange curves in Figure 3.4 for two sensor measurement errors $\boldsymbol{\varepsilon} = [\varepsilon_1, \varepsilon_2]^T$ corresponding to two statistical parameters $\mathbf{s} = [s_1, s_2]^T$ can only be determined by many simulations of the automated vehicular safety system and, second, the integration of the multivariate Gaussian pdf $f_{\boldsymbol{\varepsilon}}(\boldsymbol{\varepsilon})$ of the sensor measurement errors $\boldsymbol{\varepsilon}$ in the error acceptance region $\mathcal{A}_{\boldsymbol{\varepsilon}}$

with a possibly highly nonlinear boundary can only be performed numerically, which comes with a high computational complexity. In order to overcome both problems at the same time, one can resort to approximating the boundary of the error acceptance region \mathcal{A}_ε by just a few simulations of the automated vehicular safety system such that the integration in the resulting simplified error acceptance region becomes easy. This can be achieved by directly applying the worst-case distance approach to the robust design of automated vehicular safety systems.

5.2.1 Direct Application of Worst-Case Distance Approach to Robust Design of Automated Vehicular Safety Systems

Analogously to the worst-case distances for a finite lower bound $f_{L,i}$ and for a finite upper bound $f_{U,i}$ of the acceptance interval for the i^{th} performance property f_i in (3.59) and (3.60), the worst-case distances for a finite lower bound $q_{L,i}$ and for a finite upper bound $q_{U,i}$ of the acceptance interval for the i^{th} customer satisfaction property q_i can be defined as

$$\beta_{L,i} = \min_{\varepsilon \in \mathbb{R}^{E(n_{\text{end}}+1)}} \beta(\varepsilon) \quad \text{s.t.} \quad q_i \leq q_{L,i}, \quad (5.22)$$

and

$$\beta_{U,i} = \min_{\varepsilon \in \mathbb{R}^{E(n_{\text{end}}+1)}} \beta(\varepsilon) \quad \text{s.t.} \quad q_i \geq q_{U,i}, \quad (5.23)$$

respectively, where $\beta(\varepsilon)$ measures the distance between the sensor measurement errors ε and their mean $\boldsymbol{\mu}$. The worst-case distance $\beta_{b,i}$, $b \in \{\text{L}, \text{U}\}$, is the smallest distance between the mean $\boldsymbol{\mu}$ of the sensor measurement errors ε , at which their multivariate Gaussian pdf $f_\varepsilon(\varepsilon)$ has its peak and which is assumed to lie in the corresponding individual error acceptance region partition $\mathcal{A}_{\varepsilon,b,i}$, and the boundary of the corresponding individual error acceptance region partition $\mathcal{A}_{\varepsilon,b,i}$, where the i^{th} specification $q_{L,i} \leq q_i \leq q_{U,i}$ for the customer satisfaction is barely fulfilled, i.e., $q_i = q_{b,i}$. Following the worst-case distance approach, the Mahalanobis distance is chosen as distance measure such that the distance $\beta(\varepsilon)$ between the sensor measurement errors ε and their mean $\boldsymbol{\mu}$ is given by

$$\beta^2(\varepsilon) = (\varepsilon - \boldsymbol{\mu})^T \mathbf{C}^{-1} (\varepsilon - \boldsymbol{\mu}). \quad (5.24)$$

As a consequence, the pdf $f_\varepsilon(\varepsilon)$ of the sensor measurement errors ε reads

$$f_\varepsilon(\varepsilon) = \frac{1}{\sqrt{(2\pi)^{E(n_{\text{end}}+1)} \det(\mathbf{C})}} \exp\left(-\frac{1}{2}\beta^2(\varepsilon)\right) \quad (5.25)$$

and the set of all sensor measurement errors $\boldsymbol{\varepsilon}$ that have the same distance $\beta(\boldsymbol{\varepsilon}) = \beta = \text{const.}$ from their mean $\boldsymbol{\mu}$, i.e., all equidistant points $\boldsymbol{\varepsilon}$, is the set of all sensor measurement errors $\boldsymbol{\varepsilon}$ for which their pdf $f_{\boldsymbol{\varepsilon}}(\boldsymbol{\varepsilon})$ has the same value, i.e., a contour line of the pdf $f_{\boldsymbol{\varepsilon}}(\boldsymbol{\varepsilon})$:

$$\begin{aligned} & \left\{ \boldsymbol{\varepsilon} \in \mathbb{R}^{E(n_{\text{end}}+1)} : \beta(\boldsymbol{\varepsilon}) = \beta \right\} \\ &= \left\{ \boldsymbol{\varepsilon} \in \mathbb{R}^{E(n_{\text{end}}+1)} : f_{\boldsymbol{\varepsilon}}(\boldsymbol{\varepsilon}) = \frac{\exp\left(-\frac{1}{2}\beta^2\right)}{\sqrt{(2\pi)^{E(n_{\text{end}}+1)} \det(\mathbf{C})}} \right\} \quad (5.26) \\ &= \left\{ \boldsymbol{\varepsilon} \in \mathbb{R}^{E(n_{\text{end}}+1)} : (\boldsymbol{\varepsilon} - \boldsymbol{\mu})^T \mathbf{C}^{-1} (\boldsymbol{\varepsilon} - \boldsymbol{\mu}) = \beta^2 \right\}. \end{aligned}$$

In general, these sets for different constant distances β are hyperellipsoids whose center is the mean $\boldsymbol{\mu}$ of the sensor measurement errors $\boldsymbol{\varepsilon}$ as illustrated by the gray ellipses in Figure 3.2 and Figure 3.3 for two sensor measurement errors $\boldsymbol{\varepsilon} = [\varepsilon_1, \varepsilon_2]^T$ corresponding to the two statistical parameters $\boldsymbol{s} = [s_1, s_2]^T$ shown there with their mean \boldsymbol{s}_0 , the center of the ellipses, corresponding to the mean $\boldsymbol{\mu}$ of the sensor measurement errors. The smallest hyperellipsoid, i.e., the smallest ellipse in the two-dimensional case with two sensor measurement errors $\boldsymbol{\varepsilon} = [\varepsilon_1, \varepsilon_2]^T$, on which all sensor measurement errors $\boldsymbol{\varepsilon}$ have the same distance β from their mean $\boldsymbol{\mu}$ and that has a point with the boundary of the individual error acceptance region partition $\mathcal{A}_{\boldsymbol{\varepsilon},b,i}$ in common touches this boundary at the point where the sensor measurement errors $\boldsymbol{\varepsilon}$ on this boundary have the smallest distance $\beta(\boldsymbol{\varepsilon})$ from their mean $\boldsymbol{\mu}$. This distance is the worst-case distance $\beta_{b,i}$.

As the boundary of the individual parameter acceptance region partition $\mathcal{A}_{\boldsymbol{s},b,i}$, $b \in \{\text{L}, \text{U}\}$, is approximated by linearizing it with a tangential hyperplane to obtain an approximate individual parameter acceptance region partition $\hat{\mathcal{A}}_{\boldsymbol{s},b,i}$ bounded by this tangential hyperplane, the boundary of the individual error acceptance region partition $\mathcal{A}_{\boldsymbol{\varepsilon},b,i}$, $b \in \{\text{L}, \text{U}\}$, can also be approximated by linearizing it with a tangential hyperplane to obtain an approximate individual error acceptance region partition $\hat{\mathcal{A}}_{\boldsymbol{\varepsilon},b,i}$ bounded by this tangential hyperplane. This approximating tangential hyperplane is the tangential hyperplane that touches the boundary of the individual error acceptance region partition $\mathcal{A}_{\boldsymbol{\varepsilon},b,i}$ at the point where the sensor measurement errors $\boldsymbol{\varepsilon}$ on this boundary have the smallest distance from their mean $\boldsymbol{\mu}$, namely, the worst-case distance $\beta_{b,i}$. For two sensor measurement errors $\boldsymbol{\varepsilon} = [\varepsilon_1, \varepsilon_2]^T$, the tangential hyperplane approximating the orange boundary of the individual error acceptance region partition $\mathcal{A}_{\boldsymbol{\varepsilon},\text{L},i}$, where $q_i = q_{\text{L},i}$, in Figure 3.2 is illustrated by the violet tangential line and the tangential hyperplane approximating the orange boundary of the individual error

acceptance region partition $\mathcal{A}_{\varepsilon,U,i}$, where $q_i = q_{U,i}$, in Figure 3.3 by the magenta tangential line. The resulting approximate individual error acceptance region partitions $\hat{\mathcal{A}}_{\varepsilon,L,i}$ and $\hat{\mathcal{A}}_{\varepsilon,U,i}$ are the horizontally and vertically striped areas bounded by these violet and magenta tangential lines, respectively.

According to the expression for the probability that the statistical parameters s lie in the approximate individual parameter acceptance region partition $\hat{\mathcal{A}}_{s,b,i}$ stated in (3.65), the probability that the sensor measurement errors ε playing the role of the statistical parameters s lie in the approximate individual error acceptance region partition $\hat{\mathcal{A}}_{\varepsilon,b,i}$ corresponding to the approximate individual parameter acceptance region partition $\hat{\mathcal{A}}_{s,b,i}$ can be computed as follows to approximate the probability that they lie in the individual error acceptance region partition $\mathcal{A}_{\varepsilon,b,i}$, $b \in \{L, U\}$:

$$P(\varepsilon \in \mathcal{A}_{\varepsilon,b,i}) \approx P(\varepsilon \in \hat{\mathcal{A}}_{\varepsilon,b,i}) = \Phi(\beta_{b,i}). \quad (5.27)$$

So, the integration of the multivariate Gaussian pdf of the sensor measurement errors ε in the approximate individual error acceptance region partition $\hat{\mathcal{A}}_{\varepsilon,b,i}$ to obtain the probability $P(\varepsilon \in \hat{\mathcal{A}}_{\varepsilon,b,i})$ that the sensor measurement errors ε lie in the approximate individual error acceptance region partition $\hat{\mathcal{A}}_{\varepsilon,b,i}$ and thus approximately the probability $P(\varepsilon \in \mathcal{A}_{\varepsilon,b,i})$ that they lie in the actual individual error acceptance region partition $\mathcal{A}_{\varepsilon,b,i}$ simplifies to one evaluation of the standard normal cdf $\Phi(x)$ at the worst-case distance $\beta_{b,i}$. The peak of the multivariate Gaussian pdf of the sensor measurement errors ε at their mean μ has to lie in the individual error acceptance region partition $\mathcal{A}_{\varepsilon,b,i}$, $b \in \{L, U\}$, and it has to be rather concentrated around its peak in order to be able to achieve a large probability $P(\varepsilon \in \mathcal{A}_{\varepsilon,b,i})$ that the sensor measurement errors ε lie in the individual error acceptance region partition $\mathcal{A}_{\varepsilon,b,i}$ and thus the corresponding specification for the customer satisfaction, i.e., $q_i \geq q_{L,i}$ if $b = L$ or $q_i \leq q_{U,i}$ if $b = U$, is fulfilled, which is a requirement for achieving a high probability $P(\mathbf{q} \in \mathcal{A}_q)$ of fulfilling all specifications $q_{L,i} \leq q_i \leq q_{U,i}$, $i = 1, 2, \dots, N_q$, for the customer satisfaction. In addition, the maximum of the multivariate Gaussian pdf of the sensor measurement errors ε along the boundary of the individual error acceptance region partition $\mathcal{A}_{\varepsilon,b,i}$ occurs exactly where the tangential hyperplane, the boundary of the corresponding approximate individual error acceptance region partition $\hat{\mathcal{A}}_{\varepsilon,b,i}$, touches it and thus the approximation error between them is zero. From these facts, it can be concluded that the multivariate Gaussian pdf of the sensor measurement errors ε is small where the approximation error between the boundaries of the individual error acceptance region partition $\mathcal{A}_{\varepsilon,b,i}$ and the corresponding approximate individual error acceptance region partition $\hat{\mathcal{A}}_{\varepsilon,b,i}$ is large such that the approximation of the probability $P(\varepsilon \in \mathcal{A}_{\varepsilon,b,i})$ that the sensor measurement errors ε lie in the individual

error acceptance region partition $\mathcal{A}_{\varepsilon,b,i}$ by the probability $P(\varepsilon \in \hat{\mathcal{A}}_{\varepsilon,b,i})$ that they lie in the corresponding approximate individual error acceptance region partition $\hat{\mathcal{A}}_{\varepsilon,b,i}$ is accurate. Moreover, the boundaries of the actual and approximate individual error acceptance region partitions $\mathcal{A}_{\varepsilon,b,i}$ and $\hat{\mathcal{A}}_{\varepsilon,b,i}$, respectively, might touch or intersect at more than one point, where the approximation error is zero as well.

According to the expression for the probability $P(s \in \mathcal{A}_{s,L,i} \cap \mathcal{A}_{s,U,i})$ that the statistical parameters s lie in the intersection $\mathcal{A}_{s,L,i} \cap \mathcal{A}_{s,U,i}$ of the two individual parameter acceptance region partitions $\mathcal{A}_{s,L,i}$ and $\mathcal{A}_{s,U,i}$ in (3.66) and its approximation in (3.68), the probability $P(\varepsilon \in \mathcal{A}_{\varepsilon,L,i} \cap \mathcal{A}_{\varepsilon,U,i})$ that the sensor measurement errors ε lie in the intersection $\mathcal{A}_{\varepsilon,L,i} \cap \mathcal{A}_{\varepsilon,U,i}$ of the two individual error acceptance region partitions $\mathcal{A}_{\varepsilon,L,i}$ and $\mathcal{A}_{\varepsilon,U,i}$ can be expressed as

$$\begin{aligned} P(\varepsilon \in \mathcal{A}_{\varepsilon,L,i} \cap \mathcal{A}_{\varepsilon,U,i}) &= P(q_{L,i} \leq q_i \leq q_{U,i}) \\ &= P(\varepsilon \in \mathcal{A}_{\varepsilon,L,i}) + P(\varepsilon \in \mathcal{A}_{\varepsilon,U,i}) - 1 \end{aligned} \quad (5.28)$$

and approximated by

$$P(\varepsilon \in \mathcal{A}_{\varepsilon,L,i} \cap \mathcal{A}_{\varepsilon,U,i}) \approx \begin{cases} \Phi(\beta_{U,i}), & q_{L,i} \rightarrow -\infty \\ \Phi(\beta_{L,i}), & q_{U,i} \rightarrow \infty \\ \Phi(\beta_{L,i}) + \Phi(\beta_{U,i}) - 1, & \text{otherwise} \end{cases} \quad (5.29)$$

This is due to the fact that the sensor measurement errors ε , the customer satisfaction property q_i , the lower and upper limit of its acceptance interval $[q_{L,i}, q_{U,i}]$, and the corresponding individual error acceptance region partitions $\mathcal{A}_{\varepsilon,L,i}$ and $\mathcal{A}_{\varepsilon,U,i}$ play the role of the statistical parameters s , the performance property f_i , the lower and upper limit of its acceptance interval $[f_{L,i}, f_{U,i}]$, and the corresponding individual parameter acceptance region partitions $\mathcal{A}_{s,L,i}$ and $\mathcal{A}_{s,U,i}$, respectively. The intersection $\mathcal{A}_{\varepsilon,L,i} \cap \mathcal{A}_{\varepsilon,U,i}$ of two individual error acceptance region partitions $\mathcal{A}_{\varepsilon,L,i}$ and $\mathcal{A}_{\varepsilon,U,i}$ given by (5.20) is the set of all sensor measurement errors ε for which the i^{th} customer satisfaction property q_i lies in its acceptance interval $[q_{L,i}, q_{U,i}]$ such that the i^{th} specification $q_{L,i} \leq q_i \leq q_{U,i}$ for the customer satisfaction defined by this acceptance interval is fulfilled. It is illustrated in Figure 3.4 for the two exemplary individual error acceptance region partitions $\mathcal{A}_{\varepsilon,L,i}$ and $\mathcal{A}_{\varepsilon,U,i}$ shown in Figure 3.2 and Figure 3.3, respectively, with two sensor measurement errors $\varepsilon = [\varepsilon_1, \varepsilon_2]^T$ when replacing $f_i, f_{L,i}, f_{U,i}, s_1, s_2$ and s_0 by $q_i, q_{L,i}, q_{U,i}, \varepsilon_1, \varepsilon_2$ and μ , respectively.

Since the error acceptance region \mathcal{A}_ε is the intersection of all intersections of two individual error acceptance region partitions $\mathcal{A}_{\varepsilon,L,i}$ and $\mathcal{A}_{\varepsilon,U,i}$, $i = 1, 2, \dots, N_q$,

according to (5.19), the probability that the sensor measurement errors ε do not lie in the error acceptance region \mathcal{A}_ε , can be expressed as

$$\begin{aligned} P(\varepsilon \notin \mathcal{A}_\varepsilon) &= P\left(\varepsilon \notin \bigcap_{i=1}^{N_q} \mathcal{A}_{\varepsilon,L,i} \cap \mathcal{A}_{\varepsilon,U,i}\right) = P\left(\bigvee_{i=1}^{N_q} \varepsilon \notin \mathcal{A}_{\varepsilon,L,i} \cap \mathcal{A}_{\varepsilon,U,i}\right) \\ &\approx \sum_{i=1}^{N_q} P(\varepsilon \notin \mathcal{A}_{\varepsilon,L,i} \cap \mathcal{A}_{\varepsilon,U,i}) = \sum_{i=1}^{N_q} 1 - P(\varepsilon \in \mathcal{A}_{\varepsilon,L,i} \cap \mathcal{A}_{\varepsilon,U,i}). \end{aligned} \quad (5.30)$$

With (5.29), the probability $P(\mathbf{q} \in \mathcal{A}_q)$ of fulfilling all specifications $q_{L,i} \leq q_i \leq q_{U,i}$ for the customer satisfaction defined by the acceptance intervals $[q_{L,i}, q_{U,i}]$ for the customer satisfaction properties $q_i, i = 1, 2, \dots, N_q$, can be approximated by

$$\begin{aligned} P(\mathbf{q} \in \mathcal{A}_q) &= P(\varepsilon \in \mathcal{A}_\varepsilon) = 1 - P(\varepsilon \notin \mathcal{A}_\varepsilon) \\ &\approx 1 - \sum_{i=1}^{N_q} 1 - P(\varepsilon \in \mathcal{A}_{\varepsilon,L,i} \cap \mathcal{A}_{\varepsilon,U,i}) \\ &\approx 1 - \sum_{i=1}^{N_q} 1 - \begin{cases} \Phi(\beta_{U,i}), & q_{L,i} \rightarrow -\infty \\ \Phi(\beta_{L,i}), & q_{U,i} \rightarrow \infty \\ \Phi(\beta_{L,i}) + \Phi(\beta_{U,i}) - 1, & \text{otherwise} \end{cases} \end{aligned} \quad (5.31)$$

This direct application of the worst-case distance approach to the robust design of automated vehicular safety systems inherits the benefits from its application to the robust system design in general. The integration of the multivariate Gaussian pdf of the sensor measurement errors ε in the error acceptance region \mathcal{A}_ε from (5.21) to obtain the probability $P(\mathbf{q} \in \mathcal{A}_q)$ of fulfilling the specifications for the customer satisfaction is simplified to approximating this probability by evaluating the standard normal cdf $\Phi(x)$ at the worst-case distances $\beta_{b,i}, i = 1, 2, \dots, N_q, b = L, U$. Each required worst-case distance $\beta_{b,i}$ can be determined by solving the optimization problem (5.22) if $b = L$ and (5.23) if $b = U$, i.e., an optimization minimizing the distance between the sensor measurement errors ε on the boundary of the corresponding individual error acceptance region partition $\mathcal{A}_{\varepsilon,b,i}$ and their mean $\boldsymbol{\mu}$ without determining the whole boundary of the error acceptance region \mathcal{A}_ε . Appropriate optimization methods for solving these optimizations choose the simulations of the automated vehicular safety system required for solving the optimizations automatically in a smart way serving the achievement of the optimization goal and thus replace a computationally expensive Monte Carlo simulation, which just chooses an extensive amount of simulations of the automated

vehicular safety system according to the underlying probability distribution in a brute-force way for estimating the probability $P(\mathbf{q} \in \mathcal{A}_q)$ of fulfilling the specifications for the customer satisfaction, by a few relevant simulations that deliver the required information for approximating this probability. This is the reason why approximating the probability $P(\mathbf{q} \in \mathcal{A}_q)$ of fulfilling the specifications for the customer satisfaction by worst-case distances can lead to a significant reduction of computational complexity in the robust design of automated vehicular safety systems as compared to estimating it by a Monte Carlo simulation when a high estimation accuracy is required.

Besides these benefits, however, the direct application of the worst-case distance approach to the robust design of automated vehicular safety systems comes with the following two problems. First, solving the optimization problems (5.22) and (5.23) for determining the worst-case distances $\beta_{L,i}$ and $\beta_{U,i}$, respectively, might be difficult if the number of sensor measurement errors $E(n_{\text{end}} + 1)$ becomes large because then the optimization has to be performed with respect to a high-dimensional vector $\varepsilon \in \mathbb{R}^{E(n_{\text{end}}+1)}$ of sensor measurement errors. Second, linearizing the boundary of the individual error acceptance region partition $\mathcal{A}_{\varepsilon,b,i}$, $b \in \{L, U\}$, by just one tangential hyperplane at one point where the distance of the sensor measurement errors ε from their mean $\boldsymbol{\mu}$ is the worst-case distance $\beta_{b,i}$ limits the achievable accuracy of the approximation since this boundary is typically highly non-linear and non-smooth because of the decisions on an intervention made at the time instants t_n , $n = 0, 1, \dots, n_{\text{end}}$, independently from each other based on a decision rule $f(\cdot; \boldsymbol{\varphi})$ with the function parameters $\boldsymbol{\varphi}$ especially if the number of the considered time instants $n_{\text{end}} + 1$ becomes large.

This is illustrated by Figure 5.1 for $E = 1$ sensor measurement error $\varepsilon[n] = \varepsilon[n] \in \mathbb{R}$ with the mean $\boldsymbol{\mu}_n = \mu_n$ at a time instant t_n in the plane where only the values of the sensor measurement errors $\varepsilon[n_1]$ and $\varepsilon[n_2]$ at the specific time instants t_{n_1} and t_{n_2} , respectively, vary while the values of all other sensor measurement errors $\varepsilon[n]$ at the time instants $t_n \neq t_{n_1}, t_{n_2}$ are constant and equal to their mean, i.e., $\varepsilon[n] = \mu_n$ for $n \neq n_1, n_2$. The green area possibly including the orange boundary represents an exemplary individual error acceptance region partition $\mathcal{A}_{\varepsilon,b,i}$, $b \in \{L, U\}$, with either a finite lower bound $q_{L,i}$ if $b = L$ or a finite upper bound $q_{U,i}$ if $b = U$ in this plane under the assumption that the function must not decide for an intervention based on the sensor measurements $\mathbf{y}[n_1]$ at the time instant t_{n_1} and based on the sensor measurements $\mathbf{y}[n_2]$ at the time instant t_{n_2} using the decision rule $f(\cdot; \boldsymbol{\varphi})$ with the function parameters $\boldsymbol{\varphi}$ such that the i^{th} customer satisfaction property q_i does not lie below the lower bound $q_{L,i}$ of the acceptance interval $[q_{L,i}, q_{U,i}]$, i.e., $q_i \geq q_{L,i}$, if $b = L$ or above the upper bound $q_{U,i}$ of this acceptance interval, i.e., $q_i \leq q_{U,i}$, if $b = U$. For

given states $\mathbf{x} [n]$ of the considered dynamic system in a driving scenario at the time instants $t_n, n = 0, 1, \dots, n_{\text{end}}$, the sensor measurements $\mathbf{y} [n_1] = \mathbf{y} (\mathbf{x} [n_1], \varepsilon [n_1])$ at the time instant t_{n_1} depend only on the sensor measurement errors $\varepsilon [n_1]$ at this time instant t_{n_1} and the sensor measurements $\mathbf{y} [n_2] = \mathbf{y} (\mathbf{x} [n_2], \varepsilon [n_2])$ at the time instant t_{n_2} only on the sensor measurement errors $\varepsilon [n_2]$ at this time instant t_{n_2} . Due to the independence of the decisions made at different time instants t_{n_1} and t_{n_2} , the results of these decisions are also independent from each other in the sense that the decision result $f (\mathbf{y} [n_1]; \varphi) = f (\mathbf{y} (\mathbf{x} [n_1], \varepsilon [n_1]); \varphi)$ at the time instant t_{n_1} depends only on the sensor measurement error $\varepsilon [n_1] = \varepsilon [n_1]$ at this time instant t_{n_1} and the decision result $f (\mathbf{y} [n_2]; \varphi) = f (\mathbf{y} (\mathbf{x} [n_2], \varepsilon [n_2]); \varphi)$ at the time instant t_{n_2} depends only on the sensor measurement error $\varepsilon [n_2] = \varepsilon [n_2]$ at this time instant t_{n_2} . Therefore, the set of all sensor measurement errors ε at all considered time instants $t_n, n = 0, 1, \dots, n_{\text{end}}$, for which the decision result based on the sensor measurements $\mathbf{y} [n_1]$ at the time instant t_{n_1} is $f (\mathbf{y} [n_1]; \varphi) = f (\mathbf{y} (\mathbf{x} [n_1], \varepsilon [n_1]); \varphi) = 0$, i.e., the function does not decide for an intervention based on the sensor measurements $\mathbf{y} [n_1]$ at the time instant t_{n_1} , is the error region

$$\begin{aligned} \bar{\mathcal{I}}_{\varepsilon, n_1} &= \left\{ \varepsilon \in \mathbb{R}^{E(n_{\text{end}}+1)} : f (\mathbf{y} [n_1]; \varphi) = 0 \right\} \\ &= \left\{ \varepsilon \in \mathbb{R}^{n_{\text{end}}+1} : f (\mathbf{y} (\mathbf{x} [n_1], \varepsilon [n_1]); \varphi) = 0 \right\} \end{aligned} \quad (5.32)$$

without intervention at the time instant t_{n_1} , where the sensor measurement error $\varepsilon [n_1]$ at the time instant t_{n_1} alone determines whether $\varepsilon \in \bar{\mathcal{I}}_{\varepsilon, n_1}$. In the plane of Figure 5.1 where $\varepsilon [n] = \mu_n$ for $n \neq n_1, n_2$, this error region $\bar{\mathcal{I}}_{\varepsilon, n_1}$, where $f (\mathbf{y} [n_1]; \varphi) = 0$, is the area to the right of the dashed violet line possibly including this line. Due to the same reason, the set of all sensor measurement errors ε at all considered time instants $t_n, n = 0, 1, \dots, n_{\text{end}}$, for which the decision result based on the sensor measurements $\mathbf{y} [n_2]$ at the time instant t_{n_2} is $f (\mathbf{y} [n_2]; \varphi) = f (\mathbf{y} (\mathbf{x} [n_2], \varepsilon [n_2]); \varphi) = 0$, i.e., the function does not decide for an intervention based on the sensor measurements $\mathbf{y} [n_2]$ at the time instant t_{n_2} , is the error region

$$\begin{aligned} \bar{\mathcal{I}}_{\varepsilon, n_2} &= \left\{ \varepsilon \in \mathbb{R}^{E(n_{\text{end}}+1)} : f (\mathbf{y} [n_2]; \varphi) = 0 \right\} \\ &= \left\{ \varepsilon \in \mathbb{R}^{n_{\text{end}}+1} : f (\mathbf{y} (\mathbf{x} [n_2], \varepsilon [n_2]); \varphi) = 0 \right\} \end{aligned} \quad (5.33)$$

without intervention at the time instant t_{n_2} , where the sensor measurement error $\varepsilon [n_2]$ at the time instant t_{n_2} alone determines whether $\varepsilon \in \bar{\mathcal{I}}_{\varepsilon, n_2}$. In the plane of Figure 5.1 where $\varepsilon [n] = \mu_n$ for $n \neq n_1, n_2$, this error region $\bar{\mathcal{I}}_{\varepsilon, n_2}$, where $f (\mathbf{y} [n_2]; \varphi) = 0$, is the area above the dashed magenta line possibly including this line. The area where the areas to the right of the dashed violet line and above the dashed magenta

line possibly including these lines, which represent the error regions $\bar{\mathcal{I}}_{\varepsilon,n_1}$ and $\bar{\mathcal{I}}_{\varepsilon,n_2}$ without intervention at the time instants t_{n_1} and t_{n_2} , respectively, intersect, is the green area possibly including the orange boundary, which represents the error region without an intervention at both the time instant t_{n_1} and the time instant t_{n_2} , and thus the exemplary individual error acceptance region partition $\mathcal{A}_{\varepsilon,b,i}$ assuming that the function must not decide for an intervention based on the sensor measurements $\mathbf{y}[n_1]$ and $\mathbf{y}[n_2]$ at both time instants to fulfill $q_i \geq q_{L,i}$ if $b = L$ or $q_i \leq q_{U,i}$ if $b = U$. The smallest distance of the sensor measurement errors ε on the part of the boundary of the individual error acceptance region partition $\mathcal{A}_{\varepsilon,b,i}$ that is visualized by the upper part of the orange boundary in the plane of Figure 5.1 from their mean $\boldsymbol{\mu}$ with respect to the Mahalanobis distance is β_{n_1} while the smallest distance of the sensor measurement errors ε on the other part of this boundary from their mean $\boldsymbol{\mu}$ is β_{n_2} . The sets of all sensor measurement errors ε in the plane where $\varepsilon[n] = \mu_n$ for $n \neq n_1, n_2$ with the distances $\beta(\varepsilon) = \beta_{n_1}$ and $\beta(\varepsilon) = \beta_{n_2}$ from their mean $\boldsymbol{\mu}$ are the light and dark gray ellipses, respectively. As the dark gray ellipse is larger than the light gray ellipse, $\beta_{n_2} > \beta_{n_1}$ such that β_{n_2} cannot be the worst-case distance $\beta_{b,i}$. If there are also no other sensor measurement errors ε outside the plane where $\varepsilon[n] = \mu_n$ for $n \neq n_1, n_2$ with a distance from their mean $\boldsymbol{\mu}$ that is smaller than β_{n_1} , the worst-case distance is $\beta_{b,i} = \beta_{n_1}$. In this case, the boundary of the individual error acceptance region partition $\mathcal{A}_{\varepsilon,b,i}$ that is visualized by the orange boundary is linearized by the tangential hyperplane that is visualized by the dashed violet line and touches this boundary where the distance of the sensor measurement errors ε from their mean $\boldsymbol{\mu}$ is the worst-case distance $\beta_{b,i} = \beta_{n_1}$. By this linearization, the individual error acceptance region partition $\mathcal{A}_{\varepsilon,b,i}$ highlighted by the green area is approximated by the error region $\hat{\mathcal{I}}_{\varepsilon,n_1}$ that is bounded by the tangential hyperplane with the distance $\beta_{b,i} = \beta_{n_1}$ from $\boldsymbol{\mu}$ and represented by the horizontally striped area to the right of the dashed violet line including this line in the plane of Figure 5.1. This error region $\hat{\mathcal{I}}_{\varepsilon,n_1}$ is an approximation for the error region $\bar{\mathcal{I}}_{\varepsilon,n_1}$ without intervention at the time instant t_{n_1} , where $f(\mathbf{y}[n_1]; \boldsymbol{\varphi}) = 0$ and which is represented by the area to the right of the dashed violet line possibly including this line in the plane of Figure 5.1. Due to its highly non-linear and non-smooth boundary highlighted by the orange curve, which results from making the decisions on an intervention at the time instants t_n , $n = 0, 1, \dots, n_{\text{end}}$, independently from each other, a better approximation of the individual error acceptance region partition $\mathcal{A}_{\varepsilon,b,i}$ can be achieved by linearizing it not only by one tangential hyperplane but piecewise by several tangential hyperplanes.

This is the basic idea of the following adaptation of the worst-case distance approach to the robust design of automated vehicular safety systems. Moreover, improving the

approximation using this piecewise linearization by several tangential hyperplanes naturally leads to a decomposition of the optimization problems (5.22) and (5.23) for determining the worst-case distances $\beta_{L,i}$ and $\beta_{U,i}$, respectively, into several optimization problems that are easier to solve such that both mentioned problems of the direct application of the worst-case distance approach to the robust design of automated vehicular safety systems are tackled at the same time.

5.2.2 Adaptation of Worst-Case Distance Approach to Robust Design of Automated Vehicular Safety Systems

To better approximate the individual error acceptance region partition $\mathcal{A}_{\varepsilon,b,i}$ highlighted by the green area in the plane of Figure 5.1 where $\varepsilon[n] = \mu_n$ for $n \neq n_1, n_2$ under the assumption that the function must not decide for an intervention based on the sensor measurements $\mathbf{y}[n_1]$ and $\mathbf{y}[n_2]$ at the time instants t_{n_1} and t_{n_2} to fulfill $q_i \geq q_{L,i}$ if $b = L$ or $q_i \leq q_{U,i}$ if $b = U$, its boundary represented by the orange curve is not only linearized by the tangential hyperplane that is visualized by the dashed violet line and touches this boundary where the distance of the sensor measurement errors ε from their mean $\boldsymbol{\mu}$ is β_{n_1} , the worst-case distance $\beta_{b,i}$, but also by the tangential hyperplane that is visualized by the dashed magenta line and touches this boundary where the distance of the sensor measurement errors ε from their mean $\boldsymbol{\mu}$ is β_{n_2} . By this piecewise linearization, the error region $\bar{\mathcal{I}}_{\varepsilon,n_1}$ without intervention at the time instant t_{n_1} , where $f(\mathbf{y}[n_1]; \boldsymbol{\varphi}) = 0$ and which is represented by the area to the right of the dashed violet line possibly including this line, and the error region $\bar{\mathcal{I}}_{\varepsilon,n_2}$ without intervention at the time instant t_{n_2} , where $f(\mathbf{y}[n_2]; \boldsymbol{\varphi}) = 0$ and which is represented by the area above the dashed magenta line possibly including this line, are approximated by the error region $\hat{\bar{\mathcal{I}}}_{\varepsilon,n_1}$ that is bounded by the tangential hyperplane with the distance β_{n_1} from $\boldsymbol{\mu}$ and represented by the horizontally striped area to the right of the dashed violet line including this line and the error region $\hat{\bar{\mathcal{I}}}_{\varepsilon,n_2}$ that is bounded by the tangential hyperplane with the distance β_{n_2} from $\boldsymbol{\mu}$ and represented by the vertically striped area above the dashed magenta line including this line, respectively. Since the function must not decide for an intervention based on the sensor measurements $\mathbf{y}[n_1]$ and $\mathbf{y}[n_2]$ at the time instants t_{n_1} and t_{n_2} to fulfill $q_i \geq q_{L,i}$ if $b = L$ or $q_i \leq q_{U,i}$ if $b = U$, the individual error acceptance region partition $\mathcal{A}_{\varepsilon,b,i}$, where this is the case, lies in the intersection $\bar{\mathcal{I}}_{\varepsilon,n_1} \cap \bar{\mathcal{I}}_{\varepsilon,n_2}$ of the error regions $\bar{\mathcal{I}}_{\varepsilon,n_1}$ and $\bar{\mathcal{I}}_{\varepsilon,n_2}$ without intervention at these two time instants:

$$\mathcal{A}_{\varepsilon,b,i} \subset \bar{\mathcal{I}}_{\varepsilon,n_1} \cap \bar{\mathcal{I}}_{\varepsilon,n_2}. \quad (5.34)$$

This can be seen in the plane of Figure 5.1, where the intersection of the areas to the right of the dashed violet line possibly including this line and above the dashed magenta line possibly including this line, which represent the error regions $\bar{\mathcal{I}}_{\varepsilon,n_1}$ and $\bar{\mathcal{I}}_{\varepsilon,n_2}$ without intervention at the two time instants t_{n_1} and t_{n_2} , respectively, yields the green area possibly including the orange boundary representing the individual error acceptance region partition $\mathcal{A}_{\varepsilon,b,i}$. Using the approximate error region $\hat{\bar{\mathcal{I}}}_{\varepsilon,n_1}$ without intervention at the time instant t_{n_1} highlighted by the horizontally striped area to the right of the dashed violet line including this line and the approximate error region $\hat{\bar{\mathcal{I}}}_{\varepsilon,n_2}$ without intervention at the time instant t_{n_2} highlighted by the vertically striped area above the dashed magenta line including this line instead of the error region $\bar{\mathcal{I}}_{\varepsilon,n_1}$ without intervention at the time instant t_{n_1} and the error region $\bar{\mathcal{I}}_{\varepsilon,n_2}$ without intervention at the instant t_{n_2} , respectively, leads to the approximation of the individual error acceptance region partition $\mathcal{A}_{\varepsilon,b,i}$ represented by the green area possibly including the orange boundary by their intersection $\hat{\bar{\mathcal{I}}}_{\varepsilon,n_1} \cap \hat{\bar{\mathcal{I}}}_{\varepsilon,n_2}$ highlighted by the area that is both horizontally and vertically striped including the dashed violet and magenta boundary. This approximation of the individual error acceptance region partition $\mathcal{A}_{\varepsilon,b,i}$ using the tangential hyperplanes with the distances β_{n_1} and β_{n_2} from μ is more accurate than the original approximation by the approximate error region $\hat{\bar{\mathcal{I}}}_{\varepsilon,n_1}$ without intervention at the time instant t_{n_1} , which is highlighted by the horizontally striped area to the right of the dashed violet line including this line, alone using only the tangential hyperplane with the distance β_{n_1} , the worst-case distance $\beta_{b,i}$ of the direct application of the worst-case distance approach to the robust design of automated vehicular safety systems, from μ .

If not only the two time instants t_{n_1} and t_{n_2} but all time instants t_n with n from a set $\bar{\mathbb{I}}_{b,i} \subset \{0, 1, \dots, n_{\text{end}}\}$ are all time instants at which the function must not decide for an intervention based on the corresponding sensor measurements $\mathbf{y}[n]$ to fulfill $q_i \geq q_{L,i}$ if $b = \text{L}$ or $q_i \leq q_{U,i}$ if $b = \text{U}$, the individual error acceptance region partition $\mathcal{A}_{\varepsilon,b,i}$, where this is fulfilled, lies in the intersection of the error regions $\bar{\mathcal{I}}_{\varepsilon,n}$ without intervention at all these time instants:

$$\mathcal{A}_{\varepsilon,b,i} \subset \bigcap_{n \in \bar{\mathbb{I}}_{b,i}} \bar{\mathcal{I}}_{\varepsilon,n}. \quad (5.35)$$

This is an extension of (5.34) for the two time instants t_{n_1} and t_{n_2} to all time instants t_n , $n \in \bar{\mathbb{I}}_{b,i}$, where the error region without intervention at the time instant t_n is defined analogously to the error region $\bar{\mathcal{I}}_{\varepsilon,n_1}$ without intervention at the time instant t_{n_1} in (5.32) and the error region $\bar{\mathcal{I}}_{\varepsilon,n_2}$ without intervention at the time instant t_{n_2} in (5.33)

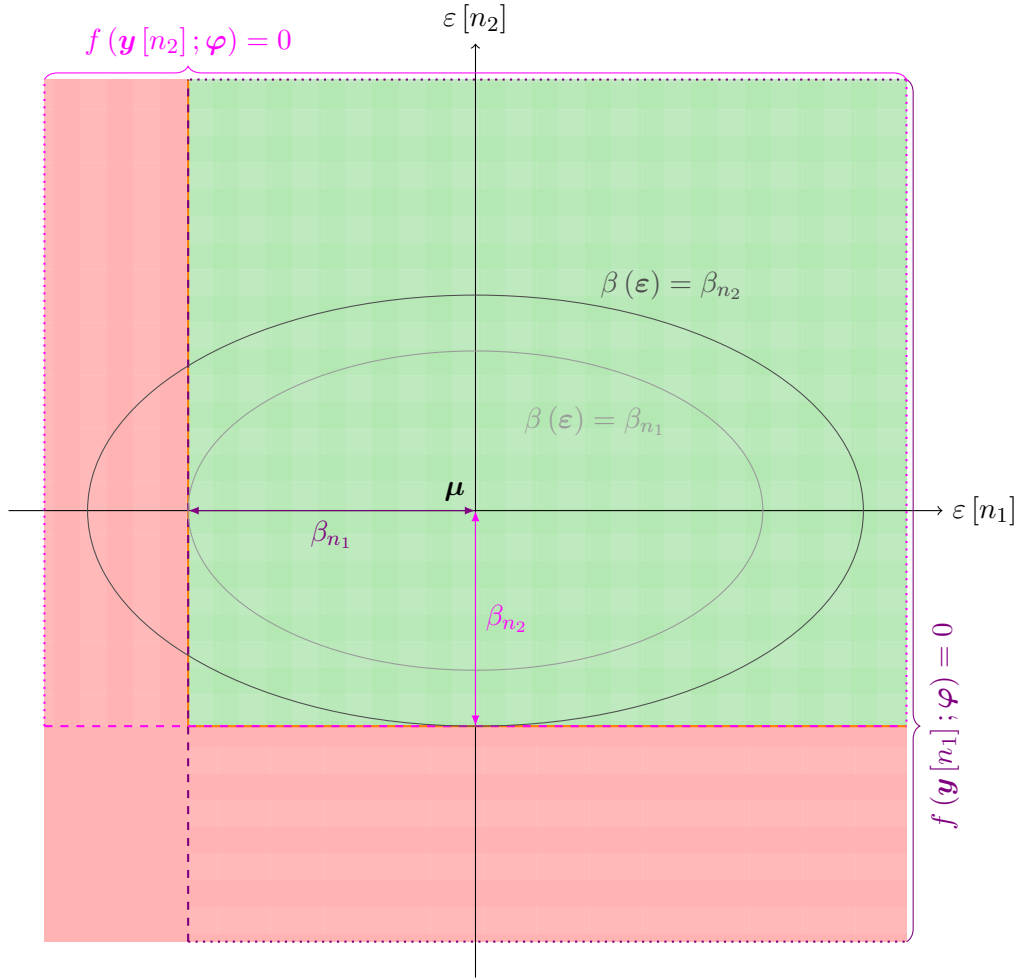


Figure 5.1: Exemplary individual error acceptance region partition $\mathcal{A}_{\varepsilon,b,i}$, $b \in \{L, U\}$, (green area possibly including dashed orange boundary) with either a finite lower bound $q_{L,i}$ if $b = L$ or a finite upper bound $q_{U,i}$ if $b = U$ for $E = 1$ sensor measurement error $\varepsilon[n]$ at a time instant t_n under the assumption that the function must not decide for an intervention based on the sensor measurements $\mathbf{y}[n_1]$ at the time instant t_{n_1} and based on the sensor measurements $\mathbf{y}[n_2]$ at the time instant t_{n_2} using the decision rule $f(\cdot; \varphi)$ such that $q_i \geq q_{L,i}$ if $b = L$ or $q_i \leq q_{U,i}$ if $b = U$, and its relationship to the error regions $\bar{\mathcal{I}}_{\varepsilon,n}$ without intervention, where $f(\mathbf{y}[n]; \varphi) = 0$, approximated by the error regions $\hat{\mathcal{I}}_{\varepsilon,n}$ corresponding to the worst-case distances β_n (horizontally and vertically striped areas including dashed violet and magenta linear boundaries, respectively) in the plane where $\varepsilon[n] = \mu_n$ for $n \neq n_1, n_2$.

as

$$\begin{aligned}\bar{\mathcal{I}}_{\varepsilon,n} &= \left\{ \varepsilon \in \mathbb{R}^{E(n_{\text{end}}+1)} : f(\mathbf{y}[n]; \varphi) = 0 \right\} \\ &= \left\{ \varepsilon \in \mathbb{R}^{n_{\text{end}}+1} : f(\mathbf{y}(\mathbf{x}[n], \varepsilon[n]); \varphi) = 0 \right\}.\end{aligned}\quad (5.36)$$

As the error region $\bar{\mathcal{I}}_{\varepsilon,n_1}$ without intervention at the time instant t_{n_1} , where $f(\mathbf{y}[n_1]; \varphi) = 0$, and the error region $\bar{\mathcal{I}}_{\varepsilon,n_2}$ without intervention at the time instant t_{n_2} , where $f(\mathbf{y}[n_2]; \varphi) = 0$, are approximated by the approximate error region $\hat{\mathcal{I}}_{\varepsilon,n_1}$ without intervention at the time instant t_{n_1} bounded by the tangential hyperplane with the distance β_{n_1} from the mean $\boldsymbol{\mu}$ of the sensor measurement errors ε and the approximate error region $\hat{\mathcal{I}}_{\varepsilon,n_2}$ without intervention at the time instant t_{n_2} bounded by the tangential hyperplane with the distance β_{n_2} from $\boldsymbol{\mu}$, respectively, the error region $\bar{\mathcal{I}}_{\varepsilon,n}$ without intervention at the time instant t_n , where $f(\mathbf{y}[n]; \varphi) = 0$, can be approximated by an approximate error region $\hat{\mathcal{I}}_{\varepsilon,n}$ without intervention at the time instant t_n bounded by the tangential hyperplane with the distance β_n from $\boldsymbol{\mu}$ for each $n \in \bar{\mathbb{I}}_{b,i}$. The distance β_n of the tangential hyperplane that is the boundary $\partial\hat{\mathcal{I}}_{\varepsilon,n}$ of the approximate error region $\hat{\mathcal{I}}_{\varepsilon,n}$ without intervention at the time instant t_n from $\boldsymbol{\mu}$ is given by the smallest distance of the sensor measurement errors ε on this hyperplane from $\boldsymbol{\mu}$, i.e.,

$$\beta_n = \min_{\varepsilon \in \mathbb{R}^{E(n_{\text{end}}+1)}} \beta(\varepsilon) \quad \text{s.t.} \quad \varepsilon \in \partial\hat{\mathcal{I}}_{\varepsilon,n}. \quad (5.37)$$

As can be seen in Figure 5.1 for the time instants t_{n_1} and t_{n_2} , the tangential hyperplane $\partial\hat{\mathcal{I}}_{\varepsilon,n}$ illustrated by the dashed violet and magenta lines for the time instants t_{n_1} and t_{n_2} , respectively, can be interpreted as the result of linearizing the boundary $\partial\bar{\mathcal{I}}_{\varepsilon,n}$ of the error region $\bar{\mathcal{I}}_{\varepsilon,n}$ without intervention at the time instant t_n , where $f(\mathbf{y}[n]; \varphi) = 0$, such that it touches this boundary at the point where the sensor measurement errors ε have the smallest distance of all sensor measurement errors ε on both the boundary $\partial\bar{\mathcal{I}}_{\varepsilon,n}$ and the tangential hyperplane $\partial\hat{\mathcal{I}}_{\varepsilon,n}$ from $\boldsymbol{\mu}$, namely, the distance β_n of the tangential hyperplane $\partial\hat{\mathcal{I}}_{\varepsilon,n}$ from $\boldsymbol{\mu}$. Therefore, this distance can alternatively be written as

$$\beta_n = \min_{\varepsilon \in \mathbb{R}^{E(n_{\text{end}}+1)}} \beta(\varepsilon) \quad \text{s.t.} \quad \varepsilon \in \partial\bar{\mathcal{I}}_{\varepsilon,n}. \quad (5.38)$$

This optimization problem can be reformulated as

$$\beta_n = \min_{\varepsilon \in \mathbb{R}^{E(n_{\text{end}}+1)}} \beta(\varepsilon) \quad \text{s.t.} \quad \varepsilon \in \partial\mathcal{I}_{\varepsilon,n} \quad (5.39)$$

because the boundary $\partial\bar{\mathcal{I}}_{\varepsilon,n}$ of the error region $\bar{\mathcal{I}}_{\varepsilon,n}$ without intervention at the time instant t_n defined in (5.36) is also the boundary $\partial\mathcal{I}_{\varepsilon,n}$ of its complement, the error

region

$$\begin{aligned}\mathcal{I}_{\varepsilon,n} &= \left\{ \varepsilon \in \mathbb{R}^{E(n_{\text{end}}+1)} : f(\mathbf{y}[n]; \boldsymbol{\varphi}) = 1 \right\} \\ &= \left\{ \varepsilon \in \mathbb{R}^{n_{\text{end}}+1} : f(\mathbf{y}(\mathbf{x}[n], \varepsilon[n]); \boldsymbol{\varphi}) = 1 \right\}\end{aligned}\quad (5.40)$$

with intervention at the time instant t_n . Using the closure

$$\text{cl}(\mathcal{I}_{\varepsilon,n}) = \mathcal{I}_{\varepsilon,n} \cup \partial\mathcal{I}_{\varepsilon,n} \quad (5.41)$$

of the error region $\mathcal{I}_{\varepsilon,n}$ with intervention at the time instant t_n , which is the union of $\mathcal{I}_{\varepsilon,n}$ and its boundary $\partial\mathcal{I}_{\varepsilon,n}$ as well as the smallest closed set containing $\mathcal{I}_{\varepsilon,n}$, this optimization problem can be equivalently rewritten as

$$\beta_n = \min_{\varepsilon \in \mathbb{R}^{E(n_{\text{end}}+1)}} \beta(\varepsilon) \quad \text{s.t.} \quad \varepsilon \in \text{cl}(\mathcal{I}_{\varepsilon,n}). \quad (5.42)$$

This is due to the fact that the sensor measurement errors ε with the smallest distance $\beta(\varepsilon)$ of all sensor measurement errors ε inside the closure $\text{cl}(\mathcal{I}_{\varepsilon,n})$ of the error region $\mathcal{I}_{\varepsilon,n}$ with intervention at the time instant t_n from their mean $\boldsymbol{\mu}$, which solve the last optimization problem, have to lie on the boundary $\partial\mathcal{I}_{\varepsilon,n} \subset \text{cl}(\mathcal{I}_{\varepsilon,n})$ of $\mathcal{I}_{\varepsilon,n}$ and thus are also the sensor measurement errors ε with the smallest distance $\beta(\varepsilon)$ of all sensor measurement errors ε on the boundary $\partial\mathcal{I}_{\varepsilon,n}$, which solve the former optimization problem.

With the complements

$$\overline{\mathcal{A}}_{s,L,i} = \{ \mathbf{s} \in \mathbb{R}^{N_s} : f_i < f_{L,i} \} \quad (5.43)$$

and

$$\overline{\mathcal{A}}_{s,U,i} = \{ \mathbf{s} \in \mathbb{R}^{N_s} : f_i > f_{U,i} \} \quad (5.44)$$

of the individual parameter acceptance region partitions $\mathcal{A}_{s,L,i}$ and $\mathcal{A}_{s,U,i}$ defined in (3.54) and (3.55), respectively, and their closure

$$\text{cl}(\overline{\mathcal{A}}_{s,L,i}) = \{ \mathbf{s} \in \mathbb{R}^{N_s} : f_i \leq f_{L,i} \} \quad (5.45)$$

and

$$\text{cl}(\overline{\mathcal{A}}_{s,U,i}) = \{ \mathbf{s} \in \mathbb{R}^{N_s} : f_i \geq f_{U,i} \}, \quad (5.46)$$

the optimization problems (3.59) and (3.60) for determining the corresponding worst-case distances $\beta_{L,i}$ and $\beta_{U,i}$, respectively, can be compactly expressed as

$$\beta_{b,i} = \min_{\mathbf{s} \in \mathbb{R}^{N_s}} \beta(\mathbf{s}) \quad \text{s.t.} \quad \mathbf{s} \in \text{cl}(\overline{\mathcal{A}}_{s,b,i}), \quad (5.47)$$

$b \in \{\text{L}, \text{U}\}$. Comparing this optimization problem with the optimization problem (5.42) unveils that the error region $\bar{\mathcal{I}}_{\varepsilon, n}$ without intervention at the time instant t_n and the corresponding smallest distance β_n of all sensor measurement errors ε in the closure of its complement from their mean $\boldsymbol{\mu}$ play the same role as the individual parameter acceptance region partition $\mathcal{A}_{s, b, i}$ and the corresponding smallest distance of all statistical parameters \boldsymbol{s} in the closure of its complement from their mean \boldsymbol{s}_0 , the worst-case distance $\beta_{b, i}$, respectively. Therefore, β_n is called worst-case distance at the time instant t_n .

For the block diagonal covariance matrix \boldsymbol{C} of the sensor measurement errors ε stated in (4.25), the square of the distance measure $\beta(\varepsilon)$ defined by (5.24) is given by (4.28):

$$\beta^2(\varepsilon) = \sum_{n=0}^{n_{\text{end}}} (\varepsilon[n] - \boldsymbol{\mu}_n)^T \boldsymbol{C}_n^{-1} (\varepsilon[n] - \boldsymbol{\mu}_n) = \sum_{n=0}^{n_{\text{end}}} \beta_n^2(\varepsilon[n]). \quad (5.48)$$

Here,

$$\beta_n^2(\varepsilon[n]) = (\varepsilon[n] - \boldsymbol{\mu}_n)^T \boldsymbol{C}_n^{-1} (\varepsilon[n] - \boldsymbol{\mu}_n) \quad (5.49)$$

is the squared Mahalanobis distance of the sensor measurement errors $\varepsilon[n]$ at the time instant t_n from their mean $\boldsymbol{\mu}_n$. For $E = 1$ sensor measurement error $\varepsilon[n] = \varepsilon[n] \in \mathbb{R}$ with the mean $\boldsymbol{\mu}_n = \mu_n$ and the covariance matrix $\boldsymbol{C}_n = \sigma_n^2$, i.e., the standard deviation σ_n , the last two equations become

$$\beta^2(\varepsilon) = \sum_{n=0}^{n_{\text{end}}} \beta_n^2(\varepsilon[n]) \quad (5.50)$$

and

$$\beta_n^2(\varepsilon[n]) = \sigma_n^{-2} (\varepsilon[n] - \mu_n)^2. \quad (5.51)$$

With this expression for the square of the distance measure $\beta(\varepsilon)$ and the definition of the error region $\mathcal{I}_{\varepsilon, n}$ with intervention at the time instant t_n in (5.40), the optimization problem (5.42) reads

$$\begin{aligned} \beta_n &= \min_{\varepsilon \in \mathbb{R}^{n_{\text{end}}+1}} \sqrt{\sum_{n'=0}^{n_{\text{end}}} \beta_{n'}^2(\varepsilon[n'])} \\ \text{s.t. } &\varepsilon \in \text{cl}(\{\varepsilon \in \mathbb{R}^{n_{\text{end}}+1} : f(\boldsymbol{y}(\boldsymbol{x}[n]), \varepsilon[n]); \boldsymbol{\varphi}) = 1\}). \end{aligned} \quad (5.52)$$

Whether $f(\boldsymbol{y}(\boldsymbol{x}[n]), \varepsilon[n]); \boldsymbol{\varphi}) = 1$ and thus the constraint of this optimization problem is fulfilled just depends on the sensor measurement error $\varepsilon[n]$ at the time instant t_n such that all other sensor measurement errors $\varepsilon[n']$, $n' \neq n$, in the vector ε can

be chosen arbitrarily without violating the constraint. They are chosen to be $\mu_{n'}$, i.e., $\varepsilon[n'] = \mu_{n'}$ for $n' \in \{0, 1, \dots, n_{\text{end}}\} \setminus \{n\}$, such that $\beta_{n'}^2(\varepsilon[n']) = 0$ and thus $\beta_{n'}^2(\varepsilon[n'])$ is minimal in order to minimize the objective for any given sensor measurement error $\varepsilon[n]$ at the time instant t_n . Hence, the optimization problem simplifies to the following optimization problem with just one scalar optimization variable $\varepsilon[n]$:

$$\begin{aligned} \beta_n &= \min_{\varepsilon[n] \in \mathbb{R}} \beta_n(\varepsilon[n]) \\ \text{s.t. } &\varepsilon[n] \in \text{cl}(\{\varepsilon[n] \in \mathbb{R} : f(\mathbf{y}(\mathbf{x}[n], \varepsilon[n]); \boldsymbol{\varphi}) = 1\}). \end{aligned} \quad (5.53)$$

As the probability $P(\boldsymbol{\varepsilon} \in \hat{\mathcal{A}}_{\varepsilon, b, i})$ that the sensor measurement errors $\boldsymbol{\varepsilon}$ lie in the approximate individual error acceptance region partition $\hat{\mathcal{A}}_{\varepsilon, b, i}$ obtained from the individual error acceptance region partition $\mathcal{A}_{\varepsilon, b, i}$, $b \in \{\text{L}, \text{U}\}$, by linearizing its boundary using a hyperplane that touches it where the distance of the sensor measurement errors $\boldsymbol{\varepsilon}$ from their mean $\boldsymbol{\mu}$ is the worst-case distance $\beta_{b, i}$ is given by $\Phi(\beta_{b, i})$ according to (5.27), the probability $P(\boldsymbol{\varepsilon} \in \hat{\mathcal{T}}_{\varepsilon, n})$ that the sensor measurement errors $\boldsymbol{\varepsilon}$ lie in the approximate error region $\hat{\mathcal{T}}_{\varepsilon, n}$ without intervention at the time instant t_n obtained from the error region $\bar{\mathcal{T}}_{\varepsilon, n}$ without intervention at the time instant t_n by linearizing its boundary using a hyperplane that touches it where the distance of the sensor measurement errors $\boldsymbol{\varepsilon}$ from their mean $\boldsymbol{\mu}$ is the worst-case distance β_n at the time instant t_n is given by

$$P(\boldsymbol{\varepsilon} \in \hat{\mathcal{T}}_{\varepsilon, n}) = \Phi(\beta_n). \quad (5.54)$$

This equation holds for the case that the mean $\boldsymbol{\mu}$ of the sensor measurement errors $\boldsymbol{\varepsilon}$ lies in the error region $\bar{\mathcal{T}}_{\varepsilon, n}$ without intervention at the time instant t_n as illustrated in Figure 5.1 for the two time instants t_{n_1} and t_{n_2} . This has to be fulfilled for all time instants t_n with $n \in \bar{\mathbb{I}}_{b, i}$ at which the function must not decide for an intervention based on the corresponding sensor measurements $\mathbf{y}[n]$ to fulfill $q_i \geq q_{\text{L}, i}$ if $b = \text{L}$ or $q_i \leq q_{\text{U}, i}$ if $b = \text{U}$ such that the mean $\boldsymbol{\mu}$ of the sensor measurement errors $\boldsymbol{\varepsilon}$ lies in the individual error acceptance region partition $\mathcal{A}_{\varepsilon, b, i}$, which is a subset of the intersection of the error regions $\bar{\mathcal{T}}_{\varepsilon, n}$ without intervention at all these time instants according to (5.35), and a high probability $P(\boldsymbol{\varepsilon} \in \mathcal{A}_{\varepsilon, b, i})$ that the sensor measurement errors $\boldsymbol{\varepsilon}$ lie in the individual error acceptance region partition $\mathcal{A}_{\varepsilon, b, i}$ and thus the corresponding specification for the customer satisfaction, i.e., $q_i \geq q_{\text{L}, i}$ if $b = \text{L}$ or $q_i \leq q_{\text{U}, i}$ if $b = \text{U}$, is fulfilled can be achieved.

If the mean $\boldsymbol{\mu}$ of the sensor measurement errors $\boldsymbol{\varepsilon}$ does not lie in the error region $\bar{\mathcal{T}}_{\varepsilon, n}$ without intervention at the time instant t_n , i.e., $\boldsymbol{\mu} \notin \bar{\mathcal{T}}_{\varepsilon, n}$, it has to lie in its

complement, the error region $\mathcal{I}_{\varepsilon,n}$ with intervention at the time instant t_n , i.e., $\boldsymbol{\mu} \in \mathcal{I}_{\varepsilon,n}$. So, the error region $\mathcal{I}_{\varepsilon,n}$ with intervention at the time instant t_n plays the same role then as the error region $\bar{\mathcal{I}}_{\varepsilon,n}$ without intervention at the time instant t_n before. Therefore, the error region $\mathcal{I}_{\varepsilon,n}$ with intervention at the time instant t_n defined in (5.40), where $f(\mathbf{y}(\mathbf{x}[n], \varepsilon[n]); \boldsymbol{\varphi}) = 1$, replaces the error region $\bar{\mathcal{I}}_{\varepsilon,n}$ without intervention at the time instant t_n defined in (5.36), where $f(\mathbf{y}(\mathbf{x}[n], \varepsilon[n]); \boldsymbol{\varphi}) = 0$, and vice versa. Accordingly, $f(\mathbf{y}(\mathbf{x}[n], \varepsilon[n]); \boldsymbol{\varphi}) = 0$ replaces $f(\mathbf{y}(\mathbf{x}[n], \varepsilon[n]); \boldsymbol{\varphi}) = 1$ in (5.53) such that the worst-case distance at the time instant t_n reads

$$\begin{aligned} \beta_n &= \min_{\varepsilon[n] \in \mathbb{R}} \beta_n(\varepsilon[n]) \\ \text{s.t. } \varepsilon[n] &\in \text{cl}(\{\varepsilon[n] \in \mathbb{R} : f(\mathbf{y}(\mathbf{x}[n], \varepsilon[n]); \boldsymbol{\varphi}) = 0\}). \end{aligned} \quad (5.55)$$

As the probability $P(\varepsilon \in \hat{\mathcal{I}}_{\varepsilon,n})$ that the sensor measurement errors ε lie in the approximate error region $\hat{\mathcal{I}}_{\varepsilon,n}$ without intervention at the time instant t_n obtained from the error region $\bar{\mathcal{I}}_{\varepsilon,n}$ without intervention at the time instant t_n by linearizing its boundary using a hyperplane that touches it where the distance of the sensor measurement errors ε from their mean $\boldsymbol{\mu}$ is the worst-case distance β_n at the time instant t_n in (5.53) is given by (5.54) if $\boldsymbol{\mu} \in \bar{\mathcal{I}}_{\varepsilon,n}$, the probability $P(\varepsilon \in \hat{\mathcal{I}}_{\varepsilon,n})$ that the sensor measurement errors ε lie in the approximate error region $\hat{\mathcal{I}}_{\varepsilon,n}$ with intervention at the time instant t_n obtained from the error region $\mathcal{I}_{\varepsilon,n}$ with intervention at the time instant t_n by linearizing its boundary using a hyperplane that touches it where distance of the sensor measurement errors ε from their mean $\boldsymbol{\mu}$ is the worst-case distance β_n at the time instant t_n in (5.55) is given by

$$P(\varepsilon \in \hat{\mathcal{I}}_{\varepsilon,n}) = \Phi(\beta_n) \quad (5.56)$$

if $\boldsymbol{\mu} \in \mathcal{I}_{\varepsilon,n}$. To sum up,

$$\Phi(\beta_n) = \begin{cases} P(\varepsilon \in \hat{\mathcal{I}}_{\varepsilon,n}), & \boldsymbol{\mu} \in \mathcal{I}_{\varepsilon,n} \\ P(\varepsilon \in \bar{\mathcal{I}}_{\varepsilon,n}), & \boldsymbol{\mu} \in \bar{\mathcal{I}}_{\varepsilon,n} \end{cases} \quad (5.57)$$

with

$$\begin{aligned} \beta_n &= \min_{\varepsilon[n] \in \mathbb{R}} \beta_n(\varepsilon[n]) \\ \text{s.t. } \varepsilon[n] &\in \text{cl}\left(\left\{\varepsilon[n] \in \mathbb{R} : f(\mathbf{y}(\mathbf{x}[n], \varepsilon[n]); \boldsymbol{\varphi}) = \begin{cases} 0, & \boldsymbol{\mu} \in \mathcal{I}_{\varepsilon,n} \\ 1, & \boldsymbol{\mu} \in \bar{\mathcal{I}}_{\varepsilon,n} \end{cases}\right\}\right). \end{aligned} \quad (5.58)$$

Since

$$\begin{aligned} \boldsymbol{\mu} \in \mathcal{I}_{\boldsymbol{\varepsilon},n} &= \{ \boldsymbol{\varepsilon} \in \mathbb{R}^{n_{\text{end}}+1} : f(\mathbf{y}(\mathbf{x}[n], \boldsymbol{\varepsilon}[n]); \boldsymbol{\varphi}) = 1 \} \\ &\Leftrightarrow f(\mathbf{y}(\mathbf{x}[n], \boldsymbol{\mu}_n); \boldsymbol{\varphi}) = 1 \end{aligned} \quad (5.59)$$

and

$$\begin{aligned} \boldsymbol{\mu} \in \bar{\mathcal{I}}_{\boldsymbol{\varepsilon},n} &= \{ \boldsymbol{\varepsilon} \in \mathbb{R}^{n_{\text{end}}+1} : f(\mathbf{y}(\mathbf{x}[n], \boldsymbol{\varepsilon}[n]); \boldsymbol{\varphi}) = 0 \} \\ &\Leftrightarrow f(\mathbf{y}(\mathbf{x}[n], \boldsymbol{\mu}_n); \boldsymbol{\varphi}) = 0, \end{aligned} \quad (5.60)$$

the results $f(\mathbf{y}(\mathbf{x}[n], \boldsymbol{\mu}_n); \boldsymbol{\varphi}) = 1$ and $f(\mathbf{y}(\mathbf{x}[n], \boldsymbol{\mu}_n); \boldsymbol{\varphi}) = 0$ of applying the decision rule $f(\cdot; \boldsymbol{\varphi})$ to the sensor measurements $\mathbf{y}(\mathbf{x}[n], \boldsymbol{\mu}_n)$ corresponding to the state $\mathbf{x}[n]$ at the time instant t_n under the assumption that the sensor measurement error $\boldsymbol{\varepsilon}[n]$ at this time instant is equal to its mean $\boldsymbol{\mu}_n$, the n^{th} entry of the mean $\boldsymbol{\mu}$ of the sensor measurement errors $\boldsymbol{\varepsilon}$, indicate that $\boldsymbol{\mu} \in \mathcal{I}_{\boldsymbol{\varepsilon},n}$ and $\boldsymbol{\mu} \in \bar{\mathcal{I}}_{\boldsymbol{\varepsilon},n}$, respectively.

The probability $P(\boldsymbol{\varepsilon} \in \mathcal{I}_{\boldsymbol{\varepsilon},n})$ that the sensor measurement errors $\boldsymbol{\varepsilon}$ lie in the error region $\mathcal{I}_{\boldsymbol{\varepsilon},n}$ with intervention at the time instant t_n and the probability $P(\boldsymbol{\varepsilon} \in \bar{\mathcal{I}}_{\boldsymbol{\varepsilon},n})$ that they lie in the error region $\bar{\mathcal{I}}_{\boldsymbol{\varepsilon},n}$ without intervention at the time instant t_n can be approximated by the probability $P(\boldsymbol{\varepsilon} \in \hat{\mathcal{I}}_{\boldsymbol{\varepsilon},n})$ that they lie in the approximate error region $\hat{\mathcal{I}}_{\boldsymbol{\varepsilon},n}$ with intervention at the time instant t_n and the probability $P(\boldsymbol{\varepsilon} \in \hat{\bar{\mathcal{I}}}_{\boldsymbol{\varepsilon},n})$ that they lie in the approximate error region $\hat{\bar{\mathcal{I}}}_{\boldsymbol{\varepsilon},n}$ without intervention at the time instant t_n , respectively:

$$P(\boldsymbol{\varepsilon} \in \mathcal{I}_{\boldsymbol{\varepsilon},n}) \approx P(\boldsymbol{\varepsilon} \in \hat{\mathcal{I}}_{\boldsymbol{\varepsilon},n}), \quad (5.61)$$

$$P(\boldsymbol{\varepsilon} \in \bar{\mathcal{I}}_{\boldsymbol{\varepsilon},n}) \approx P(\boldsymbol{\varepsilon} \in \hat{\bar{\mathcal{I}}}_{\boldsymbol{\varepsilon},n}). \quad (5.62)$$

Substituting these approximations for the probabilities $P(\boldsymbol{\varepsilon} \in \bar{\mathcal{I}}_{\boldsymbol{\varepsilon},n})$ and $P(\boldsymbol{\varepsilon} \in \mathcal{I}_{\boldsymbol{\varepsilon},n})$ into $P(\boldsymbol{\varepsilon} \in \mathcal{I}_{\boldsymbol{\varepsilon},n}) = 1 - P(\boldsymbol{\varepsilon} \in \bar{\mathcal{I}}_{\boldsymbol{\varepsilon},n})$ and $P(\boldsymbol{\varepsilon} \in \bar{\mathcal{I}}_{\boldsymbol{\varepsilon},n}) = 1 - P(\boldsymbol{\varepsilon} \in \mathcal{I}_{\boldsymbol{\varepsilon},n})$, respectively, which these probabilities have to fulfill as the two involved error regions $\mathcal{I}_{\boldsymbol{\varepsilon},n}$ and $\bar{\mathcal{I}}_{\boldsymbol{\varepsilon},n}$ are complements of each other, yields the following alternative approximations for the probabilities $P(\boldsymbol{\varepsilon} \in \mathcal{I}_{\boldsymbol{\varepsilon},n})$ and $P(\boldsymbol{\varepsilon} \in \bar{\mathcal{I}}_{\boldsymbol{\varepsilon},n})$:

$$P(\boldsymbol{\varepsilon} \in \mathcal{I}_{\boldsymbol{\varepsilon},n}) \approx 1 - P(\boldsymbol{\varepsilon} \in \hat{\bar{\mathcal{I}}}_{\boldsymbol{\varepsilon},n}), \quad (5.63)$$

$$P(\boldsymbol{\varepsilon} \in \bar{\mathcal{I}}_{\boldsymbol{\varepsilon},n}) \approx 1 - P(\boldsymbol{\varepsilon} \in \hat{\mathcal{I}}_{\boldsymbol{\varepsilon},n}). \quad (5.64)$$

If the mean $\boldsymbol{\mu}$ of the sensor measurement errors $\boldsymbol{\varepsilon}$ lies in the error region $\mathcal{I}_{\boldsymbol{\varepsilon},n}$ with intervention at the time instant t_n , i.e., $\boldsymbol{\mu} \in \mathcal{I}_{\boldsymbol{\varepsilon},n}$, the approximations in (5.61) and

(5.64) read as follows because, in this case, $P(\varepsilon \in \hat{\mathcal{I}}_{\varepsilon,n}) = \Phi(\beta_n)$ according to (5.57):

$$P(\varepsilon \in \mathcal{I}_{\varepsilon,n}) \approx \Phi(\beta_n), \quad (5.65)$$

$$P(\varepsilon \in \bar{\mathcal{I}}_{\varepsilon,n}) \approx 1 - \Phi(\beta_n) = \Phi(-\beta_n). \quad (5.66)$$

If the mean μ of the sensor measurement errors ε lies in the error region $\bar{\mathcal{I}}_{\varepsilon,n}$ without intervention at the time instant t_n , i.e., $\mu \in \bar{\mathcal{I}}_{\varepsilon,n}$, the approximations in (5.63) and (5.62) read as follows because, in this case, $P(\varepsilon \in \hat{\mathcal{I}}_{\varepsilon,n}) = \Phi(\beta_n)$ according to (5.57):

$$P(\varepsilon \in \mathcal{I}_{\varepsilon,n}) \approx 1 - \Phi(\beta_n) = \Phi(-\beta_n), \quad (5.67)$$

$$P(\varepsilon \in \bar{\mathcal{I}}_{\varepsilon,n}) \approx \Phi(\beta_n). \quad (5.68)$$

To sum up, the probability $P(\varepsilon \in \mathcal{I}_{\varepsilon,n})$ that the sensor measurement errors ε lie in the error region $\mathcal{I}_{\varepsilon,n}$ with intervention at the time instant t_n can be approximated by

$$P(\varepsilon \in \mathcal{I}_{\varepsilon,n}) \approx \begin{cases} \Phi(\beta_n), & \mu \in \mathcal{I}_{\varepsilon,n} \\ \Phi(-\beta_n), & \mu \in \bar{\mathcal{I}}_{\varepsilon,n} \end{cases}, \quad (5.69)$$

which is the combination of (5.65) and (5.67), and the probability $P(\varepsilon \in \bar{\mathcal{I}}_{\varepsilon,n})$ that they lie in the error region $\bar{\mathcal{I}}_{\varepsilon,n}$ without intervention at the time instant t_n by

$$P(\varepsilon \in \bar{\mathcal{I}}_{\varepsilon,n}) \approx \begin{cases} \Phi(-\beta_n), & \mu \in \mathcal{I}_{\varepsilon,n} \\ \Phi(\beta_n), & \mu \in \bar{\mathcal{I}}_{\varepsilon,n} \end{cases}, \quad (5.70)$$

which is the combination of (5.66) and (5.68), with the worst-case distance β_n given by (5.58).

Besides the time instants t_n with indices n from the set $\bar{\mathbb{I}}_{b,i}$, at which the function must not decide for an intervention based on the corresponding sensor measurements $\mathbf{y}[n]$ to fulfill $q_i \geq q_{L,i}$ if $b = L$ or $q_i \leq q_{U,i}$ if $b = U$, there are also time instants t_n at which the function must decide for an intervention based on the corresponding sensor measurements $\mathbf{y}[n]$ at least once to fulfill $q_i \geq q_{L,i}$ if $b = L$ or $q_i \leq q_{U,i}$ if $b = U$. The indices n of these time instants t_n are collected in the set $\mathbb{I}_{b,i} \subset \{0, 1, \dots, n_{\text{end}}\}$. For the case that this set consists of the indices n_3 and n_4 of the two time instants t_{n_3} and t_{n_4} , i.e., $\mathbb{I}_{b,i} = \{n_3, n_4\}$, the corresponding error regions $\bar{\mathcal{I}}_{\varepsilon,n_3}$ and $\bar{\mathcal{I}}_{\varepsilon,n_4}$ without intervention at the time instant t_{n_3} and t_{n_4} , respectively, are visualized by Figure 5.2 and Figure 5.3 in the plane where only the values of the sensor measurement errors

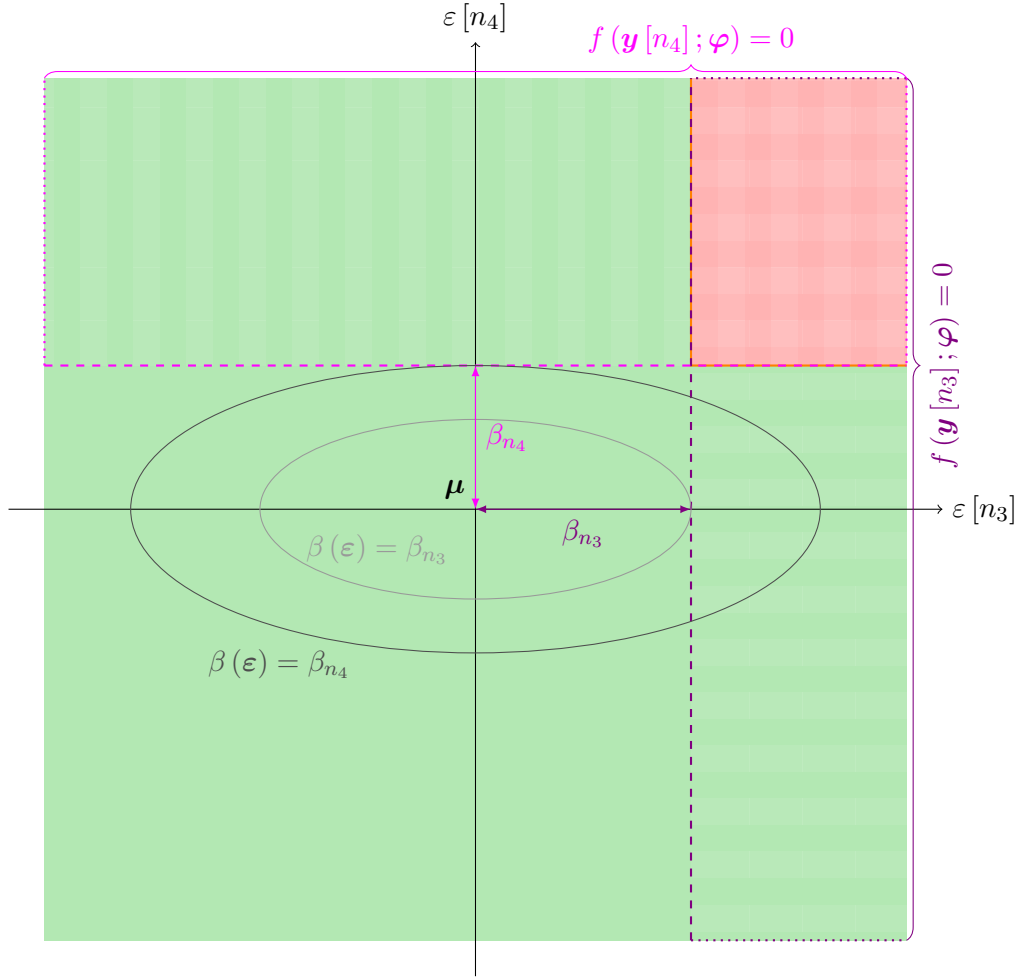


Figure 5.2: Exemplary individual error acceptance region partition $\mathcal{A}_{\varepsilon,b,i}$, $b \in \{L, U\}$, (green area possibly including dashed orange boundary) with either a finite lower bound $q_{L,i}$ if $b = L$ or a finite upper bound $q_{U,i}$ if $b = U$ for $E = 1$ sensor measurement error $\varepsilon[n]$ at a time instant t_n under the assumption that the function must decide for an intervention based on the sensor measurements $\mathbf{y}[n_3]$ and $\mathbf{y}[n_4]$ at the time instants t_{n_3} and t_{n_4} at least once using the decision rule $f(\cdot; \varphi)$ such that $q_i \geq q_{L,i}$ if $b = L$ or $q_i \leq q_{U,i}$ if $b = U$, and its relationship to the error regions $\bar{\mathcal{I}}_{\varepsilon,n}$ without intervention, where $f(\mathbf{y}[n]; \varphi) = 0$ and μ is not included, approximated by the error regions $\hat{\bar{\mathcal{I}}}_{\varepsilon,n}$ corresponding to the worst-case distances β_n (horizontally and vertically striped areas including dashed violet and magenta linear boundaries, respectively) in the plane where $\varepsilon[n] = \mu_n$ for $n \neq n_3, n_4$.

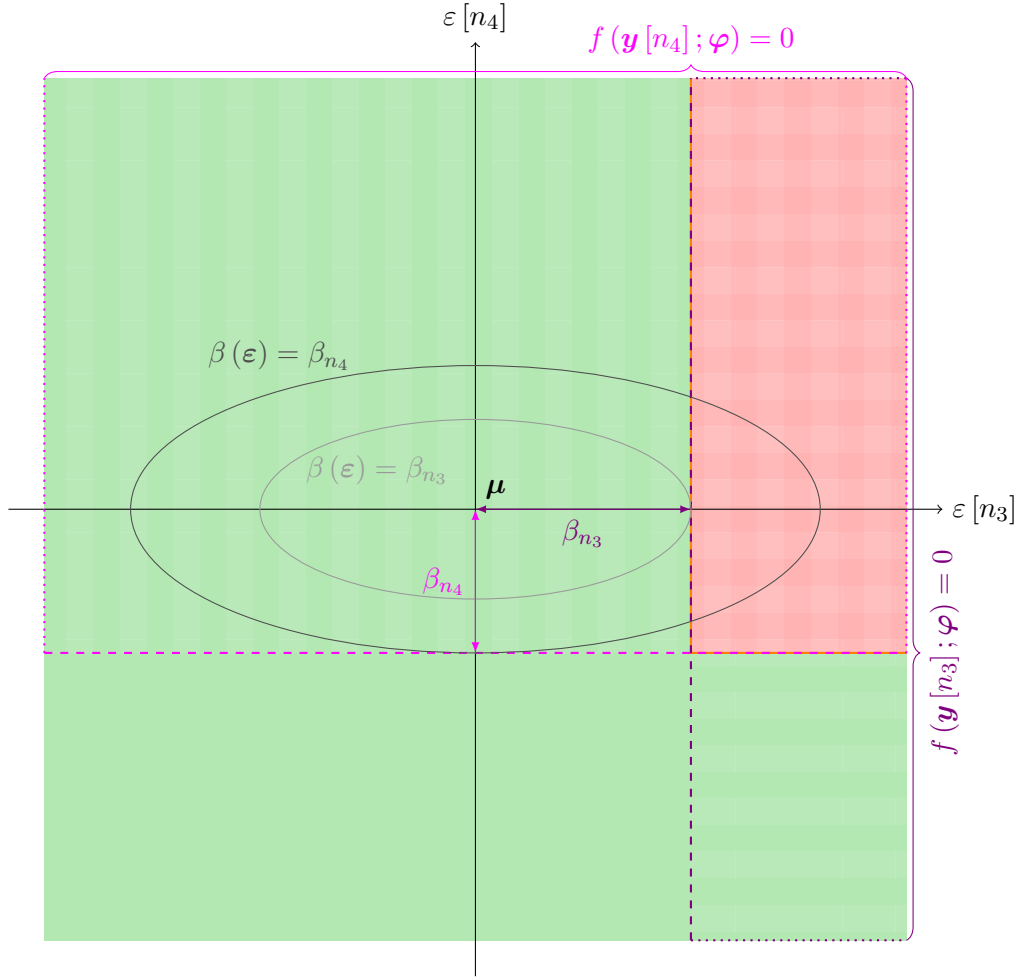


Figure 5.3: Exemplary individual error acceptance region partition $\mathcal{A}_{\epsilon,b,i}$, $b \in \{L, U\}$, (green area possibly including dashed orange boundary) with either a finite lower bound $q_{L,i}$ if $b = L$ or a finite upper bound $q_{U,i}$ if $b = U$ for $E = 1$ sensor measurement error $\epsilon[n]$ at a time instant t_n under the assumption that the function must decide for an intervention based on the sensor measurements $\mathbf{y}[n_3]$ and $\mathbf{y}[n_4]$ at the time instants t_{n_3} and t_{n_4} at least once using the decision rule $f(\cdot; \varphi)$ such that $q_i \geq q_{L,i}$ if $b = L$ or $q_i \leq q_{U,i}$ if $b = U$, and its relationship to the error regions $\bar{\mathcal{I}}_{\epsilon,n}$ without intervention, where $f(\mathbf{y}[n]; \varphi) = 0$ and $\boldsymbol{\mu}$ is partially included, approximated by the error regions $\hat{\mathcal{I}}_{\epsilon,n}$ corresponding to the worst-case distances β_n (horizontally and vertically striped areas including dashed violet and magenta linear boundaries, respectively) in the plane where $\epsilon[n] = \mu_n$ for $n \neq n_3, n_4$.

$\varepsilon [n_3]$ and $\varepsilon [n_4]$ at the specific time instants t_{n_3} and t_{n_4} , respectively, vary while the values of all other sensor measurement errors $\varepsilon [n]$ at the time instants $t_n \neq t_{n_3}, t_{n_4}$ are constant and equal to their mean, i.e., $\varepsilon [n] = \mu_n$ for $n \neq n_3, n_4$. The error region $\bar{\mathcal{I}}_{\varepsilon, n_3}$ without intervention at the time instant t_{n_3} , where $f(\mathbf{y}[n_3]; \varphi) = 0$, and the error region $\bar{\mathcal{I}}_{\varepsilon, n_4}$ without intervention at the time instant t_{n_4} , where $f(\mathbf{y}[n_4]; \varphi) = 0$, are the area to the right of the dashed violet line possibly including this line and the area above the dashed magenta line possibly including this line, respectively. Since the function must decide for an intervention based on the sensor measurements $\mathbf{y}[n_3]$ and $\mathbf{y}[n_4]$ at the time instants t_{n_3} and t_{n_4} at least once using the decision rule $f(\cdot; \varphi)$, i.e., $f(\mathbf{y}[n_3]; \varphi) = 0$ and $f(\mathbf{y}[n_4]; \varphi) = 0$ must not be the two decision results, to fulfill $q_i \geq q_{L,i}$ if $b = L$ or $q_i \leq q_{U,i}$ if $b = U$, the individual error acceptance region partition $\mathcal{A}_{\varepsilon, b, i}$, where this is the case, lies in the complement of the intersection $\bar{\mathcal{I}}_{\varepsilon, n_3} \cap \bar{\mathcal{I}}_{\varepsilon, n_4}$ of the error regions $\bar{\mathcal{I}}_{\varepsilon, n_3}$ and $\bar{\mathcal{I}}_{\varepsilon, n_4}$ without intervention at these two time instants:

$$\mathcal{A}_{\varepsilon, b, i} \subset \overline{\bar{\mathcal{I}}_{\varepsilon, n_3} \cap \bar{\mathcal{I}}_{\varepsilon, n_4}}. \quad (5.71)$$

This can be seen in Figure 5.2 and Figure 5.3, where the complement of the intersection of the areas to the right of the dashed violet line possibly including this line and above the dashed magenta line possibly including this line, which represent the error regions $\bar{\mathcal{I}}_{\varepsilon, n_3}$ and $\bar{\mathcal{I}}_{\varepsilon, n_4}$ without intervention at the two time instants t_{n_3} and t_{n_4} , respectively, yields the green area possibly including the orange boundary representing the individual error acceptance region partition $\mathcal{A}_{\varepsilon, b, i}$. In both Figure 5.2 and Figure 5.3, the mean μ of the sensor measurement errors ε lies in the individual error acceptance region partition $\mathcal{A}_{\varepsilon, b, i}$ in order to allow to achieve a high probability $P(\varepsilon \in \mathcal{A}_{\varepsilon, b, i})$ that the sensor measurement errors ε lie in the individual error acceptance region partition $\mathcal{A}_{\varepsilon, b, i}$ and thus the corresponding specification for the customer satisfaction, i.e., $q_i \geq q_{L,i}$ if $b = L$ or $q_i \leq q_{U,i}$ if $b = U$, is fulfilled. In Figure 5.2, the mean μ of the sensor measurement errors ε lies in both the complement of the error region $\bar{\mathcal{I}}_{\varepsilon, n_3}$ without intervention at the time instant t_{n_3} , namely, the error region $\mathcal{I}_{\varepsilon, n_3}$ with intervention at the time instant t_{n_3} , and the complement of the error region $\bar{\mathcal{I}}_{\varepsilon, n_4}$ without intervention at the time instant t_{n_4} , namely, the error region $\mathcal{I}_{\varepsilon, n_4}$ with intervention at the time instant t_{n_4} , whereas, in Figure 5.3, it lies in the error region $\mathcal{I}_{\varepsilon, n_3}$ with intervention at the time instant t_{n_3} and in the error region $\bar{\mathcal{I}}_{\varepsilon, n_4}$ without intervention at the time instant t_{n_4} . The error region $\hat{\bar{\mathcal{I}}}_{\varepsilon, n_3}$ that is bounded by the tangential hyperplane whose distance from the mean μ of the sensor measurement errors ε is the worst-case distance β_{n_3} at the time instant t_{n_3} and is represented by the horizontally striped area including the dashed violet line approximates the error region $\bar{\mathcal{I}}_{\varepsilon, n_3}$ without intervention at the time instant t_{n_3} and the error region $\hat{\bar{\mathcal{I}}}_{\varepsilon, n_4}$ that is

bounded by the tangential hyperplane whose distance from $\boldsymbol{\mu}$ is the worst-case distance β_{n_4} at the time instant t_{n_4} and is represented by the vertically striped area including the dashed magenta line approximates the error region $\overline{\mathcal{I}}_{\varepsilon, n_4}$ without intervention at the time instant t_{n_4} . Using the approximate error region $\widehat{\overline{\mathcal{I}}}_{\varepsilon, n_3}$ without intervention at the time instant t_{n_3} and the approximate error region $\widehat{\overline{\mathcal{I}}}_{\varepsilon, n_4}$ without intervention at the time instant t_{n_4} instead of the error region $\overline{\mathcal{I}}_{\varepsilon, n_3}$ without intervention at the time instant t_{n_3} and the error region $\overline{\mathcal{I}}_{\varepsilon, n_4}$ without intervention at the instant t_{n_4} , respectively, leads to the approximation of the individual error acceptance region partition $\mathcal{A}_{\varepsilon, b, i}$ represented by the green area possibly including the orange boundary, which lies in the complement of the intersection $\overline{\mathcal{I}}_{\varepsilon, n_3} \cap \overline{\mathcal{I}}_{\varepsilon, n_4}$ according to (5.71), by the complement of their intersection $\widehat{\overline{\mathcal{I}}}_{\varepsilon, n_3} \cap \widehat{\overline{\mathcal{I}}}_{\varepsilon, n_4}$ highlighted by the area that is both horizontally and vertically striped including the dashed violet and magenta boundary.

If there are not only two time instants t_{n_3} and t_{n_4} but an arbitrary number of time instants t_n with indices n from the set $\mathbb{I}_{b, i} \subset \{0, 1, \dots, n_{\text{end}}\}$, at which the function must decide for an intervention based on the corresponding sensor measurements $\mathbf{y}[n]$ at least once to fulfill $q_i \geq q_{L, i}$ if $b = \text{L}$ or $q_i \leq q_{U, i}$ if $b = \text{U}$, the individual error acceptance region partition $\mathcal{A}_{\varepsilon, b, i}$, where this is fulfilled, lies in the complement of the intersection of the error regions $\overline{\mathcal{I}}_{\varepsilon, n}$ without intervention at all these time instants:

$$\mathcal{A}_{\varepsilon, b, i} \subset \overline{\bigcap_{n \in \mathbb{I}_{b, i}} \overline{\mathcal{I}}_{\varepsilon, n}}. \quad (5.72)$$

This is an extension of (5.71) for the set $\mathbb{I}_{b, i} = \{n_3, n_4\}$ consisting of the indices n_3 and n_4 corresponding to the two time instants t_{n_3} and t_{n_4} to the set $\mathbb{I}_{b, i}$ consisting of the indices n corresponding to an arbitrary number of time instants t_n . Combining (5.35) and (5.72) yields

$$\mathcal{A}_{\varepsilon, b, i} \subset \bigcap_{n \in \overline{\mathbb{I}}_{b, i}} \overline{\mathcal{I}}_{\varepsilon, n} \cap \overline{\bigcap_{n \in \mathbb{I}_{b, i}} \overline{\mathcal{I}}_{\varepsilon, n}}. \quad (5.73)$$

Each sensor measurement error ε that lies in the set on the right-hand side of (5.73), where the function does not decide for an intervention based on the sensor measurements $\mathbf{y}[n]$ at the time instants t_n with indices n from $\overline{\mathbb{I}}_{b, i}$ and it decides for an intervention based on the sensor measurements $\mathbf{y}[n]$ at the time instants t_n with indices n from $\mathbb{I}_{b, i}$ at least once such that the corresponding specification for the customer satisfaction, i.e., $q_i \geq q_{L, i}$ if $b = \text{L}$ or $q_i \leq q_{U, i}$ if $b = \text{U}$, is fulfilled, also lies in the individual error acceptance region partition $\mathcal{A}_{\varepsilon, b, i}$, where this specification for the customer satisfaction is fulfilled. Hence, the individual error acceptance region

partition $\mathcal{A}_{\varepsilon,b,i}$ is not only a subset of but equal to the set on the right-hand side of (5.73):

$$\mathcal{A}_{\varepsilon,b,i} = \bigcap_{n \in \bar{\mathbb{I}}_{b,i}} \bar{\mathcal{I}}_{\varepsilon,n} \cap \overline{\bigcap_{n \in \mathbb{I}_{b,i}} \bar{\mathcal{I}}_{\varepsilon,n}}. \quad (5.74)$$

Consequently, the probability $P(\varepsilon \in \mathcal{A}_{\varepsilon,b,i})$ that the sensor measurement errors ε lie in the individual error acceptance region partition $\mathcal{A}_{\varepsilon,b,i}$ and thus the corresponding specification for the customer satisfaction, i.e., $q_i \geq q_{L,i}$ if $b = L$ or $q_i \leq q_{U,i}$ if $b = U$, is fulfilled, can be written as

$$P(\varepsilon \in \mathcal{A}_{\varepsilon,b,i}) = P\left(\varepsilon \in \bigcap_{n \in \bar{\mathbb{I}}_{b,i}} \bar{\mathcal{I}}_{\varepsilon,n} \cap \overline{\bigcap_{n \in \mathbb{I}_{b,i}} \bar{\mathcal{I}}_{\varepsilon,n}}\right). \quad (5.75)$$

In Appendix B, it is shown that the events $\{\varepsilon \in \bigcap_{n \in \mathbb{I}_1} \bar{\mathcal{I}}_{\varepsilon,n}\}$ and $\{\varepsilon \in \overline{\bigcap_{n \in \mathbb{I}_2} \bar{\mathcal{I}}_{\varepsilon,n}}\}$ that the sensor measurement errors ε lie in all error regions $\bar{\mathcal{I}}_{\varepsilon,n}$ without intervention at the time instants t_n with indices n from a set \mathbb{I}_1 and that they do not lie in all error regions $\bar{\mathcal{I}}_{\varepsilon,n}$ without intervention at the time instants t_n with indices n from a set \mathbb{I}_2 , respectively, where $\mathbb{I}_1, \mathbb{I}_2 \subset \{0, 1, \dots, n_{\text{end}}\}$ and $\mathbb{I}_1 \cap \mathbb{I}_2 = \emptyset$, are statistically independent. This applies here, where $\mathbb{I}_1 = \bar{\mathbb{I}}_{b,i}$ and $\mathbb{I}_2 = \mathbb{I}_{b,i}$. According to (B.6), the probability that the sensor measurement errors ε lie in all error regions $\bar{\mathcal{I}}_{\varepsilon,n}$ without intervention at the time instants t_n with indices $n \in \mathbb{I}_1 = \bar{\mathbb{I}}_{b,i}$ and do not lie in all error regions $\bar{\mathcal{I}}_{\varepsilon,n}$ without intervention at the time instants t_n with indices $n \in \mathbb{I}_2 = \mathbb{I}_{b,i}$ in (5.75) factorizes into the probability $P(\varepsilon \in \bigcap_{n \in \bar{\mathbb{I}}_{b,i}} \bar{\mathcal{I}}_{\varepsilon,n})$ that they lie in all error regions $\bar{\mathcal{I}}_{\varepsilon,n}$ without intervention at the time instants t_n with indices $n \in \bar{\mathbb{I}}_{b,i}$ and the probability $P(\varepsilon \in \overline{\bigcap_{n \in \mathbb{I}_{b,i}} \bar{\mathcal{I}}_{\varepsilon,n}})$ that they do not lie in all error regions $\bar{\mathcal{I}}_{\varepsilon,n}$ without intervention at the time instants t_n with indices $n \in \mathbb{I}_{b,i}$:

$$\begin{aligned} P(\varepsilon \in \mathcal{A}_{\varepsilon,b,i}) &= P\left(\varepsilon \in \bigcap_{n \in \bar{\mathbb{I}}_{b,i}} \bar{\mathcal{I}}_{\varepsilon,n}\right) P\left(\varepsilon \in \overline{\bigcap_{n \in \mathbb{I}_{b,i}} \bar{\mathcal{I}}_{\varepsilon,n}}\right) \\ &= P\left(\varepsilon \in \bigcap_{n \in \bar{\mathbb{I}}_{b,i}} \bar{\mathcal{I}}_{\varepsilon,n}\right) \left(1 - P\left(\varepsilon \in \bigcap_{n \in \mathbb{I}_{b,i}} \bar{\mathcal{I}}_{\varepsilon,n}\right)\right). \end{aligned} \quad (5.76)$$

In Appendix B, it is also shown that the events $\{\varepsilon \in \bar{\mathcal{I}}_{\varepsilon,n}\}$ that they lie in the individual error regions $\bar{\mathcal{I}}_{\varepsilon,n}$ without intervention at the time instants t_n with indices n from a set \mathbb{I} like $\bar{\mathbb{I}}_{b,i}$ and $\mathbb{I}_{b,i}$ are statistically independent. Therefore, the probability $P(\varepsilon \in \bigcap_{n \in \bar{\mathbb{I}}_{b,i}} \bar{\mathcal{I}}_{\varepsilon,n})$ that the sensor measurement errors ε lie in all error regions $\bar{\mathcal{I}}_{\varepsilon,n}$

without intervention at the time instants t_n with indices $n \in \mathbb{I} = \bar{\mathbb{I}}_{b,i}$ factorizes into the probabilities $P(\varepsilon \in \bar{\mathcal{I}}_{\varepsilon,n})$ that they lie in the individual error regions $\bar{\mathcal{I}}_{\varepsilon,n}$ without intervention at these time instants t_n and the probability $P(\varepsilon \in \bigcap_{n \in \bar{\mathbb{I}}_{b,i}} \bar{\mathcal{I}}_{\varepsilon,n})$ that the sensor measurement errors ε lie in all error regions $\bar{\mathcal{I}}_{\varepsilon,n}$ without intervention at the time instants t_n with indices $n \in \mathbb{I} = \bar{\mathbb{I}}_{b,i}$ factorizes into the probabilities $P(\varepsilon \in \bar{\mathcal{I}}_{\varepsilon,n})$ that they lie in the individual error regions $\bar{\mathcal{I}}_{\varepsilon,n}$ without intervention at these time instants t_n according to (B.2):

$$P\left(\varepsilon \in \bigcap_{n \in \bar{\mathbb{I}}_{b,i}} \bar{\mathcal{I}}_{\varepsilon,n}\right) = \prod_{n \in \bar{\mathbb{I}}_{b,i}} P(\varepsilon \in \bar{\mathcal{I}}_{\varepsilon,n}), \quad (5.77)$$

$$P\left(\varepsilon \in \bigcap_{n \in \mathbb{I}_{b,i}} \bar{\mathcal{I}}_{\varepsilon,n}\right) = \prod_{n \in \mathbb{I}_{b,i}} P(\varepsilon \in \bar{\mathcal{I}}_{\varepsilon,n}). \quad (5.78)$$

Substituting this into (5.76), yields the expression

$$P(\varepsilon \in \mathcal{A}_{\varepsilon,b,i}) = \prod_{n \in \bar{\mathbb{I}}_{b,i}} P(\varepsilon \in \bar{\mathcal{I}}_{\varepsilon,n}) \left(1 - \prod_{n \in \mathbb{I}_{b,i}} P(\varepsilon \in \bar{\mathcal{I}}_{\varepsilon,n})\right) \quad (5.79)$$

for the probability that the sensor measurement errors ε lie in the individual error acceptance region partition $\mathcal{A}_{\varepsilon,b,i}$ and thus the corresponding specification for the customer satisfaction, i.e., $q_i \geq q_{L,i}$ if $b = L$ or $q_i \leq q_{U,i}$ if $b = U$, is fulfilled. This probability can be approximated by

$$P(\varepsilon \in \mathcal{A}_{\varepsilon,b,i}) \approx \prod_{n \in \bar{\mathbb{I}}_{b,i}} \begin{cases} \Phi(-\beta_n), & \boldsymbol{\mu} \in \mathcal{I}_{\varepsilon,n} \\ \Phi(\beta_n), & \boldsymbol{\mu} \in \bar{\mathcal{I}}_{\varepsilon,n} \end{cases} \cdot \left(1 - \prod_{n \in \mathbb{I}_{b,i}} \begin{cases} \Phi(-\beta_n), & \boldsymbol{\mu} \in \mathcal{I}_{\varepsilon,n} \\ \Phi(\beta_n), & \boldsymbol{\mu} \in \bar{\mathcal{I}}_{\varepsilon,n} \end{cases}\right) \quad (5.80)$$

resulting from the approximation (5.70) for the probability $P(\varepsilon \in \bar{\mathcal{I}}_{\varepsilon,n})$ that the sensor measurement errors ε lie in the error region $\bar{\mathcal{I}}_{\varepsilon,n}$ without intervention at the time instant t_n , where the worst-case distances β_n at the time instants t_n are given by (5.58) and the check of whether $\boldsymbol{\mu} \in \mathcal{I}_{\varepsilon,n}$ or $\boldsymbol{\mu} \in \bar{\mathcal{I}}_{\varepsilon,n}$ can be performed according to (5.59) and (5.60).

If not only the individual error acceptance region partition $\mathcal{A}_{\varepsilon,b,i}$, where the corresponding specification for the customer satisfaction, i.e., $q_i \geq q_{L,i}$ if $b = L$ or

$q_i \leq q_{U,i}$ if $b = U$, is fulfilled, is considered but the intersection of all individual error acceptance region partitions $\mathcal{A}_{\varepsilon,b,i}$, $b = L, U$, $i = 1, 2, \dots, N_q$ from (5.19), namely, the error acceptance region \mathcal{A}_ε , where all specifications $q_{L,i} \leq q_i \leq q_{U,i}$ for the customer satisfaction defined by the acceptance intervals $[q_{L,i}, q_{U,i}]$ for the customer satisfaction properties q_i , $i = 1, 2, \dots, N_q$, are fulfilled, the error acceptance region \mathcal{A}_ε plays the same role as the individual error acceptance region partition $\mathcal{A}_{\varepsilon,b,i}$ before. Therefore, the probability $P(\varepsilon \in \mathcal{A}_\varepsilon)$ that the sensor measurement errors ε lie in the error acceptance region \mathcal{A}_ε , which is equal to the probability $P(\mathbf{q} \in \mathcal{A}_q)$ that all customer satisfaction properties \mathbf{q} lie in the customer satisfaction acceptance region \mathcal{A}_q and thus all specifications $q_{L,i} \leq q_i \leq q_{U,i}$ for the customer satisfaction defined for the customer satisfaction properties q_i , $i = 1, 2, \dots, N_q$, are fulfilled, can be expressed as

$$P(\mathbf{q} \in \mathcal{A}_q) = P(\varepsilon \in \mathcal{A}_\varepsilon) = \prod_{n \in \bar{\mathbb{I}}} P(\varepsilon \in \bar{\mathcal{I}}_{\varepsilon,n}) \left(1 - \prod_{n \in \mathbb{I}} P(\varepsilon \in \bar{\mathcal{I}}_{\varepsilon,n}) \right) \quad (5.81)$$

and approximated by

$$P(\mathbf{q} \in \mathcal{A}_q) = P(\varepsilon \in \mathcal{A}_\varepsilon) \approx \prod_{n \in \bar{\mathbb{I}}} \begin{cases} \Phi(-\beta_n), & \boldsymbol{\mu} \in \mathcal{I}_{\varepsilon,n} \\ \Phi(\beta_n), & \boldsymbol{\mu} \in \bar{\mathcal{I}}_{\varepsilon,n} \end{cases} \cdot \left(1 - \prod_{n \in \mathbb{I}} \begin{cases} \Phi(-\beta_n), & \boldsymbol{\mu} \in \mathcal{I}_{\varepsilon,n} \\ \Phi(\beta_n), & \boldsymbol{\mu} \in \bar{\mathcal{I}}_{\varepsilon,n} \end{cases} \right) \quad (5.82)$$

analogously to the expression and approximation for the probability $P(\varepsilon \in \mathcal{A}_{\varepsilon,b,i})$ that the sensor measurement errors ε lie in the individual error acceptance region partition $\mathcal{A}_{\varepsilon,b,i}$ in (5.79) and (5.80), respectively. Here, the worst-case distances β_n at the time instants t_n are given by (5.58) and the check of whether $\boldsymbol{\mu} \in \mathcal{I}_{\varepsilon,n}$ or $\boldsymbol{\mu} \in \bar{\mathcal{I}}_{\varepsilon,n}$ can be performed according to (5.59) and (5.60). Furthermore, $\bar{\mathbb{I}} \subset \{0, 1, \dots, n_{\text{end}}\}$ and $\mathbb{I} \subset \{0, 1, \dots, n_{\text{end}}\}$ are the set of the indices n of the time instants t_n at which the function must not decide for an intervention based on the corresponding sensor measurements $\mathbf{y}[n]$ to fulfill $q_{L,i} \leq q_i \leq q_{U,i}$, $i = 1, 2, \dots, N_q$, and the set of the indices n of the time instants t_n at which the function must decide for an intervention based on the corresponding sensor measurements $\mathbf{y}[n]$ at least once to fulfill $q_{L,i} \leq q_i \leq q_{U,i}$, $i = 1, 2, \dots, N_q$, respectively, as $\bar{\mathbb{I}}_{b,i}$ and $\mathbb{I}_{b,i}$ in (5.79) and (5.80) are the set of the indices n of the time instants t_n at which the function must not decide for an intervention based on the corresponding sensor measurements $\mathbf{y}[n]$ to fulfill $q_i \geq q_{L,i}$ if $b = L$ or $q_i \leq q_{U,i}$ if $b = U$, and the set of the indices n of the time instants t_n at

which the function must decide for an intervention based on the corresponding sensor measurements $\mathbf{y}[n]$ at least once to fulfill $q_i \geq q_{L,i}$ if $b = L$ or $q_i \leq q_{U,i}$ if $b = U$, respectively.

Although this result has been derived under the assumption of $E = 1$ sensor measurement error $\varepsilon[n] = \varepsilon[n] \in \mathbb{R}$ at a time instant t_n for ease of exposition, it also holds in the case of $E > 1$ sensor measurement errors $\varepsilon[n] \in \mathbb{R}^E$ at a time instant t_n . The only difference is that $\varepsilon[n] \in \mathbb{R}$ with the mean μ_n becomes $\varepsilon[n] \in \mathbb{R}^E$ with the mean $\boldsymbol{\mu}_n$, which implies that the vector $\varepsilon \in \mathbb{R}^{n_{\text{end}}+1}$ consisting of all sensor measurement errors becomes $\varepsilon \in \mathbb{R}^{E(n_{\text{end}}+1)}$, in (5.36), (5.40), (5.58), (5.59) and (5.60). Then, the definitions of the error regions with and without intervention at the time instant t_n read

$$\begin{aligned} \mathcal{I}_{\varepsilon,n} &= \left\{ \varepsilon \in \mathbb{R}^{E(n_{\text{end}}+1)} : f(\mathbf{y}[n]; \boldsymbol{\varphi}) = 1 \right\} \\ &= \left\{ \varepsilon \in \mathbb{R}^{E(n_{\text{end}}+1)} : f(\mathbf{y}(\mathbf{x}[n], \varepsilon[n]); \boldsymbol{\varphi}) = 1 \right\} \end{aligned} \quad (5.83)$$

and

$$\begin{aligned} \bar{\mathcal{I}}_{\varepsilon,n} &= \left\{ \varepsilon \in \mathbb{R}^{E(n_{\text{end}}+1)} : f(\mathbf{y}[n]; \boldsymbol{\varphi}) = 0 \right\} \\ &= \left\{ \varepsilon \in \mathbb{R}^{E(n_{\text{end}}+1)} : f(\mathbf{y}(\mathbf{x}[n], \varepsilon[n]); \boldsymbol{\varphi}) = 0 \right\}, \end{aligned} \quad (5.84)$$

respectively, the worst-case distances β_n at the time instants t_n are given by

$$\begin{aligned} \beta_n &= \min_{\varepsilon[n] \in \mathbb{R}^E} \beta_n(\varepsilon[n]) \\ \text{s.t. } \varepsilon[n] &\in \text{cl} \left(\left\{ \varepsilon[n] \in \mathbb{R}^E : f(\mathbf{y}(\mathbf{x}[n], \varepsilon[n]); \boldsymbol{\varphi}) = \begin{cases} 0, & \boldsymbol{\mu} \in \mathcal{I}_{\varepsilon,n} \\ 1, & \boldsymbol{\mu} \in \bar{\mathcal{I}}_{\varepsilon,n} \end{cases} \right\} \right) \end{aligned} \quad (5.85)$$

with the square of the Mahalanobis distance of the sensor measurement errors $\varepsilon[n]$ at the time instant t_n from their mean $\boldsymbol{\mu}_n$ stated in (5.49) and the check of whether $\boldsymbol{\mu} \in \mathcal{I}_{\varepsilon,n}$ or $\boldsymbol{\mu} \in \bar{\mathcal{I}}_{\varepsilon,n}$ can be performed according to

$$\begin{aligned} \boldsymbol{\mu} \in \mathcal{I}_{\varepsilon,n} &= \left\{ \varepsilon \in \mathbb{R}^{E(n_{\text{end}}+1)} : f(\mathbf{y}(\mathbf{x}[n], \varepsilon[n]); \boldsymbol{\varphi}) = 1 \right\} \\ &\Leftrightarrow f(\mathbf{y}(\mathbf{x}[n], \boldsymbol{\mu}_n); \boldsymbol{\varphi}) = 1 \end{aligned} \quad (5.86)$$

and

$$\begin{aligned} \boldsymbol{\mu} \in \bar{\mathcal{I}}_{\varepsilon,n} &= \left\{ \varepsilon \in \mathbb{R}^{E(n_{\text{end}}+1)} : f(\mathbf{y}(\mathbf{x}[n], \varepsilon[n]); \boldsymbol{\varphi}) = 0 \right\} \\ &\Leftrightarrow f(\mathbf{y}(\mathbf{x}[n], \boldsymbol{\mu}_n); \boldsymbol{\varphi}) = 0. \end{aligned} \quad (5.87)$$

The set $\bar{\mathbb{I}} \subset \{0, 1, \dots, n_{\text{end}}\}$ of the indices n of the time instants t_n at which the function must not decide for an intervention based on the corresponding sensor measurements $\mathbf{y}[n]$ to fulfill $q_{L,i} \leq q_i \leq q_{U,i}$, $i = 1, 2, \dots, N_q$, and the set $\mathbb{I} \subset \{0, 1, \dots, n_{\text{end}}\}$ of the indices n of the time instants t_n at which the function must decide for an intervention based on the corresponding sensor measurements $\mathbf{y}[n]$ at least once to fulfill $q_{L,i} \leq q_i \leq q_{U,i}$, $i = 1, 2, \dots, N_q$, can be determined by simulations of the automated vehicular safety system as follows. For each time instant t_n , $n = 0, 1, \dots, n_{\text{end}}$, the automated vehicular safety system is simulated after deciding for an intervention at one of those time instants t_n in order to map this time instant together with the given scenario parameters $\boldsymbol{\xi}$, which are the input of the simulation, to the respective values of the customer satisfaction properties \mathbf{q} , which are the output of the simulation, and determine whether all specifications $q_{L,i} \leq q_i \leq q_{U,i}$, $i = 1, 2, \dots, N_q$, for the customer satisfaction are fulfilled or not. Assuming that not all specifications $q_{L,i} \leq q_i \leq q_{U,i}$ are fulfilled if the function does not decide for an intervention based on the sensor measurements $\mathbf{y}[n]$ at any of the considered time instants t_n and that the time instants t_n for which the specifications $q_{L,i} \leq q_i \leq q_{U,i}$ are fulfilled if the function decides for an intervention based on the sensor measurements $\mathbf{y}[n]$ at one of these time instants form a block with indices n ranging from n_{min} to n_{max} , where $0 \leq n_{\text{min}} \leq n_{\text{max}} \leq n_{\text{end}}$, the function must not decide for an intervention based on the sensor measurements $\mathbf{y}[n]$ at the time instants t_n , $n = 0, 1, \dots, n_{\text{min}} - 1$, before this block and must decide for an intervention based on the sensor measurements $\mathbf{y}[n]$ at the time instants t_n , $n = n_{\text{min}}, n_{\text{min}} + 1, \dots, n_{\text{max}}$, in this block at least once to fulfill the specifications $q_{L,i} \leq q_i \leq q_{U,i}$. Consequently, the set $\bar{\mathbb{I}}$ of the indices n of the time instants t_n at which the function must not decide for an intervention based on the corresponding sensor measurements $\mathbf{y}[n]$ to fulfill $q_{L,i} \leq q_i \leq q_{U,i}$, $i = 1, 2, \dots, N_q$, and the set \mathbb{I} of the indices n of the time instants t_n at which the function must decide for an intervention based on the corresponding sensor measurements $\mathbf{y}[n]$ at least once to fulfill $q_{L,i} \leq q_i \leq q_{U,i}$, $i = 1, 2, \dots, N_q$, read

$$\bar{\mathbb{I}} = \{0, 1, \dots, n_{\text{min}} - 1\} \quad (5.88)$$

and

$$\mathbb{I} = \{n_{\text{min}}, n_{\text{min}} + 1, \dots, n_{\text{max}}\}. \quad (5.89)$$

The direct application of the worst-case distance approach to the robust design of automated vehicular safety systems determines the worst-case distances $\beta_{b,i}$, $i = 1, 2, \dots, N_q$, $b = \text{L, U}$, by solving the optimization problems (5.22) and (5.23) if $b = \text{L}$ and $b = \text{U}$, respectively, in order to approximate the probability $P(\mathbf{q} \in \mathcal{A}_q)$

of fulfilling the specifications $q_{L,i} \leq q_i \leq q_{U,i}$, $i = 1, 2, \dots, N_q$, for the customer satisfaction by evaluating the standard normal cdf $\Phi(x)$ at the determined worst-case distances $\beta_{b,i}$ according to (5.31). The adaptation of the worst-case distance approach to the robust design of automated vehicular safety systems that determines the worst-case distances β_n at the time instants t_n , $n = 0, 1, \dots, n_{\text{end}}$, by solving the optimization problems (5.85) in order to approximate the probability $P(\mathbf{q} \in \mathcal{A}_q)$ of fulfilling the specifications $q_{L,i} \leq q_i \leq q_{U,i}$, $i = 1, 2, \dots, N_q$, for the customer satisfaction by evaluating the standard normal cdf $\Phi(x)$ at the determined worst-case distances β_n according to (5.82) decomposes the original optimization problems (5.22) and (5.23) into the optimization problems (5.85), which are easier to solve. This is due to the fact that the original optimization problems (5.22) and (5.23) have to be solved with respect to the vector $\varepsilon \in \mathbb{R}^{E(n_{\text{end}}+1)}$ of the sensor measurement errors at all considered time instants t_n , $n = 0, 1, \dots, n_{\text{end}}$, and the dimension $E(n_{\text{end}} + 1)$, which requires several simulations of the automated vehicular safety system for evaluating the customer satisfaction property q_i in the constraints, whereas each of the optimization problems (5.85) has to be solved with respect to the vector $\varepsilon[n] \in \mathbb{R}^E$ of the sensor measurement errors at a single time instant t_n and the smaller dimension E , which does not require several simulations of the automated vehicular safety system but only several evaluations of the decision rule $f(\mathbf{y}(\mathbf{x}[n], \varepsilon[n]); \varphi)$ for the given states $\mathbf{x}[n]$ the considered dynamic system would have without any intervention at the time instants t_n in the constraints.

Robust Design of an Automatic Emergency Braking System

6

In the two previous chapters, the proposed methodology for the robust function and sensor design that allows to systematically design both functions and sensors of automated vehicular safety systems such that the customer requirements are fulfilled in a robust manner despite unavoidable sensor measurement errors has been described in general. This chapter demonstrates how it can be applied to the robust design of an AEB system as a typical example for an automated vehicular safety system. In order to illustrate the basic principle of the design methodology, the model of the AEB system is kept as simple as possible, which also allows to derive results in closed form at several points for an accurate evaluation of the design methodology.

In part, the application of the proposed design methodology to the robust design of an AEB system has already been published in [44–46]. While the proposed design methodology is applied for the first time in [44] to the robust design of an AEB system for one driving scenario and one predefined decision rule used for triggering an emergency brake intervention and [45] extends this to several driving scenarios and predefined decision rules by deriving closed-form expressions for the defined probabilistic quality measure Q , the AEB system is designed solely based on simulations of it without the need for deriving closed-form expressions for the probabilistic quality measure Q in [46]. The results in [44–46] will be revisited and supplemented in the following to provide a complete picture of the system model, the formulation of the design problems at hand as optimization problems using the proposed design methodology and their solution based on closed-form expressions for the probabilistic quality measure Q or solely based on simulations of the AEB system under design.

6.1 System Model for the Automatic Emergency Braking System

The system model of the considered AEB system is a special case of the general system model for an automated vehicular safety system introduced in Chapter 2. As described there in general, it can be split into a mathematical representation of the

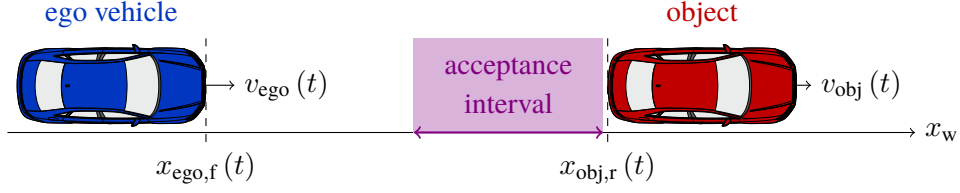


Figure 6.1: Driving scenario considered for the robust design of an AEB system at time t .

driving scenario in which the AEB system is applied and a stochastic model of the AEB system itself including sensor measurement errors.

6.1.1 Mathematical Representation of the Driving Scenario for the Robust Design of the Automatic Emergency Braking System

As in [44–46], the driving scenario illustrated in Figure 6.1, where the ego vehicle approaches an object, e.g., another vehicle, is considered for the robust design of the AEB system. At time $t \geq t_0$ within the considered time interval starting at t_0 , the front of the ego vehicle moving with the longitudinal velocity $v_{ego}(t)$ along the x_w -axis of the world coordinate system is located at the position $x_{ego,f}(t)$ with respect to this axis and the rear of the object moving with the longitudinal velocity $v_{obj}(t)$ along the x_w -axis of the world coordinate system is located at the position $x_{obj,r}(t)$ with respect to this axis. The velocity of the object is assumed to be constant over the time t . Assuming that the object is in front of the ego vehicle and slower than it at the time t_0 when the driving scenario starts, i.e., $x_{ego,f}(t_0) < x_{obj,r}(t_0)$ and $v_{ego}(t_0) > v_{obj}(t_0) \geq 0$, a collision would necessarily occur if the ego vehicle moved with constant velocity too. In order to avoid such a collision, an emergency brake intervention is triggered at time $t_b \geq t_0$, which reduces the longitudinal velocity of the ego vehicle with a constant deceleration $a > 0$. To sum up, the lateral accelerations of the ego vehicle and the object at time t are $a_{lat,ego}(t) = a_{lat,ego} = 0$ and $a_{lat,obj}(t) = a_{lat,obj} = 0$, respectively, while the longitudinal accelerations of the ego vehicle and the object at time t are

$$a_{lon,ego}(t) = \begin{cases} 0, & t < t_b \\ -a, & t \geq t_b \end{cases} \quad (6.1)$$

and $a_{lon,obj}(t) = a_{lon,obj} = 0$, respectively.

This one-dimensional motion model with piecewise constant accelerations is captured by the general motion model where the motion of each vehicle during a

6.1 System Model for the Automatic Emergency Braking System

driving maneuver is described by the system of differential equations (2.1)–(2.4). This system of differential equations describing the motion of the ego vehicle reads

$$\dot{x}_{\text{ego}}(t) = v_{\text{ego}}(t) \cos(\psi_{\text{ego}}(t)), \quad (6.2)$$

$$\dot{y}_{\text{ego}}(t) = v_{\text{ego}}(t) \sin(\psi_{\text{ego}}(t)), \quad (6.3)$$

$$\dot{v}_{\text{ego}}(t) = a_{\text{lon,ego}}, \quad (6.4)$$

$$\dot{\psi}_{\text{ego}}(t) = \min\left(\frac{a_{\text{lat,ego}}}{v_{\text{ego}}(t)}, \frac{v_{\text{ego}}(t)}{r_{\text{min,ego}}}\right) \quad (6.5)$$

with the turn radius $r_{\text{min,ego}}$ of the ego vehicle, where the state of the ego vehicle at time t is represented by the state vector $[x_{\text{ego}}(t), y_{\text{ego}}(t), v_{\text{ego}}(t), \psi_{\text{ego}}(t)]^T$ consisting of four state variables, which are the coordinates $x_{\text{ego}}(t)$ and $y_{\text{ego}}(t)$ of its center of gravity with respect to the x_w - and y_w -axis of the world coordinate system determining its position, its longitudinal velocity $v_{\text{ego}}(t)$ and its yaw angle $\psi_{\text{ego}}(t)$. Analogously, the system of differential equations describing the motion of the object reads

$$\dot{x}_{\text{obj}}(t) = v_{\text{obj}}(t) \cos(\psi_{\text{obj}}(t)), \quad (6.6)$$

$$\dot{y}_{\text{obj}}(t) = v_{\text{obj}}(t) \sin(\psi_{\text{obj}}(t)), \quad (6.7)$$

$$\dot{v}_{\text{obj}}(t) = a_{\text{lon,obj}}, \quad (6.8)$$

$$\dot{\psi}_{\text{obj}}(t) = \min\left(\frac{a_{\text{lat,obj}}}{v_{\text{obj}}(t)}, \frac{v_{\text{obj}}(t)}{r_{\text{min,obj}}}\right) \quad (6.9)$$

with the turn radius $r_{\text{min,obj}}$ of the object, where the state of the object at time t is represented by the state vector $[x_{\text{obj}}(t), y_{\text{obj}}(t), v_{\text{obj}}(t), \psi_{\text{obj}}(t)]^T$ consisting of four state variables, which are the coordinates $x_{\text{obj}}(t)$ and $y_{\text{obj}}(t)$ of its center of gravity with respect to the x_w - and y_w -axis of the world coordinate system determining its position, its longitudinal velocity $v_{\text{obj}}(t)$ and its yaw angle $\psi_{\text{obj}}(t)$.

The motion of the object with constant velocity in the considered time interval starting at t_0 is described by the differential equations (6.6)–(6.9) with $a_{\text{lon,obj}} = a_{\text{lat,obj}} = 0$. They can be solved numerically to obtain the trajectory of the object but, in this special case, a closed-form solution exists. In Appendix C, the closed-form solution (C.19)–(C.22) of the differential equations (2.1)–(2.4) describing the vehicle motion with constant velocity, i.e., $a_{\text{lon}} = a_{\text{lat}} = 0$, in the time interval starting at t_{start} under the assumption $v(t_{\text{start}}) \geq 0$ is derived. Applying this result to the differential equations (6.6)–(6.9) with $t_{\text{start}} = t_0$, $a_{\text{lon}} = a_{\text{lon,obj}} = 0$, $a_{\text{lat}} = a_{\text{lat,obj}} = 0$, $r_{\text{min}} = r_{\text{min,obj}}$, $x(t) = x_{\text{obj}}(t)$, $y(t) = y_{\text{obj}}(t)$, $v(t) = v_{\text{obj}}(t)$ and $\psi(t) = \psi_{\text{obj}}(t)$

yields their closed-form solution

$$x_{\text{obj}}(t) = v_{\text{obj}}(t_0)(t - t_0) \cos(\psi_{\text{obj}}(t_0)) + x_{\text{obj}}(t_0), \quad (6.10)$$

$$y_{\text{obj}}(t) = v_{\text{obj}}(t_0)(t - t_0) \sin(\psi_{\text{obj}}(t_0)) + y_{\text{obj}}(t_0), \quad (6.11)$$

$$v_{\text{obj}}(t) = v_{\text{obj}}(t_0), \quad (6.12)$$

$$\psi_{\text{obj}}(t) = \psi_{\text{obj}}(t_0) \quad (6.13)$$

under the assumption $v_{\text{obj}}(t_0) \geq 0$. As the yaw angle of the object in the considered driving scenario, which is illustrated in Figure 6.1, is zero, i.e., $\psi_{\text{obj}}(t_0) = 0$, the closed-form solution simplifies to

$$x_{\text{obj}}(t) = v_{\text{obj}}(t_0)(t - t_0) + x_{\text{obj}}(t_0), \quad (6.14)$$

$$y_{\text{obj}}(t) = y_{\text{obj}}(t_0), \quad (6.15)$$

$$v_{\text{obj}}(t) = v_{\text{obj}}(t_0), \quad (6.16)$$

$$\psi_{\text{obj}}(t) = 0. \quad (6.17)$$

Analogously, the differential equations (6.2)–(6.5) with $a_{\text{lon,ego}} = a_{\text{lat,ego}} = 0$, which describe the motion of the ego vehicle with constant velocity in the time interval starting at t_0 before triggering the emergency brake intervention at t_b and have exactly the same form as (6.6)–(6.9), have the closed-form solution

$$x_{\text{ego}}(t) = v_{\text{ego}}(t_0)(t - t_0) + x_{\text{ego}}(t_0), \quad (6.18)$$

$$y_{\text{ego}}(t) = y_{\text{ego}}(t_0), \quad (6.19)$$

$$v_{\text{ego}}(t) = v_{\text{ego}}(t_0), \quad (6.20)$$

$$\psi_{\text{ego}}(t) = 0 \quad (6.21)$$

such that a numerical solution is possible but not necessary to obtain the trajectory of the ego vehicle in this special case. The motion of the ego vehicle with the constant longitudinal acceleration $a_{\text{lon,ego}} = -a$ in the time interval starting at t_b when triggering the emergency brake intervention is described by the differential equations (6.2)–(6.5) with $a_{\text{lon,ego}} = -a$ and $a_{\text{lat,ego}} = 0$. They can be solved numerically to obtain the trajectory of the ego vehicle but a closed-form solution exists also in this special case. In Appendix C, the closed-form solution (C.15)–(C.18) of the differential equations (2.1)–(2.4) describing the vehicle motion with the constant longitudinal acceleration a_{lon} and the lateral acceleration $a_{\text{lat}} = 0$ in the time interval starting at t_{start} and ending at t_{end} under the assumption $v(t) \geq 0$ for $t \in [t_{\text{start}}, t_{\text{end}}]$ is derived. Applying this result to the differential equations (6.2)–(6.5) with $t_{\text{start}} = t_b$, $a_{\text{lon}} = a_{\text{lon,ego}} = -a$,

6.1 System Model for the Automatic Emergency Braking System

$a_{\text{lat}} = a_{\text{lat,ego}} = 0$, $r_{\text{min}} = r_{\text{min,ego}}$, $x(t) = x_{\text{ego}}(t)$, $y(t) = y_{\text{ego}}(t)$, $v(t) = v_{\text{ego}}(t)$ and $\psi(t) = \psi_{\text{ego}}(t)$ yields their closed-form solution

$$x_{\text{ego}}(t) = \left(-\frac{1}{2}a(t-t_b)^2 + v_{\text{ego}}(t_b)(t-t_b) \right) \cos(\psi_{\text{ego}}(t_b)) + x_{\text{ego}}(t_b), \quad (6.22)$$

$$y_{\text{ego}}(t) = \left(-\frac{1}{2}a(t-t_b)^2 + v_{\text{ego}}(t_b)(t-t_b) \right) \sin(\psi_{\text{ego}}(t_b)) + y_{\text{ego}}(t_b), \quad (6.23)$$

$$v_{\text{ego}}(t) = -a(t-t_b) + v_{\text{ego}}(t_b), \quad (6.24)$$

$$\psi_{\text{ego}}(t) = \psi_{\text{ego}}(t_b) \quad (6.25)$$

assuming $v_{\text{ego}}(t) \geq 0$ for $t \geq t_b$. With $x_{\text{ego}}(t_b) = v_{\text{ego}}(t_0)(t_b - t_0) + x_{\text{ego}}(t_0)$, $y_{\text{ego}}(t_b) = y_{\text{ego}}(t_0)$, $v_{\text{ego}}(t_b) = v_{\text{ego}}(t_0)$ and $\psi_{\text{ego}}(t_b) = 0$ resulting from substituting $t = t_b$ into the solution (6.18)–(6.21) of the differential equations (6.2)–(6.5) for the previous time interval $[t_0, t_b]$, it reads

$$\begin{aligned} x_{\text{ego}}(t) &= -\frac{1}{2}a(t-t_b)^2 + v_{\text{ego}}(t_0)(t-t_b) + v_{\text{ego}}(t_0)(t_b-t_0) + x_{\text{ego}}(t_0) \\ &= -\frac{1}{2}a(t-t_b)^2 + v_{\text{ego}}(t_0)(t-t_0) + x_{\text{ego}}(t_0), \end{aligned} \quad (6.26)$$

$$y_{\text{ego}}(t) = y_{\text{ego}}(t_0), \quad (6.27)$$

$$v_{\text{ego}}(t) = -a(t-t_b) + v_{\text{ego}}(t_0), \quad (6.28)$$

$$\psi_{\text{ego}}(t) = 0. \quad (6.29)$$

The solutions (6.18)–(6.21) and (6.26)–(6.29) of the differential equations (6.2)–(6.5) for the time intervals, where $t \leq t_b$ and $t \geq t_b$, respectively, can be combined to

$$x_{\text{ego}}(t) = \begin{cases} v_{\text{ego}}(t_0)(t-t_0) + x_{\text{ego}}(t_0), & t < t_b \\ -\frac{1}{2}a(t-t_b)^2 + v_{\text{ego}}(t_0)(t-t_0) + x_{\text{ego}}(t_0), & t \geq t_b \end{cases}, \quad (6.30)$$

$$y_{\text{ego}}(t) = y_{\text{ego}}(t_0), \quad (6.31)$$

$$v_{\text{ego}}(t) = \begin{cases} v_{\text{ego}}(t_0), & t < t_b \\ -a(t-t_b) + v_{\text{ego}}(t_0), & t \geq t_b \end{cases}, \quad (6.32)$$

$$\psi_{\text{ego}}(t) = 0. \quad (6.33)$$

The state of the considered dynamic system at time t is completely determined by the state variables of the involved vehicles at this time instant, namely, the coordinates

$x_{\text{ego}}(t)$ and $y_{\text{ego}}(t)$ of the center of gravity of the ego vehicle, its longitudinal velocity $v_{\text{ego}}(t)$ and its yaw angle $\psi_{\text{ego}}(t)$ as well as the coordinates $x_{\text{obj}}(t)$ and $y_{\text{obj}}(t)$ of the center of gravity of the object, its longitudinal velocity $v_{\text{obj}}(t)$ and its yaw angle $\psi_{\text{obj}}(t)$. Since only the relative motion of the ego vehicle and the object is relevant for the decision on whether to trigger an emergency brake intervention in this simple driving scenario, the number of state variables can be reduced by combining them. The distance

$$x(t) = x_{\text{obj},r}(t) - x_{\text{ego},f}(t) \quad (6.34)$$

between the ego vehicle and the object, and their relative velocity

$$v(t) = v_{\text{obj}}(t) - v_{\text{ego}}(t) \quad (6.35)$$

at time t sufficiently describe the state of the considered dynamic system at this time instant. They form the state vector

$$\mathbf{x}(t) = \begin{bmatrix} x(t) \\ v(t) \end{bmatrix} \quad (6.36)$$

at time t and are a combination of the state variables $x_{\text{ego}}(t)$, $y_{\text{ego}}(t)$, $v_{\text{ego}}(t)$, $\psi_{\text{ego}}(t)$, $x_{\text{obj}}(t)$, $y_{\text{obj}}(t)$, $v_{\text{obj}}(t)$ and $\psi_{\text{obj}}(t)$ of the involved vehicles, which is obvious for the relative velocity $v(t)$ and will become obvious for the distance $x(t)$ in the following.

Using the coordinate transformation (2.6) from coordinates (x_v, y_v) in the vehicle coordinate system of a vehicle with the state $[x(t), y(t), v(t), \psi(t)]^T$ at time t to coordinates (x_w, y_w) in the world coordinate system, the coordinates $(x_{v,\text{ego}}, y_{v,\text{ego}}) = (\frac{1}{2}l_{\text{ego}}, 0)$ of the middle point on the front part of the contour of the ego vehicle with the length l_{ego} in the vehicle coordinate system of the ego vehicle with the state $[x_{\text{ego}}(t), y_{\text{ego}}(t), v_{\text{ego}}(t), \psi_{\text{ego}}(t)]^T$ at time t and the coordinates $(x_{v,\text{obj}}, y_{v,\text{obj}}) = (-\frac{1}{2}l_{\text{obj}}, 0)$ of the middle point on the rear part of the contour of the object with the length l_{obj} in the vehicle coordinate system of the object with the state $[x_{\text{obj}}(t), y_{\text{obj}}(t), v_{\text{obj}}(t), \psi_{\text{obj}}(t)]^T$ at time t transform to the following coordinates $(x_{\text{ego},f}(t), y_{\text{ego},f}(t))$ and $(x_{\text{obj},r}(t), y_{\text{obj},r}(t))$ in the world coordinate system, respectively:

$$\begin{bmatrix} x_{\text{ego},f}(t) \\ y_{\text{ego},f}(t) \end{bmatrix} = \begin{bmatrix} \cos(\psi_{\text{ego}}(t)) & -\sin(\psi_{\text{ego}}(t)) \\ \sin(\psi_{\text{ego}}(t)) & \cos(\psi_{\text{ego}}(t)) \end{bmatrix} \begin{bmatrix} \frac{1}{2}l_{\text{ego}} \\ 0 \end{bmatrix} + \begin{bmatrix} x_{\text{ego}}(t) \\ y_{\text{ego}}(t) \end{bmatrix}, \quad (6.37)$$

$$\begin{bmatrix} x_{\text{obj},r}(t) \\ y_{\text{obj},r}(t) \end{bmatrix} = \begin{bmatrix} \cos(\psi_{\text{obj}}(t)) & -\sin(\psi_{\text{obj}}(t)) \\ \sin(\psi_{\text{obj}}(t)) & \cos(\psi_{\text{obj}}(t)) \end{bmatrix} \begin{bmatrix} -\frac{1}{2}l_{\text{obj}} \\ 0 \end{bmatrix} + \begin{bmatrix} x_{\text{obj}}(t) \\ y_{\text{obj}}(t) \end{bmatrix}. \quad (6.38)$$

So, the position of the front of the ego vehicle with respect to the x_w -axis of the world coordinate system reads

$$x_{\text{ego,f}}(t) = \frac{1}{2}l_{\text{ego}} \cos(\psi_{\text{ego}}(t)) + x_{\text{ego}}(t) \quad (6.39)$$

and the position of the rear of the object with respect to this axis

$$x_{\text{obj,r}}(t) = -\frac{1}{2}l_{\text{obj}} \cos(\psi_{\text{obj}}(t)) + x_{\text{obj}}(t). \quad (6.40)$$

Substituting these expressions into (6.34), yields the expression

$$x(t) = x_{\text{obj}}(t) - x_{\text{ego}}(t) - \frac{1}{2}(l_{\text{ego}} \cos(\psi_{\text{ego}}(t)) + l_{\text{obj}} \cos(\psi_{\text{obj}}(t))) \quad (6.41)$$

for the distance between the ego vehicle and the object at time t . It can be seen that the distance $x(t)$ between the ego vehicle and the object is a combination of their state variables $x_{\text{ego}}(t)$, $y_{\text{ego}}(t)$, $v_{\text{ego}}(t)$, $\psi_{\text{ego}}(t)$, $x_{\text{obj}}(t)$, $y_{\text{obj}}(t)$, $v_{\text{obj}}(t)$ and $\psi_{\text{obj}}(t)$ as their relative velocity $v(t)$ in (6.35). Therefore, they can be computed easily from these state variables after obtaining them from the numerical solution of the differential equations (6.2)–(6.5) and (6.6)–(6.9). In this special case, where the closed-form solutions (6.30)–(6.33) and (6.14)–(6.17) of these differential equations exist, the distance $x(t)$ between the ego vehicle and the object, and their relative velocity $v(t)$ can also be expressed in closed form by plugging these closed-form solutions into (6.41) and (6.35):

$$x(t) = \begin{cases} (v_{\text{obj}}(t_0) - v_{\text{ego}}(t_0))(t - t_0) \\ + x_{\text{obj}}(t_0) - x_{\text{ego}}(t_0) - \frac{1}{2}(l_{\text{ego}} + l_{\text{obj}}), & t < t_b \\ \frac{1}{2}a(t - t_b)^2 + (v_{\text{obj}}(t_0) - v_{\text{ego}}(t_0))(t - t_0) \\ + x_{\text{obj}}(t_0) - x_{\text{ego}}(t_0) - \frac{1}{2}(l_{\text{ego}} + l_{\text{obj}}), & t \geq t_b \end{cases} \quad (6.42)$$

$$= \begin{cases} v_0(t - t_0) + x_0, & t < t_b \\ \frac{1}{2}a(t - t_b)^2 + v_0(t - t_0) + x_0, & t \geq t_b \end{cases}$$

$$v(t) = \begin{cases} v_{\text{obj}}(t_0) - v_{\text{ego}}(t_0), & t < t_b \\ a(t - t_b) + v_{\text{obj}}(t_0) - v_{\text{ego}}(t_0), & t \geq t_b \end{cases} = \begin{cases} v_0, & t < t_b \\ a(t - t_b) + v_0, & t \geq t_b \end{cases}. \quad (6.43)$$

Here,

$$x_0 = x(t_0) = x_{\text{obj}}(t_0) - x_{\text{ego}}(t_0) - \frac{1}{2}(l_{\text{ego}} + l_{\text{obj}}) \quad (6.44)$$

is the initial distance between the ego vehicle and the object at the time instant t_0 when the considered driving scenario starts according to (6.41) with $\psi_{\text{ego}}(t_0) = \psi_{\text{obj}}(t_0) = 0$ and

$$v_0 = v(t_0) = v_{\text{obj}}(t_0) - v_{\text{ego}}(t_0) \quad (6.45)$$

is their initial relative velocity at this time instant according to (6.35).

The initial distance $x_0 = x_{\text{obj},r}(t_0) - x_{\text{ego},f}(t_0) > 0$ between the ego vehicle and the object, and their initial relative velocity $v_0 = v_{\text{obj}}(t_0) - v_{\text{ego}}(t_0) < 0$ forming the initial state vector

$$\mathbf{x}_0 = \begin{bmatrix} x_0 \\ v_0 \end{bmatrix} = \begin{bmatrix} x(t_0) \\ v(t_0) \end{bmatrix} = \mathbf{x}(t_0) \quad (6.46)$$

at the beginning of the considered driving scenario together with the time instant t_0 at which their driving maneuvers not initiated by the automated vehicular safety system, i.e., the AEB system, start, their longitudinal and lateral accelerations $a_{\text{lon,ego}}(t_0) = 0$, $a_{\text{lat,ego}}(t_0) = 0$, $a_{\text{lon,obj}}(t_0) = 0$ and $a_{\text{lat,obj}}(t_0) = 0$ during these driving maneuvers, their turn radii $r_{\text{min,ego}}$ and $r_{\text{min,obj}}$ as well as the coordinates $(x_{v,\text{ego}}, y_{v,\text{ego}}) = (\frac{1}{2}l_{\text{ego}}, 0)$ of the middle point on the front part of the contour of the ego vehicle with the length l_{ego} in its vehicle coordinate system and $(x_{v,\text{obj}}, y_{v,\text{obj}}) = (-\frac{1}{2}l_{\text{obj}}, 0)$ of the middle point on the rear part of the contour of the object with the length l_{obj} in its vehicle coordinate system, which are the coordinates of the points sufficiently describing their contours in the vehicle coordinate systems, completely characterize the whole considered driving scenario. They are the $N_{\xi} = 13$ scenario parameters collected in the vector

$$\xi = \begin{bmatrix} x_0 \\ v_0 \\ t_0 \\ a_{\text{lon,ego}}(t_0) \\ a_{\text{lat,ego}}(t_0) \\ a_{\text{lon,obj}}(t_0) \\ a_{\text{lat,obj}}(t_0) \\ r_{\text{min,ego}} \\ r_{\text{min,obj}} \\ x_{v,\text{ego}} \\ y_{v,\text{ego}} \\ x_{v,\text{obj}} \\ y_{v,\text{obj}} \end{bmatrix} = \begin{bmatrix} x_0 \\ v_0 \\ t_0 \\ 0 \\ 0 \\ 0 \\ 0 \\ r_{\text{min,ego}} \\ r_{\text{min,obj}} \\ \frac{1}{2}l_{\text{ego}} \\ 0 \\ -\frac{1}{2}l_{\text{obj}} \\ 0 \end{bmatrix}. \quad (6.47)$$

So, the considered driving scenario can be varied by varying the initial distance x_0 between the ego vehicle and the object, their relative velocity v_0 , the time instant t_0 at which their driving maneuvers not initiated by the AEB system start, their turn radii $r_{\min, \text{ego}}$ and $r_{\min, \text{obj}}$, and their lengths l_{ego} and l_{obj} to obtain various driving scenarios, which can be seen as instances of the same basic driving scenario.

6.1.2 Stochastic Model of the Automatic Emergency Braking System

The general mathematical model of automated vehicular safety systems depicted in Figure 2.4, which consists of a stochastic model of the sensors including their measurement errors and a mathematical model of the automated vehicular safety function, also applies to the considered AEB system.

6.1.2.1 Stochastic Model of the Sensors of the Automatic Emergency Braking System

The sensors take measurements with the sampling rate f_s at the time instants $t_n = \frac{n}{f_s}$ with the discrete time index $n = 0, 1, \dots$ and deliver the measurements $\mathbf{y}[n]$ of the M quantities observed by the sensors at the time instant t_n based on the state $\mathbf{x}[n]$ of the dynamic system at this time instant under the influence of the E sensor measurement errors $\varepsilon[n]$ at this time instant as expressed in (2.8). In case of the considered AEB system, the state vector at the time instant t_n is given by

$$\mathbf{x}[n] = \mathbf{x}(t_n) = \begin{bmatrix} x(t_n) \\ v(t_n) \end{bmatrix} = \begin{bmatrix} x[n] \\ v[n] \end{bmatrix} \quad (6.48)$$

according to (6.36) and thus consists of the distance $x[n] = x(t_n)$ between the ego vehicle and the object, and their relative velocity $v[n] = v(t_n)$ at this time instant.

As in [44–46], the sensor measurement errors in the measured distance between the ego vehicle and the object at the time instants t_n are modeled by additive i.i.d. zero-mean Gaussian random variables $\varepsilon_x[n] \sim \mathcal{N}(0, \sigma_x^2)$ of standard deviation σ_x such that the measured distance at the time instant t_n reads

$$\hat{x}[n] = x[n] + \varepsilon_x[n]. \quad (6.49)$$

Analogously, the sensor measurement errors in the measured relative velocity of the ego vehicle and the object at the time instants t_n are modeled by additive i.i.d. zero-mean Gaussian random variables $\varepsilon_v[n] \sim \mathcal{N}(0, \sigma_v^2)$ of standard deviation σ_v such that the measured relative velocity at the time instant t_n reads

$$\hat{v}[n] = v[n] + \varepsilon_v[n]. \quad (6.50)$$

Therefore, the measurement vector

$$\mathbf{y}[n] = \begin{bmatrix} \hat{x}[n] \\ \hat{v}[n] \end{bmatrix} \quad (6.51)$$

at the time instant t_n , which consists of the $M = 2$ measurements $\hat{x}[n]$ and $\hat{v}[n]$ at this time instant, is the sum of the state vector $\mathbf{x}[n]$ at the time instant t_n , which consists of the $N = 2$ state variables $x[n]$ and $v[n]$ as stated in (6.48), and the error vector

$$\boldsymbol{\varepsilon}[n] = \begin{bmatrix} \varepsilon_x[n] \\ \varepsilon_v[n] \end{bmatrix} \quad (6.52)$$

at the time instant t_n , which consists of the $E = 2$ sensor measurement errors $\varepsilon_x[n]$ and $\varepsilon_v[n]$ at this time instant. For such a special case of directly measuring the $N = M$ state variables $\mathbf{x}[n]$ with $E = M$ additive measurement errors $\boldsymbol{\varepsilon}[n]$ at the time instant t_n , this has already been expressed in (2.9). The error vector $\boldsymbol{\varepsilon}[n]$ at the time instant t_n is Gaussian, i.e., $\boldsymbol{\varepsilon}[n] \sim \mathcal{N}(\boldsymbol{\mu}_n, \mathbf{C}_n)$, and has the pdf $f_{\boldsymbol{\varepsilon}[n]}(\boldsymbol{\varepsilon}[n])$ in (2.10) with the mean

$$\boldsymbol{\mu}_n = \mathbf{0} \quad (6.53)$$

and the covariance matrix

$$\mathbf{C}_n = \begin{bmatrix} \sigma_x^2 & 0 \\ 0 & \sigma_v^2 \end{bmatrix} \quad (6.54)$$

under the assumption that the sensor measurement error $\varepsilon_x[n]$ in the measured distance between the ego vehicle and the object, and the sensor measurement error $\varepsilon_v[n]$ in the measured relative velocity of the ego vehicle and the object at the time instant t_n are statistically independent.

In this stochastic model of the sensors, the standard deviations σ_x and σ_v of their measurement errors and their sampling rate f_s are the $N_\sigma = 3$ sensor parameters that determine the sensors and are collected in the vector

$$\boldsymbol{\sigma} = \begin{bmatrix} \sigma_x \\ \sigma_v \\ f_s \end{bmatrix}. \quad (6.55)$$

6.1.2.2 Mathematical Model of the Function of the Automatic Emergency Braking System

The function of the considered AEB system derives safety-relevant information from the measurements $\mathbf{y}[n]$ at the time instant t_n in order to interpret the current driving

situation, and decides on whether to intervene by triggering an emergency brake intervention for mitigating a dangerous driving situation using a decision rule. In general, such a decision rule for an automated vehicular safety system can be represented by a decision function $f(\cdot; \varphi)$ of the form shown in (2.18), which is parameterized by the parameter vector φ consisting of N_φ adjustable parameters $\varphi_i, i = 1, 2, \dots, N_\varphi$.

In the following, three exemplary decision rules, which are represented by the decision functions $f_{\text{TTC}}(\cdot; \varphi)$, $f_{\text{adv. TTC}}(\cdot; \varphi)$ and $f_{\text{BTN}}(\cdot; \varphi)$ of this form and can be used in the considered AEB system for deciding on whether to trigger an emergency brake intervention, are described in detail. They have $N_\varphi = 1$ adjustable parameter $\varphi = \varphi \in \mathbb{R}$ and are based on typical criticality measures like the TTC and brake-threat-number (BTN) but can easily be extended or replaced by others, which might also have more parameters. As long as the used decision rule is not fulfilled, i.e., $f_c(\mathbf{y}[n]; \varphi) = 0, c \in \{\text{TTC}, \text{adv. TTC}, \text{BTN}\}$, the function does not trigger the emergency brake intervention, and, as soon as the decision rule is fulfilled for the measurements $\mathbf{y}[n]$ at a time instant t_n , i.e., $f_c(\mathbf{y}[n]; \varphi) = 1$, the function triggers the emergency brake intervention. The smallest n for which $f_c(\mathbf{y}[n]; \varphi) = 1$ is the discrete time index

$$n_b = \min_{n \in \mathbb{N}_0} n \quad \text{s.t.} \quad f_c(\mathbf{y}[n]; \varphi) = 1 \quad (6.56)$$

that corresponds to the time instant

$$t_b = t_{n_b} = \frac{n_b}{f_s} \quad (6.57)$$

at which the measurements $\mathbf{y}[n_b]$ leading to triggering the emergency brake intervention are made and also to the time instant at which the triggered emergency brake intervention starts under the simplifying assumption that it instantly starts without any delay after making these measurements.

TTC-Based Decision Rule: The first one of the three exemplary decision rules is represented by the decision function

$$f_{\text{TTC}}(\mathbf{y}[n]; \varphi) = \begin{cases} 1, & \hat{x}[n] \leq -\varphi \hat{v}[n] \\ 0, & \text{otherwise} \end{cases}. \quad (6.58)$$

So, the function decides for an intervention based on the sensor measurements $\mathbf{y}[n]$ at the time instant t_n if they fulfill the condition

$$\hat{x}[n] \leq -\varphi \hat{v}[n]. \quad (6.59)$$

If $\hat{v} [n] < 0$, this condition for triggering an emergency brake intervention based on the sensor measurements $\mathbf{y} [n]$ at the time instant t_n is equivalent to the condition $t_{\text{TTC}} [n] \leq \varphi$ for the TTC

$$t_{\text{TTC}} [n] = -\frac{\hat{x} [n]}{\hat{v} [n]} \quad (6.60)$$

at the time instant t_n , i.e., the time that remains until the ego vehicle and the object collide under the assumption that they have the distance $\hat{x} [n]$ at the time instant t_n and move with constant relative velocity $\hat{v} [n]$ from the time instant t_n on [27]. Therefore, this decision rule is called TTC-based decision rule.

Advanced TTC-Based Decision Rule: Using the second one of the three exemplary decision rules represented by the decision function

$$f_{\text{adv. TTC}} (\mathbf{y} [n]; \varphi) = \begin{cases} 1, & \hat{x} [n] - \frac{\hat{v}^2 [n]}{2a} \leq -\varphi \hat{v} [n] \\ 0, & \text{otherwise} \end{cases}, \quad (6.61)$$

the function decides for an intervention based on the sensor measurements $\mathbf{y} [n]$ at the time instant t_n if they fulfill the condition

$$\hat{x} [n] - \frac{\hat{v}^2 [n]}{2a} \leq -\varphi \hat{v} [n]. \quad (6.62)$$

This condition for triggering an emergency brake intervention based on the sensor measurements $\mathbf{y} [n]$ at the time instant t_n is equivalent to the condition $t_{\text{TTC}} [n] - t_{\text{TTC}}^* [n] \leq \varphi$ for the difference between the TTC $t_{\text{TTC}} [n]$ and the critical TTC

$$t_{\text{TTC}}^* [n] = -\frac{x^* [n]}{\hat{v} [n]} = -\frac{\hat{v} [n]}{2a} \quad (6.63)$$

at the time instant t_n corresponding to the critical distance

$$x^* [n] = \frac{\hat{v}^2 [n]}{2a} \quad (6.64)$$

at the time instant t_n if $\hat{v} [n] < 0$. This critical distance $x^* [n]$ is the distance between the ego vehicle and the object with relative velocity $\hat{v} [n]$ that is required for just avoiding the collision by the emergency brake intervention with a constant deceleration a such that their distance is 0 when their relative velocity vanishes [45]. Since this decision rule takes the critical distance $x^* [n]$ and the corresponding critical TTC $t_{\text{TTC}}^* [n]$ into account in contrast to the TTC-based decision rule represented by (6.58), it is called advanced TTC-based decision rule.

BTN-Based Decision Rule: The third and last one of the three exemplary decision rules is represented by the decision function

$$f_{\text{BTN}}(\mathbf{y}[n]; \varphi) = \begin{cases} 1, & \hat{x}[n] \leq \frac{\hat{v}^2[n]}{2\varphi} \\ 0, & \text{otherwise} \end{cases}. \quad (6.65)$$

So, the function decides for an intervention based on the sensor measurements $\mathbf{y}[n]$ at the time instant t_n if they fulfill the condition

$$\hat{x}[n] \leq \frac{\hat{v}^2[n]}{2\varphi}. \quad (6.66)$$

If $\hat{x}[n] > 0$, this condition for triggering an emergency brake intervention based on the sensor measurements $\mathbf{y}[n]$ at the time instant t_n is equivalent to the condition $a_{\text{BTN}}[n] \geq \varphi$ for the BTN

$$a_{\text{BTN}}[n] = \frac{\hat{v}^2[n]}{2\hat{x}[n]} \quad (6.67)$$

at the time instant t_n , which is the constant deceleration required for just avoiding the collision under the assumption that the ego vehicle and the object have the distance $\hat{x}[n]$ and the relative velocity $\hat{v}[n]$ when the emergency brake intervention is triggered [28]. Therefore, this decision rule is called BTN-based decision rule.

6.2 Robust Function and Sensor Design for the Automatic Emergency Braking System

The proposed methodology for the robust function and sensor design described in the two previous chapters allows to systematically design both functions and sensors of automated vehicular safety systems in general and the considered AEB system in particular such that the customer requirements are fulfilled in a robust manner despite unavoidable sensor measurement errors. The function and the sensors can be designed by solving the optimization problems (4.1), (4.9) and (4.11) formulated in Chapter 4 for the robust function design, sensor design as well as joint function and sensor design, respectively, based on closed-form expressions for the probabilistic quality measure Q or solely based on simulations of the automated vehicular safety system under design as described in Chapter 5. For the design of the considered AEB system, the following quality measure Q , which measures to what extent the function meets the customer requirements in a robust manner despite the unavoidable sensor measurement errors, can be used.

The customer is satisfied with the AEB system applied in the driving scenario illustrated in Figure 6.1 if the final distance x_{end} between the ego vehicle and the

object after an emergency brake intervention when their relative velocity vanishes is neither too small nor too large. In other words, this final distance x_{end} has to lie in an acceptance interval $[x_{\text{min}}, x_{\text{max}}]$ from the minimal tolerable final distance x_{min} to the maximal tolerable final distance x_{max} , which is visualized in Figure 6.1 by the violet area and can be chosen in a user-specific way. Hence, the final distance x_{end} is an example for one of the customer satisfaction properties q_i , $i = 1, 2, \dots, N_q$, which have to lie in certain acceptance intervals $[q_{L,i}, q_{U,i}]$ such that the intervention by an automated vehicular safety system is acceptable and the customer is satisfied with the system, and the acceptance interval $[x_{\text{min}}, x_{\text{max}}]$ for the final distance x_{end} with the lower bound x_{min} and the upper bound x_{max} corresponds to the acceptance interval $[q_{L,i}, q_{U,i}]$ for this customer satisfaction property q_i with the lower bound $q_{L,i}$ and the upper bound $q_{U,i}$.

In general, the customer satisfaction properties q_i collected in the customer satisfaction vector $\mathbf{q} = [q_1, q_2, \dots, q_{N_q}]^T = \mathbf{q}(\boldsymbol{\sigma}, \boldsymbol{\varepsilon}, f, \boldsymbol{\varphi}, \boldsymbol{\xi})$ are subject to the random sensor measurement errors $\boldsymbol{\varepsilon}[n]$ at the $n_{\text{end}} + 1$ time instants t_n , $n = 0, 1, \dots, n_{\text{end}}$, in the considered time interval collected in the vector $\boldsymbol{\varepsilon}$ given by (4.21) according to (4.22). This is also the case for the final distance x_{end} as an example for such a customer satisfaction property q_i . Consequently, it is a random variable as well and might lie inside or outside the acceptance interval $[x_{\text{min}}, x_{\text{max}}]$ such that the specification

$$x_{\text{min}} \leq x_{\text{end}} \leq x_{\text{max}} \quad (6.68)$$

for the customer satisfaction defined by this acceptance interval is fulfilled or violated as the customer satisfaction properties q_i are random variables and might lie inside or outside the acceptance intervals $[q_{L,i}, q_{U,i}]$, $i = 1, 2, \dots, N_q$, in general such that the specifications $q_{L,i} \leq q_i \leq q_{U,i}$, $i = 1, 2, \dots, N_q$, for the customer satisfaction defined by these acceptance intervals are fulfilled or violated.

The quality measure Q , which measures to what extent the function meets the customer requirements in a robust manner despite the unavoidable sensor measurement errors, is defined as the worst-case probability $P_{\text{WC}}(\mathbf{q} \in \mathcal{A}_q)$ of fulfilling the specifications for the customer satisfaction, i.e., the minimum of the probability $P(\mathbf{q} \in \mathcal{A}_q)$ that all specifications $q_{L,i} \leq q_i \leq q_{U,i}$, $i = 1, 2, \dots, N_q$, for the customer satisfaction are fulfilled in all considered driving scenarios $\boldsymbol{\xi}$ from the scenario set \mathcal{X} , in (4.33). Assuming that the final distance x_{end} is the only considered customer satisfaction property, i.e., $N_q = 1$ and $\mathbf{q} = q_1 = x_{\text{end}}$, the quality measure Q is the minimum of the probability $P(x_{\text{min}} \leq x_{\text{end}} \leq x_{\text{max}})$ that the final distance x_{end} fulfills the specification $x_{\text{min}} \leq x_{\text{end}} \leq x_{\text{max}}$ for the customer satisfaction in all considered driving scenarios $\boldsymbol{\xi}$

from the scenario set \mathcal{X} :

$$Q = \min_{\xi \in \mathcal{X}} P(x_{\min} \leq x_{\text{end}} \leq x_{\max}). \quad (6.69)$$

With this quality measure Q , the constraint of the optimization problems (4.9) and (4.11) for the sensor design as well as the joint function and sensor design, respectively, reads

$$\min_{\xi \in \mathcal{X}} P(x_{\min} \leq x_{\text{end}} \leq x_{\max}) \geq P_{\min}, \quad (6.70)$$

where the required minimum worst-case probability P_{\min} of fulfilling the specification $x_{\min} \leq x_{\text{end}} \leq x_{\max}$ for the customer satisfaction is the required minimum quality level Q_{\min} according to (4.39).

Closed-form expressions for the probability $P(x_{\min} \leq x_{\text{end}} \leq x_{\max})$ of fulfilling the specification for the customer satisfaction can be derived in the following special cases, where the TTC-based decision rule is used or the relative velocity of the ego vehicle and the object is measured without errors.

6.2.1 Probability of Fulfilling the Specification for the Customer Satisfaction in Case of the TTC-Based Decision Rule

The final distance x_{end} between the ego vehicle and the object after the emergency brake intervention when their relative velocity $v(t)$ vanishes is the distance $x(t_{\text{end}})$ at the time instant $t_{\text{end}} > t_b$ at which $v(t_{\text{end}}) = 0$. From (6.43), it follows that this time instant at which $v(t_{\text{end}}) = 0$ is

$$t_{\text{end}} = t_b - \frac{v_0}{a} \quad (6.71)$$

and, from (6.42), that the distance between the ego vehicle and the object at this time instant, their final distance, is

$$\begin{aligned} x_{\text{end}} &= x(t_{\text{end}}) = x\left(t_b - \frac{v_0}{a}\right) = \frac{1}{2}a\left(-\frac{v_0}{a}\right)^2 + v_0\left(t_b - t_0 - \frac{v_0}{a}\right) + x_0 \\ &= x_0 + v_0(t_b - t_0) - \frac{v_0^2}{2a}. \end{aligned} \quad (6.72)$$

Since $t_0 = 0$ according to (2.7) and the time instant t_b at which the emergency brake intervention is triggered is given by (6.57), the final distance can be rewritten as

$$x_{\text{end}} = x_0 + \frac{n_b v_0}{f_s} - \frac{v_0^2}{2a}. \quad (6.73)$$

Hence, this final distance x_{end} fulfills the specification $x_{\text{min}} \leq x_{\text{end}} \leq x_{\text{max}}$ for the customer satisfaction iff

$$x_{\text{min}} - x_0 + \frac{v_0^2}{2a} \leq \frac{n_b v_0}{f_s} \leq x_{\text{max}} - x_0 + \frac{v_0^2}{2a} \quad (6.74)$$

or, equivalently,

$$\frac{f_s}{v_0} \left(x_{\text{max}} - x_0 + \frac{v_0^2}{2a} \right) \leq n_b \leq \frac{f_s}{v_0} \left(x_{\text{min}} - x_0 + \frac{v_0^2}{2a} \right). \quad (6.75)$$

As the discrete time index n_b of the time instant $t_b = n_b/f_s$ at which the emergency brake intervention is triggered is a non-negative integer, the specification $x_{\text{min}} \leq x_{\text{end}} \leq x_{\text{max}}$ for the customer satisfaction is equivalent to the specification

$$n_{\text{min}} \leq n_b \leq n_{\text{max}} \quad (6.76)$$

for this discrete time index n_b with the lower bound

$$n_{\text{min}} = \max \left(0, \left\lceil \frac{f_s}{v_0} \left(x_{\text{max}} - x_0 + \frac{v_0^2}{2a} \right) \right\rceil \right) \quad (6.77)$$

and the upper bound

$$n_{\text{max}} = \left\lfloor \frac{f_s}{v_0} \left(x_{\text{min}} - x_0 + \frac{v_0^2}{2a} \right) \right\rfloor. \quad (6.78)$$

Therefore, the probability $P(x_{\text{min}} \leq x_{\text{end}} \leq x_{\text{max}})$ of fulfilling the specification $x_{\text{min}} \leq x_{\text{end}} \leq x_{\text{max}}$ for the customer satisfaction is identical to the probability $P(n_{\text{min}} \leq n_b \leq n_{\text{max}})$ of fulfilling the specification $n_{\text{min}} \leq n_b \leq n_{\text{max}}$ for the discrete time index n_b of the time instant t_b at which the emergency brake intervention is triggered:

$$P(x_{\text{min}} \leq x_{\text{end}} \leq x_{\text{max}}) = P(n_{\text{min}} \leq n_b \leq n_{\text{max}}). \quad (6.79)$$

As the discrete time indices n_b that fulfill the specification $n_{\text{min}} \leq n_b \leq n_{\text{max}}$ are the discrete time indices $n_{\text{min}}, n_{\text{min}} + 1, \dots, n_{\text{max}}$, the probability $P(n_{\text{min}} \leq n_b \leq n_{\text{max}})$ of fulfilling the specification $n_{\text{min}} \leq n_b \leq n_{\text{max}}$ is equivalent to the probability $P(n_b \in \{n_{\text{min}}, n_{\text{min}} + 1, \dots, n_{\text{max}}\})$ that the discrete time index n_b of the time instant t_b at which the emergency brake intervention is triggered is one of those discrete time indices and thus the sum of all probabilities $P(n_b = n)$ that it is one of those discrete time indices $n'_b = n_{\text{min}}, n_{\text{min}} + 1, \dots, n_{\text{max}}$:

$$\begin{aligned} P(n_{\text{min}} \leq n_b \leq n_{\text{max}}) &= P(n_b \in \{n_{\text{min}}, n_{\text{min}} + 1, \dots, n_{\text{max}}\}) \\ &= \sum_{n'_b=n_{\text{min}}}^{n_{\text{max}}} P(n_b = n'_b). \end{aligned} \quad (6.80)$$

Due to the last two equations, the probability of fulfilling the specification $x_{\min} \leq x_{\text{end}} \leq x_{\max}$ for the customer satisfaction reads

$$P(x_{\min} \leq x_{\text{end}} \leq x_{\max}) = \sum_{n'_b = n_{\min}}^{n_{\max}} P(n_b = n'_b). \quad (6.81)$$

In order to find an expression for the probability $P(n_b = n'_b)$ that the discrete time index n_b of the time instant t_b at which the emergency brake intervention is triggered is the discrete time index n'_b of the time instant $t_{n'_b}$, the condition (6.59) that has to be fulfilled for triggering an emergency brake intervention at a time instant t_n when using the TTC-based decision rule $f_{\text{TTC}}(\cdot; \varphi)$ in (6.58) is considered. With the expressions for the measured distance and relative velocity of the ego vehicle and the object in (6.49) and (6.50), respectively, this necessary and sufficient condition for $f_{\text{TTC}}(\mathbf{y}[n]; \varphi) = 1$ reads

$$x[n] + \varepsilon_x[n] \leq -\varphi(v[n] + \varepsilon_v[n]). \quad (6.82)$$

Consequently, the error region with intervention at the time instant t_n defined in (5.83) is given by

$$\begin{aligned} \mathcal{I}_{\varepsilon, n} &= \left\{ \varepsilon \in \mathbb{R}^{2(n_{\text{end}}+1)} : f_{\text{TTC}}(\mathbf{y}[n]; \varphi) = 1 \right\} \\ &= \left\{ \varepsilon \in \mathbb{R}^{2(n_{\text{end}}+1)} : x[n] + \varepsilon_x[n] \leq -\varphi(v[n] + \varepsilon_v[n]) \right\} \end{aligned} \quad (6.83)$$

and its complement, the error region without intervention at the time instant t_n defined in (5.84), by

$$\begin{aligned} \bar{\mathcal{I}}_{\varepsilon, n} &= \left\{ \varepsilon \in \mathbb{R}^{2(n_{\text{end}}+1)} : f_{\text{TTC}}(\mathbf{y}[n]; \varphi) = 0 \right\} \\ &= \left\{ \varepsilon \in \mathbb{R}^{2(n_{\text{end}}+1)} : x[n] + \varepsilon_x[n] > -\varphi(v[n] + \varepsilon_v[n]) \right\}. \end{aligned} \quad (6.84)$$

The discrete time index n_b of the time instant t_b at which the emergency brake intervention is triggered is the discrete time index n'_b of the time instant $t_{n'_b}$ iff the condition (6.82) for triggering an emergency brake intervention at a time instant t_n is fulfilled at the time instant $t_{n'_b}$, i.e., the sensor measurement errors ε lie in the error region $\mathcal{I}_{\varepsilon, n'_b}$ with intervention at this time instant $t_{n'_b}$, and not fulfilled at all time instants t_n , $n = 0, 1, \dots, n'_b - 1$, before the time instant $t_{n'_b}$, i.e., the sensor measurement errors ε lie in all error regions $\bar{\mathcal{I}}_{\varepsilon, n}$ without intervention at one of these time instants t_n . Hence, the probability $P(n_b = n'_b)$ that the discrete time index n_b of the time instant t_b at which the emergency brake intervention is triggered is the discrete time index n'_b of

the time instant $t_{n'_b}$ is identical to the probability $P\left(\varepsilon \in \bigcap_{n=0}^{n'_b-1} \bar{\mathcal{I}}_{\varepsilon,n} \cap \mathcal{I}_{\varepsilon,n'_b}\right)$ that the sensor measurement errors ε lie in the error regions $\bar{\mathcal{I}}_{\varepsilon,n}$ without intervention at the time instants $t_n, n = 0, 1, \dots, n'_b - 1$, and the error region $\mathcal{I}_{\varepsilon,n'_b}$ with intervention at the time instant $t_{n'_b}$:

$$P(n_b = n'_b) = P\left(\varepsilon \in \bigcap_{n=0}^{n'_b-1} \bar{\mathcal{I}}_{\varepsilon,n} \cap \mathcal{I}_{\varepsilon,n'_b}\right). \quad (6.85)$$

With the two disjoint sets $\mathbb{I}_1 = \{0, 1, \dots, n'_b - 1\}$ and $\mathbb{I}_2 = \{n'_b\}$, it follows from (B.6) that

$$\begin{aligned} P\left(\varepsilon \in \bigcap_{n=0}^{n'_b-1} \bar{\mathcal{I}}_{\varepsilon,n} \cap \mathcal{I}_{\varepsilon,n'_b}\right) &= P\left(\varepsilon \in \bigcap_{n \in \{0,1,\dots,n'_b-1\}} \bar{\mathcal{I}}_{\varepsilon,n} \cap \overline{\bigcap_{n \in \{n'_b\}} \bar{\mathcal{I}}_{\varepsilon,n}}\right) \\ &= P\left(\varepsilon \in \bigcap_{n \in \{0,1,\dots,n'_b-1\}} \bar{\mathcal{I}}_{\varepsilon,n}\right) P\left(\varepsilon \in \overline{\bigcap_{n \in \{n'_b\}} \bar{\mathcal{I}}_{\varepsilon,n}}\right) \\ &= P\left(\varepsilon \in \bigcap_{n=0}^{n'_b-1} \bar{\mathcal{I}}_{\varepsilon,n}\right) P\left(\varepsilon \in \mathcal{I}_{\varepsilon,n'_b}\right) \end{aligned} \quad (6.86)$$

and, with the set $\mathbb{I} = \{0, 1, \dots, n'_b - 1\}$, from (B.2) that

$$\begin{aligned} P\left(\varepsilon \in \bigcap_{n=0}^{n'_b-1} \bar{\mathcal{I}}_{\varepsilon,n}\right) &= P\left(\varepsilon \in \bigcap_{n \in \{0,1,\dots,n'_b-1\}} \bar{\mathcal{I}}_{\varepsilon,n}\right) \\ &= \prod_{n \in \{0,1,\dots,n'_b-1\}} P(\varepsilon \in \bar{\mathcal{I}}_{\varepsilon,n}) = \prod_{n=0}^{n'_b-1} P(\varepsilon \in \bar{\mathcal{I}}_{\varepsilon,n}). \end{aligned} \quad (6.87)$$

Substituting the last two equations into (6.85) leads to the factorization

$$\begin{aligned} P(n_b = n'_b) &= P\left(\varepsilon \in \mathcal{I}_{\varepsilon,n'_b}\right) \prod_{n=0}^{n'_b-1} P(\varepsilon \in \bar{\mathcal{I}}_{\varepsilon,n}) \\ &= P\left(\varepsilon \in \mathcal{I}_{\varepsilon,n'_b}\right) \prod_{n=0}^{n'_b-1} (1 - P(\varepsilon \in \mathcal{I}_{\varepsilon,n})) \end{aligned} \quad (6.88)$$

of the probability $P(n_b = n'_b)$ that the discrete time index n_b of the time instant t_b at which the emergency brake intervention is triggered is the discrete time index n'_b of

the time instant t_{n_b} . According to (6.83), the probability $P(\varepsilon \in \mathcal{I}_{\varepsilon,n})$ that the sensor measurement errors ε lie in the error region $\mathcal{I}_{\varepsilon,n}$ with intervention at the time instant t_n is equivalent to the probability that the sensor measurement errors ε fulfill the condition (6.82) for triggering an emergency brake intervention at the time instant t_n :

$$P(\varepsilon \in \mathcal{I}_{\varepsilon,n}) = P(x[n] + \varepsilon_x[n] \leq -\varphi(v[n] + \varepsilon_v[n])). \quad (6.89)$$

For time instants $t_n = \frac{n}{f_s} \leq \frac{n_b}{f_s} = t_b$ up to the time instant t_b at which the emergency brake intervention is triggered, i.e., $n \leq n_b$, it follows from (6.42) and (6.43) that the state vector at the time instant t_n from (6.48) is given by

$$\mathbf{x}[n] = \begin{bmatrix} x[n] \\ v[n] \end{bmatrix} = \begin{bmatrix} x(t_n) \\ v(t_n) \end{bmatrix} = \begin{bmatrix} v_0(t_n - t_0) + x_0 \\ v_0 \end{bmatrix} = \begin{bmatrix} x_0 + \frac{nv_0}{f_s} \\ v_0 \end{bmatrix} \quad (6.90)$$

such that the condition (6.82) that has to be fulfilled for triggering an emergency brake intervention at the time instant t_n when using the TTC-based decision rule $f_{\text{TTC}}(\cdot; \varphi)$ becomes

$$x_0 + \frac{nv_0}{f_s} + \varepsilon_x[n] \leq -\varphi(v_0 + \varepsilon_v[n]). \quad (6.91)$$

It can be rewritten to

$$\varepsilon_x[n] + \varphi\varepsilon_v[n] \leq -x_0 - \left(\frac{n}{f_s} + \varphi\right)v_0. \quad (6.92)$$

As a consequence, the probability that this condition is fulfilled is identical to the probability that the sensor measurement errors ε fulfill the condition (6.82) for triggering an emergency brake intervention at the time instant t_n and thus to the probability $P(\varepsilon \in \mathcal{I}_{\varepsilon,n})$ that they lie in the error region $\mathcal{I}_{\varepsilon,n}$ with intervention at the time instant t_n according to (6.89):

$$P(\varepsilon \in \mathcal{I}_{\varepsilon,n}) = P\left(\varepsilon_x[n] + \varphi\varepsilon_v[n] \leq -x_0 - \left(\frac{n}{f_s} + \varphi\right)v_0\right). \quad (6.93)$$

Since the sensor measurement errors $\varepsilon_x[n]$ and $\varepsilon_v[n]$ are Gaussian with zero mean and the variances σ_x^2 and σ_v^2 , respectively, and statistically independent, their linear combination $\varepsilon_x[n] + \varphi\varepsilon_v[n]$ is Gaussian as well with the mean

$$\mathbb{E}[\varepsilon_x[n] + \varphi\varepsilon_v[n]] = \underbrace{\mathbb{E}[\varepsilon_x[n]]}_{=0} + \varphi \underbrace{\mathbb{E}[\varepsilon_v[n]]}_{=0} = 0 \quad (6.94)$$

and the variance

$$\text{Var}[\varepsilon_x[n] + \varphi\varepsilon_v[n]] = \underbrace{\text{Var}[\varepsilon_x[n]]}_{=\sigma_x^2} + \varphi^2 \underbrace{\text{Var}[\varepsilon_v[n]]}_{=\sigma_v^2} = \sigma_x^2 + \varphi^2\sigma_v^2, \quad (6.95)$$

i.e., $\varepsilon_x [n] + \varphi \varepsilon_v [n] \sim \mathcal{N} (0, \sigma_x^2 + \varphi^2 \sigma_v^2)$. Therefore, the associated standardized random variable

$$\frac{\varepsilon_x [n] + \varphi \varepsilon_v [n] - \mathbb{E} [\varepsilon_x [n] + \varphi \varepsilon_v [n]]}{\sqrt{\text{Var} [\varepsilon_x [n] + \varphi \varepsilon_v [n]]}} = \frac{\varepsilon_x [n] + \varphi \varepsilon_v [n]}{\sqrt{\sigma_x^2 + \varphi^2 \sigma_v^2}} \quad (6.96)$$

is Gaussian with zero mean and unit variance, i.e., it follows the standard normal distribution $\mathcal{N} (0, 1)$, and the probability $P (\varepsilon \in \mathcal{I}_{\varepsilon, n})$ that the sensor measurement errors ε lie in the error region $\mathcal{I}_{\varepsilon, n}$ with intervention at the time instant t_n and fulfill the condition (6.92) for triggering an emergency brake intervention at the time instant t_n in (6.93) can be expressed as

$$\begin{aligned} P (\varepsilon \in \mathcal{I}_{\varepsilon, n}) &= P \left(\frac{\varepsilon_x [n] + \varphi \varepsilon_v [n]}{\sqrt{\sigma_x^2 + \varphi^2 \sigma_v^2}} \leq -\frac{x_0 + (n/f_s + \varphi) v_0}{\sqrt{\sigma_x^2 + \varphi^2 \sigma_v^2}} \right) \\ &= \Phi \left(-\frac{x_0 + (n/f_s + \varphi) v_0}{\sqrt{\sigma_x^2 + \varphi^2 \sigma_v^2}} \right). \end{aligned} \quad (6.97)$$

Hence, the probability $P (n_b = n'_b)$ that the discrete time index n_b of the time instant t_b at which the emergency brake intervention is triggered is the discrete time index n'_b of the time instant $t_{n'_b}$ from (6.88) reads

$$\begin{aligned} P (n_b = n'_b) &= \Phi \left(-\frac{x_0 + (n'_b/f_s + \varphi) v_0}{\sqrt{\sigma_x^2 + \varphi^2 \sigma_v^2}} \right) \prod_{n=0}^{n'_b-1} \left(1 - \Phi \left(-\frac{x_0 + (n/f_s + \varphi) v_0}{\sqrt{\sigma_x^2 + \varphi^2 \sigma_v^2}} \right) \right). \end{aligned} \quad (6.98)$$

Substituting this equation into (6.81) finally yields the expression

$$\begin{aligned} P (x_{\min} \leq x_{\text{end}} \leq x_{\max}) &= \sum_{n'_b=n_{\min}}^{n_{\max}} \Phi \left(-\frac{x_0 + (n'_b/f_s + \varphi) v_0}{\sqrt{\sigma_x^2 + \varphi^2 \sigma_v^2}} \right) \prod_{n=0}^{n'_b-1} \left(1 - \Phi \left(-\frac{x_0 + (n/f_s + \varphi) v_0}{\sqrt{\sigma_x^2 + \varphi^2 \sigma_v^2}} \right) \right) \end{aligned} \quad (6.99)$$

for the probability of fulfilling the specification $x_{\min} \leq x_{\text{end}} \leq x_{\max}$ for the customer satisfaction, where n_{\min} and n_{\max} are given by (6.77) and (6.78).

6.2.2 Probability of Fulfilling the Specification for the Customer Satisfaction in Case of Error-Free Relative Velocity Measurements

If the relative velocity $v [n]$ of the ego vehicle and the object at the time instant t_n is measured without error, the sensor measurement error $\varepsilon_v [n]$ in the measured relative

velocity $\hat{v}[n]$ at this time instant t_n is zero, i.e., the standard deviation σ_v of this zero-mean Gaussian random variable $\varepsilon_v[n]$ is zero. In this case, where $\sigma_v = 0$, the expression for the probability $P(\boldsymbol{\varepsilon} \in \mathcal{I}_{\boldsymbol{\varepsilon},n})$ that the sensor measurement errors $\boldsymbol{\varepsilon}$ lie in the error region $\mathcal{I}_{\boldsymbol{\varepsilon},n}$ with intervention at the time instant t_n and fulfill the condition for triggering an emergency brake intervention at the time instant t_n when using the TTC-based decision rule $f_{\text{TTC}}(\cdot; \varphi)$ in (6.97) simplifies to

$$P(\boldsymbol{\varepsilon} \in \mathcal{I}_{\boldsymbol{\varepsilon},n}) = \Phi\left(-\frac{x_0 + (n/f_s + \varphi)v_0}{\sigma_x}\right). \quad (6.100)$$

Furthermore, due to $\varepsilon_v[n] = 0$, the expressions for the measured distance $\hat{x}[n]$ and relative velocity $\hat{v}[n]$ of the ego vehicle and the object in (6.49) and (6.50) simplify to

$$\hat{x}[n] = x[n] + \varepsilon_x[n], \quad (6.101)$$

$$\hat{v}[n] = v[n]. \quad (6.102)$$

With these expressions, the necessary and sufficient condition (6.62) for $f_{\text{adv. TTC}}(\mathbf{y}[n]; \varphi) = 1$, i.e., triggering an emergency brake intervention at a time instant t_n when using the advanced TTC-based decision rule $f_{\text{adv. TTC}}(\cdot; \varphi)$ in (6.61), reads

$$x[n] + \varepsilon_x[n] - \frac{v^2[n]}{2a} \leq -\varphi v[n] \quad (6.103)$$

and the necessary and sufficient condition (6.66) for $f_{\text{BTN}}(\mathbf{y}[n]; \varphi) = 1$, i.e., triggering an emergency brake intervention at a time instant t_n when using the BTN-based decision rule $f_{\text{BTN}}(\cdot; \varphi)$ in (6.65)

$$x[n] + \varepsilon_x[n] \leq \frac{v^2[n]}{2\varphi}. \quad (6.104)$$

Consequently, the error region $\mathcal{I}_{\boldsymbol{\varepsilon},n}$ with intervention at the time instant t_n defined in (5.83) is given by

$$\begin{aligned} \mathcal{I}_{\boldsymbol{\varepsilon},n} &= \left\{ \boldsymbol{\varepsilon} \in \mathbb{R}^{2(n_{\text{end}}+1)} : f_{\text{adv. TTC}}(\mathbf{y}[n]; \varphi) = 1 \right\} \\ &= \left\{ \boldsymbol{\varepsilon} \in \mathbb{R}^{2(n_{\text{end}}+1)} : x[n] + \varepsilon_x[n] - \frac{v^2[n]}{2a} \leq -\varphi v[n] \wedge \varepsilon_v[n] = 0 \right\} \end{aligned} \quad (6.105)$$

for the advanced TTC-based decision rule, i.e., $f = f_{\text{adv. TTC}}$, and

$$\begin{aligned} \mathcal{I}_{\boldsymbol{\varepsilon},n} &= \left\{ \boldsymbol{\varepsilon} \in \mathbb{R}^{2(n_{\text{end}}+1)} : f_{\text{BTN}}(\mathbf{y}[n]; \varphi) = 1 \right\} \\ &= \left\{ \boldsymbol{\varepsilon} \in \mathbb{R}^{2(n_{\text{end}}+1)} : x[n] + \varepsilon_x[n] \leq \frac{v^2[n]}{2\varphi} \wedge \varepsilon_v[n] = 0 \right\} \end{aligned} \quad (6.106)$$

for the BTN-based decision rule, i.e., $f = f_{\text{BTN}}$. Hence, the probability $P(\varepsilon \in \mathcal{I}_{\varepsilon,n})$ that the sensor measurement errors ε lie in the error region $\mathcal{I}_{\varepsilon,n}$ with intervention at the time instant t_n is equivalent to the probability that the sensor measurement errors ε fulfill the condition (6.103) for triggering an emergency brake intervention at the time instant t_n , i.e.,

$$P(\varepsilon \in \mathcal{I}_{\varepsilon,n}) = P\left(x[n] + \varepsilon_x[n] - \frac{v^2[n]}{2a} \leq -\varphi v[n]\right), \quad (6.107)$$

if the advanced TTC-based decision rule $f_{\text{adv. TTC}}(\cdot; \varphi)$ is used and to the probability that the sensor measurement errors ε fulfill the condition (6.104) for triggering an emergency brake intervention at the time instant t_n , i.e.,

$$P(\varepsilon \in \mathcal{I}_{\varepsilon,n}) = P\left(x[n] + \varepsilon_x[n] \leq \frac{v^2[n]}{2\varphi}\right), \quad (6.108)$$

if the BTN-based decision rule $f_{\text{BTN}}(\cdot; \varphi)$ is used. With the state vector at the time instant $t_n = \frac{n}{f_s} \leq \frac{n_b}{f_s} = t_b$ in (6.90), the condition (6.103) that has to be fulfilled for triggering an emergency brake intervention at the time instant t_n when using the advanced TTC-based decision rule $f_{\text{adv. TTC}}(\cdot; \varphi)$ becomes

$$x_0 + \frac{nv_0}{f_s} + \varepsilon_x[n] - \frac{v_0^2}{2a} \leq -\varphi v_0 \quad (6.109)$$

and the condition (6.104) that has to be fulfilled for triggering an emergency brake intervention at the time instant t_n when using the BTN-based decision rule $f_{\text{BTN}}(\cdot; \varphi)$

$$x_0 + \frac{nv_0}{f_s} + \varepsilon_x[n] \leq \frac{v_0^2}{2\varphi}. \quad (6.110)$$

The former can be rewritten to

$$\varepsilon_x[n] \leq -x_0 - \left(\frac{n}{f_s} + \varphi - \frac{v_0}{2a}\right)v_0 \quad (6.111)$$

and the latter to

$$\varepsilon_x[n] \leq -x_0 - \left(\frac{n}{f_s} - \frac{v_0}{2\varphi}\right)v_0. \quad (6.112)$$

As a consequence, the probability that the former condition is fulfilled is identical to the probability that the sensor measurement errors ε fulfill the condition (6.103) for triggering an emergency brake intervention at the time instant t_n and thus to the

probability $P(\varepsilon \in \mathcal{I}_{\varepsilon,n})$ that they lie in the error region $\mathcal{I}_{\varepsilon,n}$ with intervention at the time instant t_n according to (6.107), i.e.,

$$P(\varepsilon \in \mathcal{I}_{\varepsilon,n}) = P\left(\varepsilon_x[n] \leq -x_0 - \left(\frac{n}{f_s} + \varphi - \frac{v_0}{2a}\right)v_0\right), \quad (6.113)$$

if the advanced TTC-based decision rule $f_{\text{adv. TTC}}(\cdot; \varphi)$ is used while the probability that the latter condition is fulfilled is identical to the probability that the sensor measurement errors ε fulfill the condition (6.104) for triggering an emergency brake intervention at the time instant t_n and thus to the probability $P(\varepsilon \in \mathcal{I}_{\varepsilon,n})$ that they lie in the error region $\mathcal{I}_{\varepsilon,n}$ with intervention at the time instant t_n according to (6.108), i.e.,

$$P(\varepsilon \in \mathcal{I}_{\varepsilon,n}) = P\left(\varepsilon_x[n] \leq -x_0 - \left(\frac{n}{f_s} - \frac{v_0}{2\varphi}\right)v_0\right), \quad (6.114)$$

if the BTN-based decision rule $f_{\text{BTN}}(\cdot; \varphi)$ is used. Since the sensor measurement error $\varepsilon_x[n]$ is Gaussian with zero mean, i.e., $E[\varepsilon_x[n]] = 0$, and the variance $\text{Var}[\varepsilon_x[n]] = \sigma_x^2$, and the associated standardized random variable

$$\frac{\varepsilon_x[n] - E[\varepsilon_x[n]]}{\sqrt{\text{Var}[\varepsilon_x[n]]}} = \frac{\varepsilon_x[n]}{\sigma_x} \quad (6.115)$$

is Gaussian with zero mean and unit variance, i.e., it follows the standard normal distribution $\mathcal{N}(0, 1)$, the probability $P(\varepsilon \in \mathcal{I}_{\varepsilon,n})$ that the sensor measurement errors ε lie in the error region $\mathcal{I}_{\varepsilon,n}$ with intervention at the time instant t_n when using the advanced TTC-based decision rule $f_{\text{adv. TTC}}(\cdot; \varphi)$ and fulfill the condition (6.111) for triggering an emergency brake intervention at the time instant t_n in (6.113) can be expressed as

$$\begin{aligned} P(\varepsilon \in \mathcal{I}_{\varepsilon,n}) &= P\left(\frac{\varepsilon_x[n]}{\sigma_x} \leq -\frac{x_0 + (n/f_s + \varphi - v_0/(2a))v_0}{\sigma_x}\right) \\ &= \Phi\left(-\frac{x_0 + (n/f_s + \varphi - v_0/(2a))v_0}{\sigma_x}\right). \end{aligned} \quad (6.116)$$

Due to the same reason, the probability $P(\varepsilon \in \mathcal{I}_{\varepsilon,n})$ that the sensor measurement errors ε lie in the error region $\mathcal{I}_{\varepsilon,n}$ with intervention at the time instant t_n when using the BTN-based decision rule $f_{\text{BTN}}(\cdot; \varphi)$ and fulfill the condition (6.112) for triggering an emergency brake intervention at the time instant t_n in (6.114) can be expressed as

$$\begin{aligned} P(\varepsilon \in \mathcal{I}_{\varepsilon,n}) &= P\left(\frac{\varepsilon_x[n]}{\sigma_x} \leq -\frac{x_0 + (n/f_s - v_0/(2\varphi))v_0}{\sigma_x}\right) \\ &= \Phi\left(-\frac{x_0 + (n/f_s - v_0/(2\varphi))v_0}{\sigma_x}\right). \end{aligned} \quad (6.117)$$

The expressions for the probability $P(\varepsilon \in \mathcal{I}_{\varepsilon,n})$ that the sensor measurement errors ε lie in the error region $\mathcal{I}_{\varepsilon,n}$ with intervention at the time instant t_n from (6.100), (6.116) and (6.117) in case of the TTC-based decision rule $f_{\text{TTC}}(\cdot; \varphi)$, the advanced TTC-based decision rule $f_{\text{adv. TTC}}(\cdot; \varphi)$ and the BTN-based decision rule $f_{\text{BTN}}(\cdot; \varphi)$, respectively, can be combined to

$$P(\varepsilon \in \mathcal{I}_{\varepsilon,n}) = \begin{cases} \Phi\left(-\frac{x_0 + (n/f_s + \varphi)v_0}{\sigma_x}\right), & f = f_{\text{TTC}} \\ \Phi\left(-\frac{x_0 + (n/f_s + \varphi - v_0/(2a))v_0}{\sigma_x}\right), & f = f_{\text{adv. TTC}} \\ \Phi\left(-\frac{x_0 + (n/f_s - v_0/(2\varphi))v_0}{\sigma_x}\right), & f = f_{\text{BTN}} \end{cases} \quad (6.118)$$

The probability of fulfilling the specification $x_{\min} \leq x_{\text{end}} \leq x_{\max}$ for the customer satisfaction is determined by

$$P(x_{\min} \leq x_{\text{end}} \leq x_{\max}) = \sum_{n'_b = n_{\min}}^{n_{\max}} P(\varepsilon \in \mathcal{I}_{\varepsilon, n'_b}) \prod_{n=0}^{n'_b-1} (1 - P(\varepsilon \in \mathcal{I}_{\varepsilon, n})), \quad (6.119)$$

which follows from substituting (6.88) into (6.81), with the probability $P(\varepsilon \in \mathcal{I}_{\varepsilon,n})$ that the sensor measurement errors ε lie in the error region $\mathcal{I}_{\varepsilon,n}$ with intervention at the time instant t_n from the last equation, n_{\min} from (6.77) and n_{\max} from (6.78).

6.3 Numerical Examples for the Robust Design of the Automatic Emergency Braking System

The numerical examples presented in this section illustrate the theoretical results elaborated in the previous sections and the robust design of the considered AEB system. Throughout the following numerical examples, the sampling rate is $f_s = 1$ kHz.

6.3.1 One Driving Scenario, TTC-Based Decision Rule and Error-Free Relative Velocity Measurements

In the first numerical examples, only the driving scenario that is shown in Figure 6.1 and characterized by the scenario parameters ξ_0 of the form given by (6.47) with the initial distance $x_0 = 10$ m and the initial relative velocity $v_0 = -10 \frac{\text{m}}{\text{s}}$ is considered. Furthermore, only the TTC-based decision rule $f_{\text{TTC}}(\cdot; \varphi)$ with the function parameter φ is used for triggering an emergency brake intervention and the relative velocity of the ego vehicle and the object is assumed to be measured without errors, i.e., the standard deviation of the sensor measurement errors $\varepsilon_v[n]$ in the measured relative velocity at the time instants t_n is $\sigma_v = 0$.

6.3 Numerical Examples for the Robust Design of the Automatic Emergency Braking System

In Figure 6.2, the probability $P(\varepsilon \in \mathcal{I}_{\varepsilon, n})$ that the sensor measurement errors ε lie in the error region $\mathcal{I}_{\varepsilon, n}$ with intervention at the time instant t_n and fulfill the condition for triggering an emergency brake intervention at the time instant t_n given by (6.97) is plotted over the time instants t_n for a fixed function parameter $\varphi = 0.51$ s and various values of the standard deviation σ_x of the sensor measurement errors $\varepsilon_x[n]$ in the measured distance at the time instants t_n as well as a fixed standard deviation $\sigma_x = 0.1$ m of the sensor measurement errors in the measured distance and various values of the function parameter φ . It can be observed that it is close to 0 at earlier time instants t_n , increases over time and approaches 1 at later time instants t_n for all values of the standard deviation σ_x of the sensor measurement errors in the measured distance and the function parameter φ . However, it increases in a shorter time if the standard deviation σ_x of the sensor measurement errors in the measured distance is smaller and later if the function parameter φ is smaller.

As can be seen in Figure 6.3, where the probability $P(n_b = n'_b)$ that the discrete time index n_b of the time instant $t_b = n_b/f_s$ at which the emergency brake intervention is triggered is the discrete time index n'_b of the time instant $t_{n'_b} = n'_b/f_s$ given by (6.98) is plotted over the time instants $t_{n'_b}$ for a fixed function parameter $\varphi = 0.51$ s and various values of the standard deviation σ_x of the sensor measurement errors in the measured distance as well as a fixed standard deviation $\sigma_x = 0.1$ m of the sensor measurement errors in the measured distance and various values of the function parameter φ , there is a time interval in which this probability is significantly larger than 0 for all values of σ_x and φ . Decreasing the standard deviation σ_x of the sensor measurement errors in the measured distance shifts this interval forth in time and reduces its width whereas decreasing the function parameter φ shifts it only forth in time.

For the rest of this section, the deceleration after triggering the emergency brake intervention is $a = 10 \frac{\text{m}}{\text{s}^2}$, and the minimal and maximal tolerable final distances between the ego vehicle and the object after the emergency brake intervention are $x_{\min} = 0$ and $x_{\max} = 0.5$ m. In this case, the lower and upper bound of the specification $n_{\min} \leq n_b \leq n_{\max}$ for the discrete time index n_b of the time instant $t_b = n_b/f_s$ at which the emergency brake intervention is triggered, which is equivalent to the specification $x_{\min} \leq x_{\text{end}} \leq x_{\max}$ for the customer satisfaction, are $n_{\min} = 450$ according to (6.77) and $n_{\max} = 500$ according to (6.78), respectively. So, the specification $0 = x_{\min} \leq x_{\text{end}} \leq x_{\max} = 0.5$ m for the customer satisfaction is fulfilled iff the time instant $t_b = n_b/f_s$ at which the emergency brake intervention is triggered with the discrete time index n_b lies in the time interval that starts at the time instant $t_{n_{\min}} = n_{\min}/f_s = 0.45$ s corresponding to the discrete time index $n_{\min} = 450$ and ends at the time instant

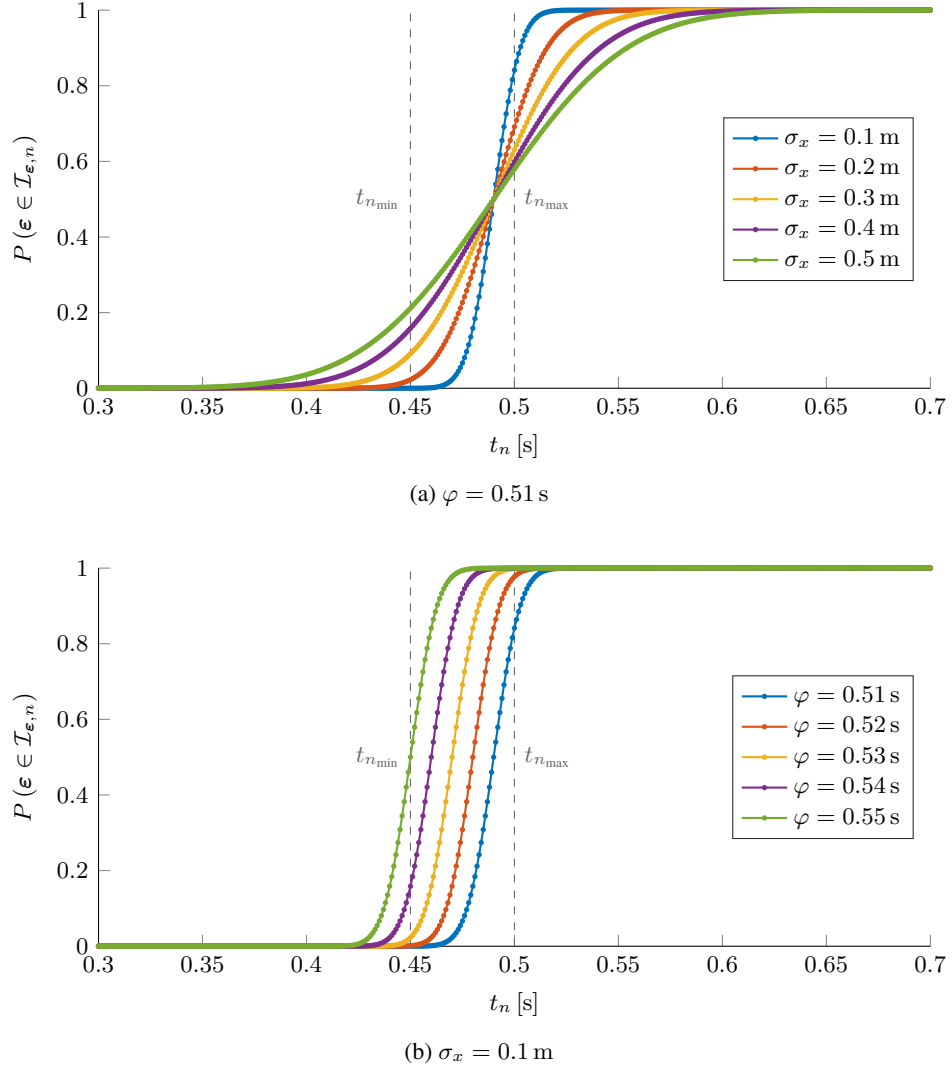


Figure 6.2: Probability that the sensor measurement errors ϵ lie in the error region $\mathcal{I}_{\epsilon,n}$ with intervention at the time instant t_n and fulfill the condition for triggering an emergency brake intervention at the time instant t_n for $\sigma_v = 0$, $x_0 = 10$ m, $v_0 = -10 \frac{\text{m}}{\text{s}}$, $f_s = 1$ kHz and the TTC-based decision rule $f_{\text{TTC}}(\cdot; \varphi)$ as well as the lower bound $t_{n_{\min}} = 0.45$ s and the upper bound $t_{n_{\max}} = 0.5$ s of the time interval in which the emergency brake intervention with the constant deceleration $a = 10 \frac{\text{m}}{\text{s}^2}$ has to be triggered to fulfill the specification $0 = x_{\min} \leq x_{\text{end}} \leq x_{\max} = 0.5$ m for the customer satisfaction.

6.3 Numerical Examples for the Robust Design of the Automatic Emergency Braking System

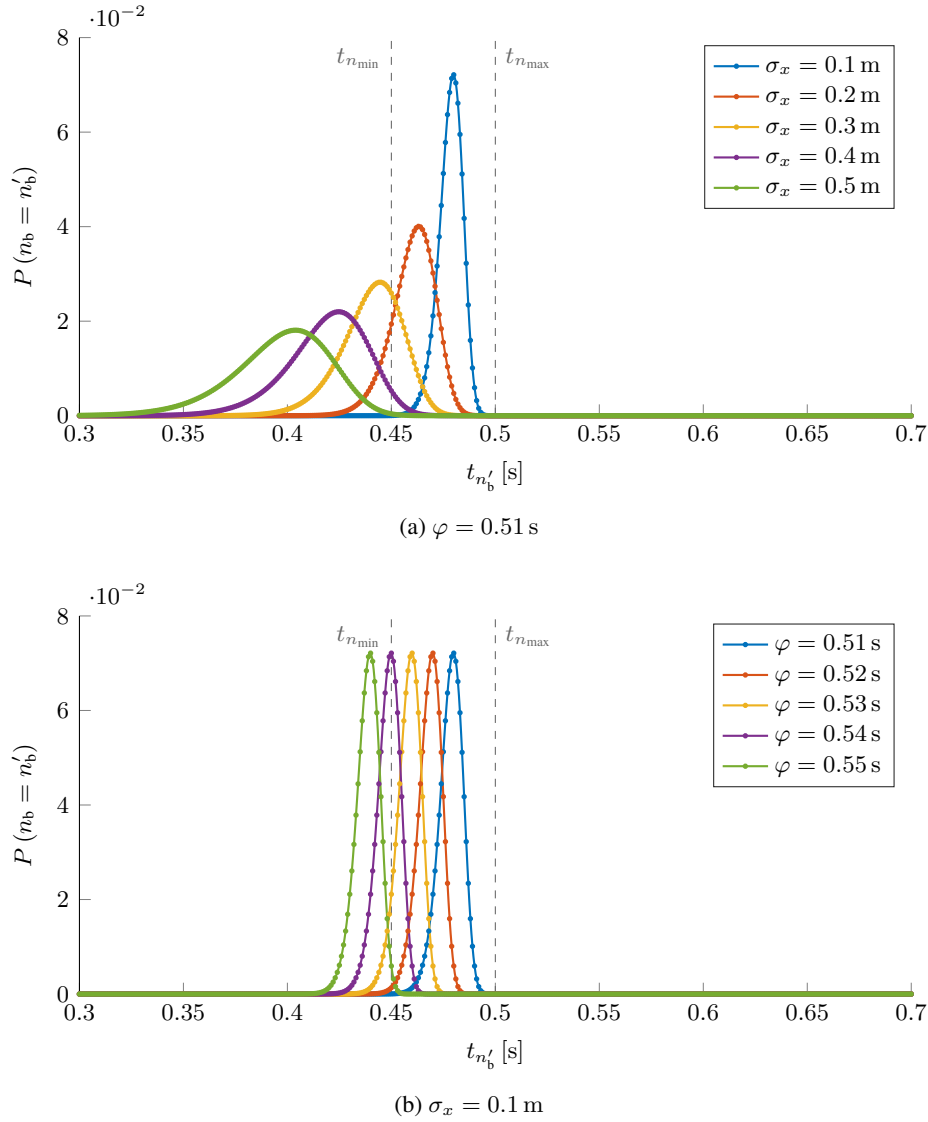


Figure 6.3: Probability that the discrete time index n_b of the time instant $t_b = n_b/f_s$ at which the emergency brake intervention is triggered is the discrete time index n'_b of the time instant $t_{n'_b} = n'_b/f_s$ for $\sigma_v = 0$, $x_0 = 10$ m, $v_0 = -10 \frac{\text{m}}{\text{s}}$, $f_s = 1$ kHz and the TTC-based decision rule $f_{\text{TTC}}(\cdot; \varphi)$ as well as the lower bound $t_{n_{\min}} = 0.45$ s and the upper bound $t_{n_{\max}} = 0.5$ s of the time interval in which the emergency brake intervention with the constant deceleration $a = 10 \frac{\text{m}}{\text{s}^2}$ has to be triggered to fulfill the specification $0 = x_{\min} \leq x_{\text{end}} \leq x_{\max} = 0.5$ m for the customer satisfaction.

$t_{n_{\max}} = n_{\max}/f_s = 0.5$ s corresponding to the discrete time index $n_{\max} = 500$. These two time instants are highlighted in the plots of Figure 6.2 and Figure 6.3.

In Figure 6.4, the probability $P(x_{\min} \leq x_{\text{end}} \leq x_{\max})$ of fulfilling the specification $x_{\min} \leq x_{\text{end}} \leq x_{\max}$ for the customer satisfaction given by (6.99) is plotted over the function parameter φ for various values of the standard deviation σ_x of the sensor measurement errors in the measured distance and over the standard deviation σ_x of the sensor measurement errors in the measured distance for various values of the function parameter φ . For all considered values of the standard deviation σ_x of the sensor measurement errors in the measured distance, this probability first increases and then decreases with an increasing function parameter φ . With a smaller standard deviation σ_x of the sensor measurement errors in the measured distance, however, a larger probability $P(x_{\min} \leq x_{\text{end}} \leq x_{\max})$ of fulfilling the specification for the customer satisfaction can be reached. For all considered values of the function parameter φ , the probability $P(x_{\min} \leq x_{\text{end}} \leq x_{\max})$ of fulfilling the specification for the customer satisfaction approaches 1 when the standard deviation σ_x of the sensor measurement errors in the measured distance decreases. If the function parameter φ is chosen appropriately, however, the same probability $P(x_{\min} \leq x_{\text{end}} \leq x_{\max})$ of fulfilling the specification for the customer satisfaction can be reached with a larger standard deviation σ_x of the sensor measurement errors in the measured distance. In order to better visualize how the probability $P(x_{\min} \leq x_{\text{end}} \leq x_{\max})$ of fulfilling the specification for the customer satisfaction depends on both the function parameter φ and the standard deviation σ_x of the sensor measurement errors in the measured distance, its contour lines are plotted in Figure 6.5.

If the sensors to be used in the considered AEB system, i.e., their parameters σ in (6.55), namely, the standard deviations σ_x and $\sigma_v = 0$ of their measurement errors in the measured distance and relative velocity, respectively, and their sampling rate $f_s = 1$ kHz, are given already, the function can be optimally adapted to the given sensors such that it meets the requirements of the customers in a robust manner despite the unavoidable sensor measurement errors to the greatest possible extent by solving the optimization problem (4.1) of the function design. As only the driving scenario ξ_0 with the initial distance $x_0 = 10$ m and the initial relative velocity $v_0 = -10 \frac{\text{m}}{\text{s}}$ is considered, i.e., the scenario set is $\mathcal{X} = \{\xi_0\}$, the quality measure Q defined in (6.69), which measures to what extent the function meets the customer requirements in a robust manner despite the unavoidable sensor measurement errors, is the probability of fulfilling the specification $x_{\min} \leq x_{\text{end}} \leq x_{\max}$ for the customer satisfaction evaluated at the driving scenario $\xi = \xi_0$, i.e., the initial distance $x_0 = 10$ m and the initial relative velocity $v_0 = -10 \frac{\text{m}}{\text{s}}$, for which the expression in (6.119) together with (6.77),

6.3 Numerical Examples for the Robust Design of the Automatic Emergency Braking System

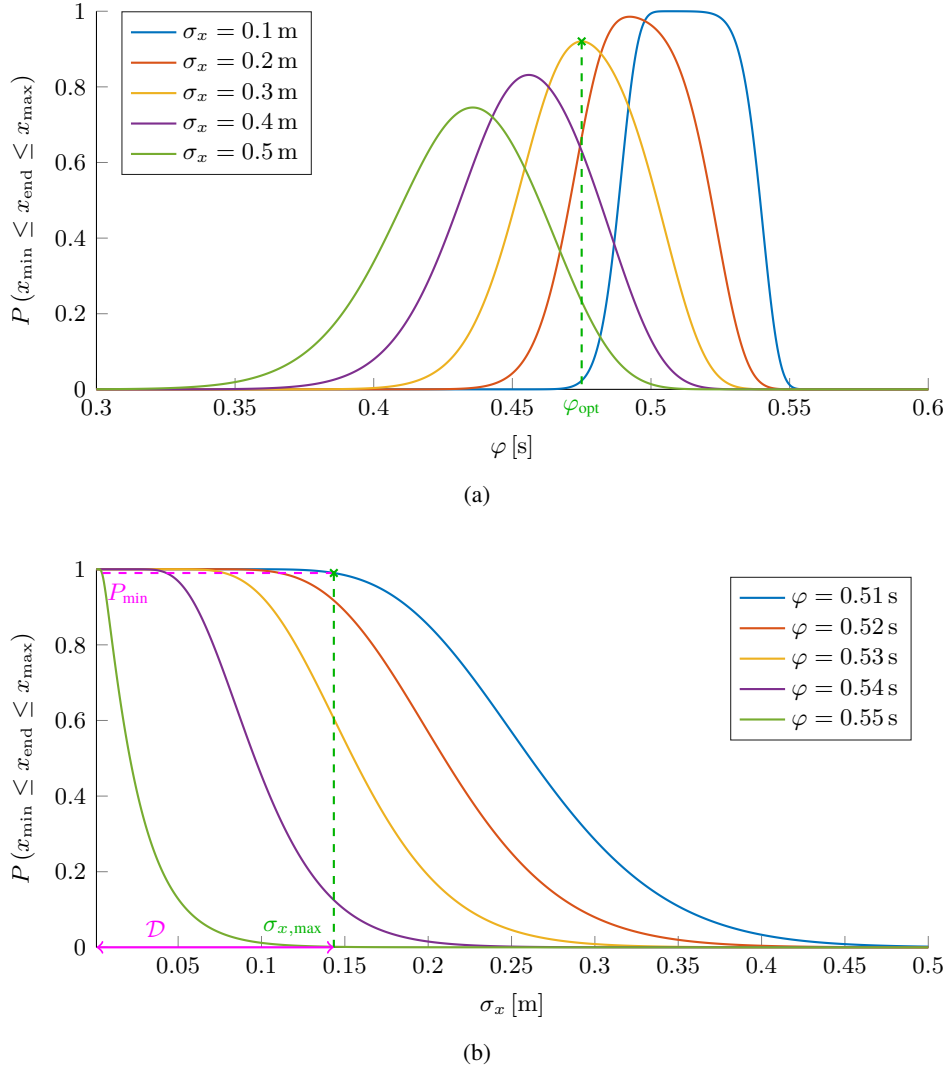


Figure 6.4: Probability that the considered AEB system fulfills the specification $x_{\min} \leq x_{\text{end}} \leq x_{\max}$ for the customer satisfaction vs. the function parameter φ (a) and the standard deviation σ_x of the sensor measurement errors in the measured distance (b) for $\sigma_v = 0$, $x_0 = 10$ m, $v_0 = -10 \frac{\text{m}}{\text{s}}$, $f_s = 1$ kHz, $a = 10 \frac{\text{m}}{\text{s}^2}$, $x_{\min} = 0$, $x_{\max} = 0.5$ m and the TTC-based decision rule $f_{\text{TTC}}(\cdot; \varphi)$ with the optimal function parameter value φ_{opt} determined by the function design for $\sigma_x = 0.3$ m and the maximal tolerable standard deviation $\sigma_{x,\max}$ of the sensor measurement errors in the measured distance determined by the sensor design for $\varphi = 0.51$ s and $P_{\min} = 0.99$, respectively.

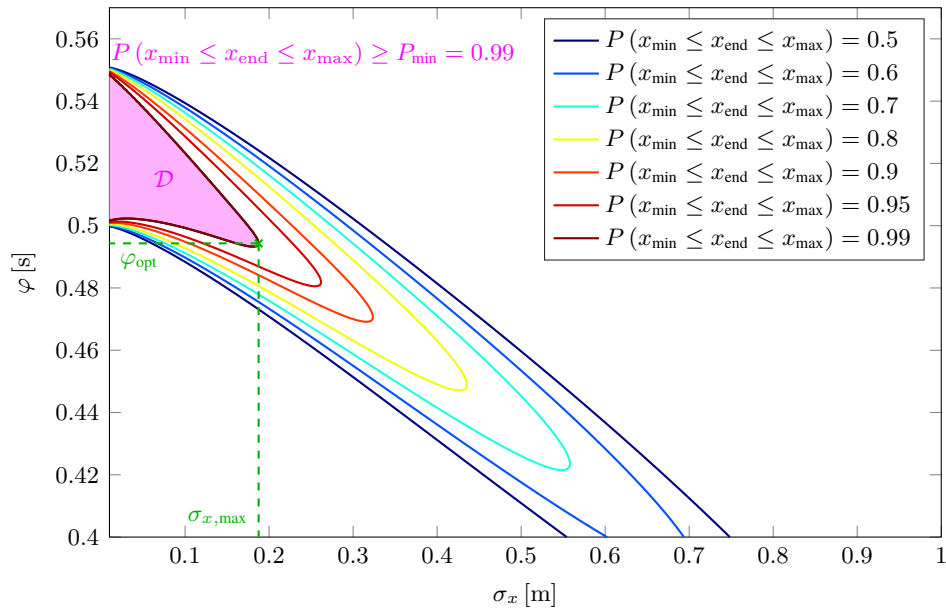


Figure 6.5: Contour lines of the probability that the considered AEB system fulfills the specification $x_{\min} \leq x_{\text{end}} \leq x_{\max}$ for the customer satisfaction for $\sigma_v = 0$, $x_0 = 10$ m, $v_0 = -10 \frac{\text{m}}{\text{s}}$, $f_s = 1$ kHz, $a = 10 \frac{\text{m}}{\text{s}^2}$, $x_{\min} = 0$, $x_{\max} = 0.5$ m and the TTC-based decision rule $f_{\text{TTC}}(\cdot; \varphi)$ with the optimal function parameter value φ_{opt} and the maximal tolerable standard deviation $\sigma_{x,\text{max}}$ of the sensor measurement errors in the measured distance determined by the joint function and sensor design for $P_{\min} = 0.99$.

6.3 Numerical Examples for the Robust Design of the Automatic Emergency Braking System

σ_x [m]	0.1	0.2	0.3	0.4	0.5
φ_{opt} [s]	0.50679	0.49234	0.47500	0.45593	0.43571
$P(x_{\min} \leq x_{\text{end}} \leq x_{\max})$	0.99998	0.98550	0.92029	0.83154	0.74535

Table 6.1: Optimal function parameter value φ_{opt} for the considered AEB system determined by the function design for $\sigma_v = 0$, $x_0 = 10$ m, $v_0 = -10 \frac{\text{m}}{\text{s}}$, $f_s = 1$ kHz, $a = 10 \frac{\text{m}}{\text{s}^2}$, $x_{\min} = 0$, $x_{\max} = 0.5$ m, the TTC-based decision rule $f_{\text{TTC}}(\cdot; \varphi)$ and various values of the standard deviation σ_x of the sensor measurement errors in the measured distance as well as the resulting probability $P(x_{\min} \leq x_{\text{end}} \leq x_{\max})$ of fulfilling the specification for the customer satisfaction.

(6.78) and (6.118) can be used:

$$\begin{aligned} Q &= P(x_{\min} \leq x_{\text{end}} \leq x_{\max})|_{\xi=\xi_0} \\ &= P(x_{\min} \leq x_{\text{end}} \leq x_{\max})|_{x_0=10 \text{ m}, v_0=-10 \frac{\text{m}}{\text{s}}}. \end{aligned} \quad (6.120)$$

Since this is the quality measure Q and only the TTC-based decision rule $f_{\text{TTC}}(\cdot; \varphi)$ with only one function parameter φ is considered, i.e., the set of the predefined decision rules for triggering the emergency brake intervention is $\mathcal{F} = \{f_{\text{TTC}}\}$ and $\varphi = \varphi$, the optimization problem (4.1) of the function design simplifies to

$$\varphi_{\text{opt}} = \underset{\varphi \in \mathbb{R}}{\text{argmax}} P(x_{\min} \leq x_{\text{end}} \leq x_{\max})|_{x_0=10 \text{ m}, v_0=-10 \frac{\text{m}}{\text{s}}, f=f_{\text{TTC}}}. \quad (6.121)$$

The solution of this optimization problem is the optimal function parameter value φ_{opt} , which maximizes the probability $P(x_{\min} \leq x_{\text{end}} \leq x_{\max})|_{x_0=10 \text{ m}, v_0=-10 \frac{\text{m}}{\text{s}}, f=f_{\text{TTC}}}$ of fulfilling the specification for the customer satisfaction evaluated at the initial distance $x_0 = 10$ m and the initial relative velocity $v_0 = -10 \frac{\text{m}}{\text{s}}$ for the TTC-based decision rule, i.e., $f = f_{\text{TTC}}$. The optimal function parameter value φ_{opt} obtained by numerically solving this optimization problem for various values of the standard deviation σ_x of the sensor measurement errors in the measured distance as well as the resulting probability $P(x_{\min} \leq x_{\text{end}} \leq x_{\max})$ of fulfilling the specification for the customer satisfaction are stated in Table 6.1. In addition, the optimal function parameter value φ_{opt} for the standard deviation $\sigma_x = 0.3$ m of the sensor measurement errors in the measured distance and the corresponding maximum value of the probability $P(x_{\min} \leq x_{\text{end}} \leq x_{\max})$ of fulfilling the specification for the customer satisfaction are illustrated in Figure 6.4.

If the function of the considered AEB system, i.e., its decision rule $f = f_{\text{TTC}}$ with the function parameter $\varphi = \varphi$, is given already, the requirements the sensors have to

fulfill such that it meets the requirements of the customers in a robust manner despite the unavoidable sensor measurement errors to the desired extent at minimal costs can be determined by solving the optimization problem (4.9) of the sensor design. Since the quality measure Q , which measures to what extent the function meets the customer requirements in a robust manner despite the unavoidable sensor measurement errors, is the probability of fulfilling the specification $x_{\min} \leq x_{\text{end}} \leq x_{\max}$ for the customer satisfaction in the driving scenario $\xi = \xi_0$ with the initial distance $x_0 = 10$ m and the initial relative velocity $v_0 = -10 \frac{\text{m}}{\text{s}}$ as stated in (6.120), the required minimum probability P_{\min} of fulfilling this specification for the customer satisfaction in the driving scenario $\xi = \xi_0$ is the required minimum quality level Q_{\min} according to (4.39). As the sampling rate has already been chosen to be $f_s = 1$ kHz, the standard deviation of the sensor measurement errors in the measured relative velocity is assumed to be $\sigma_v = 0$ and the standard deviation σ_x of the sensor measurement errors in the measured distance has to be positive, the possible domain for the values of the sensor parameters σ defined in (6.55) is

$$\begin{aligned} \mathcal{S} &= \left\{ \sigma = [\sigma_x, \sigma_v, f_s]^T \in \mathbb{R}^3 : \sigma_x \in \mathbb{R}^+ \wedge \sigma_v = 0 \wedge f_s = 1 \text{ kHz} \right\} \\ &= \left\{ \sigma = [\sigma_x, 0, 1 \text{ kHz}]^T \in \mathbb{R}^3 : \sigma_x \in \mathbb{R}^+ \right\}. \end{aligned} \quad (6.122)$$

With this possible domain \mathcal{S} of the sensor parameter values σ , the aforementioned quality measure Q in (6.120) and respective required minimum quality level $Q_{\min} = P_{\min}$ as well as the costs $C = -\sigma_x$ or, alternatively, $C = \sigma_x^{-1}$, which are chosen as simple illustrative examples, the optimization problem (4.9) of the sensor design simplifies to

$$\begin{aligned} \sigma_{x,\max} &= \underset{\sigma_x \in \mathbb{R}^+}{\operatorname{argmin}} C \\ &\text{s.t. } P(x_{\min} \leq x_{\text{end}} \leq x_{\max})|_{x_0=10 \text{ m}, v_0=-10 \frac{\text{m}}{\text{s}}, \sigma_v=0, f_s=1 \text{ kHz}} \geq P_{\min} \\ &= \underset{\sigma_x \in \mathbb{R}^+}{\operatorname{argmax}} \sigma_x \\ &\text{s.t. } P(x_{\min} \leq x_{\text{end}} \leq x_{\max})|_{x_0=10 \text{ m}, v_0=-10 \frac{\text{m}}{\text{s}}, \sigma_v=0, f_s=1 \text{ kHz}} \geq P_{\min}. \end{aligned} \quad (6.123)$$

As the chosen costs C decrease with increasing standard deviation σ_x of the sensor measurement errors in the measured distance, the minimization of the cost function C is converted into the maximization of the standard deviation σ_x of the sensor measurement errors in the measured distance. Thus, the solution of this optimization problem is the maximal tolerable standard deviation $\sigma_{x,\max}$ of the sensor measurement errors in the

6.3 Numerical Examples for the Robust Design of the Automatic Emergency Braking System

φ [s]	0.51	0.52	0.53	0.54	0.55
$\sigma_{x,\max}$ [m]	0.14341	0.11102	0.07774	0.04296	0.00430

Table 6.2: Maximal tolerable standard deviation $\sigma_{x,\max}$ of the sensor measurement errors in the measured distance for the considered AEB system determined by the sensor design for $\sigma_v = 0$, $x_0 = 10$ m, $v_0 = -10 \frac{\text{m}}{\text{s}}$, $f_s = 1$ kHz, $a = 10 \frac{\text{m}}{\text{s}^2}$, $x_{\min} = 0$, $x_{\max} = 0.5$ m, the TTC-based decision rule $f_{\text{TTC}}(\cdot; \varphi)$, $P_{\min} = 0.99$ and various values of the function parameter φ .

measured distance, which represents the accuracy requirements the sensors have to fulfill such that the probability $P(x_{\min} \leq x_{\text{end}} \leq x_{\max})|_{x_0=10 \text{ m}, v_0=-10 \frac{\text{m}}{\text{s}}, \sigma_v=0, f_s=1 \text{ kHz}}$ of fulfilling the specification for the customer satisfaction evaluated at the initial distance $x_0 = 10$ m, the initial relative velocity $v_0 = -10 \frac{\text{m}}{\text{s}}$, the standard deviation $\sigma_v = 0$ of the sensor measurement errors in the measured relative velocity and the sampling rate $f_s = 1$ kHz is at least P_{\min} as desired. The maximal tolerable standard deviation $\sigma_{x,\max}$ of the sensor measurement errors in the measured distance obtained by numerically solving this optimization problem for the required minimum probability $P_{\min} = 0.99$ of fulfilling the specification for the customer satisfaction and for various values of the function parameter φ is stated in Table 6.2. In addition, the maximal tolerable standard deviation $\sigma_{x,\max}$ of the sensor measurement errors in the measured distance for the function parameter $\varphi = 0.51$ s is illustrated in Figure 6.4. It is the largest value of the standard deviation σ_x of the sensor measurement errors in the measured distance inside the highlighted design space \mathcal{D} . According to (4.6), the design space \mathcal{D} is the set of all sensor parameter values σ in the possible domain \mathcal{S} for which the quality measure Q , i.e., the probability of fulfilling the specification $x_{\min} \leq x_{\text{end}} \leq x_{\max}$ for the customer satisfaction in the driving scenario $\xi = \xi_0$ with the initial distance $x_0 = 10$ m and the initial relative velocity $v_0 = -10 \frac{\text{m}}{\text{s}}$ as stated in (6.120), does not lie below the required minimum quality level Q_{\min} , i.e., the required minimum probability P_{\min} of fulfilling this specification for the customer satisfaction in the driving scenario $\xi = \xi_0$:

$$\mathcal{D} = \left\{ \sigma \in \mathcal{S} : P(x_{\min} \leq x_{\text{end}} \leq x_{\max})|_{x_0=10 \text{ m}, v_0=-10 \frac{\text{m}}{\text{s}}} \geq P_{\min} \right\}. \quad (6.124)$$

With the special possible domain \mathcal{S} of the sensor parameter values σ in (6.122), the design space reads

$$\mathcal{D} = \left\{ \sigma = [\sigma_x, 0, 1 \text{ kHz}]^T \in \mathbb{R}^3 : \sigma_x \in \mathbb{R}^+, \right. \\ \left. P(x_{\min} \leq x_{\text{end}} \leq x_{\max})|_{x_0=10 \text{ m}, v_0=-10 \frac{\text{m}}{\text{s}}, \sigma_v=0, f_s=1 \text{ kHz}} \geq P_{\min} \right\} \quad (6.125)$$

in this case.

If neither the sensors nor the function of the considered AEB system are given in advance, both the sensors and the function can be determined in an optimal way by solving the optimization problem (4.11) of the joint function and sensor design such that the function meets the requirements of the customers in a robust manner despite the unavoidable sensor measurement errors to the desired extent at minimal costs. With the quality measure Q in (6.120), i.e., the probability of fulfilling the specification $x_{\min} \leq x_{\text{end}} \leq x_{\max}$ for the customer satisfaction in the driving scenario $\xi = \xi_0$ with the initial distance $x_0 = 10$ m and the initial relative velocity $v_0 = -10 \frac{\text{m}}{\text{s}}$, the respective required minimum quality level $Q_{\min} = P_{\min}$, i.e., the required minimum probability P_{\min} of fulfilling this specification for the customer satisfaction in the driving scenario $\xi = \xi_0$, the same costs $C = -\sigma_x$ or, alternatively, $C = \sigma_x^{-1}$ as in the sensor design before, the possible domain \mathcal{S} of the sensor parameter values σ in (6.122) and the set $\mathcal{F} = \{f_{\text{TTC}}\}$ of the predefined decision rules for triggering the emergency brake intervention consisting of only the TTC-based decision rule $f_{\text{TTC}}(\cdot; \varphi)$ with the single function parameter $\varphi = \varphi$ as in the function design before, this optimization problem simplifies to

$$\begin{aligned}
 & (\sigma_{x,\max}, \varphi_{\text{opt}}) = \\
 & \quad \underset{\sigma_x \in \mathbb{R}^+, \varphi \in \mathbb{R}}{\operatorname{argmin}} C \\
 & \quad \text{s.t. } P(x_{\min} \leq x_{\text{end}} \leq x_{\max})|_{x_0=10 \text{ m}, v_0=-10 \frac{\text{m}}{\text{s}}, \sigma_v=0, f_s=1 \text{ kHz}, f=f_{\text{TTC}}} \geq P_{\min} \\
 & = \underset{\sigma_x \in \mathbb{R}^+, \varphi \in \mathbb{R}}{\operatorname{argmax}} \sigma_x \\
 & \quad \text{s.t. } P(x_{\min} \leq x_{\text{end}} \leq x_{\max})|_{x_0=10 \text{ m}, v_0=-10 \frac{\text{m}}{\text{s}}, \sigma_v=0, f_s=1 \text{ kHz}, f=f_{\text{TTC}}} \geq P_{\min}.
 \end{aligned} \tag{6.126}$$

As in the sensor design before, the minimization of the cost function C , whose costs C decrease with increasing standard deviation σ_x of the sensor measurement errors in the measured distance, is converted into the maximization of this standard deviation σ_x . Thus, the solution of this optimization problem is the maximal tolerable standard deviation $\sigma_{x,\max}$ of the sensor measurement errors in the measured distance and the corresponding optimal function parameter value φ_{opt} , which guarantee that the probability $P(x_{\min} \leq x_{\text{end}} \leq x_{\max})|_{x_0=10 \text{ m}, v_0=-10 \frac{\text{m}}{\text{s}}, \sigma_v=0, f_s=1 \text{ kHz}, f=f_{\text{TTC}}}$ of fulfilling the specification for the customer satisfaction evaluated at the initial distance $x_0 = 10$ m, the initial relative velocity $v_0 = -10 \frac{\text{m}}{\text{s}}$, the standard deviation $\sigma_v = 0$ of the sensor measurement errors in the measured relative velocity and the sampling rate $f_s = 1$ kHz for the TTC-based decision rule, i.e., $f = f_{\text{TTC}}$, is at least P_{\min} as

desired. The maximal tolerable standard deviation of the sensor measurement errors in the measured distance and the corresponding optimal function parameter value obtained by numerically solving this optimization problem for the required minimum probability $P_{\min} = 0.99$ of fulfilling the specification for the customer satisfaction is $\sigma_{x,\max} = 0.18754$ m and $\varphi_{\text{opt}} = 0.49433$ s, respectively. It can be observed that the so obtained maximal tolerable standard deviation $\sigma_{x,\max}$ is larger than that obtained by the sensor design for various values of the function parameter φ in Table 6.2. This is due to the larger number of optimization variables providing more degrees of freedom for solving the optimization problem as compared to the optimization problem (6.123) of the sensor design and emphasizes the power of the joint function and sensor design. The maximal tolerable standard deviation $\sigma_{x,\max}$ of the sensor measurement errors in the measured distance and the corresponding optimal function parameter value φ_{opt} resulting from the joint function and sensor design are illustrated in Figure 6.5. The pair $(\sigma_{x,\max}, \varphi_{\text{opt}})$ formed by them is the pair (σ_x, φ) with the largest standard deviation σ_x of the sensor measurement errors in the measured distance inside the design space \mathcal{D} highlighted by the magenta area and the corresponding function parameter φ , and is marked by the green cross. According to (4.16), the design space \mathcal{D} is the set of all sensor parameter values σ in the possible domain \mathcal{S} , decision rules f from the set \mathcal{F} of the predefined decision rules for triggering the emergency brake intervention and function parameter values φ for which the quality measure Q , i.e., the probability of fulfilling the specification $x_{\min} \leq x_{\text{end}} \leq x_{\max}$ for the customer satisfaction in the driving scenario $\xi = \xi_0$ with the initial distance $x_0 = 10$ m and the initial relative velocity $v_0 = -10 \frac{\text{m}}{\text{s}}$ as stated in (6.120), does not lie below the required minimum quality level Q_{\min} , i.e., the required minimum probability P_{\min} of fulfilling this specification for the customer satisfaction in the driving scenario $\xi = \xi_0$:

$$\mathcal{D} = \left\{ (\sigma, f, \varphi) \in \mathcal{S} \times \mathcal{F} \times \mathbb{R}^{N_\varphi} : \right. \\ \left. P(x_{\min} \leq x_{\text{end}} \leq x_{\max})|_{x_0=10 \text{ m}, v_0=-10 \frac{\text{m}}{\text{s}}} \geq P_{\min} \right\}. \quad (6.127)$$

With the special possible domain \mathcal{S} of the sensor parameter values σ in (6.122) and the set $\mathcal{F} = \{f_{\text{TTC}}\}$ of the predefined decision rules consisting of only the TTC-based decision rule $f_{\text{TTC}}(\cdot; \varphi)$ with the single function parameter $\varphi = \varphi$, i.e., $N_\varphi = 1$, the design space reads

$$\mathcal{D} = \left\{ (\sigma, f, \varphi) = \left([\sigma_x, 0, 1 \text{ kHz}]^T, f_{\text{TTC}}, \varphi \right) \in \mathbb{R}^3 \times \{f_{\text{TTC}}\} \times \mathbb{R} : \sigma_x \in \mathbb{R}^+, \right. \\ \left. P(x_{\min} \leq x_{\text{end}} \leq x_{\max})|_{x_0=10 \text{ m}, v_0=-10 \frac{\text{m}}{\text{s}}, \sigma_v=0, f_s=1 \text{ kHz}, f=f_{\text{TTC}}} \geq P_{\min} \right\} \quad (6.128)$$

in this case.

6.3.2 Several Driving Scenarios, Set of Decision Rules and Error-Free Relative Velocity Measurements

In order to illustrate how the AEB system can be designed for several driving scenarios, the two driving scenarios that are instances of the driving scenario shown in Figure 6.1 and characterized by the scenario parameters ξ_1 and ξ_2 of the form given by (6.47) with the same initial distance $x_0 = 50$ m but the different initial relative velocities $v_0 = -10 \frac{\text{m}}{\text{s}}$ and $v_0 = -20 \frac{\text{m}}{\text{s}}$, respectively, are considered. Hence, the scenario set \mathcal{X} for this design task consists of these two scenarios:

$$\mathcal{X} = \{\xi_1, \xi_2\}. \quad (6.129)$$

Moreover, all three introduced decision rules for triggering an emergency brake intervention, i.e., the TTC-based decision rule $f_{\text{TTC}}(\cdot; \varphi)$, the advanced TTC-based decision rule $f_{\text{adv. TTC}}(\cdot; \varphi)$ and the BTN-based decision rule $f_{\text{BTN}}(\cdot; \varphi)$, with the function parameter φ forming the set \mathcal{F} of the predefined decision rules for triggering an emergency brake intervention are considered for this design task:

$$\mathcal{F} = \{f_{\text{TTC}}, f_{\text{adv. TTC}}, f_{\text{BTN}}\}. \quad (6.130)$$

As in the previous numerical examples, the relative velocity of the ego vehicle and the object is still assumed to be measured without errors, i.e., the standard deviation of the sensor measurement errors $\varepsilon_v[n]$ in the measured relative velocity at the time instants t_n is $\sigma_v = 0$, the deceleration after triggering the emergency brake intervention is $a = 10 \frac{\text{m}}{\text{s}^2}$, and the minimal and maximal tolerable final distances between the ego vehicle and the object after the emergency brake intervention are $x_{\min} = 0$ and $x_{\max} = 0.5$ m, respectively.

According to (6.69), the quality measure Q is the minimum of the probability $P(x_{\min} \leq x_{\text{end}} \leq x_{\max})$ that the final distance x_{end} fulfills the specification $x_{\min} \leq x_{\text{end}} \leq x_{\max}$ for the customer satisfaction in the two considered driving scenarios ξ_1 and ξ_2 from the scenario set \mathcal{X} in (6.129). With this quality measure Q and the single function parameter $\varphi = \varphi$ parameterizing the TTC-based decision rule $f_{\text{TTC}}(\cdot; \varphi)$, the advanced TTC-based decision rule $f_{\text{adv. TTC}}(\cdot; \varphi)$ and the BTN-based decision rule $f_{\text{BTN}}(\cdot; \varphi)$, the optimization problem (4.1) of the function design becomes

$$(f_{\text{opt}}, \varphi_{\text{opt}}) = \underset{f \in \mathcal{F}, \varphi \in \mathbb{R}}{\operatorname{argmax}} \min_{\xi \in \mathcal{X}} P(x_{\min} \leq x_{\text{end}} \leq x_{\max}). \quad (6.131)$$

6.3 Numerical Examples for the Robust Design of the Automatic Emergency Braking System

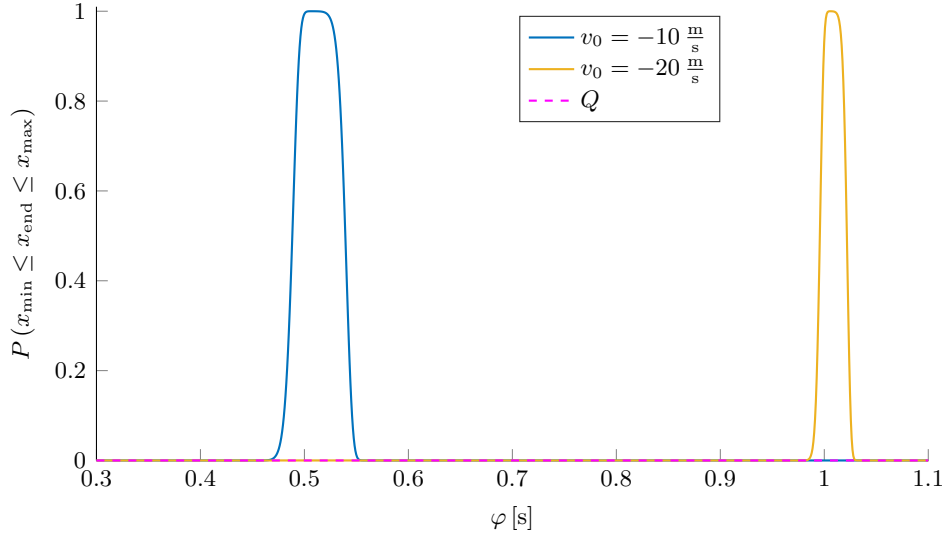


Figure 6.6: Probability that the considered AEB system fulfills the specification $x_{\min} \leq x_{\text{end}} \leq x_{\max}$ for the customer satisfaction for $v_0 = -10 \frac{\text{m}}{\text{s}}$ and $v_0 = -20 \frac{\text{m}}{\text{s}}$ as well as the minimum thereof, i.e., the quality measure Q , vs. the function parameter φ for $\sigma_x = 0.1 \text{ m}$, $\sigma_v = 0$, $x_0 = 50 \text{ m}$, $f_s = 1 \text{ kHz}$, $a = 10 \frac{\text{m}}{\text{s}^2}$, $x_{\min} = 0$, $x_{\max} = 0.5 \text{ m}$ and the TTC-based decision rule $f_{\text{TTC}}(\cdot; \varphi)$.

In Figures 6.6, 6.7 and 6.8, the probability $P(x_{\min} \leq x_{\text{end}} \leq x_{\max})$ of fulfilling the specification for the customer satisfaction in each of the two considered scenarios ξ_1 and ξ_2 with the initial relative velocities $v_0 = -10 \frac{\text{m}}{\text{s}}$ and $v_0 = -20 \frac{\text{m}}{\text{s}}$, respectively, as well as the minimum thereof, i.e., the quality measure Q from (6.69), are plotted over the function parameter φ for each of the three considered decision rules and the standard deviation $\sigma_x = 0.1 \text{ m}$ of the sensor measurement errors in the measured distance.

As can be observed, the quality measure Q is almost 0 for the TTC-based decision rule $f_{\text{TTC}}(\cdot; \varphi)$ regardless of the function parameter value φ . Hence, the maximal quality level $Q_{\max}(f_{\text{TTC}})$ from (4.3) that the TTC-based decision rule $f_{\text{TTC}}(\cdot; \varphi)$ can achieve when adjusting its function parameter $\varphi = \varphi$ is almost 0. This means that there is no function parameter value φ for which the TTC-based decision rule $f_{\text{TTC}}(\cdot; \varphi)$ can fulfill the specification $x_{\min} \leq x_{\text{end}} \leq x_{\max}$ for the customer satisfaction with high probability in both considered driving scenarios ξ_1 and ξ_2 . For the two other considered decision rules, however, such a function parameter value φ exists. The maximal achievable quality level of the advanced TTC-based decision rule $f_{\text{adv. TTC}}(\cdot; \varphi)$ and the BTN-based decision rule $f_{\text{BTN}}(\cdot; \varphi)$ is $Q_{\max}(f_{\text{adv. TTC}}) = 0.99994$ and

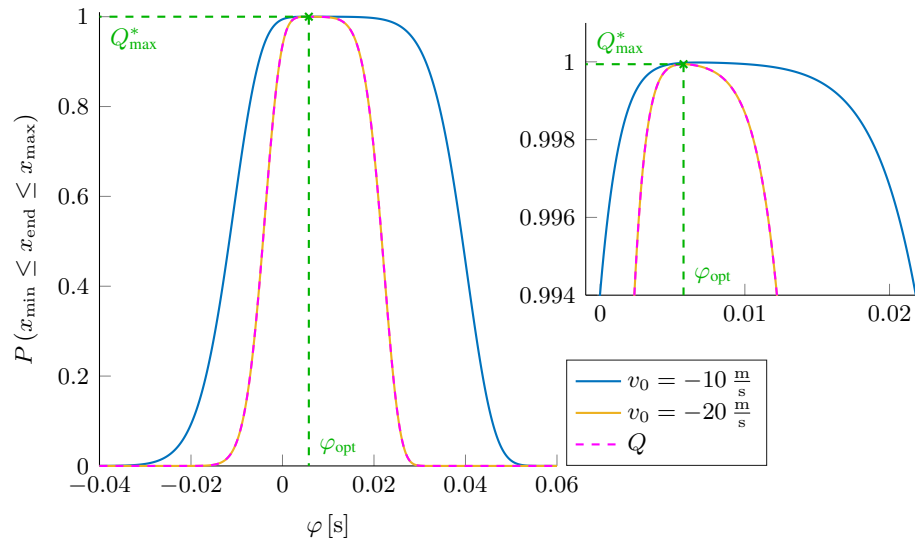


Figure 6.7: Probability that the considered AEB system fulfills the specification $x_{\min} \leq x_{\text{end}} \leq x_{\max}$ for the customer satisfaction for $v_0 = -10 \frac{\text{m}}{\text{s}}$ and $v_0 = -20 \frac{\text{m}}{\text{s}}$ as well as the minimum thereof, i.e., the quality measure Q , vs. the function parameter φ for $\sigma_x = 0.1 \text{ m}$, $\sigma_v = 0$, $x_0 = 50 \text{ m}$, $f_s = 1 \text{ kHz}$, $a = 10 \frac{\text{m}}{\text{s}^2}$, $x_{\min} = 0$, $x_{\max} = 0.5 \text{ m}$ and the advanced TTC-based decision rule $f_{\text{adv. TTC}}(\cdot; \varphi)$ with the optimal function parameter value φ_{opt} determined by the function design.

6.3 Numerical Examples for the Robust Design of the Automatic Emergency Braking System

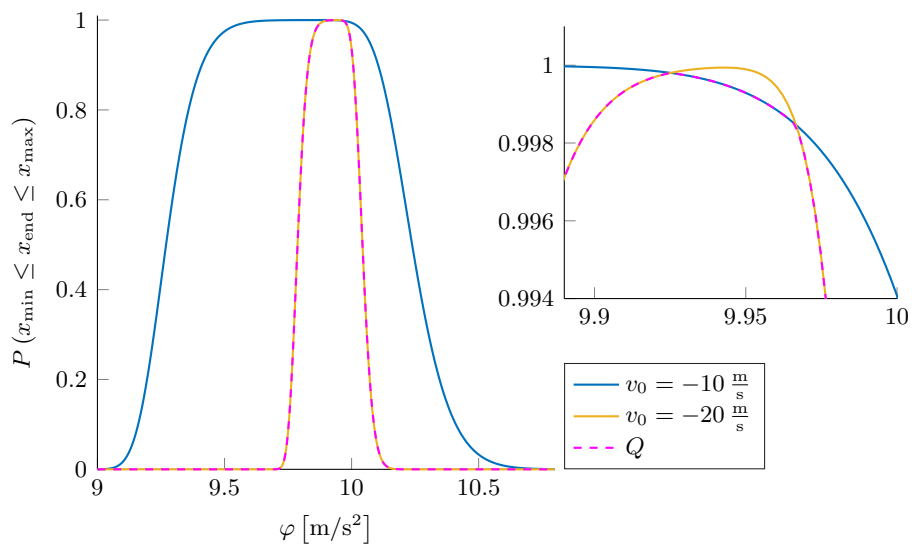


Figure 6.8: Probability that the considered AEB system fulfills the specification $x_{\min} \leq x_{\text{end}} \leq x_{\max}$ for the customer satisfaction for $v_0 = -10 \frac{\text{m}}{\text{s}}$ and $v_0 = -20 \frac{\text{m}}{\text{s}}$ as well as the minimum thereof, i.e., the quality measure Q , vs. the function parameter φ for $\sigma_x = 0.1 \text{ m}$, $\sigma_v = 0$, $x_0 = 50 \text{ m}$, $f_s = 1 \text{ kHz}$, $a = 10 \frac{\text{m}}{\text{s}^2}$, $x_{\min} = 0$, $x_{\max} = 0.5 \text{ m}$ and the BTN-based decision rule $f_{\text{BTN}}(\cdot; \varphi)$.

$Q_{\max}(f_{\text{BTN}}) = 0.99980$, respectively. Based on the ranking of three decision rules f in the set \mathcal{F} of the predefined decision rules with respect to the maximal achievable quality level $Q_{\max}(f)$, i.e., $Q_{\max}(f_{\text{TTC}}) < Q_{\max}(f_{\text{BTN}}) < Q_{\max}(f_{\text{adv. TTC}})$, the BTN-based decision rule f_{BTN} is significantly better than the TTC-based decision rule f_{TTC} and the advanced TTC-based decision rule $f_{\text{adv. TTC}}$ is even slightly better than the BTN-based decision rule f_{BTN} . Thus, the advanced TTC-based decision rule $f_{\text{adv. TTC}}$ is the best decision rule $f_{\text{opt}} = f_{\text{adv. TTC}}$ and the maximal quality level $Q_{\max}(f_{\text{adv. TTC}})$ achieved by it is the highest maximal achievable quality level Q_{\max}^* of all considered decision rules from (4.4), i.e., $Q_{\max}^* = Q_{\max}(f_{\text{adv. TTC}}) = 0.99994$. The point where the quality measure Q is equal to this highest maximal achievable quality level Q_{\max}^* is marked with a green cross and the corresponding function parameter value φ is the optimal function parameter value φ_{opt} , which together with the best decision rule $f_{\text{opt}} = f_{\text{adv. TTC}}$ forms the solution of the optimization problem (6.131) of the function design.

Using the advanced TTC-based decision rule $f_{\text{adv. TTC}}(\cdot; \varphi_{\text{opt}})$ with the optimal function parameter value φ_{opt} guarantees that the specification $x_{\min} \leq x_{\text{end}} \leq x_{\max}$ for the customer satisfaction is fulfilled with the probability $P(x_{\min} \leq x_{\text{end}} \leq x_{\max})|_{f=f_{\text{adv. TTC}}, \varphi=\varphi_{\text{opt}}}$ of at least Q_{\max}^* in each of the two considered driving scenarios ξ_1 and ξ_2 . In the driving scenario ξ_2 with the initial relative velocity $v_0 = -20 \frac{\text{m}}{\text{s}}$, the probability $P(x_{\min} \leq x_{\text{end}} \leq x_{\max})|_{f=f_{\text{adv. TTC}}, \varphi=\varphi_{\text{opt}}}$ of fulfilling this specification is exactly Q_{\max}^* while, in the driving scenario ξ_1 with the initial relative velocity $v_0 = -10 \frac{\text{m}}{\text{s}}$, it is even higher. This makes the driving scenario ξ_2 the worst-case driving scenario, which forms the set of the worst-case driving scenarios defined in (4.38):

$$\begin{aligned} \mathcal{X}_{\text{WC}} &= \left\{ \xi' \in \mathcal{X} = \{\xi_1, \xi_2\} : P(x_{\min} \leq x_{\text{end}} \leq x_{\max})|_{f=f_{\text{adv. TTC}}, \varphi=\varphi_{\text{opt}}, \xi=\xi'} \right. \\ &\quad \left. = \min_{\xi \in \mathcal{X}} P(x_{\min} \leq x_{\text{end}} \leq x_{\max})|_{f=f_{\text{adv. TTC}}, \varphi=\varphi_{\text{opt}}} = Q_{\max}^* \right\} = \{\xi_2\}. \end{aligned} \quad (6.132)$$

Although the advanced TTC-based decision rule $f_{\text{adv. TTC}}(\cdot; \varphi)$ achieves the largest minimum of the probability $P(x_{\min} \leq x_{\text{end}} \leq x_{\max})$ that the specification for the customer satisfaction is fulfilled in the two considered driving scenarios ξ_1 and ξ_2 , it can be observed that the largest probability $P(x_{\min} \leq x_{\text{end}} \leq x_{\max})$ of fulfilling this specification achieved by the considered decision rules in the individual driving scenarios when adjusting their function parameter φ is equal for all three of them. So, they would perform equally well if the function was designed for only one of the two considered driving scenarios ξ_1 and ξ_2 either with the initial relative velocity

6.3 Numerical Examples for the Robust Design of the Automatic Emergency Braking System

$v_0 = -10 \frac{\text{m}}{\text{s}}$ or $v_0 = -20 \frac{\text{m}}{\text{s}}$ while they do not if the function is designed jointly for all of them, where only a single function parameter value φ is allowed for all considered driving scenarios.

With the quality measure Q in (6.69), the constraint of the optimization problem (4.11) for the joint function and sensor design becomes the constraint in (6.70), where the required minimum worst-case probability P_{\min} of fulfilling the specification $x_{\min} \leq x_{\text{end}} \leq x_{\max}$ for the customer satisfaction is the required minimum quality level Q_{\min} according to (4.39). So, with the same costs $C = -\sigma_x$ or, alternatively, $C = \sigma_x^{-1}$ as in the joint function and sensor design for the single driving scenario ξ_0 and the TTC-based decision rule $f_{\text{TTC}}(\cdot; \varphi)$ before, the possible domain \mathcal{S} of the sensor parameter values σ in (6.122) and the single function parameter $\varphi = \varphi$ parameterizing the TTC-based decision rule $f_{\text{TTC}}(\cdot; \varphi)$, the advanced TTC-based decision rule $f_{\text{adv. TTC}}(\cdot; \varphi)$ and the BTN-based decision rule $f_{\text{BTN}}(\cdot; \varphi)$ in the set \mathcal{F} of the predefined decision rules as in the function design before, the optimization problem (4.11) of the joint function and sensor design reads

$$\begin{aligned}
 & (\sigma_{x,\max}, f_{\text{opt}}, \varphi_{\text{opt}}) = \\
 & \quad \underset{\sigma_x \in \mathbb{R}^+, f \in \mathcal{F}, \varphi \in \mathbb{R}}{\operatorname{argmin}} \quad C \\
 & \quad \text{s.t.} \quad \min_{\xi \in \mathcal{X}} P(x_{\min} \leq x_{\text{end}} \leq x_{\max})|_{\sigma_v=0, f_s=1 \text{ kHz}} \geq P_{\min} \quad (6.133) \\
 & = \quad \underset{\sigma_x \in \mathbb{R}^+, f \in \mathcal{F}, \varphi \in \mathbb{R}}{\operatorname{argmax}} \quad \sigma_x \\
 & \quad \text{s.t.} \quad \min_{\xi \in \mathcal{X}} P(x_{\min} \leq x_{\text{end}} \leq x_{\max})|_{\sigma_v=0, f_s=1 \text{ kHz}} \geq P_{\min}.
 \end{aligned}$$

Again, the minimization of the cost function C , whose costs C decrease with increasing standard deviation σ_x of the sensor measurement errors in the measured distance, is converted into the maximization of this standard deviation σ_x .

For each of the three considered decision rules in \mathcal{F} , Figures 6.9, 6.10 and 6.11 show the contour lines of the probability $P(x_{\min} \leq x_{\text{end}} \leq x_{\max})$ of fulfilling the specification for the customer satisfaction in each of the two considered driving scenarios ξ_1 and ξ_2 with the initial relative velocities $v_0 = -10 \frac{\text{m}}{\text{s}}$ and $v_0 = -20 \frac{\text{m}}{\text{s}}$, respectively, as well as of the minimum thereof, i.e., the quality measure Q from (6.69), along which they have the constant value 0.99. In case of the required minimum worst-case probability $P_{\min} = 0.99$ of fulfilling the specification for the customer satisfaction, these contour lines of the probability $P(x_{\min} \leq x_{\text{end}} \leq x_{\max})$ of fulfilling the specification for the customer satisfaction in each of the two considered driving scenarios ξ_1 and ξ_2 are the boundaries of the blue areas, where this probability is at

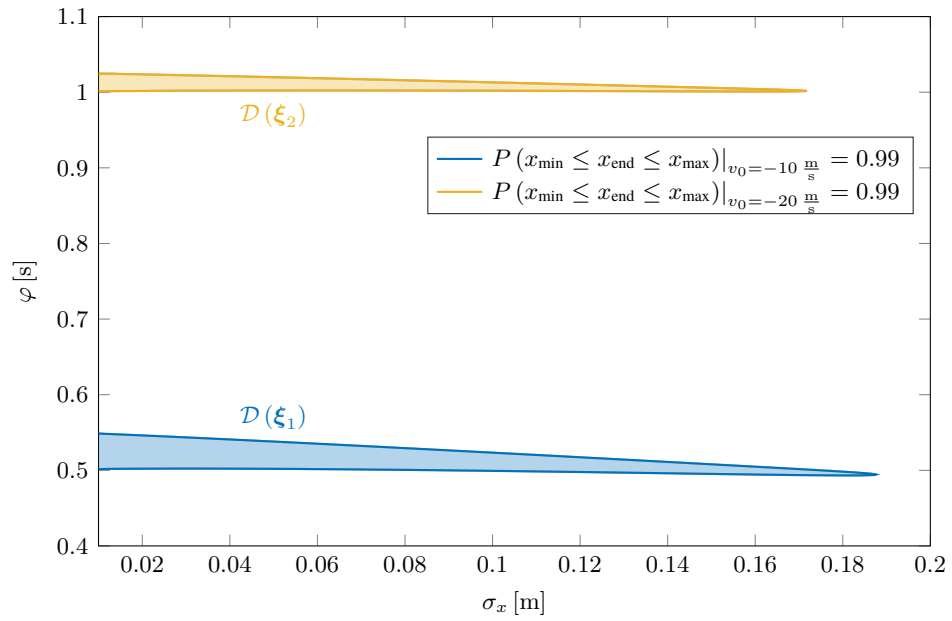


Figure 6.9: Contour lines of the probability that the considered AEB system fulfills the specification $x_{\min} \leq x_{\text{end}} \leq x_{\max}$ for the customer satisfaction for $v_0 = -10 \frac{\text{m}}{\text{s}}$ and $v_0 = -20 \frac{\text{m}}{\text{s}}$ at height 0.99, which are the boundaries of the respective individual design space partitions $\mathcal{D}(\xi_1)$ and $\mathcal{D}(\xi_2)$ in the joint function and sensor design in case of $P_{\min} = 0.99$, for $\sigma_v = 0$, $x_0 = 50$ m, $f_s = 1$ kHz, $a = 10 \frac{\text{m}}{\text{s}^2}$, $x_{\min} = 0$, $x_{\max} = 0.5$ m and the TTC-based decision rule $f_{\text{TTC}}(\cdot; \varphi)$.

6.3 Numerical Examples for the Robust Design of the Automatic Emergency Braking System

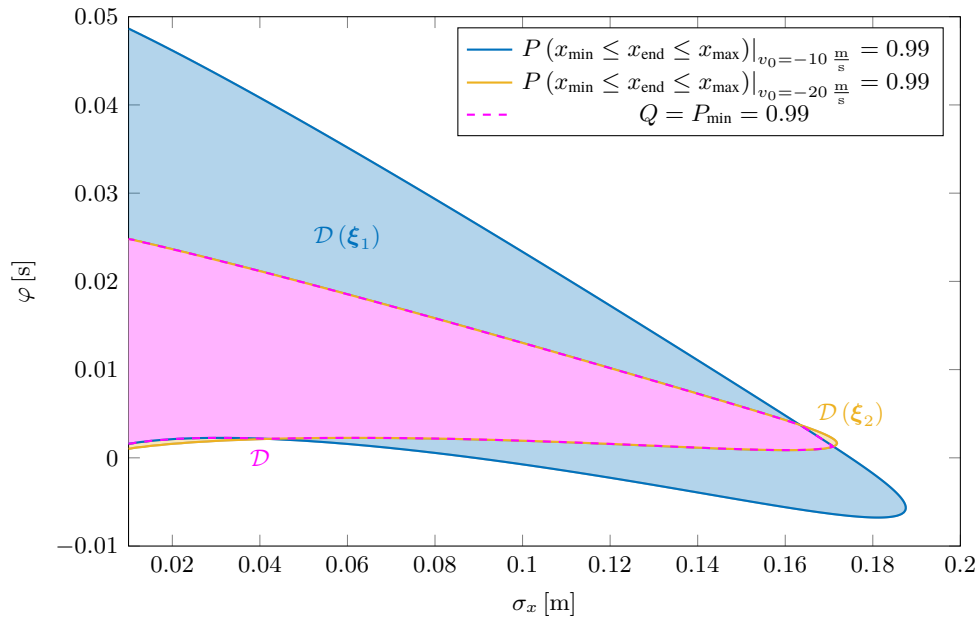


Figure 6.10: Contour lines of the probability that the considered AEB system fulfills the specification $x_{\min} \leq x_{\text{end}} \leq x_{\max}$ for the customer satisfaction for $v_0 = -10 \frac{\text{m}}{\text{s}}$ and $v_0 = -20 \frac{\text{m}}{\text{s}}$ as well as of the minimum thereof, i.e., the quality measure Q , at height 0.99, which are the boundaries of the respective individual design space partitions $\mathcal{D}(\xi_1)$ and $\mathcal{D}(\xi_2)$ and design space \mathcal{D} in the joint function and sensor design in case of $P_{\min} = 0.99$, for $\sigma_v = 0$, $x_0 = 50 \text{ m}$, $f_s = 1 \text{ kHz}$, $a = 10 \frac{\text{m}}{\text{s}^2}$, $x_{\min} = 0$, $x_{\max} = 0.5 \text{ m}$ and the advanced TTC-based decision rule $f_{\text{adv. TTC}}(\cdot; \varphi)$.

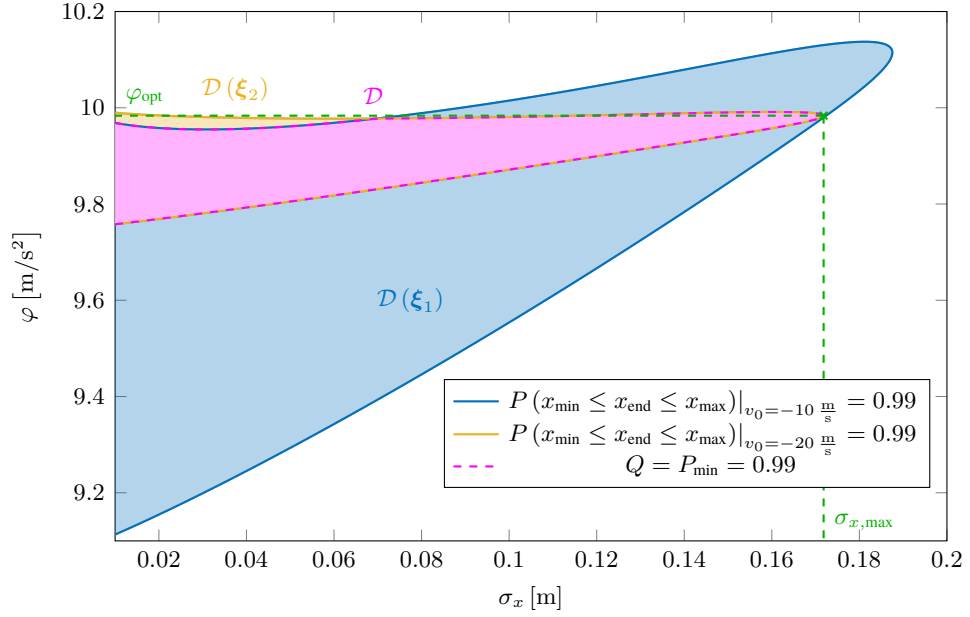


Figure 6.11: Contour lines of the probability that the considered AEB system fulfills the specification $x_{\min} \leq x_{\text{end}} \leq x_{\max}$ for the customer satisfaction for $v_0 = -10 \frac{\text{m}}{\text{s}}$ and $v_0 = -20 \frac{\text{m}}{\text{s}}$ as well as of the minimum thereof, i.e., the quality measure Q , at height 0.99, which are the boundaries of the respective individual design space partitions $\mathcal{D}(\xi_1)$ and $\mathcal{D}(\xi_2)$ and design space \mathcal{D} in the joint function and sensor design in case of $P_{\min} = 0.99$, for $\sigma_v = 0$, $x_0 = 50 \text{ m}$, $f_s = 1 \text{ kHz}$, $a = 10 \frac{\text{m}}{\text{s}^2}$, $x_{\min} = 0$, $x_{\max} = 0.5 \text{ m}$ and the BTN-based decision rule $f_{\text{BTN}}(\cdot; \varphi)$ with the optimal function parameter value φ_{opt} and the maximal tolerable standard deviation $\sigma_{x,\max}$ of the sensor measurement errors in the measured distance determined by the joint function and sensor design in case of $P_{\min} = 0.99$.

6.3 Numerical Examples for the Robust Design of the Automatic Emergency Braking System

least $P_{\min} = 0.99$ in the driving scenario ξ_1 and which represent the individual design space partition $\mathcal{D}(\xi_1)$ for the driving scenario ξ_1 , and the yellow areas, where this probability is at least $P_{\min} = 0.99$ in the driving scenario ξ_2 and which represent the individual design space partition $\mathcal{D}(\xi_2)$ for the driving scenario ξ_2 , respectively. According to (4.44), the individual design space partition $\mathcal{D}(\xi_i)$ for the driving scenario ξ_i , $i \in \{1, 2\}$, with the initial distance $x_0 = 50$ m and the initial relative velocity

$$v_{0,i} = \begin{cases} -10 \frac{\text{m}}{\text{s}}, & i = 1 \\ -20 \frac{\text{m}}{\text{s}}, & i = 2 \end{cases} \quad (6.134)$$

is the set of all sensor parameter values σ in the possible domain \mathcal{S} , decision rules f from the set \mathcal{F} of the predefined decision rules for triggering the emergency brake intervention and function parameter values φ for which the probability of fulfilling the specification $x_{\min} \leq x_{\text{end}} \leq x_{\max}$ for the customer satisfaction in the driving scenario $\xi = \xi_i$ with the initial distance $x_0 = 50$ m and the initial relative velocity $v_0 = v_{0,i}$ does not lie below the required minimum worst-case probability P_{\min} of fulfilling this specification for the customer satisfaction:

$$\mathcal{D}(\xi_i) = \left\{ (\sigma, f, \varphi) \in \mathcal{S} \times \mathcal{F} \times \mathbb{R}^{N_\varphi} : \right. \\ \left. P(x_{\min} \leq x_{\text{end}} \leq x_{\max})|_{x_0=50 \text{ m}, v_0=v_{0,i}} \geq P_{\min} \right\}. \quad (6.135)$$

With the special possible domain \mathcal{S} of the sensor parameter values σ in (6.122) and the set \mathcal{F} of the predefined decision rules in (6.130) consisting of the TTC-based decision rule $f_{\text{TTC}}(\cdot; \varphi)$, the advanced TTC-based decision rule $f_{\text{adv. TTC}}(\cdot; \varphi)$ and the BTN-based decision rule $f_{\text{BTN}}(\cdot; \varphi)$ with the single function parameter $\varphi = \varphi$, i.e., $N_\varphi = 1$, the individual design space partition $\mathcal{D}(\xi_i)$ for the driving scenario ξ_i reads

$$\mathcal{D}(\xi_i) = \left\{ (\sigma, f, \varphi) = \left([\sigma_x, 0, 1 \text{ kHz}]^T, f, \varphi \right) \right. \\ \left. \in \mathbb{R}^3 \times \{f_{\text{TTC}}, f_{\text{adv. TTC}}, f_{\text{BTN}}\} \times \mathbb{R} : \sigma_x \in \mathbb{R}^+, \right. \\ \left. P(x_{\min} \leq x_{\text{end}} \leq x_{\max})|_{x_0=50 \text{ m}, v_0=v_{0,i}, \sigma_v=0, f_s=1 \text{ kHz}} \geq P_{\min} \right\} \quad (6.136)$$

in this case.

As stated in (4.45), the intersection of the individual design space partitions $\mathcal{D}(\xi')$

for all driving scenarios ξ' from the scenario set \mathcal{X} , i.e., ξ_1 and ξ_2 , is the design space

$$\begin{aligned} \mathcal{D} &= \mathcal{D}(\xi_1) \cap \mathcal{D}(\xi_2) \\ &= \left\{ (\sigma, f, \varphi) = \left([\sigma_x, 0, 1 \text{ kHz}]^T, f, \varphi \right) \right. \\ &\quad \left. \in \mathbb{R}^3 \times \{f_{\text{TTC}}, f_{\text{adv. TTC}}, f_{\text{BTN}}\} \times \mathbb{R} : \sigma_x \in \mathbb{R}^+, \right. \\ &\quad \left. \min_{\xi \in \mathcal{X}} P(x_{\min} \leq x_{\text{end}} \leq x_{\max})|_{\sigma_v=0, f_s=1 \text{ kHz}} \geq P_{\min} \right\}. \end{aligned} \quad (6.137)$$

It is the set of all sensor parameter values σ in the possible domain \mathcal{S} from (6.122), decision rules f from the set \mathcal{F} of the predefined decision rules for triggering the emergency brake intervention in (6.130) and function parameter values $\varphi = \varphi$ for which the probability of fulfilling the specification $x_{\min} \leq x_{\text{end}} \leq x_{\max}$ for the customer satisfaction in both considered driving scenarios ξ_1 and ξ_2 with the initial relative velocities $v_0 = -10 \frac{\text{m}}{\text{s}}$ and $v_0 = -20 \frac{\text{m}}{\text{s}}$, respectively, and thus also their minimum, the quality measure Q in (6.69), do not lie below the required minimum worst-case probability P_{\min} of fulfilling this specification for the customer satisfaction, the required minimum quality level Q_{\min} , as defined by (4.16) in general and is highlighted by the magenta areas in Figures 6.9, 6.10 and 6.11. It can be observed that there is no magenta area for the TTC-based decision rule $f_{\text{TTC}}(\cdot; \varphi)$. This means that, when using the TTC-based decision rule $f_{\text{TTC}}(\cdot; \varphi)$, i.e., $f = f_{\text{TTC}}$, no pair (σ_x, φ) consisting of a value of the standard deviation σ_x of the sensor measurement errors in the measured distance and a function parameter value φ inside the design space \mathcal{D} exists that can fulfill the constraint of the optimization problem (6.133) to be solved in the joint function and sensor design such that also no maximal value $\sigma_{x,\max}(f_{\text{TTC}})$ of the standard deviation σ_x of the sensor measurement errors in the measured distance inside the design space \mathcal{D} and no minimal reachable costs $C_{\min}(f_{\text{TTC}}) = -\sigma_{x,\max}(f_{\text{TTC}})$ in case of the costs $C = -\sigma_x$ or $C_{\min}(f_{\text{TTC}}) = (\sigma_{x,\max}(f_{\text{TTC}}))^{-1}$ in case of the costs $C = \sigma_x^{-1}$ corresponding to this value $\sigma_{x,\max}(f_{\text{TTC}})$ of σ_x exist. For the advanced TTC-based decision rule $f_{\text{adv. TTC}}(\cdot; \varphi)$ and the BTN-based decision rule $f_{\text{BTN}}(\cdot; \varphi)$, however, such pairs (σ_x, φ) inside the design space \mathcal{D} exist. The maximal value of the standard deviation σ_x of the sensor measurement errors in the measured distance inside it is $\sigma_{x,\max}(f_{\text{adv. TTC}}) = 0.17101 \text{ m}$ and $\sigma_{x,\max}(f_{\text{BTN}}) = 0.17183 \text{ m}$ for the advanced TTC-based decision rule $f_{\text{adv. TTC}}(\cdot; \varphi)$ and the BTN-based decision rule $f_{\text{BTN}}(\cdot; \varphi)$, respectively. The corresponding minimal reachable costs of the advanced TTC-based decision rule $f_{\text{adv. TTC}}(\cdot; \varphi)$ and the BTN-based decision rule $f_{\text{BTN}}(\cdot; \varphi)$ are $C_{\min}(f_{\text{adv. TTC}}) = -\sigma_{x,\max}(f_{\text{adv. TTC}}) = -0.17101 \text{ m}$ in case of the costs $C = -\sigma_x$ or $C_{\min}(f_{\text{adv. TTC}}) = (\sigma_{x,\max}(f_{\text{adv. TTC}}))^{-1} = 0.17101^{-1} \text{ m}^{-1}$ in case of the

6.3 Numerical Examples for the Robust Design of the Automatic Emergency Braking System

costs $C = \sigma_x^{-1}$ and $C_{\min}(f_{\text{BTN}}) = -\sigma_{x,\max}(f_{\text{BTN}}) = -0.17183 \text{ m}$ in case of the costs $C = -\sigma_x$ or $C_{\min}(f_{\text{BTN}}) = (\sigma_{x,\max}(f_{\text{BTN}}))^{-1} = 0.17183^{-1} \text{ m}^{-1}$ in case of the costs $C = \sigma_x^{-1}$, respectively. Based on the ranking of three decision rules f in the set \mathcal{F} of the predefined decision rules with respect to the minimal reachable costs $C_{\min}(f)$, i.e., the non-existing $C_{\min}(f_{\text{TTC}})$ and $C_{\min}(f_{\text{BTN}}) < C_{\min}(f_{\text{adv. TTC}})$, the BTN-based decision rule f_{BTN} is slightly better than the advanced TTC-based decision rule $f_{\text{adv. TTC}}$. Hence, the BTN-based decision rule f_{BTN} is the best decision rule f_{opt} and the minimal costs $C_{\min}(f_{\text{BTN}})$ that are reached by it and correspond to the maximal value $\sigma_{x,\max}(f_{\text{BTN}})$ of the standard deviation σ_x of the sensor measurement errors in the measured distance inside the design space \mathcal{D} for this decision rule are the smallest minimal reachable costs C_{\min}^* of all considered decision rules from (4.15), i.e., $C_{\min}^* = C_{\min}(f_{\text{BTN}})$, which correspond to the maximal tolerable standard deviation $\sigma_{x,\max}$ of the sensor measurement errors in the measured distance, i.e., $\sigma_{x,\max} = \sigma_{x,\max}(f_{\text{BTN}}) = 0.17183 \text{ m}$. The point inside the design space \mathcal{D} where the standard deviation σ_x of the sensor measurement errors in the measured distance is equal to this maximal value $\sigma_{x,\max}$ and the corresponding costs C are equal to the smallest minimal reachable costs C_{\min}^* is marked with a green cross and the corresponding function parameter value φ is the optimal function parameter value φ_{opt} , which together with the best decision rule $f_{\text{opt}} = f_{\text{BTN}}$ and the maximal tolerable standard deviation $\sigma_{x,\max}$ of the sensor measurement errors in the measured distance forms the solution of the optimization problem (6.133) of the joint function and sensor design.

The difference in the maximal value $\sigma_{x,\max}(f)$ of the standard deviation σ_x of the sensor measurement errors in the measured distance inside the design space \mathcal{D} and thus in the minimal reachable costs $C_{\min}(f)$ for the different considered decision rules f , i.e., the TTC-, advanced TTC- and BTN-based decision rules defined by the decision functions $f_{\text{TTC}}(\cdot; \varphi)$ in (6.58), $f_{\text{adv. TTC}}(\cdot; \varphi)$ in (6.61) and $f_{\text{BTN}}(\cdot; \varphi)$ in (6.65), respectively, comes from the fact that these decision functions are different functions of the measured relative velocity $\hat{v}[n] = v[n] = v_0$, which lead to different overlaps between the individual design space partitions $\mathcal{D}(\xi_1)$ and $\mathcal{D}(\xi_2)$ for the two considered driving scenarios with the initial relative velocities $v_0 = -10 \frac{\text{m}}{\text{s}}$ and $v_0 = -20 \frac{\text{m}}{\text{s}}$, whose intersection yields the design space \mathcal{D} . For example, the decision functions $f_{\text{adv. TTC}}(\cdot; \varphi)$ and $f_{\text{BTN}}(\cdot; \varphi)$ of the advanced TTC- and the BTN-based decision rules are a function of the square of the measured relative velocity $\hat{v}[n] = v[n] = v_0$ whereas the decision function $f_{\text{TTC}}(\cdot; \varphi)$ of the TTC-based decision rule is not. However, it can be observed that the maximal value of the standard deviation σ_x of the sensor measurement errors in the measured distance inside the design space partition $\mathcal{D}(\xi_i)$ for a driving scenario ξ_i , $i \in \{1, 2\}$, is equal for all three considered

decision rules f . Hence, all three considered decision rules f would be equally good if the AEB system was designed for only one of the two considered driving scenarios ξ_1 and ξ_2 either with the initial relative velocity $v_0 = -10 \frac{\text{m}}{\text{s}}$ or $v_0 = -20 \frac{\text{m}}{\text{s}}$. There is only a difference in how good they are if the AEB system is designed jointly for all considered driving scenarios, where only a single function parameter value φ is allowed for all considered driving scenarios.

6.3.3 Erroneous Distance and Relative Velocity Measurements

After assuming the relative velocity of the ego vehicle and the object to be measured without errors so far, both their distance and relative velocity are assumed to be measured with sensor measurement errors in the following. This assumption that the standard deviation σ_v of the sensor measurement errors in the measured relative velocity is not 0 anymore but positive as the standard deviation σ_x of the sensor measurement errors in the measured distance, extends the possible domain for the values of the sensor parameters σ from (6.122) to

$$\begin{aligned} \mathcal{S} &= \left\{ \sigma = [\sigma_x, \sigma_v, f_s]^T \in \mathbb{R}^3 : \sigma_x, \sigma_v \in \mathbb{R}^+ \wedge f_s = 1 \text{ kHz} \right\} \\ &= \left\{ \sigma = [\sigma_x, \sigma_v, 1 \text{ kHz}]^T \in \mathbb{R}^3 : \sigma_x, \sigma_v \in \mathbb{R}^+ \right\}. \end{aligned} \quad (6.138)$$

As in the previous numerical examples, the deceleration after triggering the emergency brake intervention is $a = 10 \frac{\text{m}}{\text{s}^2}$, and the minimal and maximal tolerable final distances between the ego vehicle and the object after the emergency brake intervention are $x_{\min} = 0$ and $x_{\max} = 0.5$ m, respectively. For the sake of simplicity, only the driving scenario that is shown in Figure 6.1 and characterized by the scenario parameters ξ_0 of the form given by (6.47) with the initial distance $x_0 = 10$ m and the initial relative velocity $v_0 = -10 \frac{\text{m}}{\text{s}}$ is considered as in the first numerical examples. Hence, the scenario set \mathcal{X} again consist of only this single driving scenario: $\mathcal{X} = \{\xi_0\}$.

Table 6.3 states the values of the probability $P(x_{\min} \leq x_{\text{end}} \leq x_{\max})$ of fulfilling the specification for the customer satisfaction obtained by evaluating its expression in (6.99) using (6.77) and (6.78) for the TTC-based decision rule $f_{\text{TTC}}(\cdot; \varphi)$ and different values of the standard deviation σ_x of the sensor measurement errors in the measured distance, the standard deviation σ_v of the sensor measurement errors in the measured relative velocity and the function parameter φ .

The probability $P(x_{\min} \leq x_{\text{end}} \leq x_{\max})$ of fulfilling the specification $x_{\min} \leq x_{\text{end}} \leq x_{\max}$ for the customer satisfaction can also be estimated by a Monte Carlo simulation. In general, the Monte-Carlo-simulation-based estimate for the probability $P(\mathbf{q} \in \mathcal{A}_{\mathbf{q}})$ of fulfilling all specifications $q_{L,i} \leq q_i \leq q_{U,i}$, $i = 1, 2, \dots, N_{\mathbf{q}}$, for the

6.3 Numerical Examples for the Robust Design of the Automatic Emergency Braking System

	$\sigma_v = 0.1 \frac{\text{m}}{\text{s}}$	$\sigma_v = 0.2 \frac{\text{m}}{\text{s}}$	$\sigma_v = 0.3 \frac{\text{m}}{\text{s}}$	$\sigma_v = 0.4 \frac{\text{m}}{\text{s}}$
$\sigma_x = 0.1 \text{ m}$	0.01281	0.07463	0.26990	0.56125
$\sigma_x = 0.2 \text{ m}$	0.50817	0.61534	0.75049	0.85946
$\sigma_x = 0.3 \text{ m}$	0.90221	0.90384	0.89264	0.85494
$\sigma_x = 0.4 \text{ m}$	0.70521	0.67381	0.62060	0.54628

(a) $\varphi = 0.47 \text{ s}$

	$\sigma_v = 0.1 \frac{\text{m}}{\text{s}}$	$\sigma_v = 0.2 \frac{\text{m}}{\text{s}}$	$\sigma_v = 0.3 \frac{\text{m}}{\text{s}}$	$\sigma_v = 0.4 \frac{\text{m}}{\text{s}}$
$\sigma_x = 0.1 \text{ m}$	0.72458	0.89313	0.97263	0.97576
$\sigma_x = 0.2 \text{ m}$	0.98197	0.97375	0.94002	0.85727
$\sigma_x = 0.3 \text{ m}$	0.76597	0.71443	0.62608	0.50532
$\sigma_x = 0.4 \text{ m}$	0.30145	0.26714	0.21686	0.15989

(b) $\varphi = 0.49 \text{ s}$

	$\sigma_v = 0.1 \frac{\text{m}}{\text{s}}$	$\sigma_v = 0.2 \frac{\text{m}}{\text{s}}$	$\sigma_v = 0.3 \frac{\text{m}}{\text{s}}$	$\sigma_v = 0.4 \frac{\text{m}}{\text{s}}$
$\sigma_x = 0.1 \text{ m}$	0.99958	0.99041	0.91794	0.71032
$\sigma_x = 0.2 \text{ m}$	0.82285	0.72598	0.55872	0.35728
$\sigma_x = 0.3 \text{ m}$	0.26446	0.21144	0.14363	0.08191
$\sigma_x = 0.4 \text{ m}$	0.03060	0.02382	0.01568	0.00873

(c) $\varphi = 0.51 \text{ s}$

	$\sigma_v = 0.1 \frac{\text{m}}{\text{s}}$	$\sigma_v = 0.2 \frac{\text{m}}{\text{s}}$	$\sigma_v = 0.3 \frac{\text{m}}{\text{s}}$	$\sigma_v = 0.4 \frac{\text{m}}{\text{s}}$
$\sigma_x = 0.1 \text{ m}$	0.85367	0.58408	0.25591	0.07369
$\sigma_x = 0.2 \text{ m}$	0.15925	0.09322	0.03852	0.01164
$\sigma_x = 0.3 \text{ m}$	0.00732	0.00450	0.00205	0.00071
$\sigma_x = 0.4 \text{ m}$	0.00017	0.00011	0.00006	0.00002

(d) $\varphi = 0.53 \text{ s}$

Table 6.3: Probability $P(x_{\min} \leq x_{\text{end}} \leq x_{\max})$ that the considered AEB system fulfills the specification $x_{\min} \leq x_{\text{end}} \leq x_{\max}$ for the customer satisfaction for $x_0 = 10 \text{ m}$, $v_0 = -10 \frac{\text{m}}{\text{s}}$, $f_s = 1 \text{ kHz}$, $a = 10 \frac{\text{m}}{\text{s}^2}$, $x_{\min} = 0$, $x_{\max} = 0.5 \text{ m}$ and the TTC-based decision rule $f_{\text{TTC}}(\cdot; \varphi)$.

customer satisfaction in case of given sensor parameters σ , a given decision rule f , given function parameters φ and scenario parameters ξ is the frequency $\hat{P}_M(\mathbf{q} \in \mathcal{A}_q)$ of fulfilling all these specifications in the Monte Carlo simulation from (5.1). In the Monte Carlo simulation, M realizations $\varepsilon_1, \varepsilon_2, \dots, \varepsilon_M$ of all sensor measurement errors

$$\varepsilon = \left[\varepsilon_x [0] \quad \varepsilon_v [0] \quad \varepsilon_x [1] \quad \varepsilon_v [1] \quad \cdots \quad \varepsilon_x [n_{\text{end}}] \quad \varepsilon_v [n_{\text{end}}] \right]^T \in \mathbb{R}^{2(n_{\text{end}}+1)} \quad (6.139)$$

at all time instants $t_n, n = 0, 1, \dots, n_{\text{end}}$, in the considered time interval according to (4.21) and (6.52) are generated at random according to their probability distribution, i.e., the i.i.d. sensor measurement errors $\varepsilon_x [n]$ in the measured distance and the i.i.d. sensor measurement errors $\varepsilon_v [n]$ in the measured relative velocity at these time instants t_n , which are also statistically independent from each other at the same time instant t_n , are drawn from the zero-mean Gaussian distribution $\mathcal{N}(0, \sigma_x^2)$ with the standard deviation σ_x and the zero-mean Gaussian distribution $\mathcal{N}(0, \sigma_v^2)$ with the standard deviation σ_v , respectively. Here, the discrete time index n_{end} of the last time instant $t_{n_{\text{end}}}$ of the considered time interval is chosen to be that of the last time instant before the collision of the ego vehicle and the object that would occur without emergency brake intervention. In this case, where the last time instant $t_{n_{\text{end}}}$ of the considered time interval, which starts at the time instant $t_0 = 0$, lies before the time instant t_b at which the emergency brake intervention is triggered, i.e., $t_{n_{\text{end}}} < t_b$, the distance between the ego vehicle and the object at this time instant $t_{n_{\text{end}}} = n_{\text{end}}/f_s$ is

$$x(t_{n_{\text{end}}}) = v_0 t_{n_{\text{end}}} + x_0 = v_0 \frac{n_{\text{end}}}{f_s} + x_0 \quad (6.140)$$

according to (6.42). For $x(t_{n_{\text{end}}}) = 0$, the collision would start immediately after this time instant $t_{n_{\text{end}}}$ and its discrete time index n_{end} would be $-f_s x_0 / v_0$. As the discrete time index n_{end} of the last time instant before the collision is a non-negative integer, it is

$$n_{\text{end}} = \left\lfloor -f_s \frac{x_0}{v_0} \right\rfloor. \quad (6.141)$$

Each realization $\varepsilon_m, m = 1, 2, \dots, M$, of the sensor measurement errors ε together with the given sensor parameters σ , the given decision rule f , the given function parameters φ , i.e., the single function parameter $\varphi = \varphi$ parameterizing the TTC-based decision rule $f_{\text{TTC}}(\cdot; \varphi)$, the advanced TTC-based decision rule $f_{\text{adv. TTC}}(\cdot; \varphi)$ and the BTN-based decision rule $f_{\text{BTN}}(\cdot; \varphi)$, and the scenario parameters $\xi = \xi_0$ is mapped to the respective values $\mathbf{q}_m = \mathbf{q}(\sigma, \varepsilon_m, f, \varphi, \xi)$ of the customer satisfaction properties \mathbf{q} , i.e., the respective value of the final distance x_{end} between the ego vehicle and

the object, the only customer satisfaction property $\mathbf{q} = q_1 = x_{\text{end}}$ considered here, according to (4.22) by a simulation of the AEB system. After computing the measured distance $\hat{x}[n]$ in (6.49) and the measured relative velocity $\hat{v}[n]$ in (6.50) forming the measurement vector $\mathbf{y}[n]$ in (6.51) from the generated sensor measurement errors $\varepsilon_x[n]$ and $\varepsilon_v[n]$, respectively, and evaluating the used decision rule $f_c(\mathbf{y}[n]; \varphi)$, $c \in \{\text{TTC}, \text{adv. TTC}, \text{BTN}\}$, at the time instants t_n , $n = 0, 1, \dots, n_b$, to determine the discrete time index n_b of the time instant t_b at which the emergency brake intervention is triggered as the smallest discrete time index n for which the result of the evaluation of the decision function is $f_c(\mathbf{y}[n]; \varphi) = 1$ according to (6.56), the final distance x_{end} can be computed from it with (6.73). If there is not such a discrete time index n_b in the considered time interval, i.e., $n_b \notin \{0, 1, \dots, n_{\text{end}}\}$, no emergency brake intervention is triggered in this time interval such that the final distance x_{end} after the emergency brake intervention does not exist and the specification $x_{\text{min}} \leq x_{\text{end}} \leq x_{\text{max}}$ for the customer satisfaction is not fulfilled.

In the M random experiments, it is counted how often the value of the final distance x_{end} lies in the acceptance interval $[x_{\text{min}}, x_{\text{max}}]$ and thus fulfills the specification $x_{\text{min}} \leq x_{\text{end}} \leq x_{\text{max}}$ for the customer satisfaction to obtain the number $M_{1,M}$ of how often this is the case and the frequency

$$\hat{P}_M(x_{\text{min}} \leq x_{\text{end}} \leq x_{\text{max}}) = \frac{M_{1,M}}{M} \quad (6.142)$$

of fulfilling the specification $x_{\text{min}} \leq x_{\text{end}} \leq x_{\text{max}}$ for the customer satisfaction, which is an estimate for the probability $P(x_{\text{min}} \leq x_{\text{end}} \leq x_{\text{max}})$ of fulfilling this specification for the customer satisfaction. Table 6.4 states the values of the absolute error $\left| \hat{P}_{10^5}(x_{\text{min}} \leq x_{\text{end}} \leq x_{\text{max}}) - P(x_{\text{min}} \leq x_{\text{end}} \leq x_{\text{max}}) \right|$ between this Monte-Carlo-based estimate $\hat{P}_{10^5}(x_{\text{min}} \leq x_{\text{end}} \leq x_{\text{max}})$ from $M = 10^5$ simulations of the AEB system and the actual probability $P(x_{\text{min}} \leq x_{\text{end}} \leq x_{\text{max}})$ of fulfilling the specification for the customer satisfaction, whose values are given in Table 6.3, for the TTC-based decision rule $f_{\text{TTC}}(\cdot; \varphi)$ and different values of the standard deviation σ_x of the sensor measurement errors in the measured distance, the standard deviation σ_v of the sensor measurement errors in the measured relative velocity and the function parameter φ .

Moreover, the probability $P(x_{\text{min}} \leq x_{\text{end}} \leq x_{\text{max}})$ of fulfilling the specification $x_{\text{min}} \leq x_{\text{end}} \leq x_{\text{max}}$ for the customer satisfaction can also be approximated by using the adaptation of the worst-case distance approach to the robust design of automated vehicular safety systems. In general, the worst-case-distance-based approximation of the probability $P(\mathbf{q} \in \mathcal{A}_q)$ of fulfilling all specifications $q_{L,i} \leq q_i \leq q_{U,i}$, $i = 1, 2, \dots, N_q$, for the customer satisfaction is given by (5.82). Thus, in case of the AEB

	$\sigma_v = 0.1 \frac{\text{m}}{\text{s}}$	$\sigma_v = 0.2 \frac{\text{m}}{\text{s}}$	$\sigma_v = 0.3 \frac{\text{m}}{\text{s}}$	$\sigma_v = 0.4 \frac{\text{m}}{\text{s}}$
$\sigma_x = 0.1 \text{ m}$	0.00045	0.00084	0.00093	0.00141
$\sigma_x = 0.2 \text{ m}$	0.00377	0.00213	0.00108	0.00054
$\sigma_x = 0.3 \text{ m}$	0.00090	0.00057	0.00043	0.00155
$\sigma_x = 0.4 \text{ m}$	0.00203	0.00213	0.00150	0.00244

(a) $\varphi = 0.47 \text{ s}$

	$\sigma_v = 0.1 \frac{\text{m}}{\text{s}}$	$\sigma_v = 0.2 \frac{\text{m}}{\text{s}}$	$\sigma_v = 0.3 \frac{\text{m}}{\text{s}}$	$\sigma_v = 0.4 \frac{\text{m}}{\text{s}}$
$\sigma_x = 0.1 \text{ m}$	0.00108	0.00173	0.00025	0.00023
$\sigma_x = 0.2 \text{ m}$	0.00017	0.00001	0.00118	0.00158
$\sigma_x = 0.3 \text{ m}$	0.00180	0.00139	0.00311	0.00050
$\sigma_x = 0.4 \text{ m}$	0.00054	0.00051	0.00005	0.00025

(b) $\varphi = 0.49 \text{ s}$

	$\sigma_v = 0.1 \frac{\text{m}}{\text{s}}$	$\sigma_v = 0.2 \frac{\text{m}}{\text{s}}$	$\sigma_v = 0.3 \frac{\text{m}}{\text{s}}$	$\sigma_v = 0.4 \frac{\text{m}}{\text{s}}$
$\sigma_x = 0.1 \text{ m}$	0.00012	0.00011	0.00061	0.00131
$\sigma_x = 0.2 \text{ m}$	0.00099	0.00215	0.00068	0.00101
$\sigma_x = 0.3 \text{ m}$	0.00036	0.00015	0.00046	0.00076
$\sigma_x = 0.4 \text{ m}$	0.00001	0.00060	0.00033	0.00000

(c) $\varphi = 0.51 \text{ s}$

	$\sigma_v = 0.1 \frac{\text{m}}{\text{s}}$	$\sigma_v = 0.2 \frac{\text{m}}{\text{s}}$	$\sigma_v = 0.3 \frac{\text{m}}{\text{s}}$	$\sigma_v = 0.4 \frac{\text{m}}{\text{s}}$
$\sigma_x = 0.1 \text{ m}$	0.00116	0.00092	0.00046	0.00064
$\sigma_x = 0.2 \text{ m}$	0.00182	0.00035	0.00049	0.00008
$\sigma_x = 0.3 \text{ m}$	0.00004	0.00022	0.00006	0.00006
$\sigma_x = 0.4 \text{ m}$	0.00002	0.00003	0.00004	0.00000

(d) $\varphi = 0.53 \text{ s}$

Table 6.4: Absolute error $\left| \hat{P}_{10^5}(x_{\min} \leq x_{\text{end}} \leq x_{\max}) - P(x_{\min} \leq x_{\text{end}} \leq x_{\max}) \right|$ between the Monte-Carlo-based estimate $\hat{P}_{10^5}(x_{\min} \leq x_{\text{end}} \leq x_{\max})$ from $M = 10^5$ simulations of the considered AEB system and the actual probability $P(x_{\min} \leq x_{\text{end}} \leq x_{\max})$ of fulfilling the specification $x_{\min} \leq x_{\text{end}} \leq x_{\max}$ for the customer satisfaction for $x_0 = 10 \text{ m}$, $v_0 = -10 \frac{\text{m}}{\text{s}}$, $f_s = 1 \text{ kHz}$, $a = 10 \frac{\text{m}}{\text{s}^2}$, $x_{\min} = 0$, $x_{\max} = 0.5 \text{ m}$ and the TTC-based decision rule $f_{\text{TTC}}(\cdot; \varphi)$.

6.3 Numerical Examples for the Robust Design of the Automatic Emergency Braking System

system at hand, the probability $P(x_{\min} \leq x_{\text{end}} \leq x_{\max})$ of fulfilling the specification $x_{\min} \leq x_{\text{end}} \leq x_{\max}$ for the customer satisfaction can be approximated by

$$\hat{P}(x_{\min} \leq x_{\text{end}} \leq x_{\max}) = \prod_{n \in \bar{\mathbb{I}}} \begin{cases} \Phi(-\beta_n), & \boldsymbol{\mu} \in \mathcal{I}_{\boldsymbol{\varepsilon},n} \\ \Phi(\beta_n), & \boldsymbol{\mu} \in \bar{\mathcal{I}}_{\boldsymbol{\varepsilon},n} \end{cases} \cdot \left(1 - \prod_{n \in \mathbb{I}} \begin{cases} \Phi(-\beta_n), & \boldsymbol{\mu} \in \mathcal{I}_{\boldsymbol{\varepsilon},n} \\ \Phi(\beta_n), & \boldsymbol{\mu} \in \bar{\mathcal{I}}_{\boldsymbol{\varepsilon},n} \end{cases} \right). \quad (6.143)$$

The set $\bar{\mathbb{I}}$ of the indices n of the time instants $t_n, n = 0, 1, \dots, n_{\text{end}}$, in the considered time interval at which the function must not decide for an emergency brake intervention to fulfill the specification $x_{\min} \leq x_{\text{end}} \leq x_{\max}$ for the customer satisfaction is given by (5.88) and the set \mathbb{I} of the indices n of the time instants t_n in the considered time interval at which the function must decide for an emergency brake intervention at least once to fulfill this specification by (5.89), where the indices n_{\min} and n_{\max} are given by (6.77) and (6.78), respectively, but can also be determined by simulations of the AEB system as explained at the end of Chapter 5 for automated vehicular safety systems in general. The check of whether $\boldsymbol{\mu} \in \mathcal{I}_{\boldsymbol{\varepsilon},n}$ or $\boldsymbol{\mu} \in \bar{\mathcal{I}}_{\boldsymbol{\varepsilon},n}$ can be performed as described in (5.86) and (5.87). If the result of evaluating the decision rule $f_c(\cdot; \varphi)$, $c \in \{\text{TTC, adv. TTC, BTN}\}$, with a single function parameter $\varphi = \varphi$ at the mean $\boldsymbol{\mu}_n = \mathbf{0}$ of the sensor measurement errors $\boldsymbol{\varepsilon}[n]$ at the time instant t_n , i.e., the error-free measurements $\mathbf{y}(\mathbf{x}[n], \boldsymbol{\mu}_n) = \mathbf{y}(\mathbf{x}[n], \mathbf{0}) = \mathbf{x}[n]$ at the time instant t_n , is $f_c(\mathbf{y}(\mathbf{x}[n], \boldsymbol{\mu}_n); \varphi) = f_c(\mathbf{x}[n]; \varphi) = 1$, then $\boldsymbol{\mu} \in \mathcal{I}_{\boldsymbol{\varepsilon},n}$ and, otherwise, if it is $f_c(\mathbf{y}(\mathbf{x}[n], \boldsymbol{\mu}_n); \varphi) = f_c(\mathbf{x}[n]; \varphi) = 0$, then $\boldsymbol{\mu} \in \bar{\mathcal{I}}_{\boldsymbol{\varepsilon},n}$. The optimization problem in (5.85), whose solution yields the worst-case distance β_n at the time instant t_n , reads

$$\beta_n = \min_{\boldsymbol{\varepsilon}[n] \in \mathbb{R}^2} \beta_n(\boldsymbol{\varepsilon}[n])$$

$$\text{s.t. } \boldsymbol{\varepsilon}[n] \in \text{cl} \left(\left\{ \boldsymbol{\varepsilon}[n] \in \mathbb{R}^2 : f_c(\mathbf{y}(\mathbf{x}[n], \boldsymbol{\varepsilon}[n]); \varphi) = \begin{cases} 0, & \boldsymbol{\mu} \in \mathcal{I}_{\boldsymbol{\varepsilon},n} \\ 1, & \boldsymbol{\mu} \in \bar{\mathcal{I}}_{\boldsymbol{\varepsilon},n} \end{cases} \right\} \right) \quad (6.144)$$

in case of the considered AEB system using the decision rule $f_c(\cdot; \varphi)$ parameterized by a single function parameter $\varphi = \varphi$ with the square of the Mahalanobis distance $\beta_n(\boldsymbol{\varepsilon}[n])$ of the $E = 2$ sensor measurement errors $\boldsymbol{\varepsilon}[n]$ at the time instant t_n , whose mean and covariance matrix are given in (6.53) and (6.54), respectively, from their mean $\boldsymbol{\mu}_n = \mathbf{0}$ stated in (5.49). With the definition of the three considered decision

rules $f_c(\cdot; \varphi)$ in (6.58), (6.61) and (6.65), this optimization problem becomes

$$\begin{aligned} \beta_n &= \min_{\boldsymbol{\varepsilon}[n] \in \mathbb{R}^2} \beta_n(\boldsymbol{\varepsilon}[n]) \\ \text{s.t. } \boldsymbol{\varepsilon}[n] &\in \text{cl} \left(\left\{ \boldsymbol{\varepsilon}[n] \in \mathbb{R}^2 : \begin{cases} \hat{x}[n] > -\varphi \hat{v}[n], & \boldsymbol{\mu} \in \mathcal{I}_{\boldsymbol{\varepsilon},n} \\ \hat{x}[n] \leq -\varphi \hat{v}[n], & \boldsymbol{\mu} \in \bar{\mathcal{I}}_{\boldsymbol{\varepsilon},n} \end{cases} \right\} \right) \\ &= \min_{\boldsymbol{\varepsilon}[n] \in \mathbb{R}^2} \beta_n(\boldsymbol{\varepsilon}[n]) \quad \text{s.t.} \quad \begin{cases} \hat{x}[n] \geq -\varphi \hat{v}[n], & \boldsymbol{\mu} \in \mathcal{I}_{\boldsymbol{\varepsilon},n} \\ \hat{x}[n] \leq -\varphi \hat{v}[n], & \boldsymbol{\mu} \in \bar{\mathcal{I}}_{\boldsymbol{\varepsilon},n} \end{cases} \end{aligned} \quad (6.145)$$

for the TTC-based decision rule $f_{\text{TTC}}(\cdot; \varphi)$,

$$\begin{aligned} \beta_n &= \min_{\boldsymbol{\varepsilon}[n] \in \mathbb{R}^2} \beta_n(\boldsymbol{\varepsilon}[n]) \\ \text{s.t. } \boldsymbol{\varepsilon}[n] &\in \text{cl} \left(\left\{ \boldsymbol{\varepsilon}[n] \in \mathbb{R}^2 : \begin{cases} \hat{x}[n] - \frac{\hat{v}^2[n]}{2a} > -\varphi \hat{v}[n], & \boldsymbol{\mu} \in \mathcal{I}_{\boldsymbol{\varepsilon},n} \\ \hat{x}[n] - \frac{\hat{v}^2[n]}{2a} \leq -\varphi \hat{v}[n], & \boldsymbol{\mu} \in \bar{\mathcal{I}}_{\boldsymbol{\varepsilon},n} \end{cases} \right\} \right) \\ &= \min_{\boldsymbol{\varepsilon}[n] \in \mathbb{R}^2} \beta_n(\boldsymbol{\varepsilon}[n]) \quad \text{s.t.} \quad \begin{cases} \hat{x}[n] - \frac{\hat{v}^2[n]}{2a} \geq -\varphi \hat{v}[n], & \boldsymbol{\mu} \in \mathcal{I}_{\boldsymbol{\varepsilon},n} \\ \hat{x}[n] - \frac{\hat{v}^2[n]}{2a} \leq -\varphi \hat{v}[n], & \boldsymbol{\mu} \in \bar{\mathcal{I}}_{\boldsymbol{\varepsilon},n} \end{cases} \end{aligned} \quad (6.146)$$

for the advanced TTC-based decision rule $f_{\text{adv. TTC}}(\cdot; \varphi)$ and

$$\begin{aligned} \beta_n &= \min_{\boldsymbol{\varepsilon}[n] \in \mathbb{R}^2} \beta_n(\boldsymbol{\varepsilon}[n]) \\ \text{s.t. } \boldsymbol{\varepsilon}[n] &\in \text{cl} \left(\left\{ \boldsymbol{\varepsilon}[n] \in \mathbb{R}^2 : \begin{cases} \hat{x}[n] > \frac{\hat{v}^2[n]}{2\varphi}, & \boldsymbol{\mu} \in \mathcal{I}_{\boldsymbol{\varepsilon},n} \\ \hat{x}[n] \leq \frac{\hat{v}^2[n]}{2\varphi}, & \boldsymbol{\mu} \in \bar{\mathcal{I}}_{\boldsymbol{\varepsilon},n} \end{cases} \right\} \right) \\ &= \min_{\boldsymbol{\varepsilon}[n] \in \mathbb{R}^2} \beta_n(\boldsymbol{\varepsilon}[n]) \quad \text{s.t.} \quad \begin{cases} \hat{x}[n] \geq \frac{\hat{v}^2[n]}{2\varphi}, & \boldsymbol{\mu} \in \mathcal{I}_{\boldsymbol{\varepsilon},n} \\ \hat{x}[n] \leq \frac{\hat{v}^2[n]}{2\varphi}, & \boldsymbol{\mu} \in \bar{\mathcal{I}}_{\boldsymbol{\varepsilon},n} \end{cases} \end{aligned} \quad (6.147)$$

for the BTN-based decision rule $f_{\text{BTN}}(\cdot; \varphi)$.

Table 6.5 states the values of the absolute error $\left| \hat{P}(x_{\min} \leq x_{\text{end}} \leq x_{\max}) - P(x_{\min} \leq x_{\text{end}} \leq x_{\max}) \right|$ between the worst-case-distance-based approximation $\hat{P}(x_{\min} \leq x_{\text{end}} \leq x_{\max})$ and the actual probability $P(x_{\min} \leq x_{\text{end}} \leq x_{\max})$ of fulfilling the specification for the customer satisfaction, whose values are given in Table 6.3, for the TTC-based decision rule $f_{\text{TTC}}(\cdot; \varphi)$ and different values of the standard deviation σ_x of the sensor measurement errors in the measured distance, the standard deviation σ_v of the sensor measurement errors in the measured relative velocity and the function parameter φ , which are all 0.00000. This

6.3 Numerical Examples for the Robust Design of the Automatic Emergency Braking System

	$\sigma_v = 0.1 \frac{\text{m}}{\text{s}}$	$\sigma_v = 0.2 \frac{\text{m}}{\text{s}}$	$\sigma_v = 0.3 \frac{\text{m}}{\text{s}}$	$\sigma_v = 0.4 \frac{\text{m}}{\text{s}}$
$\sigma_x = 0.1 \text{ m}$	0.00000	0.00000	0.00000	0.00000
$\sigma_x = 0.2 \text{ m}$	0.00000	0.00000	0.00000	0.00000
$\sigma_x = 0.3 \text{ m}$	0.00000	0.00000	0.00000	0.00000
$\sigma_x = 0.4 \text{ m}$	0.00000	0.00000	0.00000	0.00000

(a) $\varphi = 0.47 \text{ s}$

	$\sigma_v = 0.1 \frac{\text{m}}{\text{s}}$	$\sigma_v = 0.2 \frac{\text{m}}{\text{s}}$	$\sigma_v = 0.3 \frac{\text{m}}{\text{s}}$	$\sigma_v = 0.4 \frac{\text{m}}{\text{s}}$
$\sigma_x = 0.1 \text{ m}$	0.00000	0.00000	0.00000	0.00000
$\sigma_x = 0.2 \text{ m}$	0.00000	0.00000	0.00000	0.00000
$\sigma_x = 0.3 \text{ m}$	0.00000	0.00000	0.00000	0.00000
$\sigma_x = 0.4 \text{ m}$	0.00000	0.00000	0.00000	0.00000

(b) $\varphi = 0.49 \text{ s}$

	$\sigma_v = 0.1 \frac{\text{m}}{\text{s}}$	$\sigma_v = 0.2 \frac{\text{m}}{\text{s}}$	$\sigma_v = 0.3 \frac{\text{m}}{\text{s}}$	$\sigma_v = 0.4 \frac{\text{m}}{\text{s}}$
$\sigma_x = 0.1 \text{ m}$	0.00000	0.00000	0.00000	0.00000
$\sigma_x = 0.2 \text{ m}$	0.00000	0.00000	0.00000	0.00000
$\sigma_x = 0.3 \text{ m}$	0.00000	0.00000	0.00000	0.00000
$\sigma_x = 0.4 \text{ m}$	0.00000	0.00000	0.00000	0.00000

(c) $\varphi = 0.51 \text{ s}$

	$\sigma_v = 0.1 \frac{\text{m}}{\text{s}}$	$\sigma_v = 0.2 \frac{\text{m}}{\text{s}}$	$\sigma_v = 0.3 \frac{\text{m}}{\text{s}}$	$\sigma_v = 0.4 \frac{\text{m}}{\text{s}}$
$\sigma_x = 0.1 \text{ m}$	0.00000	0.00000	0.00000	0.00000
$\sigma_x = 0.2 \text{ m}$	0.00000	0.00000	0.00000	0.00000
$\sigma_x = 0.3 \text{ m}$	0.00000	0.00000	0.00000	0.00000
$\sigma_x = 0.4 \text{ m}$	0.00000	0.00000	0.00000	0.00000

(d) $\varphi = 0.53 \text{ s}$

Table 6.5: Absolute error $\left| \hat{P}(x_{\min} \leq x_{\text{end}} \leq x_{\max}) - P(x_{\min} \leq x_{\text{end}} \leq x_{\max}) \right|$ between the worst-case-distance-based approximation $\hat{P}(x_{\min} \leq x_{\text{end}} \leq x_{\max})$ and the actual probability $P(x_{\min} \leq x_{\text{end}} \leq x_{\max})$ of fulfilling the specification $x_{\min} \leq x_{\text{end}} \leq x_{\max}$ for the customer satisfaction by the considered AEB system for $x_0 = 10 \text{ m}$, $v_0 = -10 \frac{\text{m}}{\text{s}}$, $f_s = 1 \text{ kHz}$, $a = 10 \frac{\text{m}}{\text{s}^2}$, $x_{\min} = 0$, $x_{\max} = 0.5 \text{ m}$ and the TTC-based decision rule $f_{\text{TTC}}(\cdot; \varphi)$.

is due to the fact that the inherent approximation of the error regions $\mathcal{I}_{\varepsilon,n}$ and $\bar{\mathcal{I}}_{\varepsilon,n}$ with and without intervention at the time instants t_n by linearizing their boundaries does not introduce any errors in the approximation of the probabilities that the sensor measurement errors ε lie in those error regions by the probabilities that they lie in the approximate error regions resulting from the linearization of their boundaries because they are already linear for the TTC-based decision rule $f_{\text{TTC}}(\cdot; \varphi)$. The boundary

$$\partial\mathcal{I}_{\varepsilon,n} = \partial\bar{\mathcal{I}}_{\varepsilon,n} = \left\{ \varepsilon \in \mathbb{R}^{2(n_{\text{end}}+1)} : x[n] + \varepsilon_x[n] = -\varphi(v[n] + \varepsilon_v[n]) \right\} \quad (6.148)$$

of the error regions $\mathcal{I}_{\varepsilon,n}$ and $\bar{\mathcal{I}}_{\varepsilon,n}$ with and without intervention at the time instant t_n for the TTC-based decision rule $f_{\text{TTC}}(\cdot; \varphi)$ in (6.83) and (6.84) is linear since it is described by the equation $x[n] + \varepsilon_x[n] = -\varphi(v[n] + \varepsilon_v[n])$, which is linear in the sensor measurement errors $\varepsilon_x[n]$ and $\varepsilon_v[n]$ at the time instant t_n . This equation is implied by the condition (6.59) that has to be fulfilled for triggering an emergency brake intervention at a time instant t_n when using the TTC-based decision rule $f_{\text{TTC}}(\cdot; \varphi)$ in (6.58) and its linearity in the sensor measurement errors $\varepsilon_x[n]$ and $\varepsilon_v[n]$ at the time instant t_n by the linearity of this condition in the sensor measurements $\hat{x}[n]$ and $\hat{v}[n]$ at the time instant t_n , which are linear functions of the sensor measurement errors $\varepsilon_x[n]$ and $\varepsilon_v[n]$ according to (6.49) and (6.50), respectively.

As the condition (6.66) that has to be fulfilled for triggering an emergency brake intervention at a time instant t_n when using the BTN-based decision rule $f_{\text{BTN}}(\cdot; \varphi)$ in (6.65) is not linear in the sensor measurements $\hat{x}[n]$ and $\hat{v}[n]$ at the time instant t_n , the boundary of the error regions $\mathcal{I}_{\varepsilon,n}$ and $\bar{\mathcal{I}}_{\varepsilon,n}$ with and without intervention at the time instant t_n for this decision rule is also not linear such that the inherent approximation of the error regions $\mathcal{I}_{\varepsilon,n}$ and $\bar{\mathcal{I}}_{\varepsilon,n}$ with and without intervention at the time instants t_n by linearizing their boundaries introduces approximation errors. They can be observed in Table 6.6, which states the values of the absolute error $\left| \hat{P}(x_{\min} \leq x_{\text{end}} \leq x_{\max}) - P(x_{\min} \leq x_{\text{end}} \leq x_{\max}) \right|$ between the worst-case-distance-based approximation $\hat{P}(x_{\min} \leq x_{\text{end}} \leq x_{\max})$ and the actual probability $P(x_{\min} \leq x_{\text{end}} \leq x_{\max})$ of fulfilling the specification for the customer satisfaction, i.e., the accurate Monte-Carlo-based estimate $\hat{P}_{10^8}(x_{\min} \leq x_{\text{end}} \leq x_{\max})$ from $M = 10^8$ simulations of the AEB system used as ground truth, for different values of the standard deviation σ_x of the sensor measurement errors in the measured distance, the standard deviation σ_v of the sensor measurement errors in the measured relative velocity and the function parameter φ . The accurate Monte-Carlo-based estimate $\hat{P}_{10^8}(x_{\min} \leq x_{\text{end}} \leq x_{\max})$ from $M = 10^8$ simulations of the AEB system, a very large number of simulations, is used as ground truth instead of the actual probability

6.3 Numerical Examples for the Robust Design of the Automatic Emergency Braking System

	$\sigma_v = 0.1 \frac{\text{m}}{\text{s}}$	$\sigma_v = 0.2 \frac{\text{m}}{\text{s}}$	$\sigma_v = 0.3 \frac{\text{m}}{\text{s}}$	$\sigma_v = 0.4 \frac{\text{m}}{\text{s}}$
$\sigma_x = 0.1 \text{ m}$	0.00014	0.00123	0.00046	0.00004
$\sigma_x = 0.2 \text{ m}$	0.00138	0.00226	0.00060	0.00005
$\sigma_x = 0.3 \text{ m}$	0.00071	0.00081	0.00021	0.00002
$\sigma_x = 0.4 \text{ m}$	0.00008	0.00009	0.00003	0.00000

(a) $\varphi = 9.7 \frac{\text{m}}{\text{s}^2}$

	$\sigma_v = 0.1 \frac{\text{m}}{\text{s}}$	$\sigma_v = 0.2 \frac{\text{m}}{\text{s}}$	$\sigma_v = 0.3 \frac{\text{m}}{\text{s}}$	$\sigma_v = 0.4 \frac{\text{m}}{\text{s}}$
$\sigma_x = 0.1 \text{ m}$	0.00001	0.00069	0.00093	0.00023
$\sigma_x = 0.2 \text{ m}$	0.00067	0.00285	0.00201	0.00039
$\sigma_x = 0.3 \text{ m}$	0.00116	0.00232	0.00116	0.00021
$\sigma_x = 0.4 \text{ m}$	0.00037	0.00058	0.00027	0.00005

(b) $\varphi = 9.9 \frac{\text{m}}{\text{s}^2}$

	$\sigma_v = 0.1 \frac{\text{m}}{\text{s}}$	$\sigma_v = 0.2 \frac{\text{m}}{\text{s}}$	$\sigma_v = 0.3 \frac{\text{m}}{\text{s}}$	$\sigma_v = 0.4 \frac{\text{m}}{\text{s}}$
$\sigma_x = 0.1 \text{ m}$	0.00017	0.00022	0.00095	0.00058
$\sigma_x = 0.2 \text{ m}$	0.00023	0.00186	0.00302	0.00132
$\sigma_x = 0.3 \text{ m}$	0.00112	0.00332	0.00302	0.00103
$\sigma_x = 0.4 \text{ m}$	0.00073	0.00169	0.00120	0.00036

(c) $\varphi = 10.1 \frac{\text{m}}{\text{s}^2}$

	$\sigma_v = 0.1 \frac{\text{m}}{\text{s}}$	$\sigma_v = 0.2 \frac{\text{m}}{\text{s}}$	$\sigma_v = 0.3 \frac{\text{m}}{\text{s}}$	$\sigma_v = 0.4 \frac{\text{m}}{\text{s}}$
$\sigma_x = 0.1 \text{ m}$	0.00128	0.00020	0.00062	0.00078
$\sigma_x = 0.2 \text{ m}$	0.00020	0.00079	0.00278	0.00242
$\sigma_x = 0.3 \text{ m}$	0.00067	0.00293	0.00437	0.00263
$\sigma_x = 0.4 \text{ m}$	0.00089	0.00273	0.00285	0.00135

(d) $\varphi = 10.3 \frac{\text{m}}{\text{s}^2}$

Table 6.6: Absolute error $\left| \hat{P}(x_{\min} \leq x_{\text{end}} \leq x_{\max}) - P(x_{\min} \leq x_{\text{end}} \leq x_{\max}) \right|$ between the worst-case-distance-based approximation $\hat{P}(x_{\min} \leq x_{\text{end}} \leq x_{\max})$ and the actual probability $P(x_{\min} \leq x_{\text{end}} \leq x_{\max})$ of fulfilling the specification $x_{\min} \leq x_{\text{end}} \leq x_{\max}$ for the customer satisfaction by the considered AEB system, i.e., the accurate Monte-Carlo-based estimate $\hat{P}_{10^8}(x_{\min} \leq x_{\text{end}} \leq x_{\max})$ from $M = 10^8$ simulations of the AEB system used as ground truth, for $x_0 = 10 \text{ m}$, $v_0 = -10 \frac{\text{m}}{\text{s}}$, $f_s = 1 \text{ kHz}$, $a = 10 \frac{\text{m}}{\text{s}^2}$, $x_{\min} = 0$, $x_{\max} = 0.5 \text{ m}$ and the BTN-based decision rule $f_{\text{BTN}}(\cdot; \varphi)$.

$P(x_{\min} \leq x_{\text{end}} \leq x_{\max})$ of fulfilling the specification for the customer satisfaction because no closed-form expression exists for this probability in case of the BTN-based decision rule $f_{\text{BTN}}(\cdot; \varphi)$. Its values that correspond to the stated values of the absolute error $\left| \hat{P}(x_{\min} \leq x_{\text{end}} \leq x_{\max}) - P(x_{\min} \leq x_{\text{end}} \leq x_{\max}) \right|$ can be found in Table 6.7.

For comparison, the corresponding values of the absolute error $\left| \hat{P}_{10^5}(x_{\min} \leq x_{\text{end}} \leq x_{\max}) - P(x_{\min} \leq x_{\text{end}} \leq x_{\max}) \right|$ between the Monte-Carlo-based estimate $\hat{P}_{10^5}(x_{\min} \leq x_{\text{end}} \leq x_{\max})$ from $M = 10^5$ simulations of the AEB system and the actual probability $P(x_{\min} \leq x_{\text{end}} \leq x_{\max})$ of fulfilling the specification for the customer satisfaction, i.e., the accurate Monte-Carlo-based estimate $\hat{P}_{10^8}(x_{\min} \leq x_{\text{end}} \leq x_{\max})$ from $M = 10^8$ simulations of the AEB system used as ground truth, are stated in Table 6.8. If the standard deviation of the sensor measurement errors in the measured distance is $\sigma_x = 0.1$ m, the standard deviation of the sensor measurement errors in the measured relative velocity is $\sigma_v = 0.1 \frac{\text{m}}{\text{s}}$ and the function parameter value is $\varphi = 9.9 \frac{\text{m}}{\text{s}^2}$, for example, the probability of fulfilling the specification for the customer satisfaction is

$$P(x_{\min} \leq x_{\text{end}} \leq x_{\max}) = 0.99711 \quad (6.149)$$

while the Monte-Carlo-based estimate from $M = 10^5$ simulations of the AEB system is

$$\hat{P}_{10^5}(x_{\min} \leq x_{\text{end}} \leq x_{\max}) = 0.99721 \quad (6.150)$$

and the worst-case-distance-based approximation is

$$\hat{P}(x_{\min} \leq x_{\text{end}} \leq x_{\max}) = 0.99712 \quad (6.151)$$

such that the absolute error of the Monte-Carlo-based estimate is

$$\left| \hat{P}_{10^5}(x_{\min} \leq x_{\text{end}} \leq x_{\max}) - P(x_{\min} \leq x_{\text{end}} \leq x_{\max}) \right| = 0.00010 \quad (6.152)$$

and that of the worst-case-distance-based approximation is only

$$\left| \hat{P}(x_{\min} \leq x_{\text{end}} \leq x_{\max}) - P(x_{\min} \leq x_{\text{end}} \leq x_{\max}) \right| = 0.00001 \quad (6.153)$$

as stated in Table 6.6 and Table 6.8. For this accurate worst-case-distance-based approximation, only 1,001 simulations of the AEB system and 22,095 evaluations of the BTN-based decision rule $f_{\text{BTN}}(\cdot; \varphi)$ are required. According to (5.14), the approximate number M_{req} of simulations of the automated vehicular safety system required in the Monte Carlo simulation for estimating the probability $P(\mathbf{q} \in \mathcal{A}_q) =$

6.3 Numerical Examples for the Robust Design of the Automatic Emergency Braking System

	$\sigma_v = 0.1 \frac{\text{m}}{\text{s}}$	$\sigma_v = 0.2 \frac{\text{m}}{\text{s}}$	$\sigma_v = 0.3 \frac{\text{m}}{\text{s}}$	$\sigma_v = 0.4 \frac{\text{m}}{\text{s}}$
$\sigma_x = 0.1 \text{ m}$	0.96427	0.50374	0.07416	0.00386
$\sigma_x = 0.2 \text{ m}$	0.55284	0.19271	0.02461	0.00132
$\sigma_x = 0.3 \text{ m}$	0.10534	0.03101	0.00389	0.00023
$\sigma_x = 0.4 \text{ m}$	0.00787	0.00234	0.00032	0.00002

(a) $\varphi = 9.7 \frac{\text{m}}{\text{s}^2}$

	$\sigma_v = 0.1 \frac{\text{m}}{\text{s}}$	$\sigma_v = 0.2 \frac{\text{m}}{\text{s}}$	$\sigma_v = 0.3 \frac{\text{m}}{\text{s}}$	$\sigma_v = 0.4 \frac{\text{m}}{\text{s}}$
$\sigma_x = 0.1 \text{ m}$	0.99711	0.81337	0.28426	0.03578
$\sigma_x = 0.2 \text{ m}$	0.83591	0.49513	0.13377	0.01541
$\sigma_x = 0.3 \text{ m}$	0.33303	0.15028	0.03375	0.00370
$\sigma_x = 0.4 \text{ m}$	0.05284	0.02141	0.00454	0.00051

(b) $\varphi = 9.9 \frac{\text{m}}{\text{s}^2}$

	$\sigma_v = 0.1 \frac{\text{m}}{\text{s}}$	$\sigma_v = 0.2 \frac{\text{m}}{\text{s}}$	$\sigma_v = 0.3 \frac{\text{m}}{\text{s}}$	$\sigma_v = 0.4 \frac{\text{m}}{\text{s}}$
$\sigma_x = 0.1 \text{ m}$	0.98445	0.94785	0.56662	0.14575
$\sigma_x = 0.2 \text{ m}$	0.95307	0.75821	0.35253	0.07775
$\sigma_x = 0.3 \text{ m}$	0.59901	0.36941	0.13349	0.02548
$\sigma_x = 0.4 \text{ m}$	0.17399	0.09108	0.02830	0.00500

(c) $\varphi = 10.1 \frac{\text{m}}{\text{s}^2}$

	$\sigma_v = 0.1 \frac{\text{m}}{\text{s}}$	$\sigma_v = 0.2 \frac{\text{m}}{\text{s}}$	$\sigma_v = 0.3 \frac{\text{m}}{\text{s}}$	$\sigma_v = 0.4 \frac{\text{m}}{\text{s}}$
$\sigma_x = 0.1 \text{ m}$	0.70110	0.96608	0.78701	0.34210
$\sigma_x = 0.2 \text{ m}$	0.96803	0.90221	0.59736	0.21893
$\sigma_x = 0.3 \text{ m}$	0.79557	0.60421	0.31241	0.09452
$\sigma_x = 0.4 \text{ m}$	0.36067	0.23074	0.09833	0.02577

(d) $\varphi = 10.3 \frac{\text{m}}{\text{s}^2}$

Table 6.7: Probability $P(x_{\min} \leq x_{\text{end}} \leq x_{\max})$ that the considered AEB system fulfills the specification $x_{\min} \leq x_{\text{end}} \leq x_{\max}$ for the customer satisfaction, i.e., the accurate Monte-Carlo-based estimate $\hat{P}_{10^8}(x_{\min} \leq x_{\text{end}} \leq x_{\max})$ from $M = 10^8$ simulations of the AEB system used as ground truth, for $x_0 = 10 \text{ m}$, $v_0 = -10 \frac{\text{m}}{\text{s}}$, $f_s = 1 \text{ kHz}$, $a = 10 \frac{\text{m}}{\text{s}^2}$, $x_{\min} = 0$, $x_{\max} = 0.5 \text{ m}$ and the BTN-based decision rule $f_{\text{BTN}}(\cdot; \varphi)$.

	$\sigma_v = 0.1 \frac{\text{m}}{\text{s}}$	$\sigma_v = 0.2 \frac{\text{m}}{\text{s}}$	$\sigma_v = 0.3 \frac{\text{m}}{\text{s}}$	$\sigma_v = 0.4 \frac{\text{m}}{\text{s}}$
$\sigma_x = 0.1 \text{ m}$	0.00044	0.00137	0.00090	0.00018
$\sigma_x = 0.2 \text{ m}$	0.00160	0.00120	0.00028	0.00007
$\sigma_x = 0.3 \text{ m}$	0.00089	0.00019	0.00012	0.00005
$\sigma_x = 0.4 \text{ m}$	0.00012	0.00011	0.00004	0.00004

(a) $\varphi = 9.7 \frac{\text{m}}{\text{s}^2}$

	$\sigma_v = 0.1 \frac{\text{m}}{\text{s}}$	$\sigma_v = 0.2 \frac{\text{m}}{\text{s}}$	$\sigma_v = 0.3 \frac{\text{m}}{\text{s}}$	$\sigma_v = 0.4 \frac{\text{m}}{\text{s}}$
$\sigma_x = 0.1 \text{ m}$	0.00010	0.00125	0.00008	0.00087
$\sigma_x = 0.2 \text{ m}$	0.00157	0.00049	0.00061	0.00006
$\sigma_x = 0.3 \text{ m}$	0.00073	0.00086	0.00012	0.00023
$\sigma_x = 0.4 \text{ m}$	0.00057	0.00019	0.00018	0.00001

(b) $\varphi = 9.9 \frac{\text{m}}{\text{s}^2}$

	$\sigma_v = 0.1 \frac{\text{m}}{\text{s}}$	$\sigma_v = 0.2 \frac{\text{m}}{\text{s}}$	$\sigma_v = 0.3 \frac{\text{m}}{\text{s}}$	$\sigma_v = 0.4 \frac{\text{m}}{\text{s}}$
$\sigma_x = 0.1 \text{ m}$	0.00032	0.00009	0.00013	0.00100
$\sigma_x = 0.2 \text{ m}$	0.00109	0.00093	0.00106	0.00076
$\sigma_x = 0.3 \text{ m}$	0.00348	0.00078	0.00074	0.00011
$\sigma_x = 0.4 \text{ m}$	0.00062	0.00023	0.00041	0.00009

(c) $\varphi = 10.1 \frac{\text{m}}{\text{s}^2}$

	$\sigma_v = 0.1 \frac{\text{m}}{\text{s}}$	$\sigma_v = 0.2 \frac{\text{m}}{\text{s}}$	$\sigma_v = 0.3 \frac{\text{m}}{\text{s}}$	$\sigma_v = 0.4 \frac{\text{m}}{\text{s}}$
$\sigma_x = 0.1 \text{ m}$	0.00274	0.00062	0.00034	0.00033
$\sigma_x = 0.2 \text{ m}$	0.00009	0.00110	0.00174	0.00086
$\sigma_x = 0.3 \text{ m}$	0.00179	0.00153	0.00107	0.00030
$\sigma_x = 0.4 \text{ m}$	0.00038	0.00014	0.00063	0.00031

(d) $\varphi = 10.3 \frac{\text{m}}{\text{s}^2}$

Table 6.8: Absolute error $\left| \hat{P}_{10^5}(x_{\min} \leq x_{\text{end}} \leq x_{\max}) - P(x_{\min} \leq x_{\text{end}} \leq x_{\max}) \right|$ between the Monte-Carlo-based estimate $\hat{P}_{10^5}(x_{\min} \leq x_{\text{end}} \leq x_{\max})$ from $M = 10^5$ simulations of the considered AEB system and the actual probability $P(x_{\min} \leq x_{\text{end}} \leq x_{\max})$ of fulfilling the specification $x_{\min} \leq x_{\text{end}} \leq x_{\max}$ for the customer satisfaction, i.e., the accurate Monte-Carlo-based estimate $\hat{P}_{10^8}(x_{\min} \leq x_{\text{end}} \leq x_{\max})$ from $M = 10^8$ simulations of the AEB system used as ground truth, for $x_0 = 10 \text{ m}$, $v_0 = -10 \frac{\text{m}}{\text{s}}$, $f_s = 1 \text{ kHz}$, $a = 10 \frac{\text{m}}{\text{s}^2}$, $x_{\min} = 0$, $x_{\max} = 0.5 \text{ m}$ and the BTN-based decision rule $f_{\text{BTN}}(\cdot; \varphi)$.

6.3 Numerical Examples for the Robust Design of the Automatic Emergency Braking System

$P(x_{\min} \leq x_{\text{end}} \leq x_{\max})$ of fulfilling the specifications for the customer satisfaction, i.e., the specification $x_{\min} \leq x_{\text{end}} \leq x_{\max}$, with the desired confidence levels $\kappa = 0.9$, $\kappa = 0.95$ and $\kappa = 0.99$ for the corresponding confidence interval

$$\begin{aligned} & \left[\hat{P}_M(\mathbf{q} \in \mathcal{A}_q) - \Delta P, \hat{P}_M(\mathbf{q} \in \mathcal{A}_q) + \Delta P \right] \\ & = \left[\hat{P}_M(x_{\min} \leq x_{\text{end}} \leq x_{\max}) - \Delta P, \hat{P}_M(x_{\min} \leq x_{\text{end}} \leq x_{\max}) + \Delta P \right] \end{aligned} \quad (6.154)$$

around the Monte-Carlo-based estimate $\hat{P}_M(\mathbf{q} \in \mathcal{A}_q) = \hat{P}_M(x_{\min} \leq x_{\text{end}} \leq x_{\max})$, which has the same length $2 \Delta P = 0.00004$ as the interval

$$\begin{aligned} & \left[\hat{P}(x_{\min} \leq x_{\text{end}} \leq x_{\max}) - \Delta P, \hat{P}(x_{\min} \leq x_{\text{end}} \leq x_{\max}) + \Delta P \right] \\ & = [0.99712 - 0.00002, 0.99712 + 0.00002] = [0.99710, 0.99714] \end{aligned} \quad (6.155)$$

around the worst-case-distance-based approximation $\hat{P}(x_{\min} \leq x_{\text{end}} \leq x_{\max})$ containing the true probability $P(x_{\min} \leq x_{\text{end}} \leq x_{\max})$ is 19,497,380, 27,683,305 and 47,814,092, respectively. These simulations come with even higher numbers of evaluations of the BTN-based decision rule $f_{\text{BTN}}(\cdot; \varphi)$. This example demonstrates that the adaptation of the worst-case distance approach to the robust design of automated vehicular safety systems has the potential to significantly reduce the required number of simulations of the automated vehicular safety system under design by replacing an expensive Monte Carlo simulation requiring a huge number of simulations of the automated vehicular safety system for a comparable accuracy, and with this the computational complexity, the load for simulation servers as well as the time and expenses needed for the development of automated vehicular safety systems. This becomes even more obvious when considering the following examples for the joint function and sensor design.

With the quality measure Q in (6.120), i.e., the probability of fulfilling the specification $x_{\min} \leq x_{\text{end}} \leq x_{\max}$ for the customer satisfaction in the driving scenario $\xi = \xi_0$ with the initial distance $x_0 = 10$ m and the initial relative velocity $v_0 = -10 \frac{\text{m}}{\text{s}}$, the respective required minimum quality level $Q_{\min} = P_{\min}$, i.e., the required minimum probability P_{\min} of fulfilling this specification for the customer satisfaction in the driving scenario $\xi = \xi_0$, the costs

$$C = -\sigma_x - \sigma_v, \quad (6.156)$$

which are chosen as simple illustrative example, the possible domain \mathcal{S} of the sensor parameter values σ in (6.138) and the set $\mathcal{F} = \{f_c\}$ of the predefined decision rules for triggering the emergency brake intervention consisting of only one decision rule

$f_c(\cdot; \varphi)$, $c \in \{\text{TTC}, \text{adv. TTC}, \text{BTN}\}$, with the single function parameter $\varphi = \varphi$, the optimization problem (4.11) of the joint function and sensor design reads

$$\begin{aligned} & (\sigma_{x,\text{opt}}, \sigma_{v,\text{opt}}, \varphi_{\text{opt}}) = \\ & \underset{\sigma_x \in \mathbb{R}^+, \sigma_v \in \mathbb{R}^+, \varphi \in \mathbb{R}}{\text{argmin}} \quad C \\ \text{s.t.} \quad & P(x_{\min} \leq x_{\text{end}} \leq x_{\max})|_{x_0=10 \text{ m}, v_0=-10 \frac{\text{m}}{\text{s}}, f_s=1 \text{ kHz}, f=f_c} \geq P_{\min}. \end{aligned} \quad (6.157)$$

Numerically solving this optimization problem for the required minimum probability $P_{\min} = 0.99$ of fulfilling the specification for the customer satisfaction and the TTC-based decision rule $f_{\text{TTC}}(\cdot; \varphi)$, i.e., $c = \text{TTC}$, by using the closed-form expression (6.99) for the probability $P(x_{\min} \leq x_{\text{end}} \leq x_{\max})$ of fulfilling the specification for the customer satisfaction yields the optimal values $\sigma_{x,\text{opt}} = 0.08308 \text{ m}$, $\sigma_{v,\text{opt}} = 0.34015 \frac{\text{m}}{\text{s}}$ and $\varphi_{\text{opt}} = 0.49422 \text{ s}$ for the standard deviation σ_x of the sensor measurement errors in the measured distance, the standard deviation σ_v of the sensor measurement errors in the measured relative velocity and the function parameter φ , respectively. The costs corresponding to these optimal parameter values, the minimal costs, are $C = C_{\min}^* = -0.42323$ while the corresponding probability of fulfilling the specification for the customer satisfaction is $P(x_{\min} \leq x_{\text{end}} \leq x_{\max}) = 0.99000 = P_{\min}$ as desired and enforced by the constraint of the optimization problem with $P_{\min} = 0.99$.

The same result is obtained if the optimization problem (6.157) is solved with the worst-case-distance-based approximation $\hat{P}(x_{\min} \leq x_{\text{end}} \leq x_{\max})$ instead of the actual probability $P(x_{\min} \leq x_{\text{end}} \leq x_{\max})$ of fulfilling the specification for the customer satisfaction due to the absence of any approximation errors in case of the TTC-based decision rule $f_{\text{TTC}}(\cdot; \varphi)$. Solving it with the Monte-Carlo-based estimate $\hat{P}_{10^5}(x_{\min} \leq x_{\text{end}} \leq x_{\max})$ from $M = 10^5$ simulations of the AEB system instead of the actual probability $P(x_{\min} \leq x_{\text{end}} \leq x_{\max})$ of fulfilling the specification for the customer satisfaction comes close to this result but cannot reach it exactly. The so obtained optimal parameter values are $\sigma_{x,\text{opt}} = 0.08041 \text{ m}$, $\sigma_{v,\text{opt}} = 0.34146 \frac{\text{m}}{\text{s}}$ and $\varphi_{\text{opt}} = 0.49444 \text{ s}$. For these parameter values, the probability of fulfilling the specification for the customer satisfaction is $P(x_{\min} \leq x_{\text{end}} \leq x_{\max}) = 0.99017 > 0.99 = P_{\min}$, which overfulfills the constraint of the optimization problem (6.157) due to estimation errors of the Monte-Carlo simulation and is the reason why the resulting costs $C = -0.42188$ are larger than those for the optimal parameter values obtained with the actual probability $P(x_{\min} \leq x_{\text{end}} \leq x_{\max})$ of fulfilling the specification for the customer satisfaction.

Moreover, solving the optimization problem (6.157) with the Monte-Carlo-based

6.3 Numerical Examples for the Robust Design of the Automatic Emergency Braking System

estimate $\hat{P}_{10^5}(x_{\min} \leq x_{\text{end}} \leq x_{\max})$ requires 63,100,000 simulations of the AEB system with even more evaluations of the TTC-based decision rule $f_{\text{TTC}}(\cdot; \varphi)$ while solving it with the worst-case-distance-based approximation $\hat{P}(x_{\min} \leq x_{\text{end}} \leq x_{\max})$ requires only 1,001 simulations of the AEB system with 4,104,114 evaluations of the TTC-based decision rule $f_{\text{TTC}}(\cdot; \varphi)$ although providing a more accurate result.

A similar picture emerges if the BTN-based decision rule $f_{\text{BTN}}(\cdot; \varphi)$ is used instead of the TTC-based decision rule $f_{\text{TTC}}(\cdot; \varphi)$, i.e., $c = \text{BTN}$. Solving the optimization problem (6.157) for the required minimum probability $P_{\min} = 0.99$ of fulfilling the specification for the customer satisfaction and the BTN-based decision rule $f_{\text{BTN}}(\cdot; \varphi)$ with the worst-case-distance-based approximation $\hat{P}(x_{\min} \leq x_{\text{end}} \leq x_{\max})$ instead of the actual probability $P(x_{\min} \leq x_{\text{end}} \leq x_{\max})$ of fulfilling the specification for the customer satisfaction, for which no closed-form expression exists in case of the BTN-based decision rule $f_{\text{BTN}}(\cdot; \varphi)$, yields the optimal values $\sigma_{x,\text{opt}} = 0.13547 \text{ m}$, $\sigma_{v,\text{opt}} = 0.12880 \frac{\text{m}}{\text{s}}$ and $\varphi_{\text{opt}} = 10.11366 \frac{\text{m}}{\text{s}^2}$ for the standard deviation σ_x of the sensor measurement errors in the measured distance, the standard deviation σ_v of the sensor measurement errors in the measured relative velocity and the function parameter φ , respectively. The costs corresponding to these optimal parameter values are $C = -0.26426$ while the corresponding probability of fulfilling the specification for the customer satisfaction is $P(x_{\min} \leq x_{\text{end}} \leq x_{\max}) = 0.99000 = P_{\min}$, which is the accurate Monte-Carlo-based estimate $\hat{P}_{10^8}(x_{\min} \leq x_{\text{end}} \leq x_{\max})$ from $M = 10^8$ simulations of the AEB system used as ground truth and fulfills the constraint of the optimization problem with $P_{\min} = 0.99$. By solving it with the Monte-Carlo-based estimate $\hat{P}_{10^5}(x_{\min} \leq x_{\text{end}} \leq x_{\max})$ from $M = 10^5$ simulations of the AEB system instead of the actual probability $P(x_{\min} \leq x_{\text{end}} \leq x_{\max})$ of fulfilling the specification for the customer satisfaction, the optimal parameter values $\sigma_{x,\text{opt}} = 0.14770 \text{ m}$, $\sigma_{v,\text{opt}} = 0.11473 \frac{\text{m}}{\text{s}}$ and $\varphi_{\text{opt}} = 10.12135 \frac{\text{m}}{\text{s}^2}$ are obtained, which deviate slightly from those obtained with the worst-case-distance-based approximation $\hat{P}(x_{\min} \leq x_{\text{end}} \leq x_{\max})$. For these parameter values, the probability of fulfilling the specification for the customer satisfaction is $P(x_{\min} \leq x_{\text{end}} \leq x_{\max}) = 0.99004 > 0.99 = P_{\min}$ leading to costs $C = -0.26243$, which are larger than those for the optimal parameter values obtained with the worst-case-distance-based approximation $\hat{P}(x_{\min} \leq x_{\text{end}} \leq x_{\max})$.

Similarly to the joint function and sensor design for the TTC-based decision rule $f_{\text{TTC}}(\cdot; \varphi)$ before, the 41,700,000 simulations of the AEB system with even more evaluations of the BTN-based decision rule $f_{\text{BTN}}(\cdot; \varphi)$ that solving the optimization problem (6.157) with the Monte-Carlo-based estimate $\hat{P}_{10^5}(x_{\min} \leq x_{\text{end}} \leq x_{\max})$ requires are significantly more than the 1,001 simulations of the AEB system with 2,578,523 evaluations of the BTN-based decision rule $f_{\text{BTN}}(\cdot; \varphi)$ that solving it with the worst-case-

distance-based approximation $\hat{P}(x_{\min} \leq x_{\text{end}} \leq x_{\max})$ requires although the latter provides a more accurate result than the former.

These numerical examples demonstrate that the adaptation of the worst-case distance approach to the robust design of automated vehicular safety systems can significantly reduce the required number of simulations of the automated vehicular safety system under design by replacing an expensive Monte Carlo simulation requiring a huge number of simulations of the automated vehicular safety system for a comparable accuracy, and with this the computational complexity, the load for simulation servers as well as the time and expenses needed for the development of automated vehicular safety systems.

Robust Design of an Automatic Emergency Steering System

7

After applying the proposed methodology for the robust function and sensor design that allows to systematically design both functions and sensors of automated vehicular safety systems such that the customer requirements are fulfilled in a robust manner despite unavoidable sensor measurement errors to the robust design of an AEB system in the previous chapter, this chapter demonstrates how it can also be applied to the robust design of an AES system as a typical more complex example for automated vehicular safety systems. In part, the application of the proposed design methodology to the robust design of an AES system has already been published in [47]. The published results will be revisited and supplemented in the following to provide a complete picture of the system model, the formulation of the design problems at hand as optimization problems using the proposed design methodology and their solution solely based on simulations of the AES system under design without the need for deriving closed-form expressions for the probabilistic quality measure Q . Deriving such closed-form expressions would be even more difficult for the AES system due to the two-dimensional movement of the ego vehicle during the steering maneuver as compared to the AEB system with the movement of the ego vehicle restricted to one dimension during the braking maneuver under simplifying assumptions and is not pursued since this would also not be viable for the complex automated vehicular safety systems in practice and therefore the developers of such systems have to resort to a simulation-based design anyway.

7.1 System Model for the Automatic Emergency Steering System

As the system model of the AEB system considered in the previous chapter, the system model of the considered AES system is also a special case of the general system model for an automated vehicular safety system introduced in Chapter 2, and can be split into a mathematical representation of the driving scenario in which the AES system is applied and a stochastic model of the AES system itself including sensor measurement

errors.

7.1.1 Mathematical Representation of the Driving Scenario for the Robust Design of the Automatic Emergency Steering System

The driving scenario that is considered for the robust design of the AES system is the driving scenario for the robust design of the AEB system in the previous chapter illustrated in Figure 6.1, where the ego vehicle approaches an object, e.g., another vehicle. Here, the velocity of the object is assumed to be constant over the time t . Assuming that the object is in front of the ego vehicle and slower than it at the time t_0 when the driving scenario starts, i.e., $x_{\text{ego},f}(t_0) < x_{\text{obj},r}(t_0)$ and $v_{\text{ego}}(t_0) > v_{\text{obj}}(t_0) \geq 0$, a collision would necessarily occur if the ego vehicle moved with constant velocity too. In order to avoid such a collision, an emergency steer intervention is triggered at time $t_s \geq t_0$, which steers the ego vehicle with a constant lateral acceleration $a > 0$ to the left. To sum up, the longitudinal accelerations of the ego vehicle and the object at time t are $a_{\text{lon,ego}}(t) = a_{\text{lon,ego}} = 0$ and $a_{\text{lon,obj}}(t) = a_{\text{lon,obj}} = 0$, respectively, while the lateral accelerations of the ego vehicle and the object at time t are

$$a_{\text{lat,ego}}(t) = \begin{cases} 0, & t < t_s \\ a, & t \geq t_s \end{cases} \quad (7.1)$$

and $a_{\text{lat,obj}}(t) = a_{\text{lat,obj}} = 0$, respectively.

This two-dimensional motion model with piecewise constant accelerations is captured by the general motion model where the motion of each vehicle during a driving maneuver is described by the system of differential equations (2.1)–(2.4). This system of differential equations describing the motion of the ego vehicle is given by (6.2)–(6.5) with the turn radius $r_{\text{min,ego}}$ of the ego vehicle, where the state of the ego vehicle at time t is represented by the state vector $[x_{\text{ego}}(t), y_{\text{ego}}(t), v_{\text{ego}}(t), \psi_{\text{ego}}(t)]^T$ consisting of four state variables, which are the coordinates $x_{\text{ego}}(t)$ and $y_{\text{ego}}(t)$ of its center of gravity with respect to the x_w - and y_w -axis of the world coordinate system determining its position, its longitudinal velocity $v_{\text{ego}}(t)$ and its yaw angle $\psi_{\text{ego}}(t)$. Analogously, the system of differential equations describing the motion of the object is given by (6.6)–(6.9) with the turn radius $r_{\text{min,obj}}$ of the object, where the state of the object at time t is represented by the state vector $[x_{\text{obj}}(t), y_{\text{obj}}(t), v_{\text{obj}}(t), \psi_{\text{obj}}(t)]^T$ consisting of four state variables, which are the coordinates $x_{\text{obj}}(t)$ and $y_{\text{obj}}(t)$ of its center of gravity with respect to the x_w - and y_w -axis of the world coordinate system determining its position, its longitudinal velocity $v_{\text{obj}}(t)$ and its yaw angle $\psi_{\text{obj}}(t)$.

7.1 System Model for the Automatic Emergency Steering System

The motion of the object with constant velocity in the considered time interval starting at t_0 is described by the differential equations (6.6)–(6.9) with $a_{\text{lon,obj}} = a_{\text{lat,obj}} = 0$ while the motion of the ego vehicle with constant velocity in this time interval before triggering the emergency steer intervention at t_s is described by the differential equations (6.2)–(6.5) with $a_{\text{lon,ego}} = a_{\text{lat,ego}} = 0$ and its motion with constant lateral acceleration $a_{\text{lat,ego}} = a$ in the time interval starting at t_s when triggering the emergency steer intervention by the same differential equations with $a_{\text{lon,ego}} = 0$ and $a_{\text{lat,ego}} = a$. These differential equations can be solved numerically to obtain the trajectory of both the ego vehicle and the object, i.e., their states $[x_{\text{ego}}(t), y_{\text{ego}}(t), v_{\text{ego}}(t), \psi_{\text{ego}}(t)]^T$ and $[x_{\text{obj}}(t), y_{\text{obj}}(t), v_{\text{obj}}(t), \psi_{\text{obj}}(t)]^T$ at discrete time instants

$$t = t_0 + m\delta t, \quad (7.2)$$

$m = 0, 1, \dots$, with the temporal distance δt between neighboring time instants. The state variables of these two involved vehicles, namely, the coordinates $x_{\text{ego}}(t)$ and $y_{\text{ego}}(t)$ of the center of gravity of the ego vehicle, its longitudinal velocity $v_{\text{ego}}(t)$ and its yaw angle $\psi_{\text{ego}}(t)$ as well as the coordinates $x_{\text{obj}}(t)$ and $y_{\text{obj}}(t)$ of the center of gravity of the object, its longitudinal velocity $v_{\text{obj}}(t)$ and its yaw angle $\psi_{\text{obj}}(t)$, at time t completely determine the state of the considered dynamic system at this time instant and form the state vector

$$\mathbf{x}(t) = \begin{bmatrix} x_{\text{ego}}(t) \\ y_{\text{ego}}(t) \\ v_{\text{ego}}(t) \\ \psi_{\text{ego}}(t) \\ x_{\text{obj}}(t) \\ y_{\text{obj}}(t) \\ v_{\text{obj}}(t) \\ \psi_{\text{obj}}(t) \end{bmatrix} \quad (7.3)$$

at time t .

The contours of the ego vehicle and the object are assumed to be rectangles of the lengths l_{ego} and l_{obj} , and widths w_{ego} and w_{obj} , respectively. Using the coordinate transformation (2.6) from coordinates (x_v, y_v) in the vehicle coordinate system of a vehicle with the state $[x(t), y(t), v(t), \psi(t)]^T$ at time t to coordinates $(x_w(t), y_w(t))$

in the world coordinate system, the coordinates

$$(x_{v,ego,i}, y_{v,ego,i}) = \begin{cases} \left(\frac{1}{2}l_{ego}, \frac{1}{2}w_{ego}\right), & i = 1 \\ \left(-\frac{1}{2}l_{ego}, \frac{1}{2}w_{ego}\right), & i = 2 \\ \left(-\frac{1}{2}l_{ego}, -\frac{1}{2}w_{ego}\right), & i = 3 \\ \left(\frac{1}{2}l_{ego}, -\frac{1}{2}w_{ego}\right), & i = 4 \end{cases} \quad (7.4)$$

of the four corners $i = 1, 2, 3, 4$ of the rectangle representing the contour of the ego vehicle in the vehicle coordinate system of the ego vehicle with the state $[x_{ego}(t), y_{ego}(t), v_{ego}(t), \psi_{ego}(t)]^T$ at time t and the coordinates

$$(x_{v,obj,i}, y_{v,obj,i}) = \begin{cases} \left(\frac{1}{2}l_{obj}, \frac{1}{2}w_{obj}\right), & i = 1 \\ \left(-\frac{1}{2}l_{obj}, \frac{1}{2}w_{obj}\right), & i = 2 \\ \left(-\frac{1}{2}l_{obj}, -\frac{1}{2}w_{obj}\right), & i = 3 \\ \left(\frac{1}{2}l_{obj}, -\frac{1}{2}w_{obj}\right), & i = 4 \end{cases} \quad (7.5)$$

of the four corners $i = 1, 2, 3, 4$ of the rectangle representing the contour of the object in the vehicle coordinate system of the object with the state $[x_{obj}(t), y_{obj}(t), v_{obj}(t), \psi_{obj}(t)]^T$ at time t transform to the following coordinates $(x_{ego,i}(t), y_{ego,i}(t))$ and $(x_{obj,i}(t), y_{obj,i}(t))$ in the world coordinate system, respectively:

$$\begin{bmatrix} x_{ego,i}(t) \\ y_{ego,i}(t) \end{bmatrix} = \begin{bmatrix} \cos(\psi_{ego}(t)) & -\sin(\psi_{ego}(t)) \\ \sin(\psi_{ego}(t)) & \cos(\psi_{ego}(t)) \end{bmatrix} \begin{bmatrix} x_{v,ego,i} \\ y_{v,ego,i} \end{bmatrix} + \begin{bmatrix} x_{ego}(t) \\ y_{ego}(t) \end{bmatrix}, \quad (7.6)$$

$$\begin{bmatrix} x_{obj,i}(t) \\ y_{obj,i}(t) \end{bmatrix} = \begin{bmatrix} \cos(\psi_{obj}(t)) & -\sin(\psi_{obj}(t)) \\ \sin(\psi_{obj}(t)) & \cos(\psi_{obj}(t)) \end{bmatrix} \begin{bmatrix} x_{v,obj,i} \\ y_{v,obj,i} \end{bmatrix} + \begin{bmatrix} x_{obj}(t) \\ y_{obj}(t) \end{bmatrix}, \quad (7.7)$$

$i = 1, 2, 3, 4$. This allows to compute the coordinates $(x_{ego,i}(t), y_{ego,i}(t))$ and $(x_{obj,i}(t), y_{obj,i}(t))$ of the corners of the rectangles representing the contours of the ego vehicle and the object, respectively, in the world coordinate system determining the space occupied by the ego vehicle and the object as well as the distance between them along their trajectory from their states $[x_{ego}(t), y_{ego}(t), v_{ego}(t), \psi_{ego}(t)]^T$ and $[x_{obj}(t), y_{obj}(t), v_{obj}(t), \psi_{obj}(t)]^T$ at all discrete time instants $t = t_0 + m\delta t$, $m = 0, 1, \dots$, at which these states are obtained by numerically solving the differential equations (6.2)–(6.5) and (6.6)–(6.9).

The initial coordinates $x_{ego,0} = x_{ego}(t_0)$ and $y_{ego,0} = y_{ego}(t_0)$ of the center of gravity of the ego vehicle, its initial longitudinal velocity $v_{ego,0} = v_{ego}(t_0)$ and its initial yaw angle $\psi_{ego,0} = \psi_{ego}(t_0) = 0$ as well as the initial coordinates $x_{obj,0} = x_{obj}(t_0)$

7.1 System Model for the Automatic Emergency Steering System

and $y_{\text{obj},0} = y_{\text{obj}}(t_0)$ of the center of gravity of the object, its initial longitudinal velocity $v_{\text{obj},0} = v_{\text{obj}}(t_0)$ and its initial yaw angle $\psi_{\text{obj},0} = \psi_{\text{obj}}(t_0) = 0$ forming the initial state vector

$$\mathbf{x}_0 = \begin{bmatrix} x_{\text{ego},0} \\ y_{\text{ego},0} \\ v_{\text{ego},0} \\ 0 \\ x_{\text{obj},0} \\ y_{\text{obj},0} \\ v_{\text{obj},0} \\ 0 \end{bmatrix} = \begin{bmatrix} x_{\text{ego},0} \\ y_{\text{ego},0} \\ v_{\text{ego},0} \\ \psi_{\text{ego},0} \\ x_{\text{obj},0} \\ y_{\text{obj},0} \\ v_{\text{obj},0} \\ \psi_{\text{obj},0} \end{bmatrix} = \begin{bmatrix} x_{\text{ego}}(t_0) \\ y_{\text{ego}}(t_0) \\ v_{\text{ego}}(t_0) \\ \psi_{\text{ego}}(t_0) \\ x_{\text{obj}}(t_0) \\ y_{\text{obj}}(t_0) \\ v_{\text{obj}}(t_0) \\ \psi_{\text{obj}}(t_0) \end{bmatrix} = \mathbf{x}(t_0) \quad (7.8)$$

at the beginning of the considered driving scenario together with the time instant t_0 at which their driving maneuvers not initiated by the automated vehicular safety system, i.e., the AES system, start, their longitudinal and lateral accelerations $a_{\text{lon,ego}}(t_0) = 0$, $a_{\text{lat,ego}}(t_0) = 0$, $a_{\text{lon,obj}}(t_0) = 0$ and $a_{\text{lat,obj}}(t_0) = 0$ during these driving maneuvers, their turn radii $r_{\text{min,ego}}$ and $r_{\text{min,obj}}$ as well as the coordinates $(x_{\text{v,ego},i}, y_{\text{v,ego},i})$ and $(x_{\text{v,obj},i}, y_{\text{v,obj},i})$, $i = 1, 2, 3, 4$, of the corners of the rectangles representing the contours of the ego vehicle and the object in the vehicle coordinate systems from (7.4) and (7.5), respectively, completely characterize the whole considered driving scenario.

They are the $N_\xi = 31$ scenario parameters collected in the vector

$$\xi = \begin{bmatrix} x_{\text{ego},0} \\ y_{\text{ego},0} \\ v_{\text{ego},0} \\ \psi_{\text{ego},0} \\ x_{\text{obj},0} \\ y_{\text{obj},0} \\ v_{\text{obj},0} \\ \psi_{\text{obj},0} \\ t_0 \\ a_{\text{lon,ego}}(t_0) \\ a_{\text{lat,ego}}(t_0) \\ a_{\text{lon,obj}}(t_0) \\ a_{\text{lat,obj}}(t_0) \\ r_{\text{min,ego}} \\ r_{\text{min,obj}} \\ x_{\text{v,ego},1} \\ y_{\text{v,ego},1} \\ x_{\text{v,ego},2} \\ y_{\text{v,ego},2} \\ x_{\text{v,ego},3} \\ y_{\text{v,ego},3} \\ x_{\text{v,ego},4} \\ y_{\text{v,ego},4} \\ x_{\text{v,obj},1} \\ y_{\text{v,obj},1} \\ x_{\text{v,obj},2} \\ y_{\text{v,obj},2} \\ x_{\text{v,obj},3} \\ y_{\text{v,obj},3} \\ x_{\text{v,obj},4} \\ y_{\text{v,obj},4} \end{bmatrix} = \begin{bmatrix} x_{\text{ego},0} \\ y_{\text{ego},0} \\ v_{\text{ego},0} \\ 0 \\ x_{\text{obj},0} \\ y_{\text{obj},0} \\ v_{\text{obj},0} \\ 0 \\ t_0 \\ 0 \\ 0 \\ 0 \\ 0 \\ r_{\text{min,ego}} \\ r_{\text{min,obj}} \\ \frac{1}{2}l_{\text{ego}} \\ \frac{1}{2}w_{\text{ego}} \\ -\frac{1}{2}l_{\text{ego}} \\ \frac{1}{2}w_{\text{ego}} \\ -\frac{1}{2}l_{\text{ego}} \\ -\frac{1}{2}w_{\text{ego}} \\ \frac{1}{2}l_{\text{ego}} \\ -\frac{1}{2}w_{\text{ego}} \\ \frac{1}{2}l_{\text{obj}} \\ \frac{1}{2}w_{\text{obj}} \\ -\frac{1}{2}l_{\text{obj}} \\ \frac{1}{2}w_{\text{obj}} \\ -\frac{1}{2}l_{\text{obj}} \\ -\frac{1}{2}w_{\text{obj}} \\ \frac{1}{2}l_{\text{obj}} \\ -\frac{1}{2}w_{\text{obj}} \end{bmatrix}. \quad (7.9)$$

So, the considered driving scenario can be varied by varying the initial coordinates $x_{\text{ego},0}$ and $y_{\text{ego},0}$ of the center of gravity of the ego vehicle, its initial longitudinal velocity $v_{\text{ego},0}$, its turn radius $r_{\text{min,ego}}$, and its length l_{ego} and width w_{ego} , the initial coordinates $x_{\text{obj},0}$ and $y_{\text{obj},0}$ of the center of gravity of the object, its initial longitudinal

velocity $v_{\text{obj},0}$, its turn radius $r_{\text{min,obj}}$, and its length l_{obj} and width w_{obj} as well as the time instant t_0 at which their driving maneuvers not initiated by the AES system start to obtain various driving scenarios, which can be seen as instances of the same basic driving scenario.

7.1.2 Stochastic Model of the Automatic Emergency Steering System

The general mathematical model of automated vehicular safety systems depicted in Figure 2.4, which consists of a stochastic model of the sensors including their measurement errors and a mathematical model of the automated vehicular safety function, does not only apply to the AEB system considered in the previous chapter but also to the AES system considered in this chapter.

7.1.2.1 Stochastic Model of the Sensors of the Automatic Emergency Steering System

As in the AEB system, the sensors take measurements with the sampling rate f_s at the time instants $t_n = \frac{n}{f_s}$ with the discrete time index $n = 0, 1, \dots$ and deliver the measurements $\mathbf{y}[n]$ in (6.51) consisting of the measured distance $\hat{x}[n]$ and relative velocity $\hat{v}[n]$ at the time instant t_n . The actual distance $x[n]$ between the ego vehicle and the object and their actual relative velocity $v[n]$, the $M = 2$ quantities observed by the sensors at the time instant t_n , are functions of the state $\mathbf{x}[n]$ of the dynamic system at this time instant, which, in case of the considered AES system, is given by

$$\mathbf{x}[n] = \mathbf{x}(t_n) = \begin{bmatrix} x_{\text{ego}}(t_n) \\ y_{\text{ego}}(t_n) \\ v_{\text{ego}}(t_n) \\ \psi_{\text{ego}}(t_n) \\ x_{\text{obj}}(t_n) \\ y_{\text{obj}}(t_n) \\ v_{\text{obj}}(t_n) \\ \psi_{\text{obj}}(t_n) \end{bmatrix} = \begin{bmatrix} x_{\text{ego}}[n] \\ y_{\text{ego}}[n] \\ v_{\text{ego}}[n] \\ \psi_{\text{ego}}[n] \\ x_{\text{obj}}[n] \\ y_{\text{obj}}[n] \\ v_{\text{obj}}[n] \\ \psi_{\text{obj}}[n] \end{bmatrix} \quad (7.10)$$

according to (7.3) with $N = 8$ state variables, namely, the coordinates $x_{\text{ego}}[n]$ and $y_{\text{ego}}[n]$ of the center of gravity of the ego vehicle, its longitudinal velocity $v_{\text{ego}}[n]$ and its yaw angle $\psi_{\text{ego}}[n]$ as well as the coordinates $x_{\text{obj}}[n]$ and $y_{\text{obj}}[n]$ of the center of gravity of the object, its longitudinal velocity $v_{\text{obj}}[n]$ and its yaw angle $\psi_{\text{obj}}[n]$, at the time instant t_n . The measured distance $\hat{x}[n]$ at the time instant t_n expressed in (6.49) is the sum of the actual distance $x[n]$ between the ego vehicle and the object, and the sensor measurement error $\varepsilon_x[n]$ in the measured distance at this time instant while the

measured relative velocity $\hat{v}[n]$ at the time instant t_n expressed in (6.50) is the sum of their actual relative velocity $v[n]$ and the sensor measurement error $\varepsilon_v[n]$ in the measured relative velocity at this time instant such that these measurements $\mathbf{y}[n]$ are also a function of the state $\mathbf{x}[n]$ at the time instant t_n and, in addition, of the errors $\boldsymbol{\varepsilon}[n]$ at the time instant t_n in (6.52), which consist of the $E = 2$ sensor measurement errors $\varepsilon_x[n]$ and $\varepsilon_v[n]$ at this time instant, as expressed in (2.8).

Again, the sensor measurement errors in the measured distance between the ego vehicle and the object, and their relative velocity at the time instants t_n are modeled by additive i.i.d. zero-mean Gaussian random variables $\varepsilon_x[n] \sim \mathcal{N}(0, \sigma_x^2)$ of standard deviation σ_x and $\varepsilon_v[n] \sim \mathcal{N}(0, \sigma_v^2)$ of standard deviation σ_v , respectively. Consequently, the error vector $\boldsymbol{\varepsilon}[n]$ at the time instant t_n in (6.52) is Gaussian, i.e., $\boldsymbol{\varepsilon}[n] \sim \mathcal{N}(\boldsymbol{\mu}_n, \mathbf{C}_n)$, and has the pdf $f_{\boldsymbol{\varepsilon}[n]}(\boldsymbol{\varepsilon}[n])$ in (2.10) with the mean $\boldsymbol{\mu}_n = \mathbf{0}$ from (6.53) and the covariance matrix \mathbf{C}_n from (6.54) under the assumption that the sensor measurement errors $\varepsilon_x[n]$ and $\varepsilon_v[n]$ at the time instant t_n are statistically independent.

So, the standard deviations σ_x and σ_v of the sensor measurement errors and the sampling rate f_s are the $N_\sigma = 3$ sensor parameters that determine the sensors in this stochastic model of them and are collected in the vector $\boldsymbol{\sigma}$ stated in (6.55) as in the stochastic model of the sensors in the AEB system before.

7.1.2.2 Mathematical Model of the Function of the Automatic Emergency Steering System

The function of the considered AES system derives safety-relevant information from the measurements $\mathbf{y}[n]$ at the time instant t_n in order to interpret the current driving situation, and decides on whether to intervene by triggering an emergency steer intervention for mitigating a dangerous driving situation using a decision rule. In the following, the same three exemplary decision rules as in case of the AEB system, namely, the TTC-based, the advanced TTC-based and the BTN-based decision rule, which are represented by the decision functions $f_{\text{TTC}}(\cdot; \varphi)$, $f_{\text{adv. TTC}}(\cdot; \varphi)$ and $f_{\text{BTN}}(\cdot; \varphi)$ in (6.58), (6.61) and (6.65), respectively, and can also be used for deciding on whether to trigger an emergency steer intervention instead of an emergency brake intervention, are considered. They have the form shown in (2.18) with $N_\varphi = 1$ adjustable parameter $\varphi = \varphi \in \mathbb{R}$ and can easily be extended or replaced by others, which might also have more parameters.

As long as the used decision rule is not fulfilled, i.e., $f_c(\mathbf{y}[n]; \varphi) = 0$, $c \in \{\text{TTC}, \text{adv. TTC}, \text{BTN}\}$, the function does not trigger the emergency steer intervention, and, as soon as the decision rule is fulfilled for the measurements $\mathbf{y}[n]$ at a time instant

t_n , i.e., $f_c(\mathbf{y}[n]; \varphi) = 1$, the function triggers the emergency steer intervention. The smallest n for which $f_c(\mathbf{y}[n]; \varphi) = 1$ is the discrete time index

$$n_s = \min_{n \in \mathbb{N}_0} n \quad \text{s.t.} \quad f_c(\mathbf{y}[n]; \varphi) = 1 \quad (7.11)$$

that corresponds to the time instant

$$t_s = t_{n_s} = \frac{n_s}{f_s} \quad (7.12)$$

at which the measurements $\mathbf{y}[n_s]$ leading to triggering the emergency steer intervention are made and also to the time instant at which the emergency steer intervention is triggered under the simplifying assumption that it is instantly triggered without any delay after making these measurements.

7.2 Robust Function and Sensor Design for the Automatic Emergency Steering System

The proposed methodology for the robust function and sensor design allows to systematically design both functions and sensors of automated vehicular safety systems in general and thus not only those of the AEB system considered in the previous chapter but also those of the considered AES system in particular such that the customer requirements are fulfilled in a robust manner despite unavoidable sensor measurement errors. The function and the sensors can be designed by solving the optimization problems (4.1), (4.9) and (4.11) formulated in Chapter 4 for the robust function design, sensor design as well as joint function and sensor design, respectively, based on closed-form expressions for the probabilistic quality measure Q or solely based on simulations of the automated vehicular safety system under design as described in Chapter 5. For the design of the considered AES system, the following quality measure Q , which measures to what extent the function meets the customer requirements in a robust manner despite the unavoidable sensor measurement errors, can be used.

The customer is satisfied with the AES system applied in the driving scenario illustrated in Figure 6.1 if the smallest distance d between the ego vehicle and the object during an emergency steer intervention is neither too small nor too large. In other words, this smallest distance d has to lie in an acceptance interval $[d_{\min}, d_{\max}]$ from the minimal tolerable smallest distance d_{\min} to the maximal tolerable smallest distance d_{\max} , which can be chosen in a user-specific way. Hence, besides the final distance x_{end} after an emergency brake intervention, the smallest distance d during an emergency steer intervention is a further example for one of the customer satisfaction properties q_i , $i = 1, 2, \dots, N_q$, which have to lie in certain acceptance intervals $[q_{L,i}, q_{U,i}]$ such

that the intervention by an automated vehicular safety system is acceptable and the customer is satisfied with the system, and the acceptance interval $[d_{\min}, d_{\max}]$ for the smallest distance d with the lower bound d_{\min} and the upper bound d_{\max} corresponds to the acceptance interval $[q_{L,i}, q_{U,i}]$ for this customer satisfaction property q_i with the lower bound $q_{L,i}$ and the upper bound $q_{U,i}$.

In general, the customer satisfaction properties q_i collected in the customer satisfaction vector $\mathbf{q} = [q_1, q_2, \dots, q_{N_q}]^T = \mathbf{q}(\boldsymbol{\sigma}, \boldsymbol{\varepsilon}, f, \boldsymbol{\varphi}, \boldsymbol{\xi})$ are subject to the random sensor measurement errors $\boldsymbol{\varepsilon}[n]$ at the $n_{\text{end}} + 1$ time instants $t_n, n = 0, 1, \dots, n_{\text{end}}$, in the considered time interval collected in the vector $\boldsymbol{\varepsilon}$ given by (4.21) according to (4.22). This is also the case for the smallest distance d as an example for such a customer satisfaction property q_i . Consequently, it is a random variable as well and might lie inside or outside the acceptance interval $[d_{\min}, d_{\max}]$ such that the specification

$$d_{\min} \leq d \leq d_{\max} \quad (7.13)$$

for the customer satisfaction defined by this acceptance interval is fulfilled or violated as the customer satisfaction properties q_i are random variables and might lie inside or outside the acceptance intervals $[q_{L,i}, q_{U,i}], i = 1, 2, \dots, N_q$, in general such that the specifications $q_{L,i} \leq q_i \leq q_{U,i}, i = 1, 2, \dots, N_q$, for the customer satisfaction defined by these acceptance intervals are fulfilled or violated.

The quality measure Q , which measures to what extent the function meets the customer requirements in a robust manner despite the unavoidable sensor measurement errors, is defined as the worst-case probability $P_{\text{WC}}(\mathbf{q} \in \mathcal{A}_{\mathbf{q}})$ of fulfilling the specifications for the customer satisfaction, i.e., the minimum of the probability $P(\mathbf{q} \in \mathcal{A}_{\mathbf{q}})$ that all specifications $q_{L,i} \leq q_i \leq q_{U,i}, i = 1, 2, \dots, N_q$, for the customer satisfaction are fulfilled in all considered driving scenarios $\boldsymbol{\xi}$ from the scenario set \mathcal{X} in (4.33). Assuming that the smallest distance d is the only considered customer satisfaction property, i.e., $N_q = 1$ and $\mathbf{q} = q_1 = d$, the quality measure Q is the minimum of the probability $P(d_{\min} \leq d \leq d_{\max})$ that the smallest distance d fulfills the specification $d_{\min} \leq d \leq d_{\max}$ for the customer satisfaction in all considered driving scenarios $\boldsymbol{\xi}$ from the scenario set \mathcal{X} :

$$Q = \min_{\boldsymbol{\xi} \in \mathcal{X}} P(d_{\min} \leq d \leq d_{\max}). \quad (7.14)$$

With this quality measure Q , the constraint of the optimization problems (4.9) and (4.11) for the sensor design as well as the joint function and sensor design, respectively, reads

$$\min_{\boldsymbol{\xi} \in \mathcal{X}} P(d_{\min} \leq d \leq d_{\max}) \geq P_{\min}, \quad (7.15)$$

7.3 Numerical Examples for the Robust Design of the Automatic Emergency Steering System

where the required minimum worst-case probability P_{\min} of fulfilling the specification $d_{\min} \leq d \leq d_{\max}$ for the customer satisfaction is the required minimum quality level Q_{\min} according to (4.39).

Deriving closed-form expressions for the probability of fulfilling the specification for the customer satisfaction and thus for the quality measure Q would be even more difficult for the AES system due to the two-dimensional movement of the ego vehicle during the steering maneuver as compared to the AEB system with the movement of the ego vehicle restricted to one dimension during the braking maneuver under simplifying assumptions and is not pursued since this would also not be viable for the complex automated vehicular safety systems in practice and therefore the developers of such systems have to resort to a simulation-based design anyway. Due to this fact, the solution of the optimization problems (4.1), (4.9) and (4.11) for the robust function design, sensor design as well as joint function and sensor design, respectively, solely based on simulations of the AES system under design without the need for deriving closed-form expressions for the probabilistic quality measure Q is chosen to design its function and sensors.

7.3 Numerical Examples for the Robust Design of the Automatic Emergency Steering System

The numerical examples presented in this section demonstrate how the function and the sensors of the considered AES system can be designed with the proposed methodology for the robust function and sensor design. Throughout these numerical examples, the sampling rate is $f_s = 1$ kHz, the lateral acceleration after triggering the emergency steer intervention is $a = 5 \frac{\text{m}}{\text{s}^2}$, and the minimal and maximal tolerable smallest distances between the ego vehicle and the object during the emergency steer intervention are $d_{\min} = 0$ and $d_{\max} = 0.5$ m, respectively.

For the sake of simplicity, only the driving scenario that is shown in Figure 6.1 and characterized by the scenario parameters ξ_0 of the form given by (7.9) with the initial coordinates $x_{\text{ego},0} = 0$ and $y_{\text{ego},0} = 0$ of the center of gravity of the ego vehicle, its initial longitudinal velocity $v_{\text{ego},0} = 10 \frac{\text{m}}{\text{s}}$, its turn radius $r_{\min,\text{ego}} = 10$ m, and its length $l_{\text{ego}} = 4$ m and width $w_{\text{ego}} = 2$ m, the initial coordinates $x_{\text{obj},0} = 20$ m and $y_{\text{obj},0} = 0$ of the center of gravity of the object, its initial longitudinal velocity $v_{\text{obj},0} = 0$, and its length $l_{\text{obj}} = 4$ m and width $w_{\text{obj}} = 2$ m is considered. Hence, the scenario set \mathcal{X} consists of only this single driving scenario: $\mathcal{X} = \{\xi_0\}$. As a consequence, the quality measure Q defined in (7.14), which measures to what extent the function meets the customer requirements in a robust manner despite the

unavoidable sensor measurement errors, is the probability of fulfilling the specification $d_{\min} \leq d \leq d_{\max}$ for the customer satisfaction evaluated at this driving scenario $\xi = \xi_0$:

$$Q = P(d_{\min} \leq d \leq d_{\max})|_{\xi=\xi_0}. \quad (7.16)$$

As in the robust design of the AEB system with sensor measurement errors in both the measured distance and measured relative velocity before, the possible domain for the values of the sensor parameters σ is given by (6.138) and the same costs C in (6.156) are chosen as simple illustrative example. With this possible domain \mathcal{S} of the sensor parameter values σ and these costs C as well as the quality measure Q in (7.16), i.e., the probability of fulfilling the specification $d_{\min} \leq d \leq d_{\max}$ for the customer satisfaction in the driving scenario $\xi = \xi_0$, the respective required minimum quality level $Q_{\min} = P_{\min}$, i.e., the required minimum probability P_{\min} of fulfilling this specification for the customer satisfaction in the driving scenario $\xi = \xi_0$, and the set $\mathcal{F} = \{f_c\}$ of the predefined decision rules for triggering the emergency steer intervention consisting of only one decision rule $f_c(\cdot; \varphi)$, $c \in \{\text{TTC, adv. TTC, BTN}\}$, with the single function parameter $\varphi = \varphi$, the optimization problem (4.11) of the joint function and sensor design reads

$$\begin{aligned} & (\sigma_{x,\text{opt}}, \sigma_{v,\text{opt}}, \varphi_{\text{opt}}) = \\ & \underset{\sigma_x \in \mathbb{R}^+, \sigma_v \in \mathbb{R}^+, \varphi \in \mathbb{R}}{\text{argmin}} \quad C \quad \text{s.t.} \quad P(d_{\min} \leq d \leq d_{\max})|_{\xi=\xi_0, f_s=1 \text{ kHz}, f=f_c} \geq P_{\min}. \end{aligned} \quad (7.17)$$

The probability $P(d_{\min} \leq d \leq d_{\max})$ of fulfilling the specification $d_{\min} \leq d \leq d_{\max}$ for the customer satisfaction can be estimated by a Monte Carlo simulation. In general, the Monte-Carlo-simulation-based estimate for the probability $P(q \in \mathcal{A}_q)$ of fulfilling all specifications $q_{L,i} \leq q_i \leq q_{U,i}$, $i = 1, 2, \dots, N_q$, for the customer satisfaction in case of given sensor parameters σ , a given decision rule f , given function parameters φ and scenario parameters ξ is the frequency $\hat{P}_M(q \in \mathcal{A}_q)$ of fulfilling all these specifications in the Monte Carlo simulation from (5.1). In the Monte Carlo simulation, M realizations $\varepsilon_1, \varepsilon_2, \dots, \varepsilon_M$ of all sensor measurement errors stated in (6.139), i.e., the sensor measurement errors $\varepsilon_x[n]$ and $\varepsilon_v[n]$ in the measured distance and relative velocity, respectively, at all time instants t_n , $n = 0, 1, \dots, n_{\text{end}}$, in the considered time interval are generated at random according to their probability distribution, i.e., the i.i.d. sensor measurement errors $\varepsilon_x[n]$ in the measured distance and the i.i.d. sensor measurement errors $\varepsilon_v[n]$ in the measured relative velocity at these time instants t_n , which are also statistically independent from each other at the same time instant t_n , are drawn from the zero-mean Gaussian distribution $\mathcal{N}(0, \sigma_x^2)$

7.3 Numerical Examples for the Robust Design of the Automatic Emergency Steering System

with the standard deviation σ_x and the zero-mean Gaussian distribution $\mathcal{N}(0, \sigma_v^2)$ with the standard deviation σ_v , respectively. Here, the discrete time index n_{end} of the last time instant $t_{n_{\text{end}}}$ of the considered time interval is chosen to be that of the last time instant before the collision of the ego vehicle and the object that would occur without emergency steer intervention and is given by (6.141) as in the previous robust design of the AEB system. Each realization ε_m , $m = 1, 2, \dots, M$, of the sensor measurement errors ε together with the given sensor parameters σ , the given decision rule f , the given function parameters φ , i.e., the single function parameter $\varphi = \varphi$ parameterizing the TTC-based decision rule $f_{\text{TTC}}(\cdot; \varphi)$, the advanced TTC-based decision rule $f_{\text{adv. TTC}}(\cdot; \varphi)$ and the BTN-based decision rule $f_{\text{BTN}}(\cdot; \varphi)$, and the scenario parameters $\xi = \xi_0$ is mapped to the respective values $q_m = q(\sigma, \varepsilon_m, f, \varphi, \xi)$ of the customer satisfaction properties q , i.e., the respective value of the smallest distance d between the ego vehicle and the object, the only customer satisfaction property $q = q_1 = d$ considered here, according to (4.22) by a simulation of the AES system. After computing the measured distance $\hat{x}[n]$ in (6.49) and the measured relative velocity $\hat{v}[n]$ in (6.50) forming the measurement vector $\mathbf{y}[n]$ in (6.51) from the generated sensor measurement errors $\varepsilon_x[n]$ and $\varepsilon_v[n]$, respectively, and evaluating the used decision rule $f_c(\mathbf{y}[n]; \varphi)$, $c \in \{\text{TTC}, \text{adv. TTC}, \text{BTN}\}$, at the time instants t_n , $n = 0, 1, \dots, n_s$, to determine the discrete time index n_s of the time instant t_s at which the emergency steer intervention is triggered as the smallest discrete time index n for which the result of the evaluation of the decision function is $f_c(\mathbf{y}[n]; \varphi) = 1$ according to (7.11), the smallest distance d is determined numerically by taking the minimum of all distances between the ego vehicle and the object during the steering maneuver at the discrete time instants of the simulation in (7.2) with the temporal distance $\delta t = 10^{-4}$ s between neighboring time instants. If there is not such a discrete time index n_s in the considered time interval, i.e., $n_s \notin \{0, 1, \dots, n_{\text{end}}\}$, no emergency steer intervention is triggered in this time interval such that the ego vehicle and the object collide. Whenever they collide, the smallest distance d between them is set to $-\infty$ and the specification $d_{\min} \leq d \leq d_{\max}$ for the customer satisfaction is not fulfilled.

In the M random experiments, it is counted how often the value of the smallest distance d lies in the acceptance interval $[d_{\min}, d_{\max}]$ and thus fulfills the specification $d_{\min} \leq d \leq d_{\max}$ for the customer satisfaction to obtain the number $M_{1,M}$ of how often this is the case and the frequency

$$\hat{P}_M(d_{\min} \leq d \leq d_{\max}) = \frac{M_{1,M}}{M} \quad (7.18)$$

of fulfilling the specification $d_{\min} \leq d \leq d_{\max}$ for the customer satisfaction, which is

an estimate for the probability $P(d_{\min} \leq d \leq d_{\max})$ of fulfilling this specification for the customer satisfaction.

Alternatively, the probability $P(d_{\min} \leq d \leq d_{\max})$ of fulfilling the specification $d_{\min} \leq d \leq d_{\max}$ for the customer satisfaction can also be approximated by using the adaptation of the worst-case distance approach to the robust design of automated vehicular safety systems. In general, the worst-case-distance-based approximation of the probability $P(\mathbf{q} \in \mathcal{A}_{\mathbf{q}})$ of fulfilling all specifications $q_{L,i} \leq q_i \leq q_{U,i}$, $i = 1, 2, \dots, N_{\mathbf{q}}$, for the customer satisfaction is given by (5.82). Thus, in case of the AES system at hand, the probability $P(d_{\min} \leq d \leq d_{\max})$ of fulfilling the specification $d_{\min} \leq d \leq d_{\max}$ for the customer satisfaction can be approximated by

$$\hat{P}(d_{\min} \leq d \leq d_{\max}) = \prod_{n \in \bar{\mathbb{I}}} \begin{cases} \Phi(-\beta_n), & \boldsymbol{\mu} \in \mathcal{I}_{\boldsymbol{\varepsilon},n} \\ \Phi(\beta_n), & \boldsymbol{\mu} \in \bar{\mathcal{I}}_{\boldsymbol{\varepsilon},n} \end{cases} \cdot \left(1 - \prod_{n \in \mathbb{I}} \begin{cases} \Phi(-\beta_n), & \boldsymbol{\mu} \in \mathcal{I}_{\boldsymbol{\varepsilon},n} \\ \Phi(\beta_n), & \boldsymbol{\mu} \in \bar{\mathcal{I}}_{\boldsymbol{\varepsilon},n} \end{cases} \right). \quad (7.19)$$

The set $\bar{\mathbb{I}}$ of the indices n of the time instants t_n , $n = 0, 1, \dots, n_{\text{end}}$, in the considered time interval at which the function must not decide for an emergency steer intervention to fulfill the specification $d_{\min} \leq d \leq d_{\max}$ for the customer satisfaction is given by (5.88) and the set \mathbb{I} of the indices n of the time instants t_n in the considered time interval at which the function must decide for an emergency steer intervention at least once to fulfill this specification by (5.89), where the indices n_{\min} and n_{\max} are determined by simulations of the AES system as explained at the end of Chapter 5 for automated vehicular safety systems in general. For each time instant t_n , $n = 0, 1, \dots, n_{\text{end}}$, the AES system is simulated after deciding for an emergency steer intervention and triggering it at one of those time instants t_n in order to map this time instant together with the given scenario parameters $\boldsymbol{\xi} = \boldsymbol{\xi}_0$ to the respective values of the customer satisfaction properties \mathbf{q} , i.e., the respective value of the smallest distance d between the ego vehicle and the object, the only customer satisfaction property $\mathbf{q} = q_1 = d$ considered here, where the smallest distance d is determined numerically by taking the minimum of all distances between the ego vehicle and the object during the steering maneuver at the discrete time instants of the simulation in (7.2) with the temporal distance $\delta t = 10^{-4}$ s between neighboring time instants as in the Monte Carlo simulation. The so obtained smallest distances d fulfill the specification $d_{\min} \leq d \leq d_{\max}$ for the customer satisfaction if the time instant t_n at which the emergency steer intervention is triggered has a discrete time index n between 775 and 884, i.e., $n \in \{775, 776, \dots, 884\}$. Since these time instants t_n for

which the specification $d_{\min} \leq d \leq d_{\max}$ for the customer satisfaction is fulfilled if the function decides for an emergency steer intervention based on the sensor measurements $\mathbf{y}[n]$ at one of these time instants form a block with indices n ranging from n_{\min} to n_{\max} , where $0 \leq n_{\min} = 775 \leq n_{\max} = 884 \leq n_{\text{end}} = 1,600$, and this specification for the customer satisfaction is not fulfilled if the function does not decide for an emergency steer intervention based on the sensor measurements $\mathbf{y}[n]$ at any of the considered time instants t_n , which inevitably leads to a collision, the function must not decide for an intervention based on the sensor measurements $\mathbf{y}[n]$ at the time instants t_n , $n = 0, 1, \dots, n_{\min} - 1$, before this block and must decide for an intervention based on the sensor measurements $\mathbf{y}[n]$ at the time instants t_n , $n = n_{\min}, n_{\min} + 1, \dots, n_{\max}$, in this block at least once to fulfill the specification $d_{\min} \leq d \leq d_{\max}$ for the customer satisfaction. Consequently, the set $\bar{\mathbb{I}}$ of the indices n of the time instants t_n at which the function must not decide for an emergency steer intervention based on the corresponding sensor measurements $\mathbf{y}[n]$ to fulfill the specification $d_{\min} \leq d \leq d_{\max}$ for the customer satisfaction, and the set \mathbb{I} of the indices n of the time instants t_n at which the function must decide for an emergency steer intervention based on the corresponding sensor measurements $\mathbf{y}[n]$ at least once to fulfill the specification $d_{\min} \leq d \leq d_{\max}$ for the customer satisfaction read $\bar{\mathbb{I}} = \{0, 1, \dots, 774\}$ and $\mathbb{I} = \{775, 776, \dots, 884\}$, respectively. So, they have the form in (5.88) and (5.89) with $n_{\min} = 775$ and $n_{\max} = 884$.

As in the robust design of the AEB system, the check of whether $\boldsymbol{\mu} \in \mathcal{I}_{\varepsilon, n}$ or $\boldsymbol{\mu} \in \bar{\mathcal{I}}_{\varepsilon, n}$ can be performed as described in (5.86) and (5.87). If the result of evaluating the decision rule $f_c(\cdot; \varphi)$, $c \in \{\text{TTC}, \text{adv. TTC}, \text{BTN}\}$, with a single function parameter $\varphi = \varphi$ at the mean $\boldsymbol{\mu}_n = \mathbf{0}$ of the sensor measurement errors $\boldsymbol{\varepsilon}[n]$ at the time instant t_n , i.e., the error-free measurements $\mathbf{y}(\mathbf{x}[n], \boldsymbol{\mu}_n) = \mathbf{y}(\mathbf{x}[n], \mathbf{0})$ at the time instant t_n , is $f_c(\mathbf{y}(\mathbf{x}[n], \boldsymbol{\mu}_n); \varphi) = f_c(\mathbf{y}(\mathbf{x}[n], \mathbf{0}); \varphi) = 1$, then $\boldsymbol{\mu} \in \mathcal{I}_{\varepsilon, n}$ and, otherwise, if it is $f_c(\mathbf{y}(\mathbf{x}[n], \boldsymbol{\mu}_n); \varphi) = f_c(\mathbf{y}(\mathbf{x}[n], \mathbf{0}); \varphi) = 0$, then $\boldsymbol{\mu} \in \bar{\mathcal{I}}_{\varepsilon, n}$.

The optimization problem in (5.85), whose solution yields the worst-case distance β_n at the time instant t_n , is given by (6.144) in case of both the previously considered AEB system and the considered AES system using the decision rule $f_c(\cdot; \varphi)$ parameterized by a single function parameter $\varphi = \varphi$ with the square of the Mahalanobis distance $\beta_n(\boldsymbol{\varepsilon}[n])$ of the $E = 2$ sensor measurement errors $\boldsymbol{\varepsilon}[n]$ at the time instant t_n , whose mean and covariance matrix are given in (6.53) and (6.54), respectively, from their mean $\boldsymbol{\mu}_n = \mathbf{0}$ stated in (5.49). With the definition of three considered decision rules $f_c(\cdot; \varphi)$ in (6.58), (6.61) and (6.65), this optimization problem transforms to (6.145), (6.146) and (6.147) for the TTC-based decision rule $f_{\text{TTC}}(\cdot; \varphi)$, the advanced TTC-based decision rule $f_{\text{adv. TTC}}(\cdot; \varphi)$ and the BTN-based decision rule $f_{\text{BTN}}(\cdot; \varphi)$,

respectively.

Solving the optimization problem (7.17) for the required minimum probability $P_{\min} = 0.99$ of fulfilling the specification for the customer satisfaction and the BTN-based decision rule $f_{\text{BTN}}(\cdot; \varphi)$, i.e., $c = \text{BTN}$, with the worst-case-distance-based approximation $\hat{P}(d_{\min} \leq d \leq d_{\max})$ instead of the actual probability $P(d_{\min} \leq d \leq d_{\max})$ of fulfilling the specification for the customer satisfaction yields the optimal values $\sigma_{x,\text{opt}} = 0.37099 \text{ m}$, $\sigma_{v,\text{opt}} = 0.18155 \frac{\text{m}}{\text{s}}$ and $\varphi_{\text{opt}} = 7.34528 \frac{\text{m}}{\text{s}^2}$ for the standard deviation σ_x of the sensor measurement errors in the measured distance, the standard deviation σ_v of the sensor measurement errors in the measured relative velocity and the function parameter φ , respectively. The costs corresponding to these optimal parameter values are $C = -0.55254$ while the corresponding probability of fulfilling the specification for the customer satisfaction is $P(d_{\min} \leq d \leq d_{\max}) = 0.98991 < P_{\min} = 0.99$, which is the accurate Monte-Carlo-based estimate $\hat{P}_{10^8}(d_{\min} \leq d \leq d_{\max})$ from $M = 10^8$ simulations of the AES system used as ground truth and approximately fulfills the constraint of the optimization problem with $P_{\min} = 0.99$ but slightly violates it due to approximation errors of the worst-case-distance-based approximation. By solving it with the Monte-Carlo-based estimate $\hat{P}_{10^5}(d_{\min} \leq d \leq d_{\max})$ from $M = 10^5$ simulations of the AES system instead of the actual probability $P(d_{\min} \leq d \leq d_{\max})$ of fulfilling the specification for the customer satisfaction, the optimal parameter values $\sigma_{x,\text{opt}} = 0.38636 \text{ m}$, $\sigma_{v,\text{opt}} = 0.16424 \frac{\text{m}}{\text{s}}$ and $\varphi_{\text{opt}} = 7.32785 \frac{\text{m}}{\text{s}^2}$ are obtained, which deviate slightly from those obtained with the worst-case-distance-based approximation $\hat{P}(d_{\min} \leq d \leq d_{\max})$. For these parameter values, the costs are $C = -0.55059$, which are larger than those for the optimal parameter values obtained with the worst-case-distance-based approximation $\hat{P}(d_{\min} \leq d \leq d_{\max})$, and the probability of fulfilling the specification for the customer satisfaction is $P(d_{\min} \leq d \leq d_{\max}) = 0.98999 < P_{\min} = 0.99$, which approximately fulfills the constraint of the optimization problem with $P_{\min} = 0.99$ but slightly violates it due to estimation errors of the Monte Carlo simulation. The problem of slightly violating the constraint of the optimization problem with the required minimum probability $P_{\min} = 0.99$ of fulfilling the specification for the customer satisfaction by both the Monte-Carlo- and worst-case-distance-based solution of the optimization problem because of estimation and approximation errors, respectively, can be handled by slightly increasing the required minimum probability P_{\min} in the constraint of the optimization problem such that it is slightly larger than the actual required minimum probability $P'_{\min} = 0.99$ of fulfilling the specification for the customer satisfaction and the probability $P(d_{\min} \leq d \leq d_{\max})$ of fulfilling this specification resulting from solving the optimization problem is not smaller than the actual required minimum

7.3 Numerical Examples for the Robust Design of the Automatic Emergency Steering System

probability $P'_{\min} = 0.99$ as desired despite estimation and approximation errors.

Similarly to the joint function and sensor design for the AEB system in the previous chapter, the 51,700,000 simulations of the AES system with even more evaluations of the BTN-based decision rule $f_{\text{BTN}}(\cdot; \varphi)$ that solving the optimization problem (7.17) with the Monte-Carlo-based estimate $\hat{P}_{10^5}(d_{\min} \leq d \leq d_{\max})$ requires are significantly more than the 1,601 simulations of the AES system with 4,497,559 evaluations of the BTN-based decision rule $f_{\text{BTN}}(\cdot; \varphi)$ that solving it with the worst-case-distance-based approximation $\hat{P}(d_{\min} \leq d \leq d_{\max})$ requires although the latter provides a result of similar accuracy as the former. This demonstrates once again that the adaptation of the worst-case distance approach to the robust design of automated vehicular safety systems can significantly reduce the required number of simulations of the automated vehicular safety system under design by replacing an expensive Monte Carlo simulation requiring a huge number of simulations of the automated vehicular safety system for a comparable accuracy, and with this the computational complexity, the load for simulation servers as well as the time and expenses needed for the development of automated vehicular safety systems.

Conclusion 8

In this thesis, a new methodology for the robust design of automated vehicular safety systems considering unavoidable sensor measurement errors has been developed. It is the first general design methodology with which both sensors and functions for a variety of automated vehicular safety systems can be systematically designed while taking both the unavoidable sensor measurement errors and the customer satisfaction into account. This is of high importance because the functions of automated vehicular safety systems use the measurements of sensors sensing the environment of the vehicle in order to interpret the driving situation and trigger appropriate actions in dangerous driving situations, e.g., an emergency brake intervention, such that they are typically very vulnerable to sensor imperfections and unavoidable sensor measurement errors have a negative impact on both the safety and the satisfaction of the customer.

8.1 Summary

After introducing the system model, which can be split into a mathematical representation of the considered driving scenario in which the automated vehicular safety system is applied and a stochastic model of the automated vehicular safety system itself including sensor measurement errors, a general overview of a robust system design as performed in integrated circuit design is given in order to understand how ideas from integrated circuit design, a completely different application area, can be transferred to the design of automated vehicular safety systems, which marks a paradigm shift. Several analogies to the design of integrated circuits considering manufacturing tolerances help to formulate the robust design of automated vehicular safety systems considering sensor measurement errors as optimization problems based on the introduced system model, which allow for a systematic solution of the design problems. In particular, three basic design problems have been considered, which application engineers having to select sensors with appropriate properties and to adjust the functions in the development of automated vehicular safety systems are typically confronted with, namely, the function design for given sensors, the sensor design for a given function as well as the joint function and sensor design. For each of these three basic design problems, an

optimization problem has been formulated by elaborating on the analogies to a robust system design as performed in integrated circuit design, which demonstrates that the performance properties, the statistical parameters and the operating parameters in such a robust system design correspond to the customer satisfaction properties, the random variables modeling the sensor measurement errors and the scenario parameters in the robust design of automated vehicular safety systems considering sensor measurement errors, respectively. Solving the formulated optimization problems yields the optimal sensor parameter values, the best decision rule for triggering the respective action by the function and the optimal function parameter values of the automated vehicular safety system under design with respect to a quality measure. As the worst-case probability of fulfilling the performance specifications, i.e., the minimum of the probability that all performance specifications defined by acceptance intervals for the performance properties are fulfilled in the whole tolerance region of the operating parameters, is used as quality measure for the robust system design, the worst-case probability of fulfilling the specifications for the customer satisfaction, i.e., the minimum of the probability that all specifications for the customer satisfaction defined by acceptance intervals for the customer satisfaction properties are fulfilled in all driving scenarios with the various scenario parameter values from the set of considered driving scenarios, is used as quality measure for the robust design of automated vehicular safety systems in order to take the unavoidable sensor measurement errors and the customer satisfaction into account.

The solution of the optimization problem formulated for the function design maximizes this quality measure, which measures to what extent the function meets the customer requirements in a robust manner despite the unavoidable sensor measurement errors, such that the requirements of the customers are met in a robust manner despite the unavoidable sensor measurement errors to the greatest possible extent. Moreover, the constraints of the optimization problems formulated for the sensor as well as joint function and sensor design define design spaces, from which application engineers have to choose the sensor parameter values, the decision rule and the function parameter values such that the quality measure is not smaller than the required minimum quality level and thus the customer requirements are met in a robust manner despite the unavoidable sensor measurement errors to the desired extent. Hence, application engineers are provided with design spaces that represent the requirements the sensors have to fulfill, which is of particular importance for the overall design task in an industrial environment. The solution of the optimization problems formulated for the sensor as well as joint function and sensor design minimizes the costs inside the design spaces such that the quality measure does not lie below the required minimum quality level

and thus the customer requirements are met in a robust manner despite the unavoidable sensor measurement errors to the desired extent at minimal costs.

With the formulation of the optimization problems and the definition of the quality measure, a new methodology for the robust design of automated vehicular safety systems considering unavoidable sensor measurement errors has been developed. Solving the formulated optimization problems requires several evaluations of the quality measure. As there is usually no closed-form expression for the quality measure due to the high complexity of automated vehicular safety systems in practice, it has to be evaluated based on simulations of the automated vehicular safety system under design. To this end, different possibilities for such a simulation-based evaluation of the quality measure again based on analogies to a robust system design as performed in integrated circuit design have been suggested. This eventually leads to a new methodology for the robust design of automated vehicular safety systems that allows to systematically design both functions and sensors of automated vehicular safety systems by solving the formulated optimization problems solely based on simulations of the automated vehicular safety system under design such that the customer requirements are fulfilled in a robust manner despite unavoidable sensor measurement errors.

The Monte Carlo simulation is one possibility for the simulation-based evaluation of the quality measure, which has been defined to be the minimum of the probability of fulfilling the specifications for the customer satisfaction in all considered driving scenarios. As the probability of fulfilling the performance specifications in the robust system design, the probability of fulfilling the specifications for the customer satisfaction is estimated by a Monte Carlo simulation. The estimate for the probability of fulfilling the specifications for the customer satisfaction obtained by such a Monte Carlo simulation is the frequency of fulfilling the specifications for the customer satisfaction in the repeated simulations of the automated vehicular safety system with realizations of the sensor measurement errors drawn at random from their probability distribution. Estimating the probability of fulfilling the specifications for the customer satisfaction in this way has a beneficial advantage but also an important drawback. On the one hand, it can be implemented easily and it is easy to apply it to different automated vehicular safety systems due to its generality. On the other hand, however, a large number of simulations of the automated vehicular safety system has to be performed in order to obtain an accurate estimate for the probability of fulfilling the specifications for the customer satisfaction, which might lead to a prohibitively large computational complexity in practice.

In order to overcome this problem, the probability of fulfilling the specifications for the customer satisfaction can alternatively be approximated by using worst-case

distances, which have already been used in the integrated circuit design considering manufacturing tolerances for approximating the probability of fulfilling the performance specifications. The direct application of this worst-case distance approach to the robust design of automated vehicular safety systems inherits the benefits from its application to the integrated circuit design. The integration of the multivariate Gaussian pdf of the sensor measurement errors in the error acceptance region defined as the set of all values of the sensor measurement errors for which the automated vehicular safety system fulfills the specifications for the customer satisfaction to obtain the probability of fulfilling the specifications for the customer satisfaction is simplified to approximating this probability by evaluating the standard normal cdf at worst-case distances. Each required worst-case distance can be determined by an optimization minimizing the distance between the sensor measurement errors on the boundary of one of the individual error acceptance region partitions into which the error acceptance region can be decomposed and their mean. Appropriate optimization methods for solving these optimizations choose the simulations of the automated vehicular safety system required for solving the optimizations automatically in a smart way serving the achievement of the optimization goal and thus replace a computationally expensive Monte Carlo simulation, which just chooses an extensive amount of simulations of the automated vehicular safety system according to the underlying probability distribution in a brute-force way for estimating the probability of fulfilling the specifications for the customer satisfaction, by a few relevant simulations that deliver the required information for approximating this probability. This is the reason why approximating the probability of fulfilling the specifications for the customer satisfaction by worst-case distances can lead to a significant reduction of computational complexity in the robust design of automated vehicular safety systems as compared to estimating it by a Monte Carlo simulation when a high estimation accuracy is required.

In order to achieve a better approximation of the probability of fulfilling the specifications for the customer satisfaction and simplify the optimizations for determining the required worst-case distances at the same time, the worst-case distance approach has been adapted to the robust design of automated vehicular safety systems by analyzing and exploiting the special structure of the error acceptance region. More precisely, this adaptation of the worst-case distance approach to the robust design of automated vehicular safety systems decomposes the original optimization problems for determining the required worst-case distances into optimization problems that are easier to solve, and more accurately approximates the probability of fulfilling the specifications for the customer satisfaction by evaluating the standard normal cdf at the worst-case distances determined by solving these optimization problems. This mainly requires

only several evaluations of the decision rule for triggering the respective action besides a few simulations of the automated vehicular safety system.

With the two considered possibilities for the simulation-based evaluation of the quality measure, namely, the Monte Carlo simulation and the worst-case distance approach, the design task can be performed solely based on simulations of the automated vehicular safety system under design. This makes the developed methodology for the robust function and sensor design considering sensor measurement errors applicable to various automated vehicular safety systems.

After developing the methodology for the robust design of automated vehicular safety systems considering unavoidable sensor measurement errors, it has finally been applied to two typical examples for automated vehicular safety systems, namely, an AEB and an AES system. These application examples provide a complete picture of the system model, the formulation of the design problems at hand as optimization problems using the proposed design methodology and their solution based on closed-form expressions for the quality measure or solely based on simulations of the AEB or AES system under design without the need for deriving closed-form expressions for the quality measure. Deriving such closed-form expressions would also not be viable for the complex automated vehicular safety systems in practice and therefore the developers of such systems have to resort to a simulation-based design. In particular, the model of the AEB system has been kept as simple as possible in order to illustrate the basic principle of the design methodology and allow for the derivation of results in closed form at several points for an accurate evaluation of the design methodology. The considered numerical examples demonstrate that the adaptation of the worst-case distance approach to the robust design of automated vehicular safety systems can significantly reduce the required number of simulations of the automated vehicular safety system under design by replacing an expensive Monte Carlo simulation requiring a huge number of simulations of the automated vehicular safety system for a comparable accuracy, and with this the computational complexity, the load for simulation servers as well as the time and expenses needed for the development of automated vehicular safety systems.

8.2 Future Work

Although the developed methodology for the robust design of automated vehicular safety systems considering unavoidable sensor measurement errors has successfully been applied to an AEB and AES system as a proof of concept, the uncomplicated usage of the design methodology by application engineers in the development of

automated vehicular safety systems requires an extension of the developed simulation-based design methodology to an easy-to-use software tool. It must automatically select one of the two considered possibilities for the simulation-based evaluation of the quality measure, namely, the Monte Carlo simulation and the worst-case distance approach, depending on the desired accuracy, available computational resources and the fulfillment of the assumptions to be fulfilled for the applicability of the worst-case distance approach such that application engineers do not need any a priori knowledge about the details of the simulation techniques inside the software tool in order to design automated vehicular safety systems with it.

For a wide applicability of the worst-case distance approach inside the software tool allowing for a significant reduction of the computational complexity at a high accuracy, the worst-case distance approach has to be adapted to the robust design of automated vehicular safety systems without making the simplifying assumptions in this thesis. So far, it has been assumed that the sensor measurement errors at different time instants are statistically independent and the function decides on whether to trigger the respective action based on sensor measurements at a single time instant. As the sensor measurement errors at different time instants might be statistically dependent and the function might decide on whether to trigger the respective action based on sensor measurements at several time instants in practice, it is of high importance to adapt the worst-case distance approach to the robust design of automated vehicular safety systems also for these cases.

Furthermore, the worst-case distance approach exploits the properties of the normal distribution of the sensor measurement errors, which are assumed to be Gaussian. In certain scenarios, this assumption of Gaussian sensor measurement errors might be justified. Even if this Gaussian assumption is not justified, one can still proceed with the Gaussian random variables, which can be considered as a kind of virtual sensor measurement errors, as they can be transformed to random variables with a different probability distribution modeling the actual sensor measurement errors and this transformation can be considered to be part of the sensors. However, finding this transformation for a given target probability distribution of the actual sensor measurement errors is not trivial. First of all, it has to be examined for which target probability distributions such a transformation can be found before finding the transformation of the virtual sensor measurement errors to the actual sensor measurement errors itself can be automated. This transformation has to be automated in the software tool and, more precisely, integrated into the simulations of the automated vehicular safety system under design that have to be performed according to the methodology for the robust design of automated vehicular safety systems such that application engineers do not

have to care about the necessary transformation in case of actual sensor measurement errors that are not Gaussian when designing automated vehicular safety systems.

Finding the transformation of the virtual sensor measurement errors to the actual sensor measurement errors for a given target probability distribution requires the knowledge of this probability distribution. This emphasizes that the developed methodology for the robust design of automated vehicular safety systems considering unavoidable sensor measurement errors heavily relies on accurate sensor models describing the probability distribution of the sensor measurement errors. In this thesis, it has been assumed that those sensor models are available, i.e., the probability distribution of the sensor measurement errors is known. In practice, however, accurate realistic sensor models are often not available. Using techniques from machine learning in order to obtain such sensor models, i.e., learn them, from real sensor data is a promising approach for future work.

Probability that the Statistical Parameters \mathbf{s} Lie in $\hat{\mathcal{A}}_{\mathbf{s},b,i}$



The probability that the statistical parameters \mathbf{s} lie in the approximate individual parameter acceptance region partition $\hat{\mathcal{A}}_{\mathbf{s},b,i}$ bounded by the tangential hyperplane touching the boundary of the individual parameter acceptance region partition $\mathcal{A}_{\mathbf{s},b,i}$ at the point $\mathbf{s}_{b,i}$ where the distance between the statistical parameters \mathbf{s} on this boundary and their mean \mathbf{s}_0 is minimum, namely, the worst-case distance $\beta_{b,i}$, is derived in the following.

As any other hyperplane, the tangential hyperplane touching the boundary of the individual parameter acceptance region partition $\mathcal{A}_{\mathbf{s},b,i}$ at the point $\mathbf{s}_{b,i}$ can be described as the set

$$\{\mathbf{s} \in \mathbb{R}^{N_s} : \mathbf{n}_{b,i}^T \mathbf{C}^{-1} \mathbf{s} = \delta_{b,i}\} \quad (\text{A.1})$$

of statistical parameters \mathbf{s} with a normal vector $\mathbf{n}_{b,i} \in \mathbb{R}^{N_s}$ normalized such that it has unit norm $\|\mathbf{n}_{b,i}\|_{\mathbf{C}} = 1$ and a parameter $\delta_{b,i} \in \mathbb{R}$, which are scaled such that

$$\mathbf{n}_{b,i}^T \mathbf{C}^{-1} \mathbf{s}_0 \leq \delta_{b,i}. \quad (\text{A.2})$$

Here, the inner product

$$\langle \mathbf{s}_1, \mathbf{s}_2 \rangle_{\mathbf{C}} = \mathbf{s}_2^T \mathbf{C}^{-1} \mathbf{s}_1 \quad (\text{A.3})$$

between $\mathbf{s}_1 \in \mathbb{R}^{N_s}$ and $\mathbf{s}_2 \in \mathbb{R}^{N_s}$, and the norm

$$\|\mathbf{s}\|_{\mathbf{C}} = \sqrt{\langle \mathbf{s}, \mathbf{s} \rangle_{\mathbf{C}}} = \sqrt{\mathbf{s}^T \mathbf{C}^{-1} \mathbf{s}} \quad (\text{A.4})$$

induced by this inner product is used, which also allows to express the Mahalanobis distance $\beta(\mathbf{s})$ used as distance measure in terms of this norm:

$$\beta(\mathbf{s}) = \sqrt{(\mathbf{s} - \mathbf{s}_0)^T \mathbf{C}^{-1} (\mathbf{s} - \mathbf{s}_0)} = \|\mathbf{s} - \mathbf{s}_0\|_{\mathbf{C}}. \quad (\text{A.5})$$

As the tangential hyperplane touches the boundary of the individual parameter acceptance region partition $\mathcal{A}_{\mathbf{s},b,i}$ at the point $\mathbf{s}_{b,i}$ where the hyperellipsoid on which all

Appendix A. Probability that the Statistical Parameters \mathbf{s} Lie in $\hat{\mathcal{A}}_{\mathbf{s},b,i}$

statistical parameters \mathbf{s} have the worst-case distance $\beta_{b,i}$ from their mean \mathbf{s}_0 touches the boundary of $\mathcal{A}_{\mathbf{s},b,i}$, this hyperellipsoid also touches the tangential hyperplane, the boundary of the corresponding approximate individual parameter acceptance region partition $\hat{\mathcal{A}}_{\mathbf{s},b,i}$ at the point $\mathbf{s}_{b,i}$. This can also be observed for the two statistical parameters $\mathbf{s} = [s_1, s_2]^T$ in Figure 3.2 and Figure 3.3, where the tangential hyperplanes are tangential lines and the hyperellipsoids are ellipses. As the distance $\beta(\mathbf{s})$ of the statistical parameters \mathbf{s} on the boundary of the individual parameter acceptance region partition $\mathcal{A}_{\mathbf{s},b,i}$ is minimum at the point $\mathbf{s}_{b,i}$, the distance $\beta(\mathbf{s})$ of the statistical parameters \mathbf{s} on the boundary of the corresponding approximate individual parameter acceptance region partition $\hat{\mathcal{A}}_{\mathbf{s},b,i}$ is also minimum at this point. Therefore, the worst-case distance $\beta_{b,i}$, $b \in \{L, U\}$, obtained by minimizing the distance $\beta(\mathbf{s})$ of the statistical parameters \mathbf{s} on the boundary of the individual parameter acceptance region partition $\mathcal{A}_{\mathbf{s},b,i}$ according to (3.59) and (3.60) is the same as the worst-case distance obtained by minimizing the distance $\beta(\mathbf{s})$ of the statistical parameters \mathbf{s} on the boundary of the corresponding approximate individual parameter acceptance region partition $\hat{\mathcal{A}}_{\mathbf{s},b,i}$ described by the set of statistical parameters \mathbf{s} stated in (A.1):

$$\begin{aligned}\beta_{b,i} &= \min_{\mathbf{s} \in \mathbb{R}^{N_s}} \beta(\mathbf{s}) \quad \text{s.t.} \quad f_i = f_{b,i} \\ &= \min_{\mathbf{s} \in \mathbb{R}^{N_s}} \beta(\mathbf{s}) \quad \text{s.t.} \quad \mathbf{n}_{b,i}^T \mathbf{C}^{-1} \mathbf{s} = \delta_{b,i}.\end{aligned}\tag{A.6}$$

Furthermore, the point $\mathbf{s}_{b,i}$ where the hyperellipsoid on which all statistical parameters \mathbf{s} have the worst-case distance $\beta_{b,i}$ from their mean \mathbf{s}_0 touches the boundaries of both the individual parameter acceptance region partition $\mathcal{A}_{\mathbf{s},b,i}$ and the corresponding approximate individual parameter acceptance region partition $\hat{\mathcal{A}}_{\mathbf{s},b,i}$ is the minimizer in these minimization problems:

$$\begin{aligned}\mathbf{s}_{b,i} &= \operatorname{argmin}_{\mathbf{s} \in \mathbb{R}^{N_s}} \beta(\mathbf{s}) \quad \text{s.t.} \quad f_i = f_{b,i} \\ &= \operatorname{argmin}_{\mathbf{s} \in \mathbb{R}^{N_s}} \beta(\mathbf{s}) \quad \text{s.t.} \quad \mathbf{n}_{b,i}^T \mathbf{C}^{-1} \mathbf{s} = \delta_{b,i}.\end{aligned}\tag{A.7}$$

As

$$\forall \mathbf{s}_1, \mathbf{s}_2 \in \mathbb{R}^{N_s} : \beta(\mathbf{s}_1) < \beta(\mathbf{s}_2) \Leftrightarrow \beta^2(\mathbf{s}_1) < \beta^2(\mathbf{s}_2),\tag{A.8}$$

the objective $\beta(\mathbf{s})$ of these minimization problems can be replaced by $\beta^2(\mathbf{s})$ such that the minimizer in these minimization problems is also the minimizer in the following

minimization problems:

$$\begin{aligned}
\mathbf{s}_{b,i} &= \underset{\mathbf{s} \in \mathbb{R}^{N_s}}{\operatorname{argmin}} \beta^2(\mathbf{s}) \quad \text{s.t.} \quad f_i = f_{b,i} \\
&= \underset{\mathbf{s} \in \mathbb{R}^{N_s}}{\operatorname{argmin}} (\mathbf{s} - \mathbf{s}_0)^\top \mathbf{C}^{-1} (\mathbf{s} - \mathbf{s}_0) \quad \text{s.t.} \quad \mathbf{n}_{b,i}^\top \mathbf{C}^{-1} \mathbf{s} = \delta_{b,i} \\
&= \underset{\mathbf{s} \in \mathbb{R}^{N_s}}{\operatorname{argmin}} \mathbf{s}^\top \mathbf{C}^{-1} \mathbf{s} - \mathbf{s}_0^\top \mathbf{C}^{-1} \mathbf{s} - \mathbf{s}^\top \mathbf{C}^{-1} \mathbf{s}_0 \quad \text{s.t.} \quad \mathbf{n}_{b,i}^\top \mathbf{C}^{-1} \mathbf{s} = \delta_{b,i}.
\end{aligned} \tag{A.9}$$

Due to the symmetry of the covariance matrix \mathbf{C} and its inverse \mathbf{C}^{-1} , it simplifies to

$$\begin{aligned}
\mathbf{s}_{b,i} &= \underset{\mathbf{s} \in \mathbb{R}^{N_s}}{\operatorname{argmin}} \mathbf{s}^\top \mathbf{C}^{-1} \mathbf{s} - (\mathbf{s}_0^\top \mathbf{C}^{-1} \mathbf{s})^\top - \mathbf{s}^\top \mathbf{C}^{-1} \mathbf{s}_0 \quad \text{s.t.} \quad (\mathbf{n}_{b,i}^\top \mathbf{C}^{-1} \mathbf{s})^\top = \delta_{b,i} \\
&= \underset{\mathbf{s} \in \mathbb{R}^{N_s}}{\operatorname{argmin}} \mathbf{s}^\top \mathbf{C}^{-1} \mathbf{s} - \mathbf{s}^\top (\mathbf{C}^{-1})^\top \mathbf{s}_0 - \mathbf{s}^\top \mathbf{C}^{-1} \mathbf{s}_0 \quad \text{s.t.} \quad \mathbf{s}^\top (\mathbf{C}^{-1})^\top \mathbf{n}_{b,i} = \delta_{b,i} \\
&= \underset{\mathbf{s} \in \mathbb{R}^{N_s}}{\operatorname{argmin}} \mathbf{s}^\top \mathbf{C}^{-1} \mathbf{s} - 2\mathbf{s}^\top \mathbf{C}^{-1} \mathbf{s}_0 \quad \text{s.t.} \quad \mathbf{s}^\top \mathbf{C}^{-1} \mathbf{n}_{b,i} - \delta_{b,i} = 0.
\end{aligned} \tag{A.10}$$

The Lagrangian function for this constrained optimization problem reads

$$\mathcal{L}(\mathbf{s}, \lambda) = \mathbf{s}^\top \mathbf{C}^{-1} \mathbf{s} - 2\mathbf{s}^\top \mathbf{C}^{-1} \mathbf{s}_0 + \lambda (\mathbf{s}^\top \mathbf{C}^{-1} \mathbf{n}_{b,i} - \delta_{b,i}). \tag{A.11}$$

Setting its derivative with respect to the statistical parameters \mathbf{s}

$$\begin{aligned}
\frac{\partial}{\partial \mathbf{s}} \mathcal{L}(\mathbf{s}, \lambda) &= \left(\mathbf{C}^{-1} + (\mathbf{C}^{-1})^\top \right) \mathbf{s} - 2\mathbf{C}^{-1} \mathbf{s}_0 + \lambda \mathbf{C}^{-1} \mathbf{n}_{b,i} \\
&= 2\mathbf{C}^{-1} (\mathbf{s} - \mathbf{s}_0) + \lambda \mathbf{C}^{-1} \mathbf{n}_{b,i}
\end{aligned} \tag{A.12}$$

to 0 yields

$$2\mathbf{C}^{-1} (\mathbf{s} - \mathbf{s}_0) = -\lambda \mathbf{C}^{-1} \mathbf{n}_{b,i} \tag{A.13}$$

and

$$\mathbf{s} = -\frac{\lambda}{2} \mathbf{n}_{b,i} + \mathbf{s}_0. \tag{A.14}$$

Substituting this into the constraint of the optimization problem (A.9) results in

$$\begin{aligned}
-\frac{\lambda}{2} \mathbf{n}_{b,i}^\top \mathbf{C}^{-1} \mathbf{n}_{b,i} + \mathbf{n}_{b,i}^\top \mathbf{C}^{-1} \mathbf{s}_0 &= -\frac{\lambda}{2} \|\mathbf{n}_{b,i}\|_{\mathbf{C}}^2 + \mathbf{n}_{b,i}^\top \mathbf{C}^{-1} \mathbf{s}_0 \\
&= -\frac{\lambda}{2} + \mathbf{n}_{b,i}^\top \mathbf{C}^{-1} \mathbf{s}_0 = \delta_{b,i}
\end{aligned} \tag{A.15}$$

and

$$\lambda = -2 (\delta_{b,i} - \mathbf{n}_{b,i}^\top \mathbf{C}^{-1} \mathbf{s}_0). \tag{A.16}$$

Appendix A. Probability that the Statistical Parameters \mathbf{s} Lie in $\hat{\mathcal{A}}_{\mathbf{s},b,i}$

This is plugged into (A.14) to obtain the solution of the optimization problem (A.10):

$$\mathbf{s}_{b,i} = (\delta_{b,i} - \mathbf{n}_{b,i}^T \mathbf{C}^{-1} \mathbf{s}_0) \mathbf{n}_{b,i} + \mathbf{s}_0. \quad (\text{A.17})$$

Since this solution $\mathbf{s}_{b,i}$ is the minimizer in the original minimization problem (A.6), its distance $\beta(\mathbf{s}_{b,i})$ from the mean of the statistical parameters \mathbf{s}_0 is the worst-case distance $\beta_{b,i}$:

$$\begin{aligned} \beta^2(\mathbf{s}_{b,i}) &= (\mathbf{s}_{b,i} - \mathbf{s}_0)^T \mathbf{C}^{-1} (\mathbf{s}_{b,i} - \mathbf{s}_0) \\ &= (\delta_{b,i} - \mathbf{n}_{b,i}^T \mathbf{C}^{-1} \mathbf{s}_0)^2 \mathbf{n}_{b,i}^T \mathbf{C}^{-1} \mathbf{n}_{b,i} \\ &= (\delta_{b,i} - \mathbf{n}_{b,i}^T \mathbf{C}^{-1} \mathbf{s}_0)^2 \|\mathbf{n}_{b,i}\|_{\mathbf{C}}^2 \\ &= (\delta_{b,i} - \mathbf{n}_{b,i}^T \mathbf{C}^{-1} \mathbf{s}_0)^2 = \beta_{b,i}^2. \end{aligned} \quad (\text{A.18})$$

As the normal vector $\mathbf{n}_{b,i}$ and $\delta_{b,i}$ describing the boundary of the approximate individual parameter acceptance region partition $\hat{\mathcal{A}}_{\mathbf{s},b,i}$ as the set of statistical parameters \mathbf{s} in (A.1) have been scaled such that (A.2) is fulfilled, i.e., $\delta_{b,i} - \mathbf{n}_{b,i}^T \mathbf{C}^{-1} \mathbf{s}_0 \geq 0$, this implies that

$$\beta_{b,i} = \delta_{b,i} - \mathbf{n}_{b,i}^T \mathbf{C}^{-1} \mathbf{s}_0. \quad (\text{A.19})$$

Substituting this into (A.17) yields the final expression for the point $\mathbf{s}_{b,i}$ where the hyperellipsoid on which all statistical parameters \mathbf{s} have the worst-case distance $\beta_{b,i}$ from their mean \mathbf{s}_0 touches the boundaries of both the individual parameter acceptance region partition $\mathcal{A}_{\mathbf{s},b,i}$ and the corresponding approximate individual parameter acceptance region partition $\hat{\mathcal{A}}_{\mathbf{s},b,i}$:

$$\mathbf{s}_{b,i} = \beta_{b,i} \mathbf{n}_{b,i} + \mathbf{s}_0. \quad (\text{A.20})$$

From (A.19), it follows that

$$\delta_{b,i} = \beta_{b,i} + \mathbf{n}_{b,i}^T \mathbf{C}^{-1} \mathbf{s}_0 \quad (\text{A.21})$$

such that the set of statistical parameters \mathbf{s} in (A.1) describing the boundary of the approximate individual parameter acceptance region partition $\hat{\mathcal{A}}_{\mathbf{s},b,i}$ reads

$$\begin{aligned} \{\mathbf{s} \in \mathbb{R}^{N_s} : \mathbf{n}_{b,i}^T \mathbf{C}^{-1} \mathbf{s} = \delta_{b,i}\} &= \{\mathbf{s} \in \mathbb{R}^{N_s} : \mathbf{n}_{b,i}^T \mathbf{C}^{-1} \mathbf{s} = \beta_{b,i} + \mathbf{n}_{b,i}^T \mathbf{C}^{-1} \mathbf{s}_0\} \\ &= \{\mathbf{s} \in \mathbb{R}^{N_s} : \mathbf{n}_{b,i}^T \mathbf{C}^{-1} (\mathbf{s} - \mathbf{s}_0) = \beta_{b,i}\} \\ &= \{\mathbf{s} \in \mathbb{R}^{N_s} : \langle \mathbf{s} - \mathbf{s}_0, \mathbf{n}_{b,i} \rangle_{\mathbf{C}} = \beta_{b,i}\}. \end{aligned} \quad (\text{A.22})$$

This hyperplane, on which $\mathbf{n}_{b,i}^T \mathbf{C}^{-1} \mathbf{s} = \delta_{b,i}$, divides the space \mathbb{R}^{N_s} into the two open half-spaces in one of which $\mathbf{n}_{b,i}^T \mathbf{C}^{-1} \mathbf{s} < \delta_{b,i}$ while in the other one $\mathbf{n}_{b,i}^T \mathbf{C}^{-1} \mathbf{s} > \delta_{b,i}$.

The open half-space where $\mathbf{n}_{b,i}^T \mathbf{C}^{-1} \mathbf{s} > \delta_{b,i}$ never contains the mean $\mathbf{s}_0 \in \hat{\mathcal{A}}_{s,b,i}$ of the statistical parameters \mathbf{s} fulfilling (A.2). Therefore, it cannot be the half-space included in the approximate individual parameter acceptance region partition $\hat{\mathcal{A}}_{s,b,i}$, in which the mean \mathbf{s}_0 of the statistical parameters \mathbf{s} lies because it is assumed to lie in the individual parameter acceptance region partition $\mathcal{A}_{s,b,i}$. Consequently, the open half-space where $\mathbf{n}_{b,i}^T \mathbf{C}^{-1} \mathbf{s} < \delta_{b,i}$ together with the bounding hyperplane where $\mathbf{n}_{b,i}^T \mathbf{C}^{-1} \mathbf{s} = \delta_{b,i}$ form the approximate individual parameter acceptance region partition $\hat{\mathcal{A}}_{s,b,i}$, where $\mathbf{n}_{b,i}^T \mathbf{C}^{-1} \mathbf{s} \leq \delta_{b,i}$:

$$\hat{\mathcal{A}}_{s,b,i} = \{ \mathbf{s} \in \mathbb{R}^{N_s} : \mathbf{n}_{b,i}^T \mathbf{C}^{-1} \mathbf{s} \leq \delta_{b,i} \}. \quad (\text{A.23})$$

With (A.21), the approximate individual parameter acceptance region partition can be expressed in terms of the worst-cased distance $\beta_{b,i}$:

$$\begin{aligned} \hat{\mathcal{A}}_{s,b,i} &= \{ \mathbf{s} \in \mathbb{R}^{N_s} : \mathbf{n}_{b,i}^T \mathbf{C}^{-1} \mathbf{s} \leq \beta_{b,i} + \mathbf{n}_{b,i}^T \mathbf{C}^{-1} \mathbf{s}_0 \} \\ &= \{ \mathbf{s} \in \mathbb{R}^{N_s} : \mathbf{n}_{b,i}^T \mathbf{C}^{-1} (\mathbf{s} - \mathbf{s}_0) \leq \beta_{b,i} \} \\ &= \{ \mathbf{s} \in \mathbb{R}^{N_s} : \langle \mathbf{s} - \mathbf{s}_0, \mathbf{n}_{b,i} \rangle_{\mathbf{C}} \leq \beta_{b,i} \}. \end{aligned} \quad (\text{A.24})$$

As the statistical parameters \mathbf{s} are Gaussian with mean

$$\mathbb{E} [\mathbf{s}] = \mathbf{s}_0 \quad (\text{A.25})$$

and covariance

$$\mathbb{E} [(\mathbf{s} - \mathbb{E}[\mathbf{s}]) (\mathbf{s} - \mathbb{E}[\mathbf{s}])^T] = \mathbb{E} [(\mathbf{s} - \mathbf{s}_0) (\mathbf{s} - \mathbf{s}_0)^T] = \mathbf{C}, \quad (\text{A.26})$$

the random variable $\langle \mathbf{s} - \mathbf{s}_0, \mathbf{n}_{b,i} \rangle_{\mathbf{C}} = \mathbf{n}_{b,i}^T \mathbf{C}^{-1} (\mathbf{s} - \mathbf{s}_0)$ is Gaussian as well with mean

$$\mathbb{E} [\langle \mathbf{s} - \mathbf{s}_0, \mathbf{n}_{b,i} \rangle_{\mathbf{C}}] = \mathbb{E} [\mathbf{n}_{b,i}^T \mathbf{C}^{-1} (\mathbf{s} - \mathbf{s}_0)] = \mathbf{n}_{b,i}^T \mathbf{C}^{-1} (\mathbb{E}[\mathbf{s}] - \mathbf{s}_0) = 0 \quad (\text{A.27})$$

and variance

$$\begin{aligned} &\mathbb{E} [(\langle \mathbf{s} - \mathbf{s}_0, \mathbf{n}_{b,i} \rangle_{\mathbf{C}} - \mathbb{E} [\langle \mathbf{s} - \mathbf{s}_0, \mathbf{n}_{b,i} \rangle_{\mathbf{C}}])^2] = \mathbb{E} [(\langle \mathbf{s} - \mathbf{s}_0, \mathbf{n}_{b,i} \rangle_{\mathbf{C}})^2] \\ &= \mathbb{E} [(\mathbf{n}_{b,i}^T \mathbf{C}^{-1} (\mathbf{s} - \mathbf{s}_0))^2] = \mathbb{E} [(\mathbf{n}_{b,i}^T \mathbf{C}^{-1} (\mathbf{s} - \mathbf{s}_0)) (\mathbf{n}_{b,i}^T \mathbf{C}^{-1} (\mathbf{s} - \mathbf{s}_0))^T] \\ &= \mathbb{E} [\mathbf{n}_{b,i}^T \mathbf{C}^{-1} (\mathbf{s} - \mathbf{s}_0) (\mathbf{s} - \mathbf{s}_0)^T (\mathbf{C}^{-1})^T \mathbf{n}_{b,i}] \\ &= \mathbf{n}_{b,i}^T \mathbf{C}^{-1} \mathbb{E} [(\mathbf{s} - \mathbf{s}_0) (\mathbf{s} - \mathbf{s}_0)^T] \mathbf{C}^{-1} \mathbf{n}_{b,i} \\ &= \mathbf{n}_{b,i}^T \mathbf{C}^{-1} \mathbf{C} \mathbf{C}^{-1} \mathbf{n}_{b,i} = \mathbf{n}_{b,i}^T \mathbf{C}^{-1} \mathbf{n}_{b,i} = \|\mathbf{n}_{b,i}\|_{\mathbf{C}}^2 = 1, \end{aligned} \quad (\text{A.28})$$

Appendix A. Probability that the Statistical Parameters \mathbf{s} Lie in $\hat{\mathcal{A}}_{\mathbf{s},b,i}$

i.e., standard Gaussian:

$$\langle \mathbf{s} - \mathbf{s}_0, \mathbf{n}_{b,i} \rangle_{\mathbf{C}} = \mathbf{n}_{b,i}^{\mathbf{T}} \mathbf{C}^{-1} (\mathbf{s} - \mathbf{s}_0) \sim \mathcal{N}(0, 1). \quad (\text{A.29})$$

The probability that the statistical parameters \mathbf{s} lie in the approximate individual parameter acceptance region partition $\hat{\mathcal{A}}_{\mathbf{s},b,i}$ can thus be computed as follows:

$$P(\mathbf{s} \in \hat{\mathcal{A}}_{\mathbf{s},b,i}) = P(\langle \mathbf{s} - \mathbf{s}_0, \mathbf{n}_{b,i} \rangle_{\mathbf{C}} \leq \beta_{b,i}) = \Phi(\beta_{b,i}). \quad (\text{A.30})$$

Properties Implied by Statistical Independence of Sensor Measurement Errors

B

The statistical independence of the sensor measurement errors $\varepsilon[n_1]$ and $\varepsilon[n_2]$ at different time instants t_{n_1} and t_{n_2} , $n_1, n_2 \in \mathbb{N}_0, n_1 \neq n_2$, implies the following properties.

The probability that the vector ε consisting of the sensor measurement errors $\varepsilon[n]$ at the time instants $t_n, n = 0, 1, \dots, n_{\text{end}}$, as stated in (4.21) lies in the intersection $\bigcap_{n \in \mathbb{I}} \bar{\mathcal{I}}_{\varepsilon, n}$ of the error regions $\bar{\mathcal{I}}_{\varepsilon, n}$ without intervention at the time instants t_n with indices n from a set $\mathbb{I} \subset \{0, 1, \dots, n_{\text{end}}\}$ as defined in (5.84) reads

$$\begin{aligned}
 P\left(\varepsilon \in \bigcap_{n \in \mathbb{I}} \bar{\mathcal{I}}_{\varepsilon, n}\right) &= \int_{\bigcap_{n \in \mathbb{I}} \bar{\mathcal{I}}_{\varepsilon, n}} f_{\varepsilon}(\varepsilon) \, d\varepsilon \\
 &= \int_{\bigcap_{n \in \{n_1, n_2, \dots, n_{\text{end}, \mathbb{I}}\}} \left\{ \varepsilon \in \mathbb{R}^{E(n_{\text{end}}+1)} : f(\mathbf{y}(\mathbf{x}[n], \varepsilon[n]); \varphi) = 0 \right\}} f_{\varepsilon}(\varepsilon) \, d\varepsilon \\
 &= \int_{\{\varepsilon[n_1] \in \mathbb{R}^E : f(\mathbf{y}(\mathbf{x}[n_1], \varepsilon[n_1]); \varphi) = 0\}} \dots \int_{\{\varepsilon[n_{\text{end}, \mathbb{I}}] \in \mathbb{R}^E : f(\mathbf{y}(\mathbf{x}[n_{\text{end}, \mathbb{I}}], \varepsilon[n_{\text{end}, \mathbb{I}}]); \varphi) = 0\}} \\
 &\quad \int_{\mathbb{R}^E} \dots \int_{\mathbb{R}^E} f_{\varepsilon}(\varepsilon) \, d\varepsilon[\bar{n}_{\text{end}, \mathbb{I}}] \dots d\varepsilon[\bar{n}_1] \, d\varepsilon[n_{\text{end}, \mathbb{I}}] \dots d\varepsilon[n_1].
 \end{aligned} \tag{B.1}$$

Here, $n_1, n_2, \dots, n_{\text{end}, \mathbb{I}}$ denote the indices in the set $\mathbb{I} = \{n_1, n_2, \dots, n_{\text{end}, \mathbb{I}}\}$ and $\bar{n}_1, \bar{n}_2, \dots, \bar{n}_{\text{end}, \mathbb{I}}$ the other indices in the set $\{0, 1, \dots, n_{\text{end}}\}$, i.e., $\{0, 1, \dots, n_{\text{end}}\} / \mathbb{I} = \{\bar{n}_1, \bar{n}_2, \dots, \bar{n}_{\text{end}, \mathbb{I}}\}$. Since the pdf $f_{\varepsilon}(\varepsilon)$ of all sensor measurement errors ε factorizes into the pdfs $f_{\varepsilon[n]}(\varepsilon[n])$ of the sensor measurement errors $\varepsilon[n]$ at the time instants

Appendix B. Properties Implied by Statistical Independence of Sensor Measurement Errors

$t_n, n = 0, 1, \dots, n_{\text{end}}$, as stated in (4.23) due to their statistical independence,

$$\begin{aligned}
& P \left(\boldsymbol{\varepsilon} \in \bigcap_{n \in \mathbb{I}} \bar{\mathcal{I}}_{\boldsymbol{\varepsilon}, n} \right) \\
&= \int_{\{\boldsymbol{\varepsilon}[n_1] \in \mathbb{R}^E : f(\mathbf{y}(\mathbf{x}[n_1], \boldsymbol{\varepsilon}[n_1]); \boldsymbol{\varphi}) = 0\}} \cdots \int_{\{\boldsymbol{\varepsilon}[n_{\text{end}, \mathbb{I}}] \in \mathbb{R}^E : f(\mathbf{y}(\mathbf{x}[n_{\text{end}, \mathbb{I}}], \boldsymbol{\varepsilon}[n_{\text{end}, \mathbb{I}}]); \boldsymbol{\varphi}) = 0\}} \\
&\quad \int_{\mathbb{R}^E} \cdots \int_{\mathbb{R}^E} \prod_{n=0}^{n_{\text{end}}} f_{\boldsymbol{\varepsilon}[n]}(\boldsymbol{\varepsilon}[n]) \, \mathrm{d}\boldsymbol{\varepsilon}[n_{\text{end}, \mathbb{I}}] \cdots \mathrm{d}\boldsymbol{\varepsilon}[\bar{n}_1] \, \mathrm{d}\boldsymbol{\varepsilon}[n_{\text{end}, \mathbb{I}}] \cdots \mathrm{d}\boldsymbol{\varepsilon}[n_1] \\
&= \int_{\{\boldsymbol{\varepsilon}[n_1] \in \mathbb{R}^E : f(\mathbf{y}(\mathbf{x}[n_1], \boldsymbol{\varepsilon}[n_1]); \boldsymbol{\varphi}) = 0\}} f_{\boldsymbol{\varepsilon}[n_1]}(\boldsymbol{\varepsilon}[n_1]) \cdots \\
&\quad \int_{\{\boldsymbol{\varepsilon}[n_{\text{end}, \mathbb{I}}] \in \mathbb{R}^E : f(\mathbf{y}(\mathbf{x}[n_{\text{end}, \mathbb{I}}], \boldsymbol{\varepsilon}[n_{\text{end}, \mathbb{I}}]); \boldsymbol{\varphi}) = 0\}} f_{\boldsymbol{\varepsilon}[n_{\text{end}, \mathbb{I}}]}(\boldsymbol{\varepsilon}[n_{\text{end}, \mathbb{I}}]) \\
&\quad \int_{\mathbb{R}^E} f_{\boldsymbol{\varepsilon}[\bar{n}_1]}(\boldsymbol{\varepsilon}[\bar{n}_1]) \cdots \int_{\mathbb{R}^E} f_{\boldsymbol{\varepsilon}[\bar{n}_{\text{end}, \mathbb{I}}]}(\boldsymbol{\varepsilon}[\bar{n}_{\text{end}, \mathbb{I}}]) \\
&\quad \mathrm{d}\boldsymbol{\varepsilon}[\bar{n}_{\text{end}, \mathbb{I}}] \cdots \mathrm{d}\boldsymbol{\varepsilon}[\bar{n}_1] \, \mathrm{d}\boldsymbol{\varepsilon}[n_{\text{end}, \mathbb{I}}] \cdots \mathrm{d}\boldsymbol{\varepsilon}[n_1] \\
&= \underbrace{\int_{\{\boldsymbol{\varepsilon}[n_1] \in \mathbb{R}^E : f(\mathbf{y}(\mathbf{x}[n_1], \boldsymbol{\varepsilon}[n_1]); \boldsymbol{\varphi}) = 0\}} f_{\boldsymbol{\varepsilon}[n_1]}(\boldsymbol{\varepsilon}[n_1]) \, \mathrm{d}\boldsymbol{\varepsilon}[n_1] \cdots}_{=P(f(\mathbf{y}(\mathbf{x}[n_1], \boldsymbol{\varepsilon}[n_1]); \boldsymbol{\varphi}) = 0)} \\
&\quad \underbrace{\int_{\{\boldsymbol{\varepsilon}[n_{\text{end}, \mathbb{I}}] \in \mathbb{R}^E : f(\mathbf{y}(\mathbf{x}[n_{\text{end}, \mathbb{I}}], \boldsymbol{\varepsilon}[n_{\text{end}, \mathbb{I}}]); \boldsymbol{\varphi}) = 0\}} f_{\boldsymbol{\varepsilon}[n_{\text{end}, \mathbb{I}}]}(\boldsymbol{\varepsilon}[n_{\text{end}, \mathbb{I}}]) \, \mathrm{d}\boldsymbol{\varepsilon}[n_{\text{end}, \mathbb{I}}]}_{=P(f(\mathbf{y}(\mathbf{x}[n_{\text{end}, \mathbb{I}}], \boldsymbol{\varepsilon}[n_{\text{end}, \mathbb{I}}]); \boldsymbol{\varphi}) = 0)} \\
&\quad \underbrace{\int_{\mathbb{R}^E} f_{\boldsymbol{\varepsilon}[\bar{n}_1]}(\boldsymbol{\varepsilon}[\bar{n}_1]) \, \mathrm{d}\boldsymbol{\varepsilon}[\bar{n}_1]}_{=1} \cdots \underbrace{\int_{\mathbb{R}^E} f_{\boldsymbol{\varepsilon}[\bar{n}_{\text{end}, \mathbb{I}}]}(\boldsymbol{\varepsilon}[\bar{n}_{\text{end}, \mathbb{I}}]) \, \mathrm{d}\boldsymbol{\varepsilon}[\bar{n}_{\text{end}, \mathbb{I}}]}_{=1} \\
&= \prod_{n \in \mathbb{I}} P(f(\mathbf{y}(\mathbf{x}[n], \boldsymbol{\varepsilon}[n]); \boldsymbol{\varphi}) = 0) = \prod_{n \in \mathbb{I}} P(\boldsymbol{\varepsilon} \in \bar{\mathcal{I}}_{\boldsymbol{\varepsilon}, n}).
\end{aligned} \tag{B.2}$$

So, the probability $P(\boldsymbol{\varepsilon} \in \bigcap_{n \in \mathbb{I}} \bar{\mathcal{I}}_{\boldsymbol{\varepsilon}, n})$ that the sensor measurement errors $\boldsymbol{\varepsilon}$ lie in all error regions $\bar{\mathcal{I}}_{\boldsymbol{\varepsilon}, n}$ without intervention at the time instants t_n with indices $n \in \mathbb{I}$ factorizes into the probabilities $P(\boldsymbol{\varepsilon} \in \bar{\mathcal{I}}_{\boldsymbol{\varepsilon}, n})$ that they lie in the individual error regions $\bar{\mathcal{I}}_{\boldsymbol{\varepsilon}, n}$ without intervention at these time instants t_n . This shows that the events $\{\boldsymbol{\varepsilon} \in \bar{\mathcal{I}}_{\boldsymbol{\varepsilon}, n}\}$ that they lie in the individual error regions $\bar{\mathcal{I}}_{\boldsymbol{\varepsilon}, n}$ without intervention at

the time instants $t_n, n \in \mathbb{I}$, are statistically independent.

If the set \mathbb{I} is considered to be the union of two disjoint sets \mathbb{I}_1 and \mathbb{I}_2 , i.e., $\mathbb{I} = \mathbb{I}_1 \cup \mathbb{I}_2$ with $\mathbb{I}_1, \mathbb{I}_2 \subset \{0, 1, \dots, n_{\text{end}}\}$ and $\mathbb{I}_1 \cap \mathbb{I}_2 = \emptyset$, it follows from (B.2) that

$$\begin{aligned}
P\left(\varepsilon \in \bigcap_{n \in \mathbb{I}_1} \bar{\mathcal{I}}_{\varepsilon, n} \cap \bigcap_{n \in \mathbb{I}_2} \bar{\mathcal{I}}_{\varepsilon, n}\right) &= P\left(\varepsilon \in \bigcap_{n \in \mathbb{I}_1 \cup \mathbb{I}_2} \bar{\mathcal{I}}_{\varepsilon, n}\right) \\
&= \prod_{n \in \mathbb{I}_1 \cup \mathbb{I}_2} P(\varepsilon \in \bar{\mathcal{I}}_{\varepsilon, n}) \\
&= \underbrace{\prod_{n \in \mathbb{I}_1} P(\varepsilon \in \bar{\mathcal{I}}_{\varepsilon, n})}_{=P(\varepsilon \in \bigcap_{n \in \mathbb{I}_1} \bar{\mathcal{I}}_{\varepsilon, n})} \underbrace{\prod_{n \in \mathbb{I}_2} P(\varepsilon \in \bar{\mathcal{I}}_{\varepsilon, n})}_{=P(\varepsilon \in \bigcap_{n \in \mathbb{I}_2} \bar{\mathcal{I}}_{\varepsilon, n})} \\
&= P\left(\varepsilon \in \bigcap_{n \in \mathbb{I}_1} \bar{\mathcal{I}}_{\varepsilon, n}\right) P\left(\varepsilon \in \bigcap_{n \in \mathbb{I}_2} \bar{\mathcal{I}}_{\varepsilon, n}\right).
\end{aligned} \tag{B.3}$$

Since

$$\begin{aligned}
&P\left(\varepsilon \in \bigcap_{n \in \mathbb{I}_1} \bar{\mathcal{I}}_{\varepsilon, n} \cap \bigcap_{n \in \mathbb{I}_2} \bar{\mathcal{I}}_{\varepsilon, n}\right) + P\left(\varepsilon \in \bigcap_{n \in \mathbb{I}_1} \bar{\mathcal{I}}_{\varepsilon, n} \cap \overline{\bigcap_{n \in \mathbb{I}_2} \bar{\mathcal{I}}_{\varepsilon, n}}\right) \\
&= P\left(\varepsilon \in \bigcap_{n \in \mathbb{I}_1} \bar{\mathcal{I}}_{\varepsilon, n}\right),
\end{aligned} \tag{B.4}$$

the last result leads to

$$\begin{aligned}
&P\left(\varepsilon \in \bigcap_{n \in \mathbb{I}_1} \bar{\mathcal{I}}_{\varepsilon, n} \cap \overline{\bigcap_{n \in \mathbb{I}_2} \bar{\mathcal{I}}_{\varepsilon, n}}\right) \\
&= P\left(\varepsilon \in \bigcap_{n \in \mathbb{I}_1} \bar{\mathcal{I}}_{\varepsilon, n}\right) - P\left(\varepsilon \in \bigcap_{n \in \mathbb{I}_1} \bar{\mathcal{I}}_{\varepsilon, n} \cap \bigcap_{n \in \mathbb{I}_2} \bar{\mathcal{I}}_{\varepsilon, n}\right) \\
&= P\left(\varepsilon \in \bigcap_{n \in \mathbb{I}_1} \bar{\mathcal{I}}_{\varepsilon, n}\right) - P\left(\varepsilon \in \bigcap_{n \in \mathbb{I}_1} \bar{\mathcal{I}}_{\varepsilon, n}\right) P\left(\varepsilon \in \bigcap_{n \in \mathbb{I}_2} \bar{\mathcal{I}}_{\varepsilon, n}\right) \\
&= P\left(\varepsilon \in \bigcap_{n \in \mathbb{I}_1} \bar{\mathcal{I}}_{\varepsilon, n}\right) \underbrace{\left(1 - P\left(\varepsilon \in \bigcap_{n \in \mathbb{I}_2} \bar{\mathcal{I}}_{\varepsilon, n}\right)\right)}_{=P(\varepsilon \in \overline{\bigcap_{n \in \mathbb{I}_2} \bar{\mathcal{I}}_{\varepsilon, n}})}.
\end{aligned} \tag{B.5}$$

This factorization

$$P\left(\varepsilon \in \bigcap_{n \in \mathbb{I}_1} \bar{\mathcal{I}}_{\varepsilon,n} \cap \overline{\bigcap_{n \in \mathbb{I}_2} \bar{\mathcal{I}}_{\varepsilon,n}}\right) = P\left(\varepsilon \in \bigcap_{n \in \mathbb{I}_1} \bar{\mathcal{I}}_{\varepsilon,n}\right) P\left(\varepsilon \in \overline{\bigcap_{n \in \mathbb{I}_2} \bar{\mathcal{I}}_{\varepsilon,n}}\right) \quad (\text{B.6})$$

of the probability $P\left(\varepsilon \in \bigcap_{n \in \mathbb{I}_1} \bar{\mathcal{I}}_{\varepsilon,n} \cap \overline{\bigcap_{n \in \mathbb{I}_2} \bar{\mathcal{I}}_{\varepsilon,n}}\right)$ that the sensor measurement errors ε lie in all error regions $\bar{\mathcal{I}}_{\varepsilon,n}$ without intervention at the time instants t_n with indices $n \in \mathbb{I}_1$ and do not lie in all error regions $\bar{\mathcal{I}}_{\varepsilon,n}$ without intervention at the time instants t_n with indices $n \in \mathbb{I}_2$ into the probability $P\left(\varepsilon \in \bigcap_{n \in \mathbb{I}_1} \bar{\mathcal{I}}_{\varepsilon,n}\right)$ that they lie in all error regions $\bar{\mathcal{I}}_{\varepsilon,n}$ without intervention at the time instants t_n with indices $n \in \mathbb{I}_1$ and the probability $P\left(\varepsilon \in \overline{\bigcap_{n \in \mathbb{I}_2} \bar{\mathcal{I}}_{\varepsilon,n}}\right)$ that they do not lie in all error regions $\bar{\mathcal{I}}_{\varepsilon,n}$ without intervention at the time instants t_n with indices $n \in \mathbb{I}_2$ demonstrates that the events $\{\varepsilon \in \bigcap_{n \in \mathbb{I}_1} \bar{\mathcal{I}}_{\varepsilon,n}\}$ and $\{\varepsilon \in \overline{\bigcap_{n \in \mathbb{I}_2} \bar{\mathcal{I}}_{\varepsilon,n}}\}$ that the sensor measurement errors ε lie in all error regions $\bar{\mathcal{I}}_{\varepsilon,n}$ without intervention at the time instants t_n with indices $n \in \mathbb{I}_1$ and that they do not lie in all error regions $\bar{\mathcal{I}}_{\varepsilon,n}$ without intervention at the time instants t_n with indices $n \in \mathbb{I}_2$, respectively, are statistically independent.

Closed-Form Solutions of Differential Equations Describing Vehicle Motion



Closed-form solutions of the differential equations (2.1)–(2.4) describing the vehicle motion during a driving maneuver starting at t_{start} and ending at t_{end} exist for the special cases of constant longitudinal and lateral acceleration. They are derived in the following.

C.1 Vehicle Motion with Constant Longitudinal Acceleration

If the vehicle moves with the constant longitudinal acceleration a_{lon} while its lateral acceleration is $a_{\text{lat}} = 0$ and its longitudinal velocity $v(t)$ is assumed to be nonnegative at all times t in the considered time interval $[t_{\text{start}}, t_{\text{end}}]$, (2.4) simplifies to

$$\dot{\psi}(t) = 0. \quad (\text{C.1})$$

This means that the yaw angle $\psi(t)$ is constant in the considered time interval $[t_{\text{start}}, t_{\text{end}}]$, i.e.,

$$\psi(t) = \psi(t_{\text{start}}). \quad (\text{C.2})$$

Due to (2.3), the expression for the longitudinal velocity $v(t)$ must have the form

$$v(t) = a_{\text{lon}}t + C_v \quad (\text{C.3})$$

with a constant C_v . For $t = t_{\text{start}}$, it reads $v(t_{\text{start}}) = a_{\text{lon}}t_{\text{start}} + C_v$, which implies that $C_v = v(t_{\text{start}}) - a_{\text{lon}}t_{\text{start}}$ and

$$v(t) = a_{\text{lon}}t + v(t_{\text{start}}) - a_{\text{lon}}t_{\text{start}} = a_{\text{lon}}(t - t_{\text{start}}) + v(t_{\text{start}}). \quad (\text{C.4})$$

With (C.2) and (C.4), (2.1) and (2.2) become

$$\dot{x}(t) = (a_{\text{lon}}(t - t_{\text{start}}) + v(t_{\text{start}})) \cos(\psi(t_{\text{start}})), \quad (\text{C.5})$$

$$\dot{y}(t) = (a_{\text{lon}}(t - t_{\text{start}}) + v(t_{\text{start}})) \sin(\psi(t_{\text{start}})). \quad (\text{C.6})$$

Therefore, the expressions for the coordinates $x(t)$ and $y(t)$ of the center of gravity of the vehicle with respect to the x_w - and y_w -axis of the world coordinate system determining its position must have the form

$$x(t) = \left(\frac{1}{2} a_{\text{lon}} (t - t_{\text{start}})^2 + v(t_{\text{start}}) t \right) \cos(\psi(t_{\text{start}})) + C_x, \quad (\text{C.7})$$

$$y(t) = \left(\frac{1}{2} a_{\text{lon}} (t - t_{\text{start}})^2 + v(t_{\text{start}}) t \right) \sin(\psi(t_{\text{start}})) + C_y \quad (\text{C.8})$$

with constants C_x and C_y . For $t = t_{\text{start}}$, it holds that

$$x(t_{\text{start}}) = v(t_{\text{start}}) t_{\text{start}} \cos(\psi(t_{\text{start}})) + C_x, \quad (\text{C.9})$$

$$y(t_{\text{start}}) = v(t_{\text{start}}) t_{\text{start}} \sin(\psi(t_{\text{start}})) + C_y, \quad (\text{C.10})$$

which implies that

$$C_x = x(t_{\text{start}}) - v(t_{\text{start}}) t_{\text{start}} \cos(\psi(t_{\text{start}})), \quad (\text{C.11})$$

$$C_y = y(t_{\text{start}}) - v(t_{\text{start}}) t_{\text{start}} \sin(\psi(t_{\text{start}})) \quad (\text{C.12})$$

and

$$\begin{aligned} x(t) &= \left(\frac{1}{2} a_{\text{lon}} (t - t_{\text{start}})^2 + v(t_{\text{start}}) t \right) \cos(\psi(t_{\text{start}})) + x(t_{\text{start}}) \\ &\quad - v(t_{\text{start}}) t_{\text{start}} \cos(\psi(t_{\text{start}})) \\ &= \left(\frac{1}{2} a_{\text{lon}} (t - t_{\text{start}})^2 + v(t_{\text{start}}) (t - t_{\text{start}}) \right) \cos(\psi(t_{\text{start}})) + x(t_{\text{start}}), \end{aligned} \quad (\text{C.13})$$

$$\begin{aligned} y(t) &= \left(\frac{1}{2} a_{\text{lon}} (t - t_{\text{start}})^2 + v(t_{\text{start}}) t \right) \sin(\psi(t_{\text{start}})) + y(t_{\text{start}}) \\ &\quad - v(t_{\text{start}}) t_{\text{start}} \sin(\psi(t_{\text{start}})) \\ &= \left(\frac{1}{2} a_{\text{lon}} (t - t_{\text{start}})^2 + v(t_{\text{start}}) (t - t_{\text{start}}) \right) \sin(\psi(t_{\text{start}})) + y(t_{\text{start}}). \end{aligned} \quad (\text{C.14})$$

To sum up, the solution of the differential equations (2.1)–(2.4) describing the vehicle motion during a driving maneuver starting at t_{start} and ending at t_{end} with the constant longitudinal acceleration a_{lon} and the lateral acceleration $a_{\text{lat}} = 0$ under the

C.2 Vehicle Motion with Constant Lateral Acceleration

assumption $v(t) \geq 0$ for $t \in [t_{\text{start}}, t_{\text{end}}]$ is given by (C.13), (C.14), (C.4) and (C.2):

$$x(t) = \left(\frac{1}{2} a_{\text{lon}} (t - t_{\text{start}})^2 + v(t_{\text{start}}) (t - t_{\text{start}}) \right) \cos(\psi(t_{\text{start}})) + x(t_{\text{start}}), \quad (\text{C.15})$$

$$y(t) = \left(\frac{1}{2} a_{\text{lon}} (t - t_{\text{start}})^2 + v(t_{\text{start}}) (t - t_{\text{start}}) \right) \sin(\psi(t_{\text{start}})) + y(t_{\text{start}}), \quad (\text{C.16})$$

$$v(t) = a_{\text{lon}} (t - t_{\text{start}}) + v(t_{\text{start}}), \quad (\text{C.17})$$

$$\psi(t) = \psi(t_{\text{start}}). \quad (\text{C.18})$$

If the constant longitudinal acceleration is zero, i.e., $a_{\text{lon}} = 0$, in addition, the vehicle moves with constant velocity and the solution of the differential equations (2.1)–(2.4) simplifies to

$$x(t) = v(t_{\text{start}}) (t - t_{\text{start}}) \cos(\psi(t_{\text{start}})) + x(t_{\text{start}}), \quad (\text{C.19})$$

$$y(t) = v(t_{\text{start}}) (t - t_{\text{start}}) \sin(\psi(t_{\text{start}})) + y(t_{\text{start}}), \quad (\text{C.20})$$

$$v(t) = v(t_{\text{start}}), \quad (\text{C.21})$$

$$\psi(t) = \psi(t_{\text{start}}) \quad (\text{C.22})$$

and the assumption $v(t) \geq 0$ for $t \in [t_{\text{start}}, t_{\text{end}}]$ to $v(t_{\text{start}}) \geq 0$.

C.2 Vehicle Motion with Constant Lateral Acceleration

If the vehicle moves with the constant lateral acceleration a_{lat} while its longitudinal acceleration is $a_{\text{lon}} = 0$, (2.3) reads

$$\dot{v}(t) = 0. \quad (\text{C.23})$$

This means that the longitudinal velocity $v(t)$ is constant in the considered time interval $[t_{\text{start}}, t_{\text{end}}]$, i.e.,

$$v(t) = v(t_{\text{start}}). \quad (\text{C.24})$$

Assuming that the lateral acceleration a_{lat} is small enough such that $\frac{a_{\text{lat}}}{v(t)} < \frac{v(t)}{r_{\text{min}}}$ for this constant longitudinal velocity, (2.4) simplifies to

$$\dot{\psi}(t) = \frac{a_{\text{lat}}}{v(t_{\text{start}})}. \quad (\text{C.25})$$

Due to this, the expression for the yaw angle $\psi(t)$ must have the form

$$\psi(t) = \frac{a_{\text{lat}}}{v(t_{\text{start}})} t + C_{\psi} \quad (\text{C.26})$$

Appendix C. Closed-Form Solutions of Differential Equations Describing Vehicle Motion

with a constant C_ψ . For $t = t_{\text{start}}$, it reads $\psi(t_{\text{start}}) = \frac{a_{\text{lat}}}{v(t_{\text{start}})}t_{\text{start}} + C_\psi$, which implies that $C_\psi = \psi(t_{\text{start}}) - \frac{a_{\text{lat}}}{v(t_{\text{start}})}t_{\text{start}}$ and

$$\psi(t) = \frac{a_{\text{lat}}}{v(t_{\text{start}})}t + \psi(t_{\text{start}}) - \frac{a_{\text{lat}}}{v(t_{\text{start}})}t_{\text{start}} = \frac{a_{\text{lat}}}{v(t_{\text{start}})}(t - t_{\text{start}}) + \psi(t_{\text{start}}). \quad (\text{C.27})$$

With (C.24) and (C.27), (2.1) and (2.2) become

$$\dot{x}(t) = v(t_{\text{start}}) \cos\left(\frac{a_{\text{lat}}}{v(t_{\text{start}})}(t - t_{\text{start}}) + \psi(t_{\text{start}})\right), \quad (\text{C.28})$$

$$\dot{y}(t) = v(t_{\text{start}}) \sin\left(\frac{a_{\text{lat}}}{v(t_{\text{start}})}(t - t_{\text{start}}) + \psi(t_{\text{start}})\right). \quad (\text{C.29})$$

Therefore, the expressions for the coordinates $x(t)$ and $y(t)$ of the center of gravity of the vehicle with respect to the x_w - and y_w -axis of the world coordinate system determining its position must have the form

$$x(t) = \frac{v^2(t_{\text{start}})}{a_{\text{lat}}} \sin\left(\frac{a_{\text{lat}}}{v(t_{\text{start}})}(t - t_{\text{start}}) + \psi(t_{\text{start}})\right) + C_x, \quad (\text{C.30})$$

$$y(t) = -\frac{v^2(t_{\text{start}})}{a_{\text{lat}}} \cos\left(\frac{a_{\text{lat}}}{v(t_{\text{start}})}(t - t_{\text{start}}) + \psi(t_{\text{start}})\right) + C_y \quad (\text{C.31})$$

with constants C_x and C_y . For $t = t_{\text{start}}$, it holds that

$$x(t_{\text{start}}) = \frac{v^2(t_{\text{start}})}{a_{\text{lat}}} \sin(\psi(t_{\text{start}})) + C_x, \quad (\text{C.32})$$

$$y(t_{\text{start}}) = -\frac{v^2(t_{\text{start}})}{a_{\text{lat}}} \cos(\psi(t_{\text{start}})) + C_y, \quad (\text{C.33})$$

which implies that

$$C_x = x(t_{\text{start}}) - \frac{v^2(t_{\text{start}})}{a_{\text{lat}}} \sin(\psi(t_{\text{start}})), \quad (\text{C.34})$$

$$C_y = y(t_{\text{start}}) + \frac{v^2(t_{\text{start}})}{a_{\text{lat}}} \cos(\psi(t_{\text{start}})) \quad (\text{C.35})$$

and

$$\begin{aligned}
 x(t) &= \frac{v^2(t_{\text{start}})}{a_{\text{lat}}} \sin\left(\frac{a_{\text{lat}}}{v(t_{\text{start}})}(t - t_{\text{start}}) + \psi(t_{\text{start}})\right) + x(t_{\text{start}}) \\
 &\quad - \frac{v^2(t_{\text{start}})}{a_{\text{lat}}} \sin(\psi(t_{\text{start}}))
 \end{aligned} \tag{C.36}$$

$$\begin{aligned}
 &= \frac{v^2(t_{\text{start}})}{a_{\text{lat}}} \left(\sin\left(\frac{a_{\text{lat}}}{v(t_{\text{start}})}(t - t_{\text{start}}) + \psi(t_{\text{start}})\right) - \sin(\psi(t_{\text{start}})) \right) \\
 &\quad + x(t_{\text{start}}), \\
 y(t) &= -\frac{v^2(t_{\text{start}})}{a_{\text{lat}}} \cos\left(\frac{a_{\text{lat}}}{v(t_{\text{start}})}(t - t_{\text{start}}) + \psi(t_{\text{start}})\right) + y(t_{\text{start}}) \\
 &\quad + \frac{v^2(t_{\text{start}})}{a_{\text{lat}}} \cos(\psi(t_{\text{start}})) \\
 &= \frac{v^2(t_{\text{start}})}{a_{\text{lat}}} \left(\cos(\psi(t_{\text{start}})) - \cos\left(\frac{a_{\text{lat}}}{v(t_{\text{start}})}(t - t_{\text{start}}) + \psi(t_{\text{start}})\right) \right) \\
 &\quad + y(t_{\text{start}}).
 \end{aligned} \tag{C.37}$$

To sum up, the solution of the differential equations (2.1)–(2.4) describing the vehicle motion during a driving maneuver starting at t_{start} and ending at t_{end} with the constant lateral acceleration a_{lat} and the longitudinal acceleration $a_{\text{lon}} = 0$ under the assumption $\frac{a_{\text{lat}}}{v(t_{\text{start}})} < \frac{v(t_{\text{start}})}{r_{\text{min}}}$ is given by (C.36), (C.37), (C.24) and (C.27):

$$\begin{aligned}
 x(t) &= \frac{v^2(t_{\text{start}})}{a_{\text{lat}}} \left(\sin\left(\frac{a_{\text{lat}}}{v(t_{\text{start}})}(t - t_{\text{start}}) + \psi(t_{\text{start}})\right) - \sin(\psi(t_{\text{start}})) \right) \\
 &\quad + x(t_{\text{start}}),
 \end{aligned} \tag{C.38}$$

$$\begin{aligned}
 y(t) &= \frac{v^2(t_{\text{start}})}{a_{\text{lat}}} \left(\cos(\psi(t_{\text{start}})) - \cos\left(\frac{a_{\text{lat}}}{v(t_{\text{start}})}(t - t_{\text{start}}) + \psi(t_{\text{start}})\right) \right) \\
 &\quad + y(t_{\text{start}}),
 \end{aligned} \tag{C.39}$$

$$v(t) = v(t_{\text{start}}), \tag{C.40}$$

$$\psi(t) = \frac{a_{\text{lat}}}{v(t_{\text{start}})}(t - t_{\text{start}}) + \psi(t_{\text{start}}). \tag{C.41}$$

Bibliography

- [1] McKinsey & Company, “Automotive revolution - perspective towards 2030,” Jan. 2016.
- [2] SAE International Standard J3016, *Taxonomy and Definitions for Terms Related to Driving Automation Systems for On-Road Motor Vehicles*, Jun. 2018. [Online]. Available: https://doi.org/10.4271/J3016_201806
- [3] SAE International, *Summary of SAE International’s Levels of Driving Automation for On-Road Vehicles*, 2014. [Online]. Available: https://www.sae.org/binaries/content/assets/cm/content/news/press-releases/pathway-to-autonomy/automated_driving.pdf
- [4] H. Winner, S. Hakuli, F. Lotz, and C. Singer, *Handbook of Driver Assistance Systems*, 1st ed. Springer International Publishing, 2016.
- [5] A. Lambert, D. Gruyer, G. S. Pierre, and A. N. Ndjeng, “Collision probability assessment for speed control,” in *2008 11th International IEEE Conference on Intelligent Transportation Systems*, Oct. 2008, pp. 1043–1048.
- [6] J. Ward, G. Agamennoni, S. Worrall, and E. Nebot, “Vehicle collision probability calculation for general traffic scenarios under uncertainty,” in *2014 IEEE Intelligent Vehicles Symposium Proceedings*, Jun. 2014, pp. 986–992.
- [7] C. Braeuchle, J. Ruenz, F. Flehmig, W. Rosenstiel, and T. Kropf, “Situation analysis and decision making for active pedestrian protection using Bayesian networks,” in *6. Tagung Fahrerassistenzsysteme*, München, 2013.
- [8] A. Houénou, P. Bonnifait, and V. Cherfaoui, “Risk assessment for collision avoidance systems,” in *17th International IEEE Conference on Intelligent Transportation Systems (ITSC)*, Oct. 2014, pp. 386–391.
- [9] M. Schreier, V. Willert, and J. Adamy, “Bayesian, maneuver-based, long-term trajectory prediction and criticality assessment for driver assistance systems,”

Bibliography

- in *17th International IEEE Conference on Intelligent Transportation Systems (ITSC)*, Oct. 2014, pp. 334–341.
- [10] D. Åsljung, M. Westlund, and J. Fredriksson, “A probabilistic framework for collision probability estimation and an analysis of the discretization precision,” in *2019 IEEE Intelligent Vehicles Symposium (IV)*, Jun. 2019, pp. 52–57.
- [11] A. Berthelot, A. Tamke, T. Dang, and G. Breuel, “Handling uncertainties in criticality assessment,” in *2011 IEEE Intelligent Vehicles Symposium (IV)*, Jun. 2011, pp. 571–576.
- [12] N. E. Du Toit and J. W. Burdick, “Probabilistic collision checking with chance constraints,” *IEEE Transactions on Robotics*, vol. 27, no. 4, pp. 809–815, Aug. 2011.
- [13] S. Patil, J. van den Berg, and R. Alterovitz, “Estimating probability of collision for safe motion planning under Gaussian motion and sensing uncertainty,” in *2012 IEEE International Conference on Robotics and Automation*, May 2012, pp. 3238–3244.
- [14] M. Metro, J. Ghosh, and C. Bhat, “Optimal alarms for vehicular collision detection,” in *2017 IEEE Intelligent Vehicles Symposium (IV)*, Jun. 2017, pp. 277–282.
- [15] C. M. Hruschka, D. Töpfer, and S. Zug, “Risk assessment for integral safety in automated driving,” in *2019 2nd International Conference on Intelligent Autonomous Systems (ICoIAS)*, Feb. 2019, pp. 102–109.
- [16] Ö. S. Tas and C. Stiller, “Limited visibility and uncertainty aware motion planning for automated driving,” in *2018 IEEE Intelligent Vehicles Symposium (IV)*, Jun. 2018, pp. 1171–1178.
- [17] R. Karlsson, J. Jansson, and F. Gustafsson, “Model-based statistical tracking and decision making for collision avoidance application,” in *Proceedings of the 2004 American Control Conference*, vol. 4, Jun. 2004, pp. 3435–3440.
- [18] M. Brännström, F. Sandblom, and L. Hammarstrand, “A probabilistic framework for decision-making in collision avoidance systems,” *IEEE Transactions on Intelligent Transportation Systems*, vol. 14, no. 2, pp. 637–648, Jun. 2013.
- [19] S. Lefèvre, R. Bajcsy, and C. Laugier, “Probabilistic decision making for collision avoidance systems: Postponing decisions,” in *2013 IEEE/RSJ International Conference on Intelligent Robots and Systems*, Nov. 2013, pp. 4370–4375.

- [20] C. Braeuchle, F. Flehmig, W. Rosenstiel, and T. Kropf, “Maneuver decision for active pedestrian protection under uncertainty,” in *16th International IEEE Conference on Intelligent Transportation Systems (ITSC 2013)*, Oct. 2013, pp. 646–651.
- [21] P. Themann, J. Kotte, D. Raudszus, and L. Eckstein, “Impact of positioning uncertainty of vulnerable road users on risk minimization in collision avoidance systems,” in *2015 IEEE Intelligent Vehicles Symposium (IV)*, Jun. 2015, pp. 1201–1206.
- [22] F. Zhang, C. M. Martinez, D. Clarke, D. Cao, and A. Knoll, “Neural network based uncertainty prediction for autonomous vehicle application,” *Frontiers in Neurorobotics*, vol. 13, p. 12, 2019.
- [23] P. Zheng and M. McDonald, “The effect of sensor errors on the performance of collision warning systems,” in *Proceedings of the 2003 IEEE International Conference on Intelligent Transportation Systems*, vol. 1, Oct. 2003, pp. 469–474.
- [24] J. Hillenbrand, K. Kroschel, and V. Schmid, “Situation assessment algorithm for a collision prevention assistant,” in *2005 IEEE Intelligent Vehicles Symposium*, Jun. 2005, pp. 459–465.
- [25] T. Dirndorfer, M. Botsch, and A. Knoll, “Model-based analysis of sensor-noise in predictive passive safety algorithms,” in *Proceedings of the 22nd Enhanced Safety of Vehicles Conference*, 2011.
- [26] A. Berthelot, A. Tamke, T. Dang, and G. Breuel, “A novel approach for the probabilistic computation of time-to-collision,” in *2012 IEEE Intelligent Vehicles Symposium*, Jun. 2012, pp. 1173–1178.
- [27] J. E. Stellet, J. Schumacher, W. Branz, and J. M. Zöllner, “Uncertainty propagation in criticality measures for driver assistance,” in *2015 IEEE Intelligent Vehicles Symposium (IV)*, Jun. 2015, pp. 1187–1194.
- [28] J. E. Stellet, P. Vogt, J. Schumacher, W. Branz, and J. M. Zöllner, “Analytical derivation of performance bounds of autonomous emergency brake systems,” in *2016 IEEE Intelligent Vehicles Symposium (IV)*, Jun. 2016, pp. 220–226.
- [29] J. Nilsson, A. C. E. Ödöblom, and J. Fredriksson, “Worst-case analysis of automotive collision avoidance systems,” *IEEE Transactions on Vehicular Technology*, vol. 65, no. 4, pp. 1899–1911, Apr. 2016.

Bibliography

- [30] J. E. Stellet, C. Heigele, F. Kuhnt, J. M. Zöllner, and D. Schramm, “Performance evaluation and statistical analysis of algorithms for ego-motion estimation,” in *17th International IEEE Conference on Intelligent Transportation Systems (ITSC)*, Oct. 2014, pp. 2125–2131.
- [31] A. Kelly, “Linearized error propagation in odometry,” *The International Journal of Robotics Research*, vol. 23, no. 2, pp. 179–218, 2004.
- [32] Lee Yang, Ji Hyun Yang, E. Feron, and V. Kulkarni, “Development of a performance-based approach for a rear-end collision warning and avoidance system for automobiles,” in *IEEE IV2003 Intelligent Vehicles Symposium*, Jun. 2003, pp. 316–321.
- [33] J. Nilsson and M. Ali, “Sensitivity analysis and tuning for active safety systems,” in *13th International IEEE Conference on Intelligent Transportation Systems*, Sep. 2010, pp. 161–167.
- [34] J. E. Stellet, J. Schumacher, O. Lange, W. Branz, F. Niewels, and J. M. Zöllner, “Statistical modelling of object detection in stereo vision-based driver assistance,” in *Intelligent Autonomous Systems 13*. Springer International Publishing, 2016, pp. 749–761.
- [35] J. Rohde, J. E. Stellet, H. Mielenz, and J. M. Zöllner, “Model-based derivation of perception accuracy requirements for vehicle localization in urban environments,” in *2015 IEEE 18th International Conference on Intelligent Transportation Systems*, Sep. 2015, pp. 712–718.
- [36] ———, “Localization accuracy estimation with application to perception design,” in *2016 IEEE International Conference on Robotics and Automation (ICRA)*, May 2016, pp. 4777–4783.
- [37] A. M. Hasofer and N. C. Lind, “Exact and invariant second-moment code format,” *Journal of the Engineering Mechanics Division*, vol. 100, no. EM1, pp. 111–121, Feb. 1974.
- [38] R. Rackwitz and B. Fiessler, “Structural reliability under combined random load sequences,” *Computers & Structures*, vol. 9, no. 5, pp. 489 – 494, 1978.
- [39] W. Utschick, “Ein sequentiell quadratisches Optimierverfahren zur Toleranzanalyse integrierter Schaltungen,” Diplomarbeit, TUM, 1993.

- [40] H. E. Graeb, C. U. Wieser, and K. J. Antreich, “Improved methods for worst-case analysis and optimization incorporating operating tolerances,” in *30th ACM/IEEE Design Automation Conference*, Jun. 1993, pp. 142–147.
- [41] K. J. Antreich, H. E. Graeb, and C. U. Wieser, “Practical methods for worst-case and yield analysis of analog integrated circuits,” *International Journal of High Speed Electronics and Systems*, vol. 04, no. 03, pp. 261–282, 1993.
- [42] ———, “Circuit analysis and optimization driven by worst-case distances,” *IEEE Transactions on Computer-Aided Design of Integrated Circuits and Systems*, vol. 13, no. 1, pp. 57–71, Jan. 1994.
- [43] H. E. Graeb, *Analog Design Centering and Sizing*. Springer Publishing Company, Incorporated, 2007.
- [44] C. Stöckle, W. Utschick, S. Herrmann, and T. Dirndorfer, “Robust design of an automatic emergency braking system considering sensor measurement errors,” in *21st IEEE International Conference on Intelligent Transportation Systems (ITSC)*, Nov. 2018, pp. 2018–2023.
- [45] ———, “Robust function and sensor design considering sensor measurement errors applied to automatic emergency braking,” in *30th IEEE Intelligent Vehicles Symposium (IV)*, Jun. 2019, pp. 2284–2290.
- [46] M. L. Leyrer, C. Stöckle, S. Herrmann, T. Dirndorfer, and W. Utschick, “An efficient approach to simulation-based robust function and sensor design applied to an automatic emergency braking system,” in *31st IEEE Intelligent Vehicles Symposium (IV)*, Oct. 2020, pp. 617–622.
- [47] K.-F. Lin, C. Stöckle, S. Herrmann, T. Dirndorfer, and W. Utschick, “Robust function and sensor design considering sensor measurement errors applied to automatic emergency steering,” in *31st IEEE Intelligent Vehicles Symposium (IV)*, Oct. 2020, pp. 610–616.
- [48] C. Stöckle, S. Herrmann, T. Dirndorfer, and W. Utschick, “Automated vehicular safety systems: Robust function and sensor design,” *IEEE Signal Processing Magazine*, vol. 37, no. 4, pp. 24–33, Jul. 2020.
- [49] N. Kaempchen, B. Schiele, and K. Dietmayer, “Situation assessment of an autonomous emergency brake for arbitrary vehicle-to-vehicle collision scenarios,”

Bibliography

IEEE Transactions on Intelligent Transportation Systems, vol. 10, no. 4, pp. 678–687, Dec. 2009.

- [50] X. Rong Li and V. P. Jilkov, “Survey of maneuvering target tracking. Part I: Dynamic models,” *IEEE Transactions on Aerospace and Electronic Systems*, vol. 39, no. 4, pp. 1333–1364, Oct. 2003.
- [51] D. Schramm, M. Hiller, and R. Bardini, *Vehicle Dynamics: Modeling and Simulation*, 2nd ed. Springer Publishing Company, Incorporated, 2018.